# THE PETROLOGY AND GEOCHEMISTRY OF PERALKALINE GRANITE AND VOLCANICS NEAR DAVIS INLET, LABRADOR



CHARLOTTE ANNE WHITE


CENTRE FOR NFLD. STUDIES
MAR 23 198
MEMORIAL UNIVERSITY
OF NEWFOUNDLAND

# THE PETROLOGY AND GEOCHEMISTRY OF PERALKALINE GRANITE AND VOLCANIC ROCKS NEAR DAVIS INLET, LABRADOR

by

© Charlotte Anne White, B.A., B. Sc.

A thesis submitted in partial fulfillment
of the requirements for the degree
of Master of Science

Department of Geology
Memorial University of Newfoundland

December 1980

St. John's Newfoundland

The Davis Inlet area is underlain by Archean gneisses and younger igneous rocks which range in composition from gabbroic to granitic. Two granites and a volcanic unit were sampled during the field season of 1978.

Detailed petrographic and geochemical studies indicate the non-peralkaline nature of the clinopyroxene-fayalite granite and the peralkaline character of the arfvedsonite-riebeckite granite and its associated volcanics. Mineralogical characteristics such as the presence of poikolitic aegirine-augite and arfvedsonite-riebeckite with needles of riebeckite nucleating on grain boundaries, and extensive albitization reflect the peralkaline nature and intense volatile activity in the peralkaline granite.

Chemical characteristics such as agpaitic indices (Molecular $Na_2O+K_2O/Al_2O_3$), normative acmite and sodium metasilicate and trace element behaviour can be used to separate the granitic suites according to their peralkaline and non-peralkaline natures.

The enigma of the Nuiklavick volcanic suite has been dealt with primarily on the basis of trace (including RE) element data. Extreme enrichment of Zr, Nb, Y, Th, Zn, Ni and the REE along with severely depleted Ba, Sr, Ca, and Mg are a strong indication of a very peralkaline character. Trace element trends and concentrations observed in samples examined cannot be explained by conventional differentiation models. Systematic trace element enrichment patterns indicate a high degree of continuity between the peralkaline granite and volcanic samples reflecting transport of elements to the top of the magma chamber as cationic com-

plexes in a fluid/volatile phase. From the data observed in this study and in others it is possible to suggest that over saturated peralkaline rocks reflect intense volatile activity which produces their characteristic petrography and geochemistry.

## ACKNOWLEDGMENTS

Sample collection and mapping for this thesis were supervised by Dr. B.J. Fryer and Dr. J.D. Hill while the author was employed by the Newfoundland Department of Mines and Energy as a field assistant. Thin sections and polished thin sections were provided by L. Warford and F. Thornhill. Samples were prepared for geochemical analyses with the assistance of D. Dumka. D. Press, C. Andrews and P. Davis assisted and advised on matters concerning geochemical techniques and processing. R.P, Taylor assisted with the microprobe analyses which were supervised by Dr. H. Longerich. Fluid inclusion sections were made and examined by Alex Kay. Photographic work was done by W. Marsh and the manuscript was prepared by C. Neary.

Discussions with Dr. B.J. Fryer and R.P. Taylor were very useful in the formulation of the ideas expressed in this thesis. The thesis work was supervised by Dr. B.J. Fryer to whom the author is grateful for his patience, time and effort put into discussion. Financial support for this study was provided through a Memorial University Graduate Fellowship and a NSERC research grant to B.J. Fryer.

TABLE OF CONTENTS

## CHAPTER 3

## GEOCHEMISTRY



## CHAPTER 4

## DISCUSSION



## CHAPTER 5

LIST OF PHOTOMICROGRAPHS

LIST OF PHOTOMICROGRAPHS (cont'd)

# LIST OF PLATES

## LIST OF FIGURES

LIST OF FIGURES (cont'd)

LIST OF FIGURES (cont'd)

LIST OF FIGURES (cont'd)

# LIST OF TABLES

LIST OF TABLES (cont'd)

# CHAPTER 1

## SCOPE AND PURPOSE OF STUDY

The major purpose of this study is to examine geochemical trends and their implications in an oversaturated alkaline/peralkaline environment. An attempt will be made to document on petrologic and geochemical grounds, the significance of volatiles and/or metasomatic fluids in the evolution of alkaline/peralkaline magmas.

The genetic relationship of the Nuiklavick Volcanics to the associated arfvedsonite-riebeckite granite will be defined by using rare earth element patterns to study mineralogical relationships. The absence of a direct genetic relationship between the arfvedsonite-riebeckite granite and the clinopyroxene-fayalite granite will be discussed.

## LOCATION AND ACCESS

Davis Inlet is a small native community located on the Labrador Coast at approximately 56°N latitude and 61°W longitude (Fig. 1). It is approximately 300 km north of Goose Bay and 80 km south of Nain. Access to Davis Inlet is by air (float plane) or by C.N. Marine coastal boat which operates during the ice-fee season - late spring to early autumn. Samples were collected from areas 1, 2 and 3 (Fig. 1) by boat and helicopter during the field season of 1978. The areas samples were mapped primarily by Hill during the field seasons of 1977 and 1978 assisted by the author in 1978 (Hill, 1978a,b, 1979).

## PHYSIOGRAPHY

The physiography of the Davis Inlet area, as described by Hill (1978b) is characterized by a peneplain that rises gradually from 300 m near the coast to 700 m inland with a maximum relief of 500 m. Deep erosional dissection by numerous streams and rivers has resulted in the formation of a series of rugged hills separated by drift and forest-covered valleys. Outcrop is abundant but occurs only on the hill tops above the tree line which is at about 200 m.

## PREVIOUS WORK

The first published description of the geology of the Davis Inlet area was by Wheeler (1942) who defined the Nain Igneous Complex following several years of mapping the Labrador Coast and some inland areas (Wheeler, 1942, 1955, 1960, 1961). Subsequent work by Taylor (1972) included a description of the Davis Inlet area as part of a large scale, helicopter-supported, reconnaissance mapping project in which the presence of the quartz-feldspar porphyry was reported. Ryan (1974) mapped and studied the metamorphic and structural relationships of the gneissic terrane near Flowers Bay in the Davis Inlet area but Collerson et al. (1974) were the first to recognize the alkaline nature of the granitic rocks in the Davis Inlet area. The area is presently being mapped and studied in greater detail than previously by Hill (1978a,b, 1979, 1980) who recognized the peralkalic nature of the arfvedsonite-riebeckite granite.

## GEOLOGICAL SETTING

The Davis Inlet area is underlain by undeformed igneous rocks of Helikian age which intrude Archean gneisses belonging to the Nain Structural Province of the Canadian Shield (Taylor, 1971). Geological descriptions and field relationships as reported by Hill (1978a,b, 1979, 1980) are summarized below.

### Archean Gneiss

Archean gneisses (unit 1, Table 1) occur bordering the younger igneous rocks to the east and north as well as forming discrete screens between separate intrusions (Fig. 1). The gneisses have been divided into several subunits on the basis of metamorphic facies (amphibolite-granulite), stages of deformation and composition.

### Gabbroic Rocks

Gabbroic plutons of varying compositions occur in at least nine separate areas and as three distinct phases namely: anorthosite plutons, olivine-norite dykes cross cutting marginal zones of the anorthosite plutons and as older anorthosite xenoliths in chill zones of the younger anorthosite plutons (Unit 2, Table 1). All phases intrude the Archean gneisses and are themselves intruded by younger more felsic igneous rocks and occasionally occur as roof pendants overlying the younger igneous rocks. The plutons consist of fine-grained olivine gabbro border phases which grade into coarser-grained troctolitic and anorthositic interiors commonly displaying rhythmic layering. Contact zones are often characterized by extensive brecciation and thermal aureoles reaching pyroxene hornfels metamorphic grade.

TABLE 1A

LEGEND FOR ALL MAPS

(Modified after Hill, 1979)

HELIKIAN

5. Medium to coarse grained massive undivided granite composed of arfvedsonite-riebeckite, fayalite, clinopyroxene, hornblende, and biotite bearing varieties; minor associated pegmatite and aplite dikes.

4. Massive quartz-feldspar porphyry, flow banded felsite, lithic tuff and minor breccia and agglomerate.

3. Syenite, monzonite and monzodiorite - olivine-pyroxene syenite, olivine-pyroxene monzonite and monzodiorite, foliated plagioclase cumulate with intercumulus clinopyroxene.

2. Gabbroic rocks - fine to medium grained olivine gabbro and leuco-gabbro, coarse to very coarse grained plagioclase and plagioclase olivine clumulate, locally contains thin layers of olivine-oxide and plagioclase-apatite clumulates.

ARCHEAN

1. Banded biotite-feldspar quartz gneiss; plagioclase-amphibole, plagioclase-pyroxene and amphibole gneiss, locally mixed with granitoid gneiss and pegmatite; interlayered, banded tonalite, granodiorite and minor granite gneiss; coarse grained granodiorite and granite augen gneiss; massive to faintly gneissic biotite granite.

SYMBOLS

Geologic boundary (observed, approximate, assumed, gradational, dip indicated, observed intrusive contact with younger unit indicated) .....

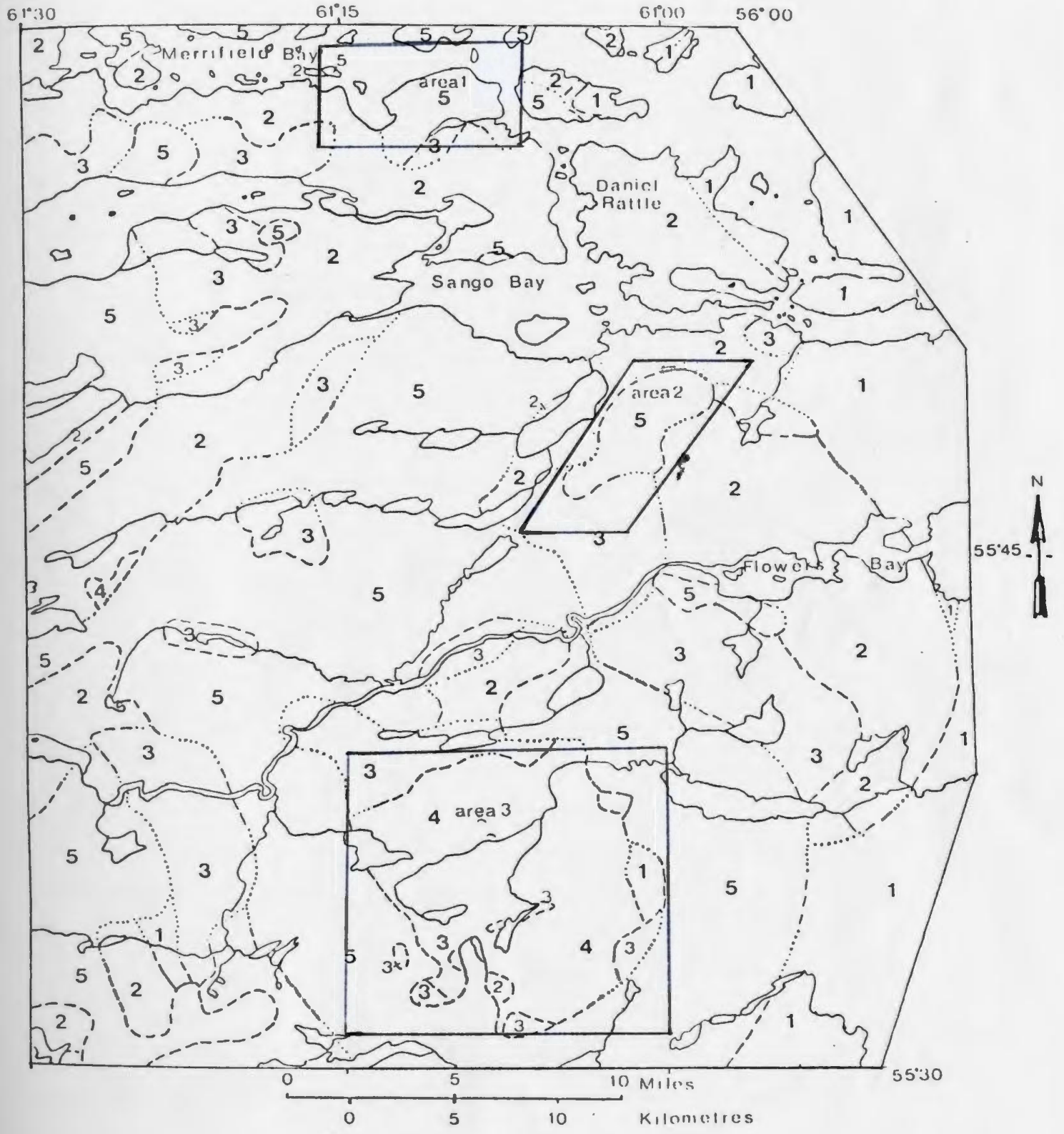


Fig.1: Geology Map of the Davis Inlet Area (modified after Hill, 1979)

TABLE 1

STRATIGRAPHIC COLUMN OF ROCK UNITS IN THE DAVIS INLET AREA

(Modified after Hill, 1978b, 1979)

HELIKIAN

5. Medium to coarse grained, massive undivided granite composed of arfvedsonite-riebeckite, aegirine, fayalite, clinopyroxene, hornblende and biotite bearing varieties; minor amounts of associated pegmatite and aplite dykes.

4. Massive quartz-feldspar porphyry, flow-banded felsite, lithic tuff, minor breccia and agglomerate.

3. (a) Olivine-pyroxene syenite

   (b) Olivine-pyroxene monzonite and monzodiorite

   (c) Foliated plagioclase cumulate with intercumulus clinopyroxene.

2. (a) Fine to medium grained olivine gabbro and leucogabbro

   (b) Coarse to very coarse grained plagioclase and plagioclase-olivine cumulate; locally contains thin layers of olivine-oxide cumulate and plagioclase-apatite cumulate.

ARCHEAN

1. (a) Banded biotite-feldpsar-quartz gneiss

   (b) Plagioclase-amphibole, plagioclase-pyroxene and amphibole gneiss, locally mixed with granitoid gneiss and pegmatite

   (c) Interlayered, banded tonalite, granodiorite and minor granite gneiss, local inclusions of 1b

   (d) Coarse grained granodiorite and granite augen gneiss

   (e) Massive to faintly gneissic biotite granite.

Syenite, Monzonite and Monzodiorite

Small homogeneous plutons of pyroxene-olivine syenite, monzonite and monzodiorite occur throughout the area (Unit 3, Table 1). These plutons which have been assigned a tentative Rb-Sr age of 1325 ± 55 Ma (Char Lake Monzonite, Brooks, 1980) intrude the gabbroic plutons and are themselves intruded by younger granitic rocks of Unit 5. Relationships with the Nuiklavick Volcanics have not been determined to date. The homogeneous plutons are syenitic to monzodioritic in composition and contain quartz-rich lenses which are gradational with the host rocks and chilled margins that may contain phenocrysts of plagioclase and/or orthopyroxene. The Char Lake pluton is the largest of these and is less homogeneous than most. It has chilled margins of monzodiorite with an interior composition which ranges from gabbro to granite.

Felsic Volcanic Rocks - Nuiklavick Volcanics

The Nuiklavick Volcanics (Bevan, 1954) occur in the highland areas south of Flowers River (Fig. 1) where relatively poor exposure prohibits identification of details in the volcanic stratigraphy. The Nuiklavick Volcanics consist of quartz and quartz-feldspar porphyry, flow banded felsite/rhyolite, lithic tuff and volcanic breccia (Unit 4, Table 1). All of the volcanic outcrops are rhyolitic with the exception of one which contains plagioclase phenocrysts and is considered dacitic. The dominant lithology is a massive quartz-feldspar porphyry which is accompanied by subordinate aphyric and porphyritic rhyolite (felsite). The rhyolite may exhibit flow banding with northerly strikes and gentle northeasterly dips (one exception is steeply dipping - Fig. 4).

Lithic tuff generally occurs topographically overlying the porphyry and may suggest a stratigraphic sequence. Volcanic breccia and/or agglomerate contain bombs of quartz-feldspar porphyry that may reach 40 cm in diameter and seem to lack secondary deformation.

The relative age of the Nuiklavick Volcanics is uncertain but it is younger than the gabbroic rocks since porphyry dykes cut plagioclase cumulate and one isolated xenolith of plagioclase cumulate occurs in porphyry. It is, however, older than the granite of Unit 5 (Table 1) which invariably cuts the volcanics when the two occur together. Roof pendants of porphyry have been found overlying granite bodies.

Granite

Three varieties of coarse grained granitic rocks (Unit 5, Table 1) form the dominant lithologies of the map area (Fig. 1). Arfvedsonite-riebeckite granite occurs predominantly south of Sango Bay. Clinopyroxene-fayalite granite is more common in the west with a few outcrops north of Sango Bay. A hornblende-biotite granite outcrops in two locations, one is on a small island in Merrifield Bay, the other is just south of Sango Bay.

The arfvedsonite-riebeckite granite appears to form relatively thin, flat-lying sheet-like bodies which are younger than the clinopyroxene-fayalite granite on the basis of intrusive relationships and Rb-Sr dating (Clinopyroxene-fayalite granite 1217 $\pm$ 24 m.y. arfvedsonite-riebeckite granite 835 $\pm$ 50 m.y. (Brooks, 1980)). The arfvedsonite-riebeckite granite

is undeformed but does contain some areas of brecciation which have been interpreted as the product of release of gases during intrusion (Hill, 1980). Associated pegmatite, miarolitic cavities and patchy coarse and fine grained areas provide further evidence of extensive volatile/gaseous activity.

## NOMENCLATURE

With one exception, the rock and unit names used in this study are those used by Hill (1978a,b, 1979, 1980) during mapping. The unit called Gabbroic Plutons has been changed to Gabbroic Rocks because the unit includes three gabbroic phases not all of which are plutons. The rock units are described in Table 1.

Identifications of microcline and orthoclase are based upon the presence or absence of cross-hatch twinning which is characteristic of microcline (Smith, 1974).

The term peralkaline has been defined in various ways by several different people. In this thesis, it is used to indicate any or one or combination of the following:

1. The presence of sodium-rich pyroxene (aegirine-augite) or amphibole (arfvedsonite-riebeckite) (Carmichael et al., 1974).

2. An agpaitic index (molecular $Na_2O+K_2O/Al_2O_3$) greater than one (Carmichael et al., 1974).

3. The appearance of acmite or sodium metasilicate in the CIPW normative analyses (Bailey and Schairer, 1966).

4. High concentrations of a suite of trace elements referred to as residual, agpaitic or lithophile elements which include Zr, Nb, Be, Y, Zr, REE, Th (Tauson, 1967; Taylor et al., 1980).

5. Depletion of Mg, Ca, Ba, Sr, Eu (Cr and Ni - to be revised in Chapters 3 and 4) (Nicholls and Carmichael, 1969; Ferrara and Treuil, 1974).

The term residual element, as used here, refers to those trace elements listed above which are characteristically enriched in peralkaline melts. As defined here, residual element does not necessarily comply with the strict definition whereby residual elements must obey Henry's Law and cannot readily enter the crystal structures of the common rock forming minerals (Arth, 1976). In particular, zinc has been included as a residual element by a number of people (Nicholls and Carmichael, 1969; Bailey and MacDonald, 1976). Further proof of the residual nature of zinc will be provided in a subsequent section of this work.

$\Sigma$Ce or Ce earths refer to La + Ce + Nd + Sm; $\Sigma$Y or Y earths refers to Gd + Dy + Er + Yb + Y (Mineyev, 1966).

Pseudoperthite, as used in this thesis, refers to altered perthite crystals which in thin section have pale green iron-magnesium rich lamellae and hosts that are sericitized or recrystallized. In the field, these are dark green to black and resemble mafic phenocrysts.

# CHAPTER 2

# PETROGRAPHY

Approximately fifty samples of clinopyroxene-fayalite granite, arfvedsonite-riebeckite granite and Nuiklavick volcanics from the Davis Inlet area have been examined petrographically. Sample locations are presented as Figures 2-4 and individual sample descriptions are given in Appendix A. The purposes of the petrographic study are to:

1. compare the two granites
2. document hydrothermal activity associated with the arfvedsonite-riebeckite granite
3. attempt to separate the Nuiklavick Volcanics into sub-volcanic and extrusive subunits.

## CLINOPYROXENE-FAYALITE GRANITE

Eight samples of clinopyroxene-fayalite granite were collected from a well exposed section of coastline, extending north from Daniel Rattle and south of Merrifield Bay (Fig. 2). In the field, it is often difficult to distinguish this granite from the syenite/monzonites of Unit 3 and arfvedsonite-riebeckite granite. It is quite melanocratic, with 5-10% mafic minerals, medium to coarse grained and inequigranular (Plate 1) with an average modal analysis of:

| | |
|---|---|
| 25% | quartz |
| 5 -20% | orthoclase |
| 30 -65% | perthite |
| 0 -20% | plagioclase |
| 5 -10% | mafic minerals. |

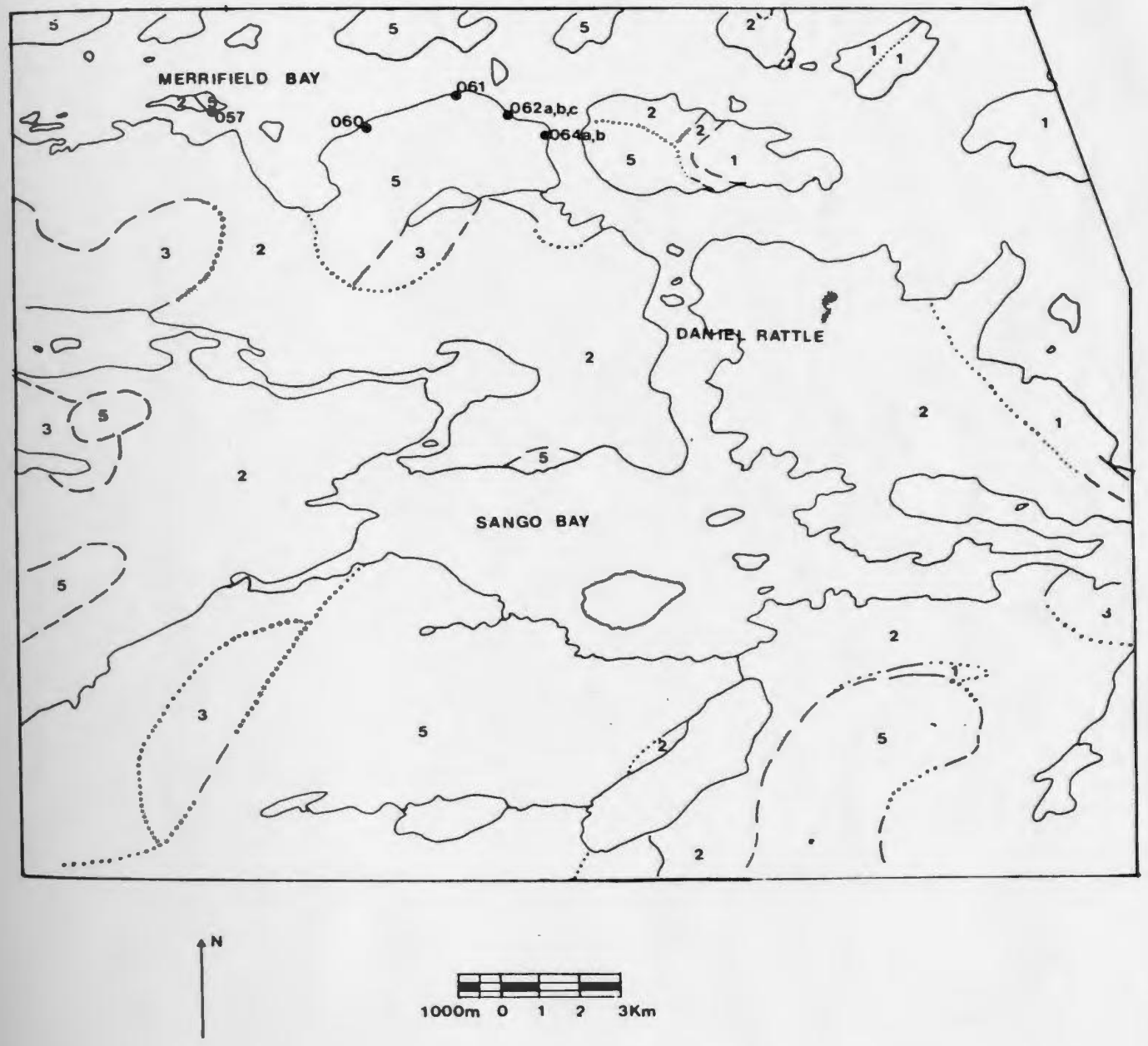


Fig.2: Clinopyroxene-fayalite granite Sample Map


Plate 1: Handspecimen of clinopyroxene-fayalite granite

In thin section quartz occurs as interstitial grains between alkali feldspars which are the most common minerals.

The alkali feldspars are predominantly mesoperthite accompanied by some orthoclase which may actually be perthite with sub-microscopic lamellae (Smith, 1974). Plagioclase occurs only as hydrothermally formed albite.

Optical identifications of mafic phases as ferrohastingsite, hedenbergite/ferrohedenbergite and fayalite have been confirmed by electron microprobe analyses (Table 2). Ferrohastingsite seems to be the most abundant mafic phase in the samples studied. All three mafic phases are intimately intergrown and their sequence of crystallization is difficult to determine but it seems to be fayalite → hedenbergite → ferrohastingsite (photomicrograph 1). Ferrohastingsite occurs as oikocrysts (photomicrograph 2). Occasionally, biotite or a blue-green amphibole, which may be arfvedsonitic, is found replacing ferrohastingsite (photomicrograph 3) (Deer et al., 1963).

Common accessory minerals include iron-titanium oxides, allanite, zircon, apatite and rutile. The oxides are by far the most common of the accessory minerals.

ARFVEDSONITE-RIEBECKITE GRANITE

Seventeen samples of arfvedsonite-riebeckite granite were collected from Merrifield Mountain (Fig. 3) and examined petrographically for the purpose of confirming their peralkaline nature and the petrographic-petrochemical relationships of the minerals in this rock unit.

TABLE 2

ELECTRON MICROPROBE ANALYSES OF MAFIC PHASES OF CLINOPYROXENE-FAYALITE GRANITE

| | A | B | C |
|---|---|---|---|
| $SiO_2$ | 41.8 | 50.24 | 29.5 |
| $Al_2O_3$ | 8.39 | 0.25 | 0.07 |
| FeO | 26.69 | 22.66 | 64.68 |
| MgO | 4.99 | 5.00 | 2.5 |
| CaO | 9.97 | 20.21 | 0.05 |
| $Na_2O$ | 1.99 | 0.20 | - |
| $K_2O$ | 1.24 | -* | - |
| $TiO_2$ | 1.89 | 0.1 | - |
| MnO | 0.26 | 0.53 | 1.48 |
| TOTAL | 97.23 | 99.19 | 98.29 |

A - hastingsite $(Na_{.3}, K_{.1})\ Ca_{1.8}\ (Mg_{1.2}, Fe_{3.7})\ (Si_7\ Al_{.8}\ O_{22})\ OH, F$

B - hedenbergite $Ca_{.89}\ (Mg_{.3}, Fe_{.7})\ Si_2O_6$

C - fayalite $(Mg_{.1}, Fe_{1.9})\ SiO_4$

*in all tables a dash means values were below limits of detection

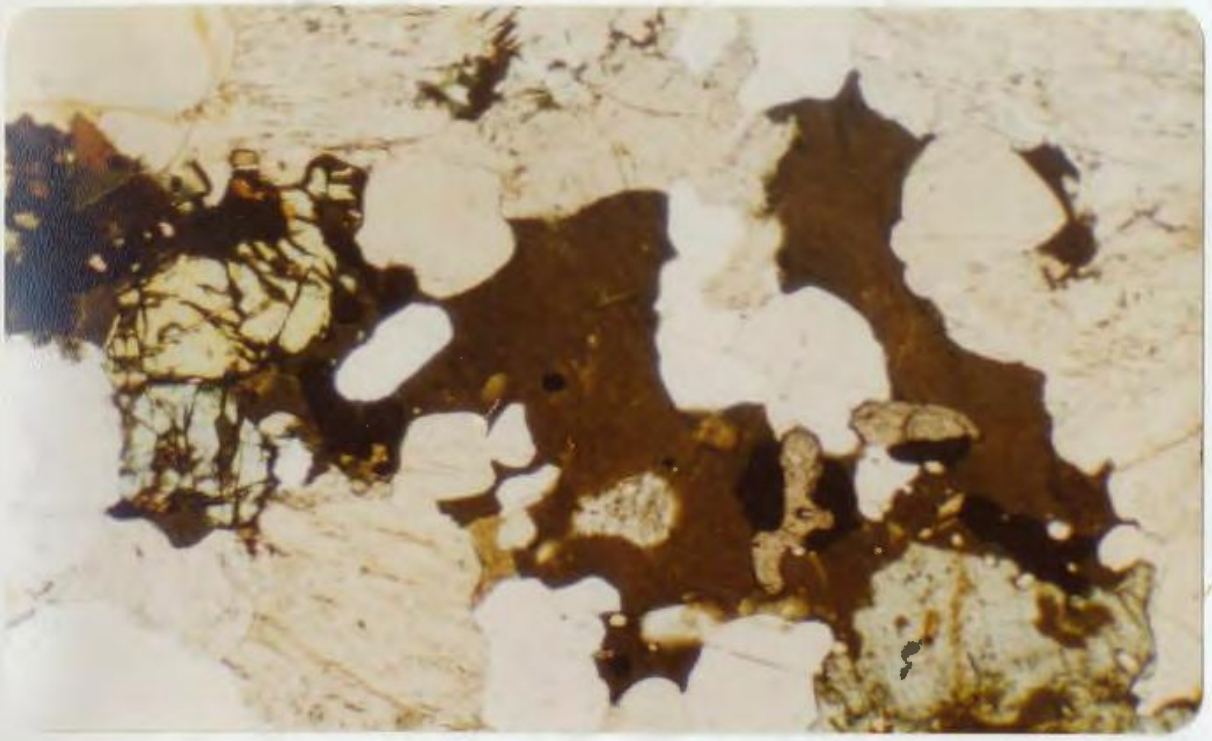

Photomicrograph 1: Association of mafic minerals in clinopyroxene-fayalite granite. Green mineral is ferrohastingsite, yellow tinged high relief mineral is fayalite and pale nearly colourless mineral in ferrohastingsite is hedenbergite.

(40x) - all photomicrographs are in plane polarized light unless otherwise stated

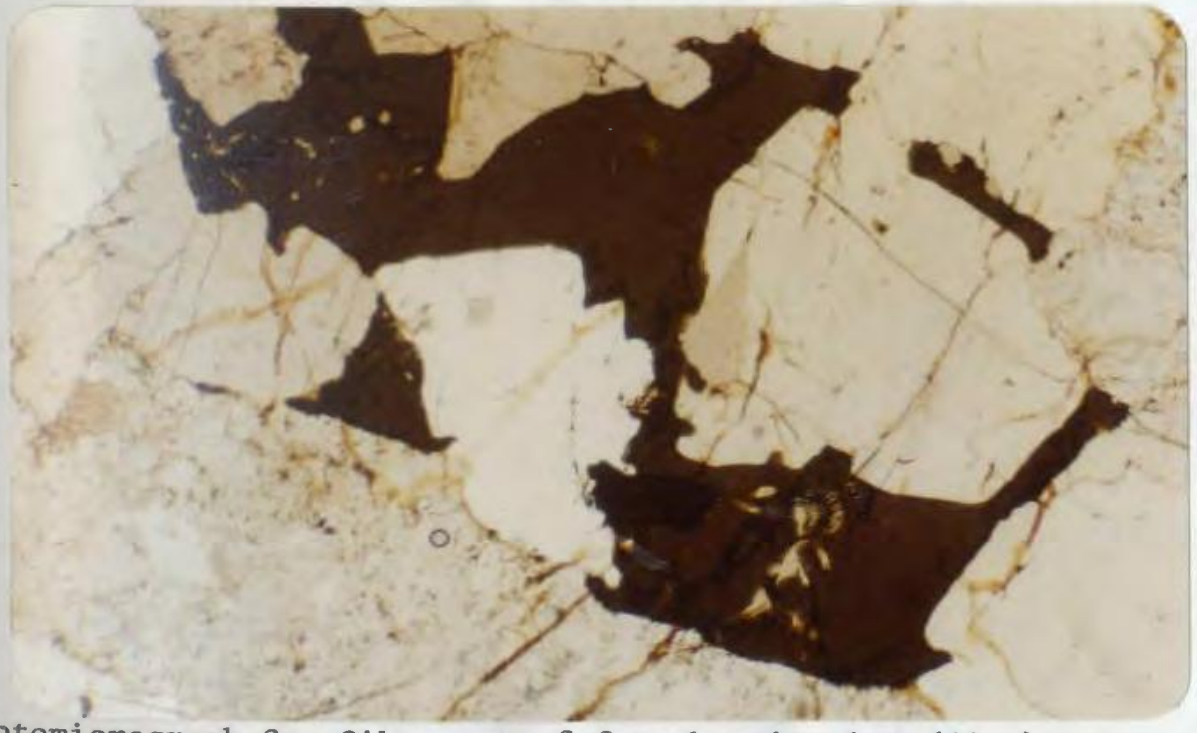

Photomicrograph 2: Oikocryst of ferrohastingsite (40 x)

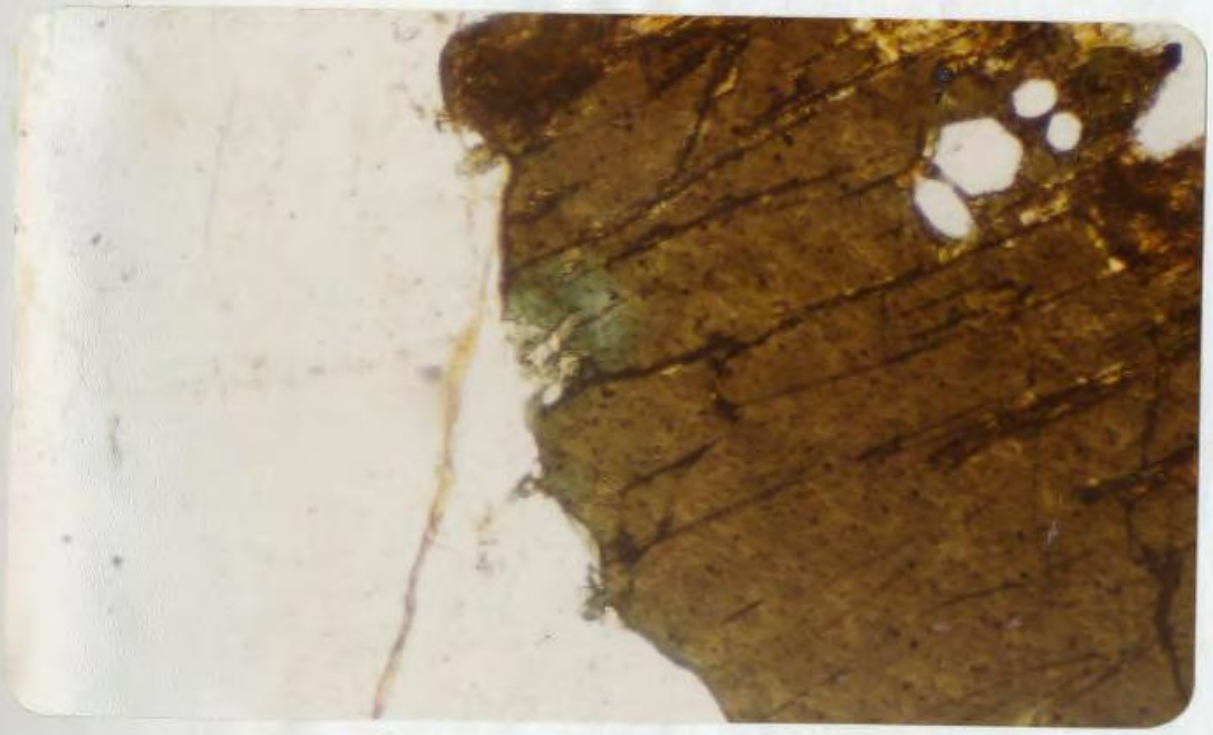

Photomicrograph 3: Blue-green amphibole that may be arfvedsonitic, replacing ferrohastingsite along grain boundary (125 x)

The arfvedsonite-riebeckite granite is leucocratic (white-pink), medium to coarse grained and equigranular (Plate 2). In contact zones it tends to be fine grained and prophyritic with phenocrysts of quartz, feldspar and locally arfvedsonite-riebeckite (Plate 3) or it may develop a graphic intergrowth of quartz and feldspar (Plate 4). The average modal composition is:

25-30% quartz
65-70% perthitic alkali feldspar
3-5 % mafic minerals
up to 1% accessory minerals.

In thin section, quartz commonly occurs as interstitial crystals or as vermicular or graphic intergrowths with feldspar. The bulk of the rock consists of microperthitic alkali feldspar with microcline/orthoclase hosts and albitic lamellae. Several textural varieties of microperthite have been identified - rod, stringer, braided, and patch or rim albitization (photomicrographs 4, 5) (Smith 1974; Taylor et al., 1980).

The mafic components are primarily sodic pyroxene (generally aegirine-augite), and sodic amphibole (arfvedsonite-riebeckite) accompanied by aenigmatite and astrophyllite which are usually present only in accessory amounts.

Aegirine-augite is pleochroic in green with the following pleochroic scheme: $\alpha$ - deep green, $\beta$- grass green, $\gamma$ - brownish green. Arfvedsonite-riebeckite is also pleochroic in green and blue with $\alpha$ - light yellow, brown-pale blue grey, $\beta$ - dark green-bright blue, $\gamma$ - dark blue, green-dark green. The darkest colours reflect the most riebeckitic compositions

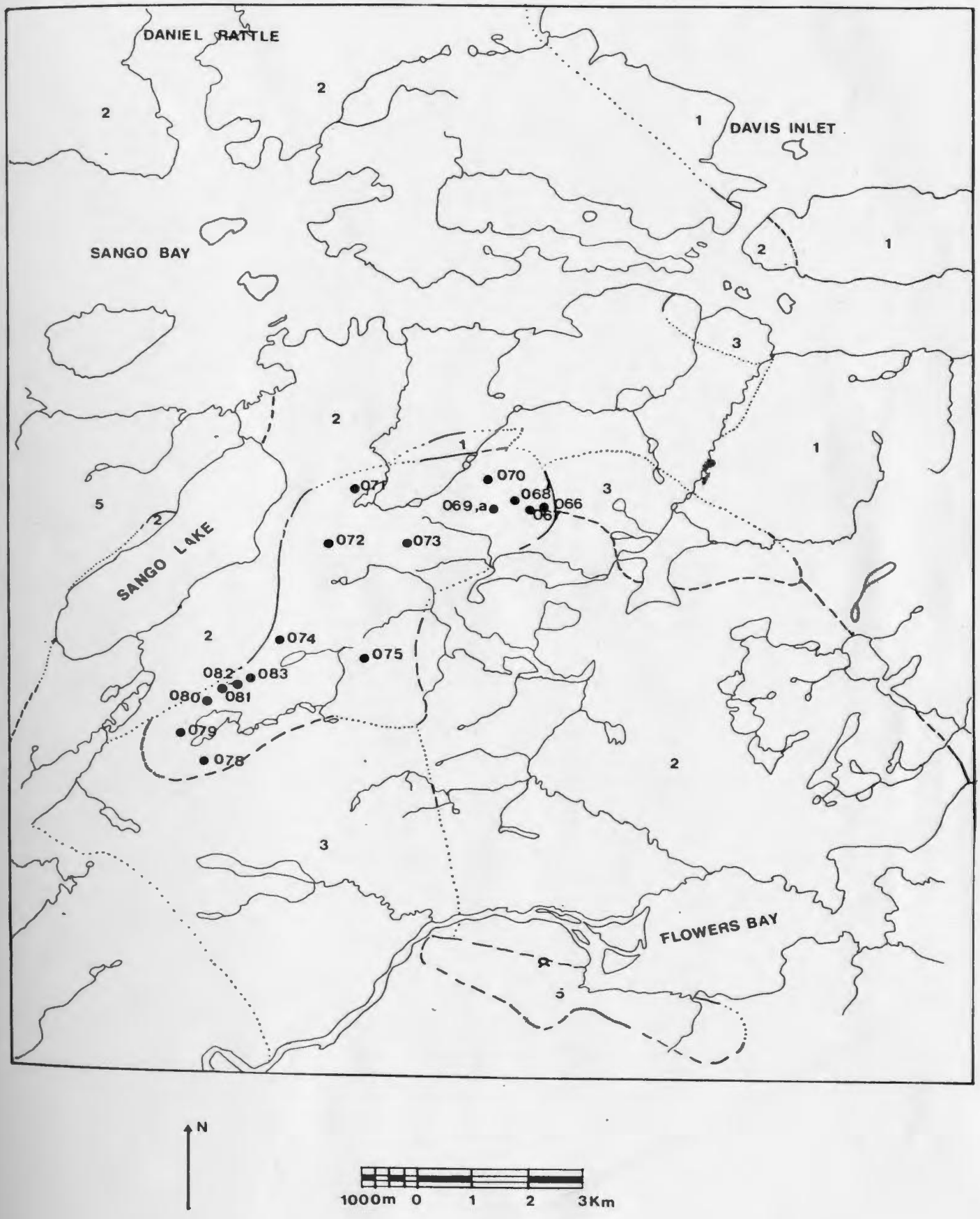


Fig. 3: Arfvedsonite-riebeckite granite Sample Map

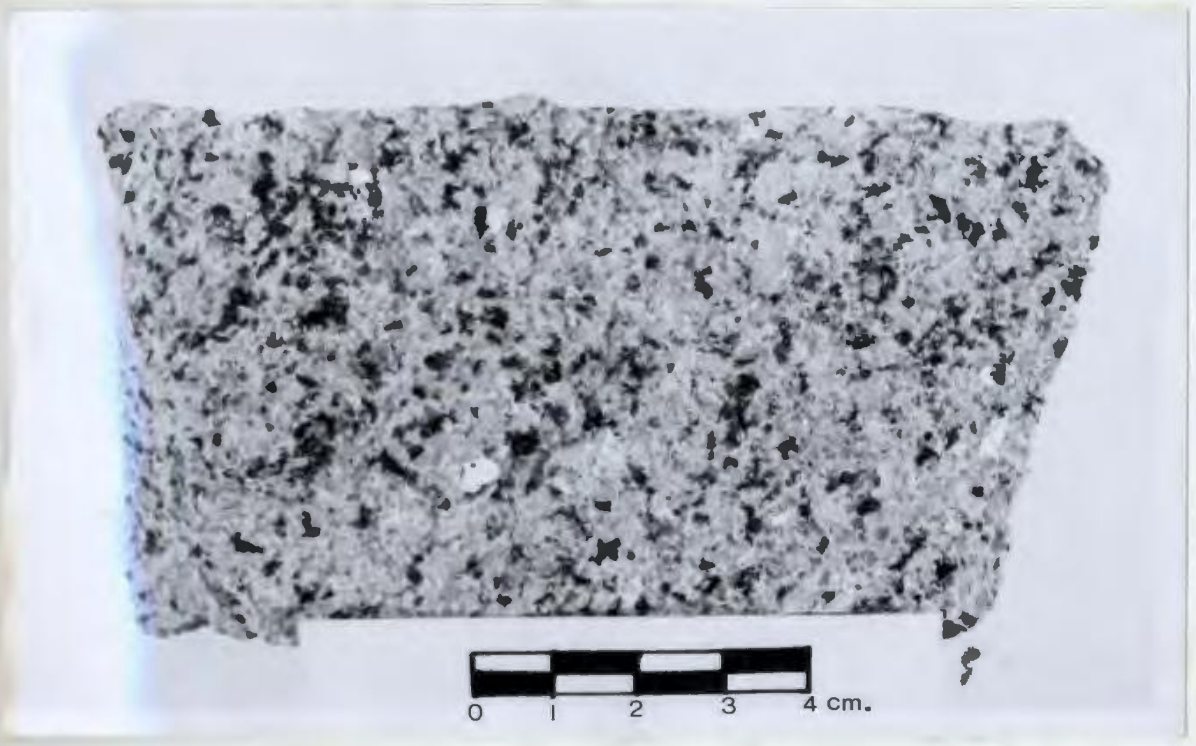


Plate 2: Handspecimen of arfvedsonite-riebeckite granite


Plate 3: Poikolitic arfvedsonite-riebeckite and aegirine-augite in fine grained groundmass. Sample from chilled margin near gneiss


Plate 4: Graphic intergrowth of quartz and feldspar. Sample from near chilled margin

Photomicrograph 4: Rim albitization in arfvedsonite-riebeckite granite (40 x, crossed nicols)


Photomicrograph 5: Albitization with associated allanite and aegirine-augite (50 x, crossed nicols)

and are much less common than arfvedsonitic compositions). The mafic phases are intimately associated, commonly with the most sodium- and iron-rich phases surrounding the less sodium- and iron-rich cores, i.e. aegirine-augite rimmed by a thin corona of arfvedsonite-riebeckite (photomicrograph 6) or green arfvedsonitic amphibole rimmed by bluer more riebeckitic compositions. Electron microprobe analyses of aegirine-augite and arfvedsonite-riebeckite confirm that the compositions vary from the core to rim becoming increasingly sodium- and iron-rich (Table 3).

Aenigmatic is red pleochroic, often with a very dark nearly opaque core. It often seems to be replacing the pyroxene or amphibole but it is difficult to determine the real sequence (photomicrograph 7).

The mafic minerals, including aenigmatite and astrophyllite occur in several crystal forms:

1. primary igneous minerals (pyroxene, amphibole, possibly aenigmatite) (photomicrograph 8)

2. oikocrysts (late stage poikolitic growths) - primarily pyroxene and amphibole (photomicrograph 9)

3. secondary replacement minerals especially along cleavage planes and as thin coronas (photomicrographs 6 and 10)

4. as small acicular crystals or radiating clusters which nucleate on grain boundaries of earlier formed crystals or peppering the felsic phases (photomicrographs 11, 12 and 13).

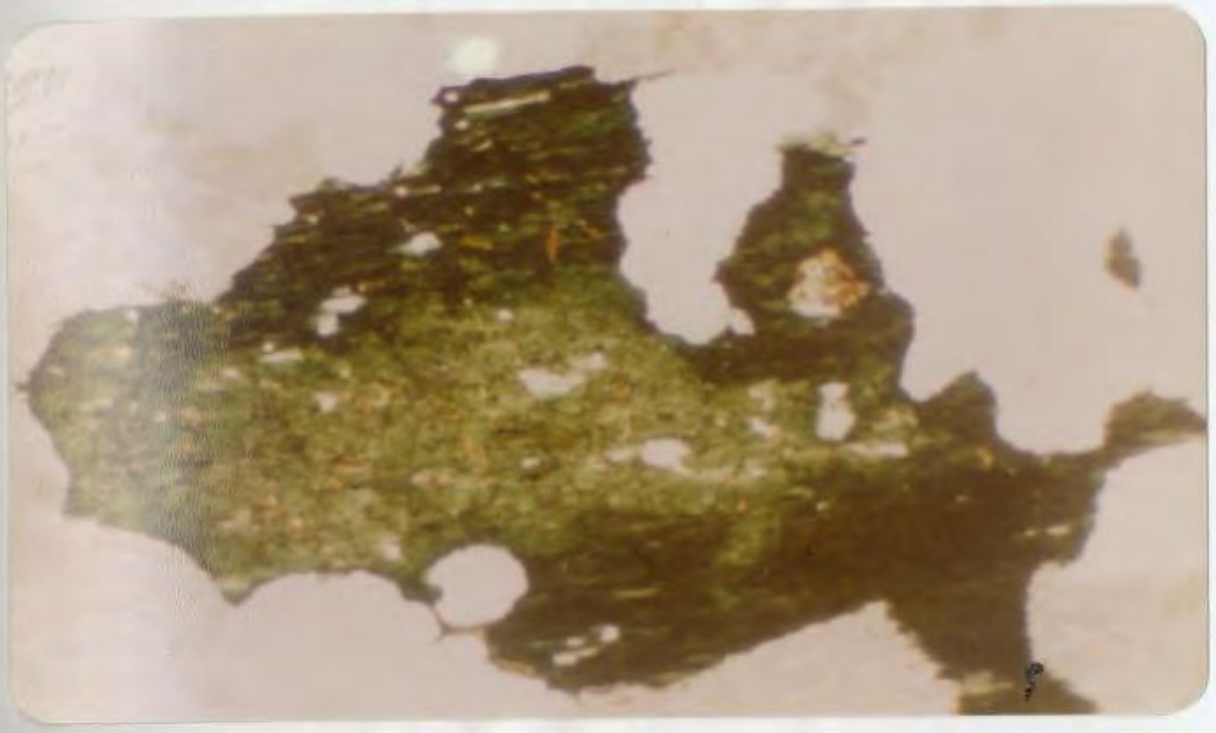

Photomicrograph 6: Arfvedsonite-riebeckite (corona) replacing aegirine-augite (40 x)

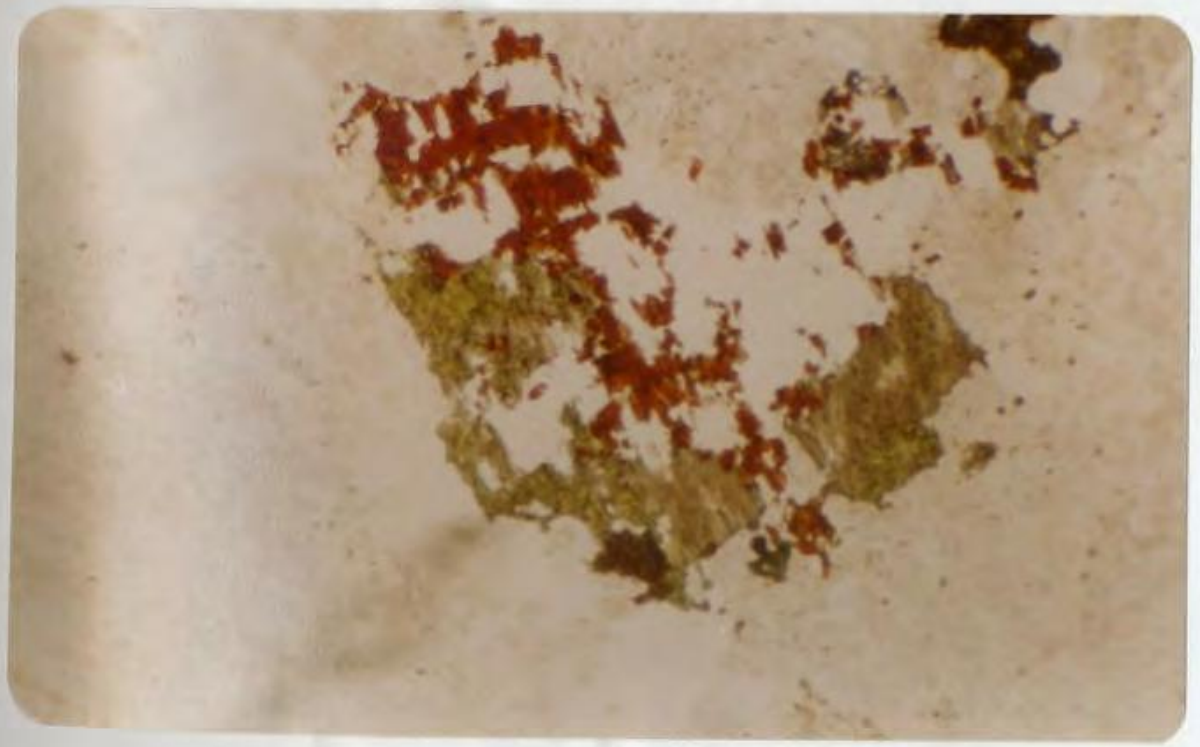

Photomicrograph 7: Aenigmatite replacing arfvedsonite-riebeckite and and aegirine-augite. In lower left hand corner, arfvedsonite-riebeckite has a bluer riebeckite material on edge of grain (50 x)

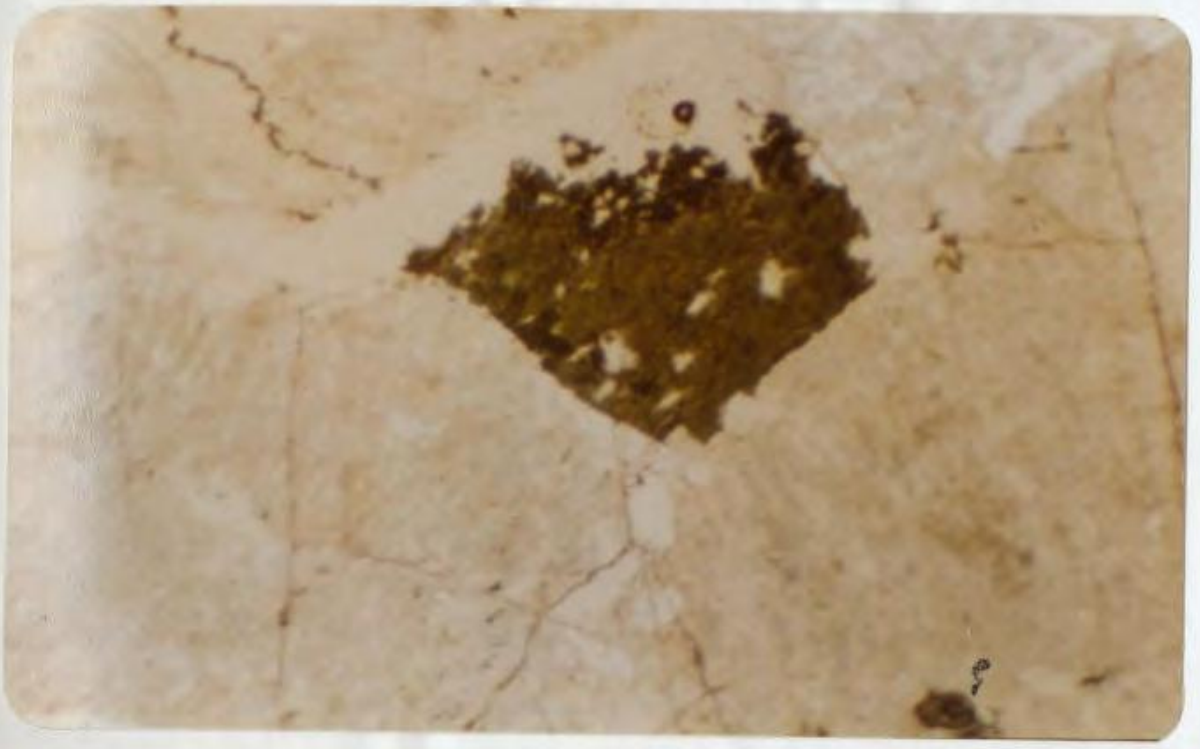

Photomicrograph 8: Arfvedsonite-riebeckite that crystallized magmatically and was subsequently corroded by a hydrothermal fluid phase (40 x)

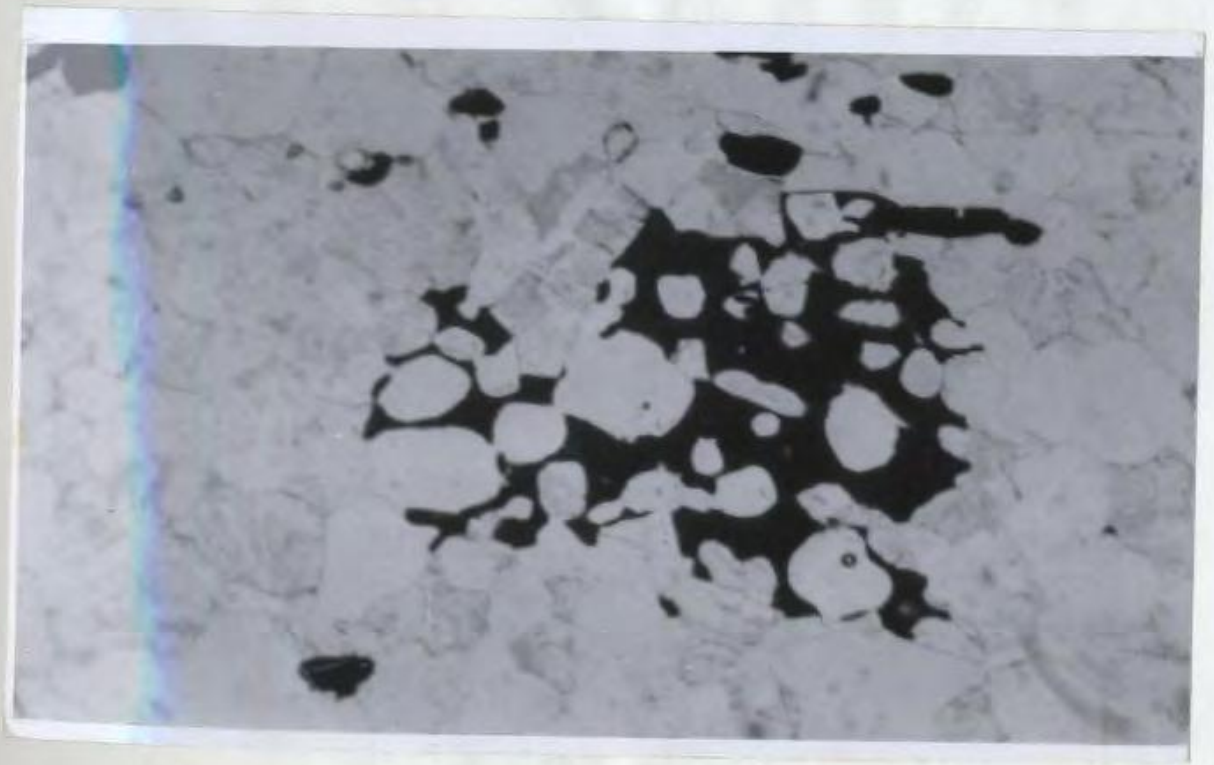

Photomicrograph 9: Oikocryst of arfvedsonite-riebeckite (40 x)

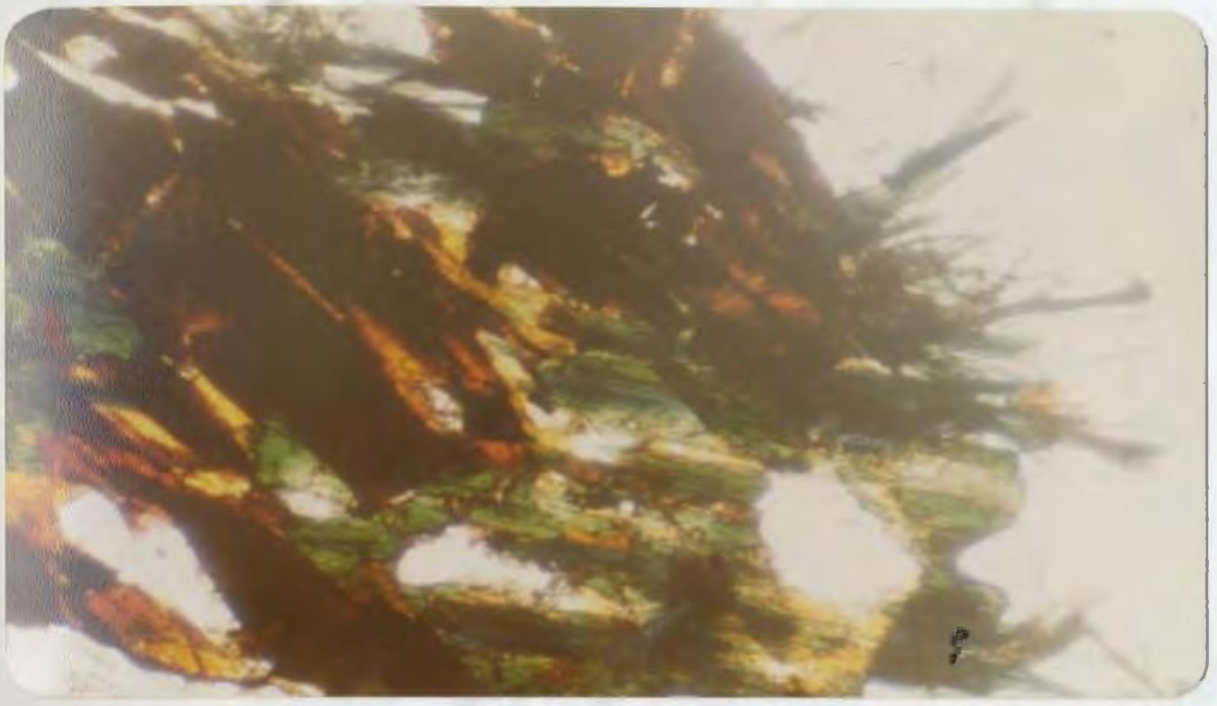

Photomicrograph 10: Blue riebeckitic material replacing arfvedsonite or aegirine-augite along grain boundaries. Also, riebeckite needles nucleating on grain boundaries and very dark coloured, nearly opaque aenigmatite (125 x)

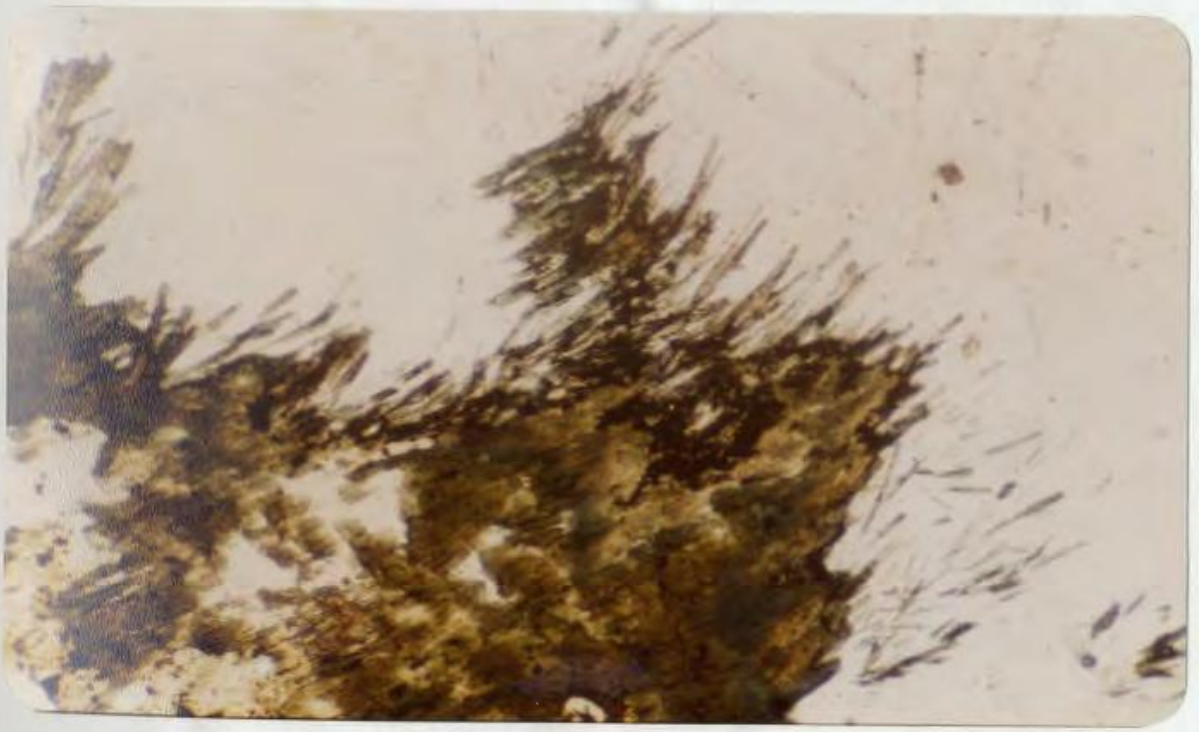

Photomicrograph 11: Riebeckitic crystals nucleating along grain boundary of arfvedsonite-riebeckite which is being replaced by riebeckitic material (125 x)

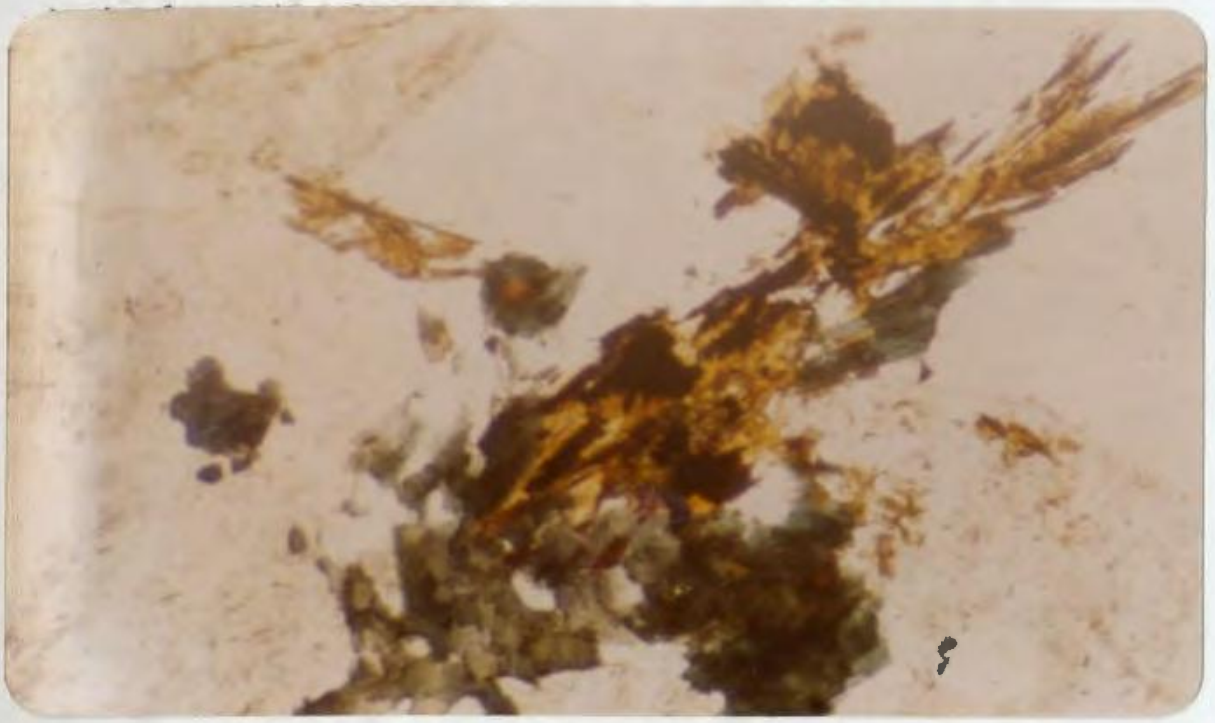

Photomicrograph 12: Radiating cluster of astrophyllite needles nucleating on edge of arfvedsonite-riebeckite crystal (125 x)

Photomicrograph 13: Clusters of riebeckite needles in feldspar (125 x)

TABLE 3

RESULTS OF ELECTRON MICROPROBE ANALYSES OF SOME PYROXENES, AMPHIBOLES AND ZIRCONS FROM THE ARFVEDSONITE-RIEBECKITE GRANITE

| | A | B | C | D | E | F | G |
|---|---|---|---|---|---|---|---|
| $SiO_2$ | 49.51 | 48.07 | 47.96 | 48.75 | 25.35 | 40.32 | 38.93 |
| $Al_2O_3$ | .18 | .16 | .98 | .64 | 23.12 | | |
| FeO | 28.69 | 32.20 | 26.82 | 35.11 | 34.47 | .04 | |
| MgO | .41 | .09 | .45 | .20 | 1.13 | | |
| CaO | 17.25 | 15.71 | 3.05 | 1.60 | 0.10 | .01 | .03 |
| $Na_2O$ | 2.55 | 4.15 | 5.83 | 10.02 | 0.04 | .11 | .02 |
| $K_2O$ | .01 | .23 | 1.49 | .02 | 2.13 | .02 | |
| $TiO_2$ | .42 | .47 | .95 | .77 | 0.43 | .02 | |
| MnO | .51 | | | | 0.21 | | |
| $Y_2O_3$ | | | | | | .03 | .88 |
| $ZrO_2$ | | | | | | 58.50 | 49.38 |
| $Ce_2O_3$ | | | | | | .05 | |
| ZnO | | | | | | .16 | .05 |
| TOTAL | 99.53 | 97.48 | 93.45 | 89.36 | 86.98 | 99.33 | 89.33 |

A - pyroxene centre $(Na_{.1}, Ca_{.7})$ $(Fe_{.94}, Mg_{.01})$ $Si_2O_6$

B - pyroxene rim $(Na_{.2}, Ca_{.7})$ $(Fe_{1.0}, Mg_{.01})$ $Si_2O_6$

C - amphibole near contact with pyroxene $Na_{2.9}$ $Fe_{5.0}$ $Al_{.2}$ $(Si_{8.4}O_{22})$ (OH,F)

D - amphibole rim $Na_{3.8}$ $Fe_{4.2}$ $Al_{.1}$ $(Si_{8.7}O_{22})$ (OH,F)

E - alteration material, pseudomorphic after mafic phenocryst(?)

F - altered zircon

G - unaltered zircon

A variety of accessory minerals have been identified including allanite, zircon, fluorite, rutile, calcite, and very occasional Fe-Ti oxides. Allanite occurs as small euhedral crystals which are characterized by a dark (often brown) core and a lighter yellow pleochroic rim - a combination which probably reflects metamictization (photomicrograph 14).

Two generations of zircons occur and will be referred to here and subsequently as types one and two. Type one occurs as large crystals up to .75 mm in diameter, that tend to be altered (possibly metamict) and corroded (photomicrograph 15). Type two form small (0.05 mm) euhedral and colourless crystals (photomicrograph 16).

Discussion of Hydrothermally Related Petrographic Relationships

Some of the petrographic relationships just documented reflect extensive hydrothermal activity which seems to play a major role in the development of alkaline/peralkaline granitic rocks. Extensive development of rim albitization/patch perthite (photomicrographs 4 and 5) reflects the presence of hydrothermal fluids circulating along grain boundaries and invading fractures and holes in previously formed crystals (Smith, 1974; Taylor et al., 1980). The association of small (acicular) crystals of aegirine-augite and/or arfvedsonite-riebeckite in association with rim albitization suggests that the fluids may have been albitic-acmitic in composition as suggested by Bowden and Turner (1974) (photomicrographs 5 and 17). However, the exact composition of the fluid phase(s) in peralkaline environments is still a matter of much speculation.

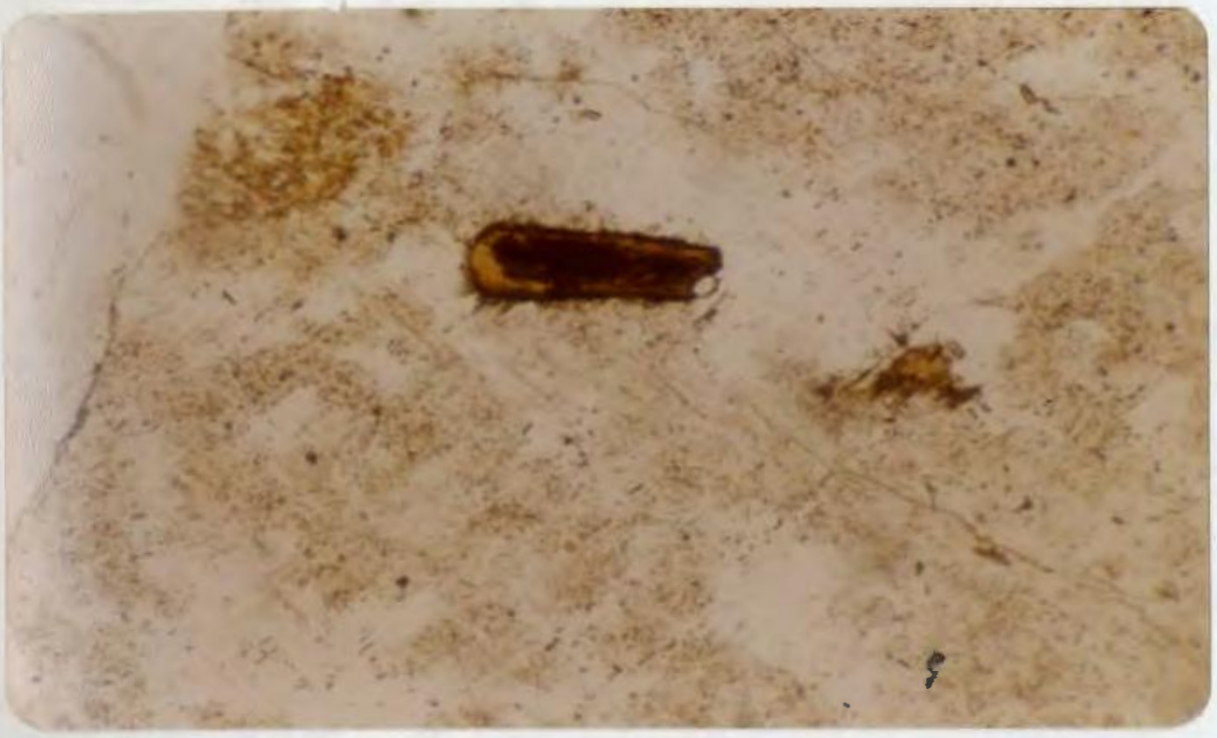

Photomicrograph 14: Allanite which has a dark brown opaque core and a lighter yellow rim (125 x) •

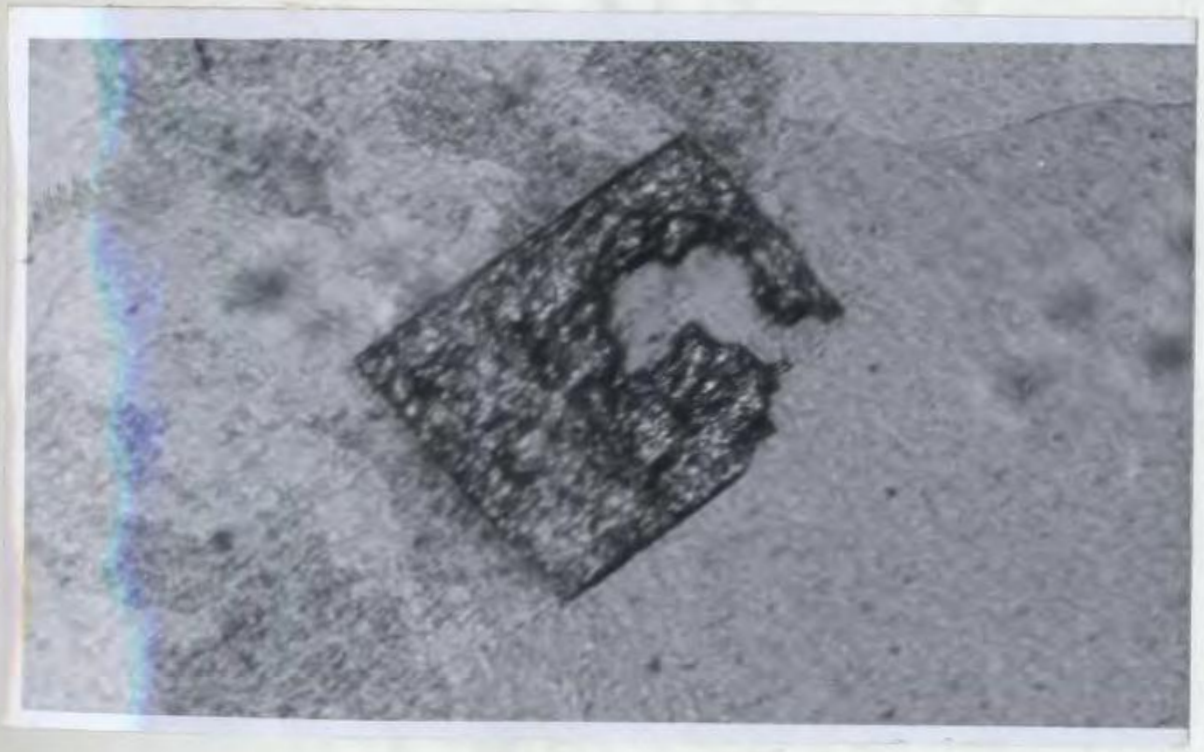

Photomicrograph 15: Type 1 zircon which is large, altered and corroded

Photomicrograph 16: Type 2 zircon which is small, unaltered and well formed (125 x)

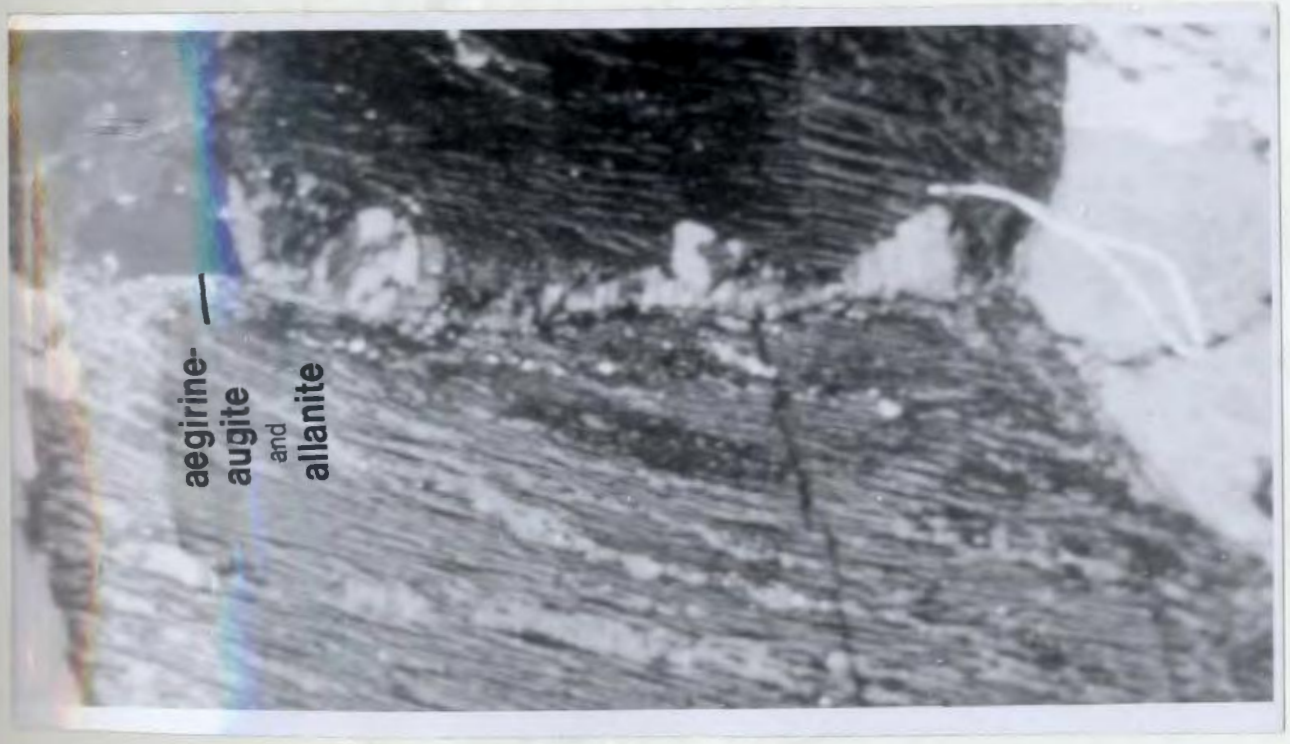


Photomicrograph 17: Arfvedsonite-riebeckite in association with rim albitization (40 x, crossed nicols)

Many of the crystal forms and associations of the mafic minerals support the hypothesis that hydrothermal fluids played a major role in their crystallization. The crystallization sequence of the mafic phases is difficult to interpret optically but generally it seems to be aegirine-augite → arfvedsonite-riebeckite → aenigmatite, followed by astrophyllite, allanite and other accessory minerals.

It has been demonstrated that aegirine-augite is stable under conditions necessary for igneous crystallization (Ernst, 1962; Bailey, 1969). Arfvedsonite-riebeckite oikocrysts and coronas could have been the product of a reaction between aegirine-augite and a residual peralkaline melt during primary crystallization as part of a discontinuous reaction series (Ernst, 1962; Bailey, 1969).

However, the oikocrysts and coronas appear to be the result of hydrothermal activity and experimental evidence indicates that the presence of riebeckite almost undoubtably reflects hydrothermal activity (Ernst, 1962). Acicular crystals of all the mafic components (including aenigmatite and astrophyllite) that nucleate on crystal boundaries, occur peppering the felsic phases or occur in association with albitization are almost certainly hydrothermal in origin. Similar occurrences of this type have been documented as hydrothermal growths by other workers (Hawley, 1937; Frohberg, 1939; Taylor et al., 1980).

Compositional zoning observed optically in aegirine-augite and arfvedsonite-riebeckite reflects chemical zonation. In both over-and undersaturated peralkaline rocks, pyroxenes and aenigmatite tend to

become enriched in Na, Ti, Fe and Mn from core to rim (Neumann, 1976; Larsen, 1977; Ferguson, 1978; Grapes et al., 1979; Taylor, pers. comm., 1980; Table 3). In amphiboles, Fe, Na, and Mn are enriched from core to rim but Ti, Al, Mg and Ca are depleted (Table 3; Ferguson, 1978; Grapes et al., 1979). It should be noted that in aenigmatite, total iron decreases from core to rim but $Fe_2O_3$ increases (Larsen, 1977; Grapes et al., 1979). It has been observed that when aegirine-augite and arfvedsonite-riebeckite occur in contact, elements such as Ca, Mg, Fe, Na, and Ti tend to be intermediate in concentration near the contact (Table 3).

Ferguson (1978) suggested that the early crystallization of microperthite results in a peralkaline residual, interstitial liquid rich in Na, Fe, Ti, and Mn from which aegirine-augite may crystallize followed by more sodium-rich aegirine (2nd generation), arfvedsonite and aenigmatite. The crystallization sequence is strongly related to volatile pressure, composition, temperature and oxygen fugacity. In particular, the crystallization of arfvedsonite is closely related to an increase in volatile pressure and bulk composition whereby the substitution of $F^-$ for $OH^-$ extends its stability to higher temperature ranges (Grapes et al., 1979). The dependence of the crystallization sequence on so many factors permits variation in the order of crystallization in various parts of the body because all these factors are not constant throughout the whole of a large body of magma.

Astrophyllite generally occurs in the form of acicular needles or clusters which appear to be hydrothermal. Astrophyllite analyses of MacDonald and Saunders (1973) show high concentrations of Zr, Zn, Nb, Rb, Cs and Ta, and REE. Assuming a hydrothermal origin, this indicates that the fluids associated with peralkaline magmas were rich in these and probably other trace elements. It has been found as well that many of the trace elements characteristic of peralkaline melts, especially Zr and Zn are especially concentrated in late crystallizing ferromagnesian minerals (Nicholls and Carmichael, 1969; MacDonald and Saunders, 1973).

The zircons described previously as types 1 and 2 have been the subject of a somewhat cursory microprobe study with no conclusive results. It will be tentatively suggested that the altered variety, type 1, may be slightly enriched in $Na_2O$ and Zn with a slight depletion of Y (Table 3) and may represent an early magmatic phase.

## NUIKLAVICK VOLCANICS

Petrographic examination of twenty-four samples of Nuiklavick volcanics (Fig. 4) allow subdivision of the unit into subvolcanic quartz-feldspar prophyry, extrusive rhyolite and tuff and volcanic breccia.

### Quartz-feldspar Porphyry

The quartz-feldspar porphyry samples are yellowish-red to grey-green in colour with a fine grained to aphanitic groundmass. Feldspar phenocrysts are more abundant than quartz, usually euhedral, pink, white

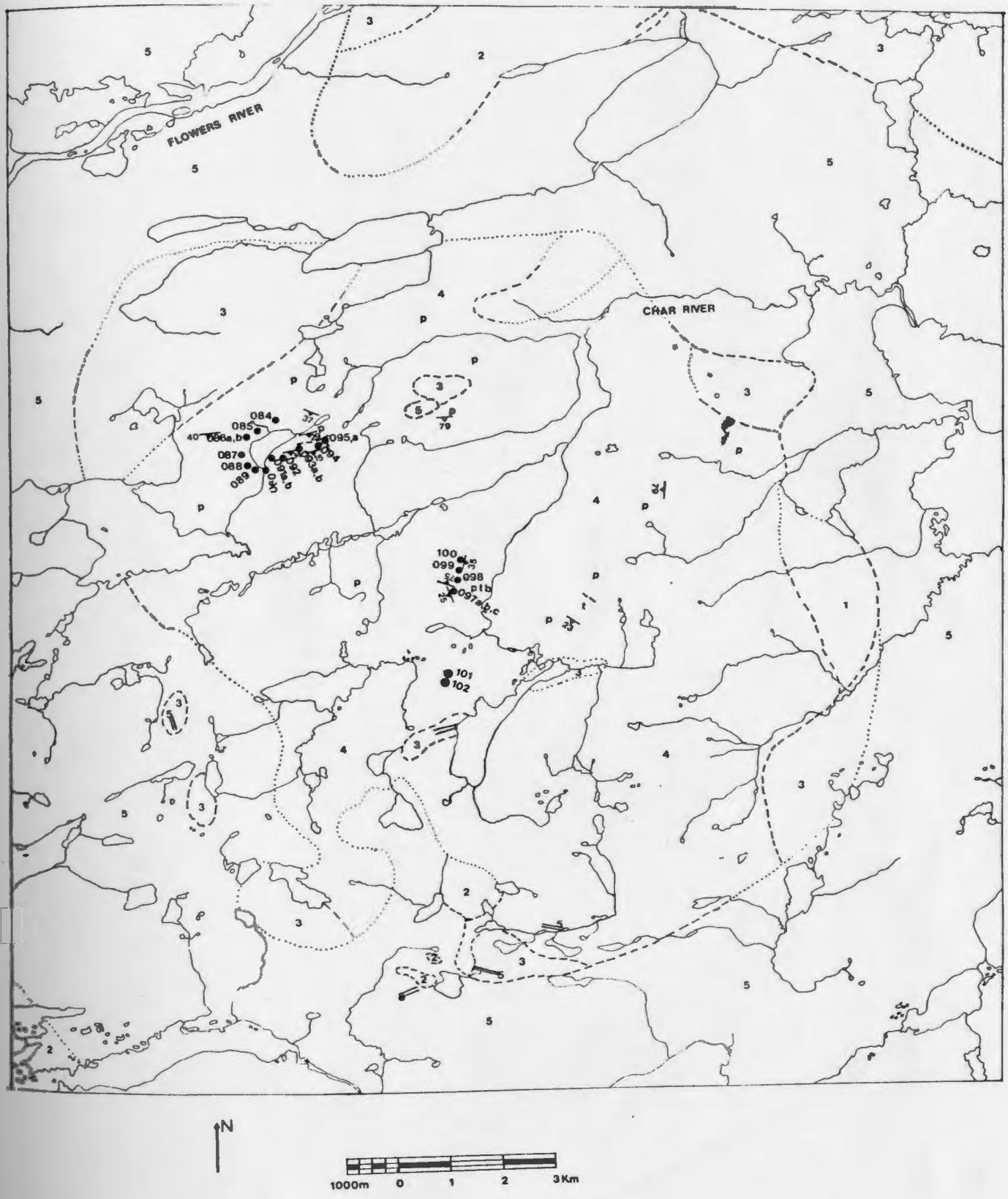


Fig. 4: Nuiklavick Volcanics Sample Map

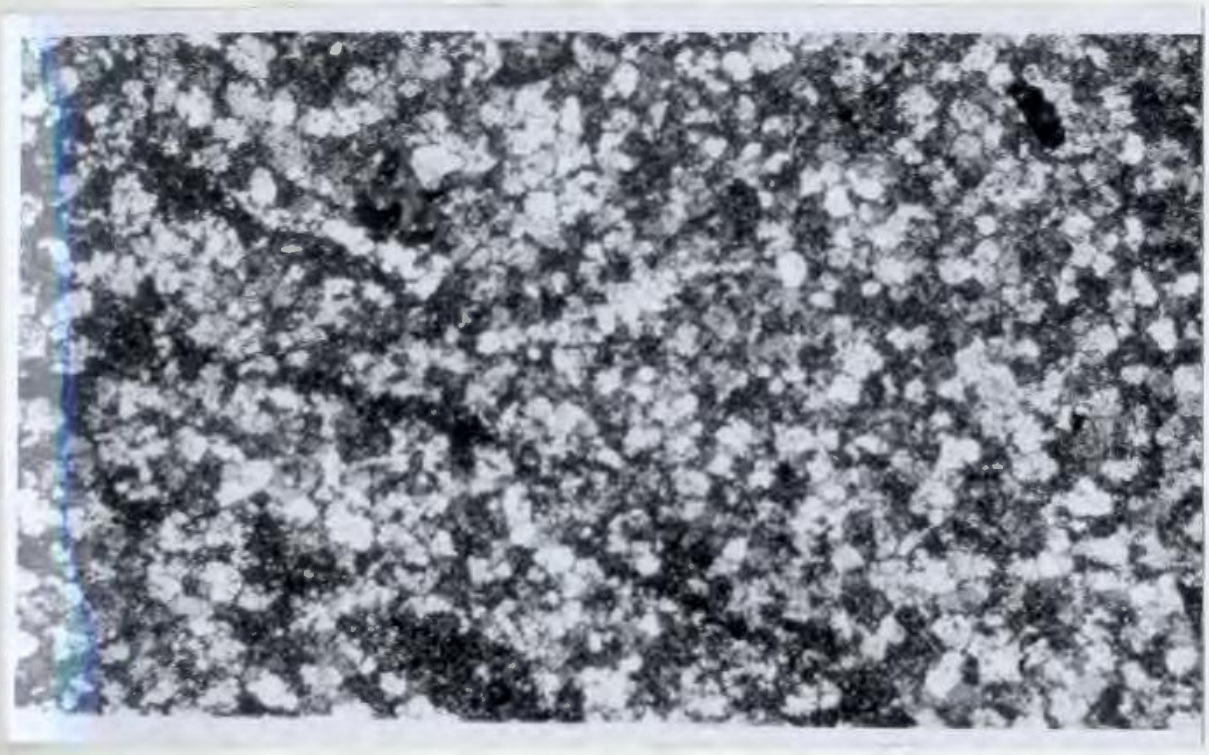

Photomicrograph 18: Felsitic texture: a microcrystalline mosaic of quartz and feldspar (40 x)

Photomicrograph 19: Altered perthite (pseudoperthite which has a sericitized host and lamellae that are composed of an iron-rich alteration material (40 x)

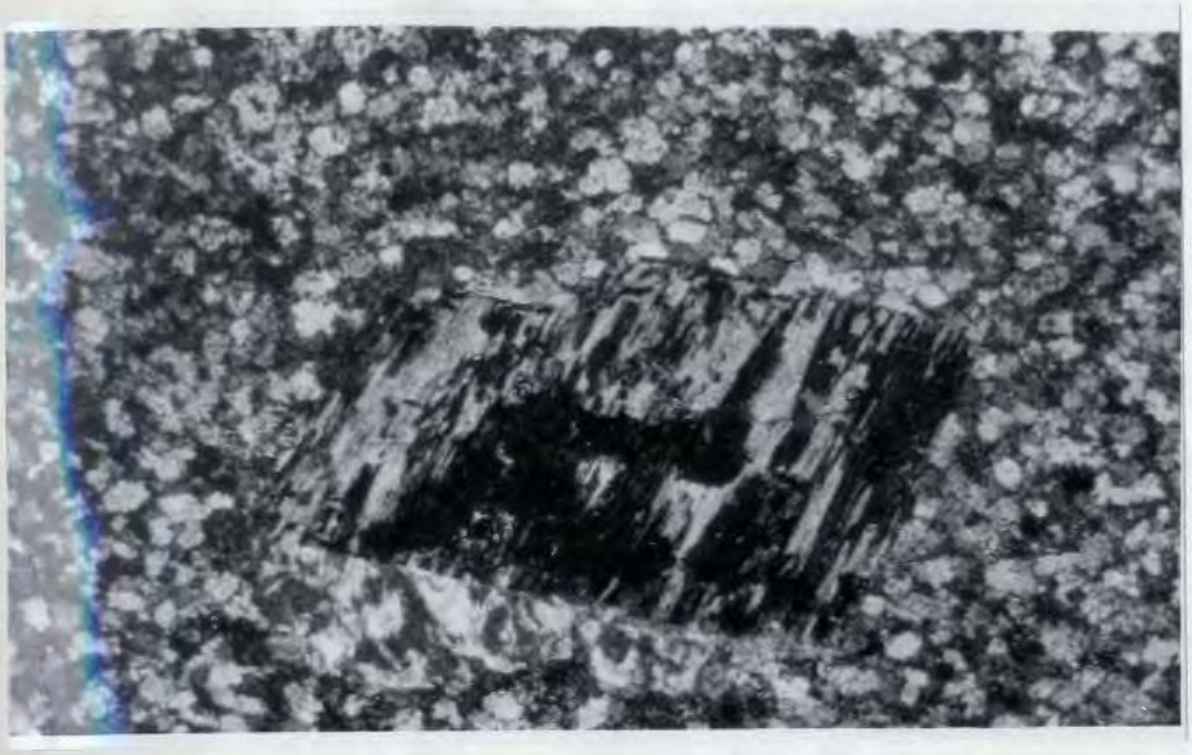

Photomicrograph 20: Relatively unaltered perthite phenocryst (40 x, crossed nicols)

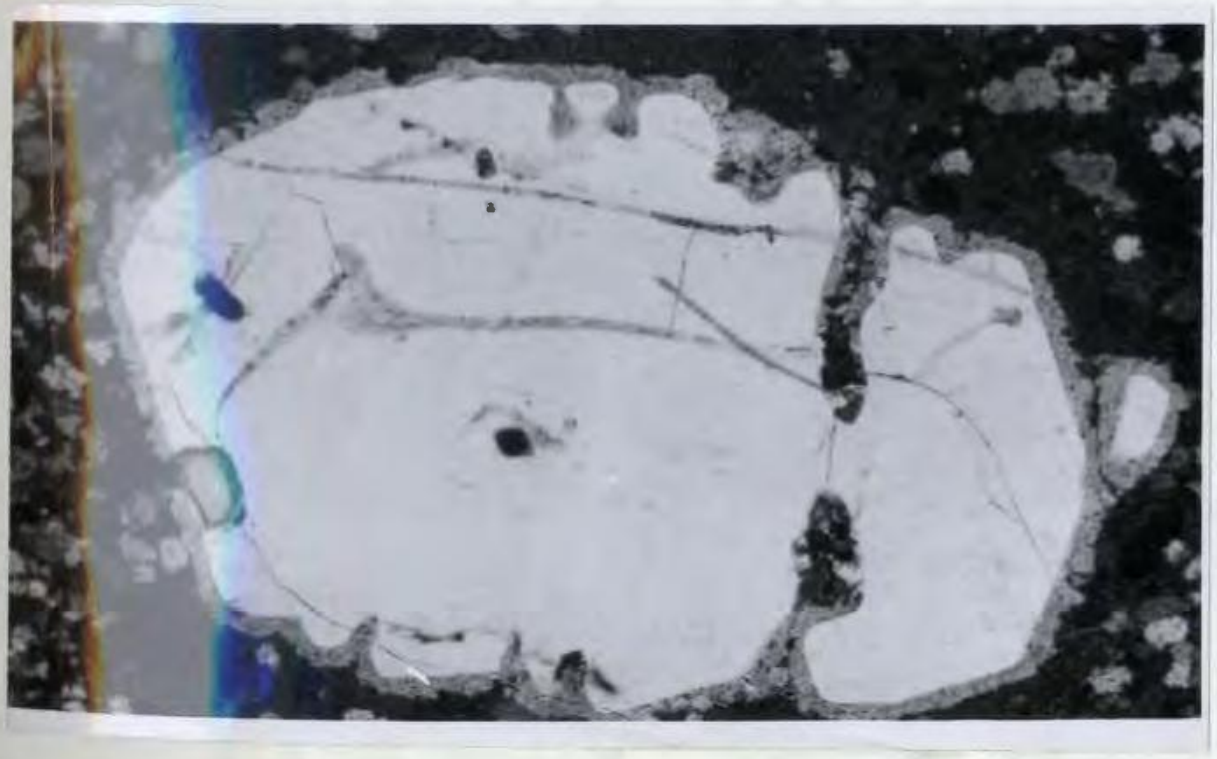

Photomicrograph 21: Quartz phenocryst with lacy overgrowth in optical continuity (40 x, crossed nicols)

or stained green-black in colour and are up to 4.5 mm in size (Plate 5). Green-black stained feldspar phenocrysts were mistaken for mafic phenocrysts in the field but thin section and microprobe study confirm their identification as altered perthite. The groundmass adjacent to stained phenocrysts may be altered resulting in patchy-mottled colouring (Plate 6). Quartz phenocrysts are euhedral, colourless and generally about 0.5 mm in size. Angular xenoliths of volcanic ash are occasionally present in a few of the samples examined (Plate 7).

Thin section study reveals a groundmass with an average grain size of 0.1 mm consisting of a microcrystalline mosaic of quartz and feldspar with a felsitic texture (photomicrograph 18).

Phenocrysts of quartz and feldspar ranging in size from 0.5mm to 4.5mm consisting of a microcrystalline mosaic of quartz and feldspar with a felsitic texture (photomicrograph 18).

Phenocrysts of quartz and feldspar ranging in size from 0.5 mm to 4.5 mm comprise up to 50% of the rock by volume. Euhedral-subhedral feldspar phenocrysts may very occasionally be orthoclase but perthite or pseudoperthite ( as defined previously) are much more predominant. Pseudoperthite phenocrysts have pale green lamellae but the host ranges from virtually unaltered to very sericitized or recrystallized (Plate 8, photomicrograph 19) whereas phenocrysts of perthite are relatively unaltered (photomicrograph 20). Electron microprobe analyses of the green lamallae in pseudoperthites give very low totals. They are depleted in silicon and sodium and enriched in aluminum, iron, magnesium, and titanium (Table 4).


Plate 5: Pink euhedral feldspar phenocrysts in quartz-feldspar porphyry


Plate 6: Patchy-mottled colouring due to leaching around feldspar phenocrysts in quartz-feldspar porphyry


Plate 7: Angular xenolith of volcanic ash in quartz-feldspar porphyry

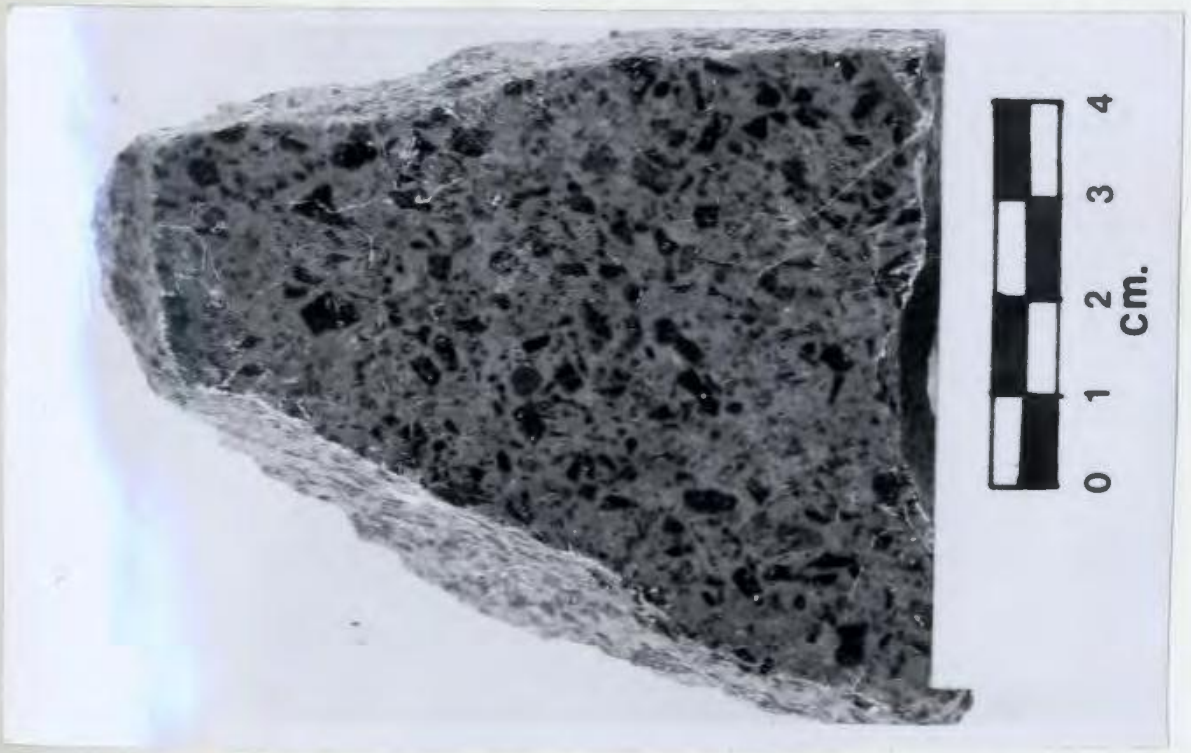


Plate 8: Pseudoperthite phenocrysts that are black to dark green in handspecimen

TABLE 4

ELECTRON MICROPROBE ANALYSES OF CONSTITUENTS OF QUARTZ-FELDSPAR PORPHYRY

| | A | B | C | D | E |
|---|---|---|---|---|---|
| $SiO_2$ | 60.96 | 65.78 | 47.93 | 25.35 | 76.5 |
| $Al_2O_3$ | 19.48 | 21.42 | 34.11 | 23.12 | 7.6 |
| FeO | 0.04 | 0.04 | 3.02 | 34.47 | 3.44 |
| MgO | - | 0.03 | 0.19 | 1.13 | 0.13 |
| CaO | - | 0.06 | 0.11 | 0.10 | 0.03 |
| $Na_2O$ | 0.31 | 9.30 | 0.32 | 0.04 | 0.34 |
| $K_2O$ | 14.09 | 0.44 | 8.14 | 2.13 | 2.47 |
| $TiO_2$ | .01 | - | 0.13 | 0.43 | 0.06 |
| MnO | - | - | 0.06 | 0.21 | 0.02 |
| TOTAL | 94.87 | 97.08 | 93.81 | 86.98 | 90.57 |

A - unaltered feldspar host (average of 2)

B - relatively unaltered feldspar lamallae (average of 2)

C - altered feldspar lamallae (average of 2)

D - green alteration material - relict mafic phenocryst (average of 3)

E - groundmass composition (average of 10)

Two possible reasons for low totals of which number 2 is considered most likely:

1. concentration of trace elements that were not analyzed
2. poor calibration on electron microprobe
3. the presence of volatiles for which there are no analyses

Quartz phenocrysts are euhedral-subhedral (may be embayed) dipyramidal pseudomorphs after beta quartz and are characterized by inclusions, bubble trains and lacy overgrowths in optical continuity (photomicrograph 21). Electron microprobe analyses of the lacy overgrowths on the quartz crystals show that they are also quartz.

Mafic phenocrysts are absent in the samples examined, however, Hill (pers. comm., 1980), has found a riebeckitic crystal in one sample. In the samples examined, there are some patches of green alteration material which may be pseudomorphs after mafic phenocrysts. Microprobe analyses indicate that these patches are enriched in iron, alumina, calcium, titania and manganese but depleted in silica and sodium similar to the lamellae of the pseudoperthites (Table 4).

Quartz and Quartz-feldspar Porphyritic Rhyolite and Lithic Tuff

Rhyolite and tuff samples are described together because of their extrusive nature and their petrographic similarities, the only major difference being the presence or absence of lithic fragments. They are classified according to the classification scheme compiled in Table 5.

The rhyolite and tuff samples have a black grey or dark red aphanitic groundmass, with phenocrysts or crystal fragments of quartz and feldspar in the rhyolite and lithic fragments in the tuff.

Lithic fragments are usually quartz-feldspar porphyry and tend to be angular but are often stretched and contorted and range in size from 1 to 9 cm (Plate 9). Crystal fragments/phenocrysts in both the rhyolite


Plate 9: Lithic fragments in tuff


Plate 10: Discontinuous flow banding in lithic tuff


Plate 11: Autobrecciated volcanic breccia

TABLE 5

CLASSIFICATION SCHEME MODIFIED AFTER
WENTWORTH AND WILLIAMS (1932) AND FISHER (1960)

| Fragment Size | Fragment Type | Indurated Aggregate |
|---|---|---|
| 32 mm | Bombs - plastic at time of eruption | Agglomerate |
| | Blocks - previously solidified volcanic rocks of cognate origin, broken angular forms | Volcanic Breccia |
| 32 mm-4 mm | Lapilli - essential, accidental or accessory ejecta, may be of any type of igneous, metamorphic or sedimentary rocks | Lapilli tuff |
| 4 mm-.25 mm | Coarse Ash:<br>Vitric - 75% glass | Coarse tuff:<br>Vitric tuff |
| | Crystal - 75% crystals | Crystal tuff |
| | Lithic - dominantly stony detritus | Lithic tuff |
| .25 mm | Fine ash: same types as above | Fine tuff: as above |

and tuff are predominantly quartz that has been broken and/or fractured. Subordinate perthite phenocrysts or crystal fragments occur in some samples. Crystal fragments/phenocrysts reach a maximum of 1 mm in size, but many are microcrystalline.

In thin section, the groundmass is microcrystalline to cryptocrystalline (much less than 0.05 mm - maximum 0.1 mm) making identification of its components nearly impossible. Phenocrysts/crystal fragments account for a maximum of 10% of the rock by volume. Quartz phenocrysts/crystal fragments (contain bubble trains but few other inclusions and have no lacy overgrowths) are more common than feldspar phenocrysts or crystal fragments (photomicrograph 22). Feldspar phenocrysts/crystal fragments are intratelluric crystals of microperthite that have been fractured and/or broken, often resorbed and very severely altered in a manner similar to the pseudoperthites described in the subvolcanic porphyry section (photomicrograph 23). As in the case of the porphyry, some rare patches of green alteration material may be pseudomorphs after mafic phenocrysts. Lithic fragments are of quartz-feldspar porphyry composition that often contain phenocrysts (photomicrograph 24) and of flow banded rhyolite.

Intense devitrification and recrystallization are ubiquitous but some textural evidence of an original glassy nature has survived. Some textural characteristics of extrusive rocks common to both the Nuiklavick volcanics and younger volcanics are listed below and accompanied by photomicrographs of each for comparison:

Photomicrograph 22: Quartz phenocryst/crystal fragment in an extrusive rock (40 x, crossed nicols)

Photomicrograph 23: Broken and fractured phenocrysts/crystal fragments in an extrusive rock (40 x, crossed nicols)

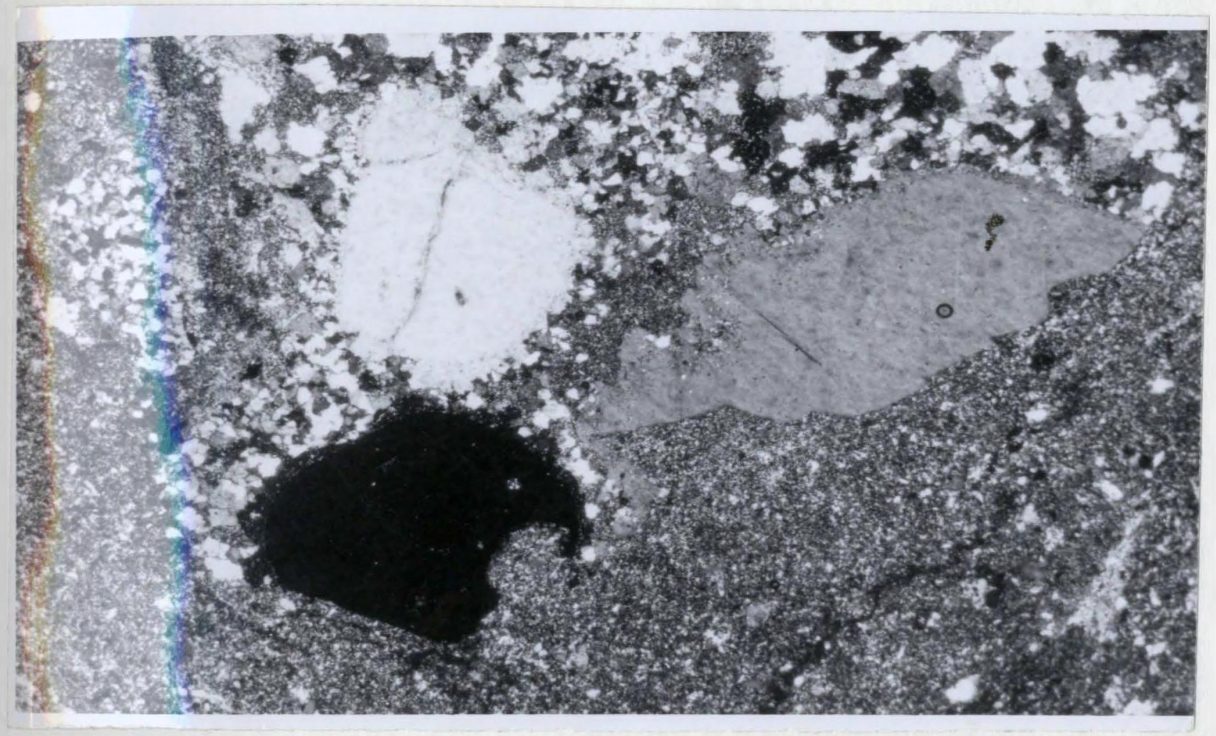

Photomicrograph 24: Fragment of porphyry in tuff (40 x, crossed nicols)

1. sperulites (photomicrographs 25 and 26)
2. eutaxitic structure (photomicrographs 27 and 28) (Martin, 1959)
3. lenticular inclusions (Plate 9, photomicrographs 29 and 30) (Martin, 1959)
4. intratelluric crystals (photomicrograph 24)
5. flow banding (Plate 10)
6. autobrecciation (Plate 11)

Volcanic Breccia

Volcanic breccia associated with the Nuiklavick volcanics is commonly light coloured (samples studied) with angular lithic fragments of porphyry, rhyolite or tuff that may reach 40 cm in diameter (Hill, 1979) (Plate 11). The volcanic breccia samples studies are very rich in phenocrysts/crystal fragments without much groundmass (photomicrograph 31). They appear to have suffered autobrecciation, because upon careful examination the fragments seem to fit together suggesting little mechanical disruption.

Discussion of Subvolcanic vs Extrusive Natures for Felsic Volcanic Sequences

As noted previously, it is not possible to determine a stratigraphic sequence for the Nuiklavick Volcanics; however, an attempt has been made to separate subvolcanic and extrusive rocks and to some extent pyroclastic from non-pyroclastic rhyolites.

Field evidence for some samples such as their massive nature, fine grain size and lack of internal structures, combined with petrographic evidence suggest that some of the samples collected may be shallow

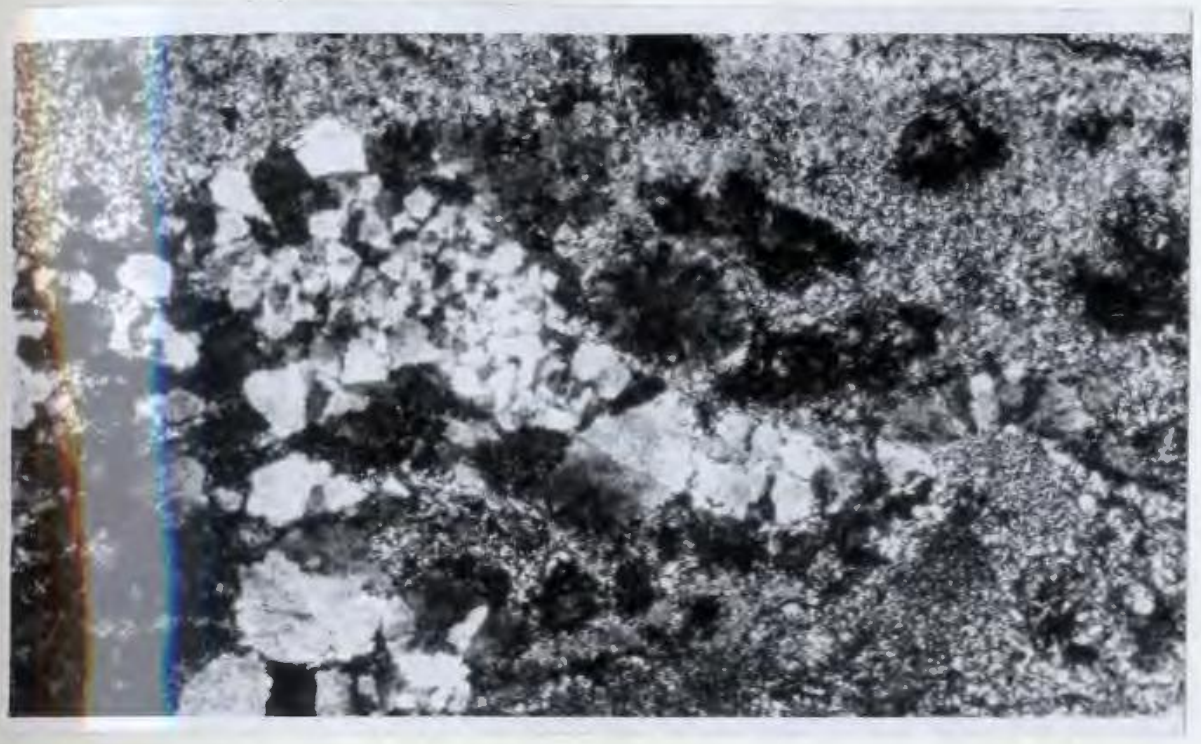

Photomicrograph 25: Spherulites in tuff from Davis Inlet (50 x, crossed nicols)

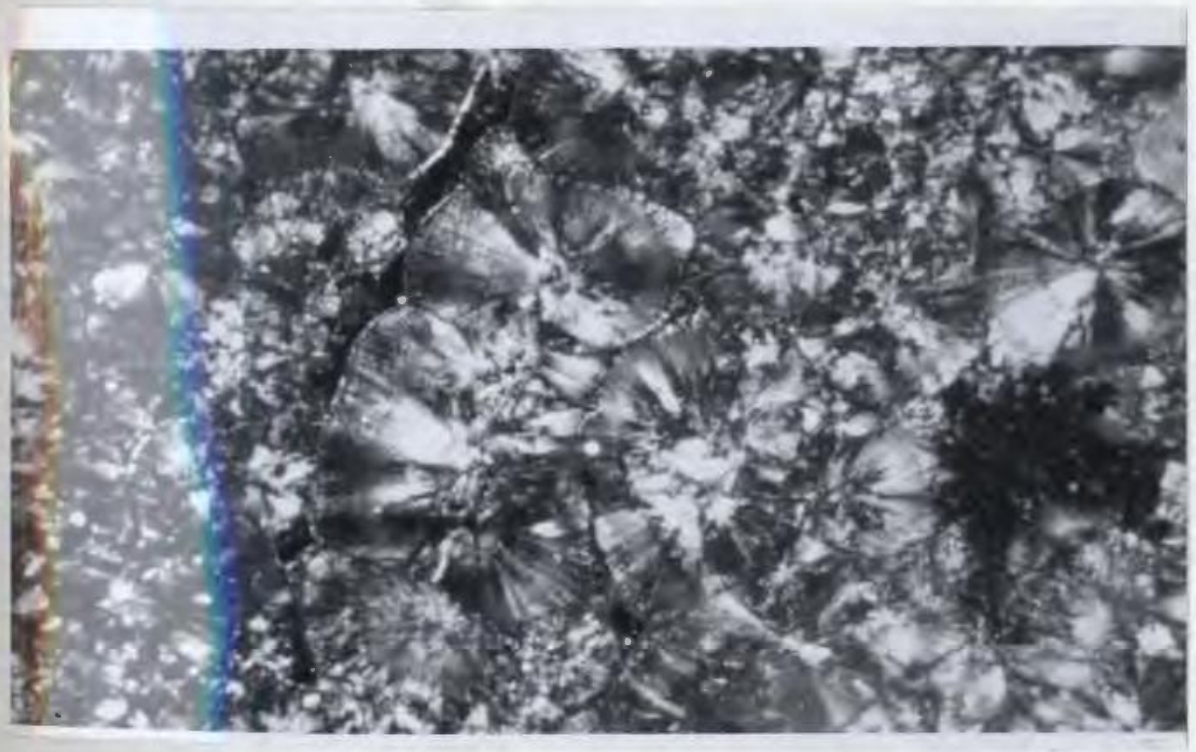

Photomicrograph 26: Spherulites in tuff from New Zealand (50 x, crossed nicols)

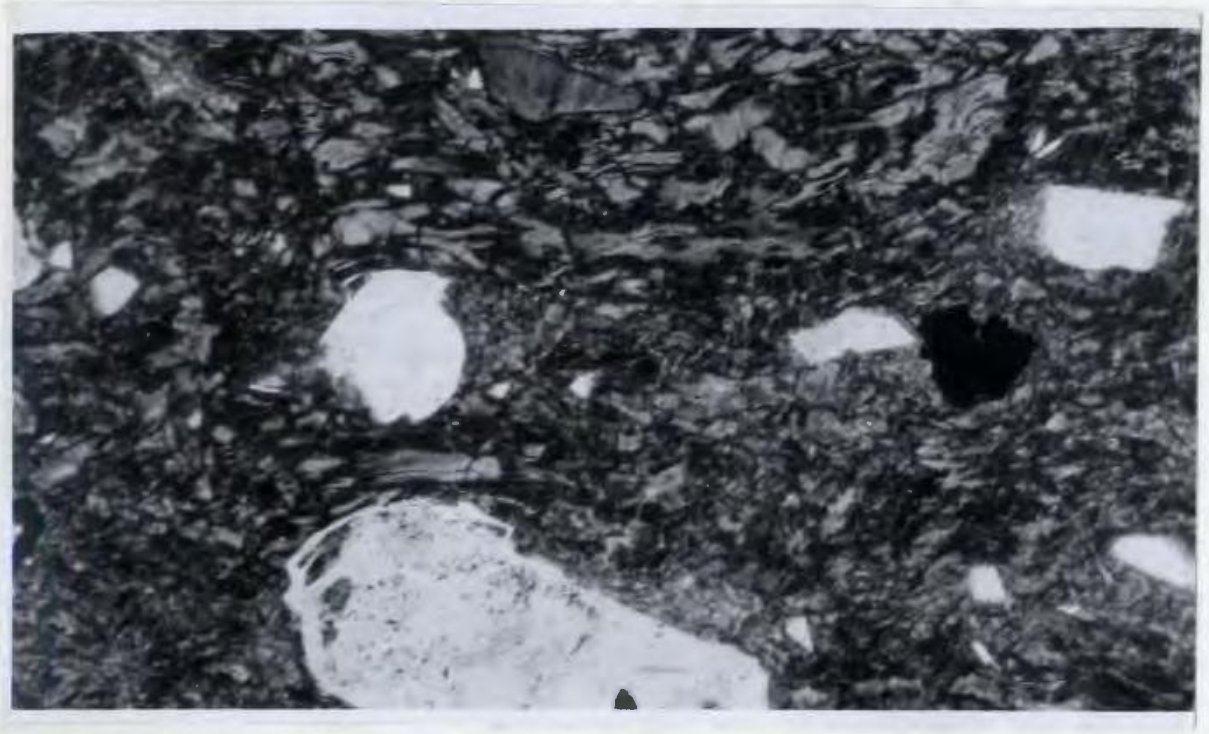

Photomicrograph 27: Eutaxitic structure in tuff from Davis Inlet (40 x)

Photomicrograph 28: Eutaxitic structure in the Bishop Tuff (40 x)

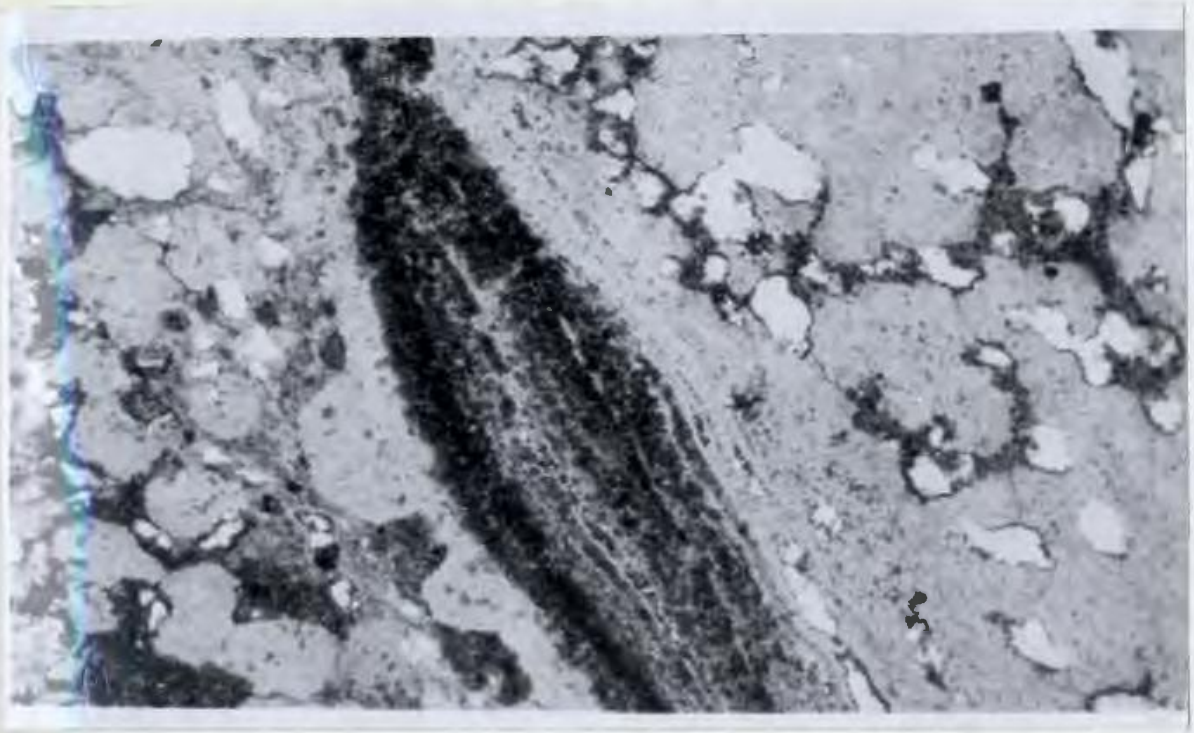

Photomicrograph 29: Lenticular inclusion, relict glass shard, in tuff from Davis inlet (40 x)

Photomicrograph 30: Lenticular inclusion, relict glass shard, in the Bishop Tuff (40 x)

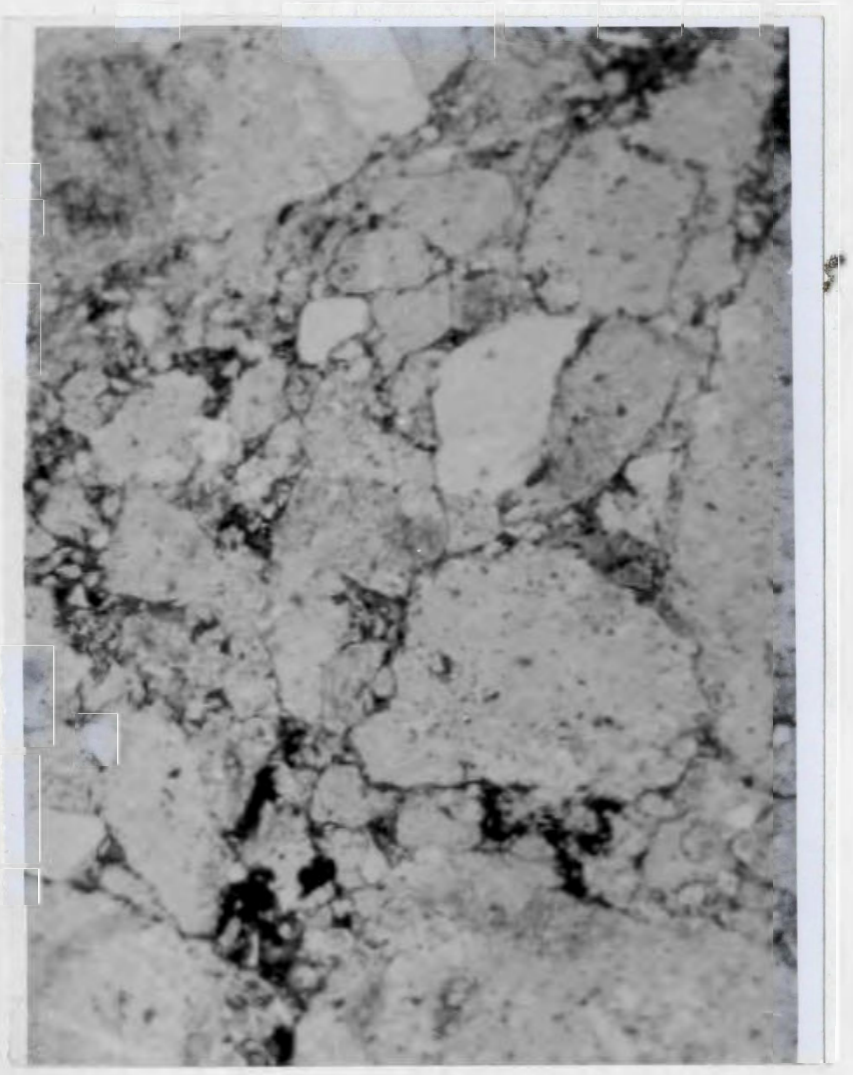

Photomicrograph 31: Volcanic breccia (40 x)

intrusives. These samples occur topographically below those which have extrusive characteristics. Although no contacts have been found, at one location (Fig. 4) porphyry occurs immediately below tuff, indicating an abrupt change and possible contact (Hill pers. comm., 1980).

Table 6 is a list of pertinent criteria used in this study to separate subvolcanic porphyry from extrusive volcanic rocks. Of the criteria used, the only one not applicable to the prophyry samples is the presence of a visibly granular groundmass. Although the groundmass in the porphyry is not visibly granular, those samples are distinctly more coarsely grained than the extrusive types.

Table 7 presents textural criteria suggestive of an extrusive nature plus useful evidence for distinguishing pyroclastic and non-pyroclastic types. In this work the separation of the extrusive rocks into pyroclastic and non-pyroclastic varieties is considered less important than separation of subvolcanic and extrusive rocks. The descriptions of individual samples in Appendix A provides a compilation of all the points in Tables 6 and 7 relative to the samples used.

## SUMMARY

Petrographically the clinopyroxene-fayalite granite and the arfvedsonite-riebeckite granite are quite different. The arfvedsonite-riebeckite granite reflects a more sodium-and less iron-rich environment than the clinopyroxene-fayalite granite. The presence of such sodic

TABLE 6

CRITERIA FOR DISTINGUISHING BETWEEN RHYOLITIC FLOWS AND SUBVOLCANIC PORPHYRY COMPILED FROM MOOREHOUSE (1959) AND HATCH ET AL. (1972)

| Rhyolitic Flow | Subvolcanic Porphyry |
|---|---|
| 1. Light coloured except where glassy | 1. Abundant phenocrysts |
| 2. may be porphyritic | 2. matrix visibly granular in handspeciman and a microcrystalline mosaic of quartz and feldspar in thin section |
| 3. often flow banded<br>i.e. colour banded alternating glassy and stony stripes, streams of vesicles, crystallites or phenocrysts, lines of spherulites | 3. quartz phenocrysts are less abundant and smaller than feldspar |
| 4. the presence of vesicles or amydules | 4. quartz phenocrysts are more corroded and embayed than feldspar |
| 5. perlitic fractures | 5. quartz phenocrysts are bipyrimidal, dihexagonal |
| 6. lithophysae | 6. secondary enlargement of quartz phenocrysts by lacy rims in optical continuity |

TABLE 7

TEXTURAL VARIATIONS BETWEEN PYROCLASTIC AND NON-PYROCLASTIC EXTRUSIVE FELSIC VOLCANICS

(Compiled from Martin, 1959; Ross and Smith, 1961; Hatch et al., 1972; Lillijequist and Svensen, 1974)

| Textural Characteristic | Non-pyroclastic Flow | Pyroclastic Rocks Tuff/Ignimbrite |
|---|---|---|
| Flow Banding continuous discontinous | + | x |
| Alternating and fine-grained bands representing vitreous and non-vitreous layers | + (91a) | |
| Spherulites | + | x |
| Autobrecciation | + | x |
| Eutaxitic | | x |
| Lenticular Structures | + | x |

+ indicates the presence of the specific textural feature in non-pyroclastic flow

x indicates its presence in pyroclastic rocks

minerals as arfvedsonite-riebeckite and aegirine augite are evidence of the peralkalic affinity of the arfvedsonite-riebeckite granite. Some textural features are common to both, i.e. similar types of associations of mafic minerals and the occurrence of mafic minerals with coronas and oikocrysts (photomicrographs 2, 3, 6 and 10) suggesting that similar processes may be involved in the development of both the alkaline and the peralkaline magmas. The most important petrographic difference between the two granites is that the various hydrothermally formed minerals are better developed and more common in the peralkaline arfvedsonite-riebeckite granite. The crystallization and assemblage of late stage, hydrothermal minerals provides conclusive evidence of the presence and activity of fluids and volatiles that are considered instrumental in the evolution of peralkaline (alkaline) rocks in general.

The Nuiklavick volcanics can be separated into subvolcanic and extrusive subunits on the basis of petrography through relict textural features. The altered feldspar phenocrysts have probably been affected by fluids similar to those present during the crystallization of the arfvedsonite-riebeckite granite as evidenced by the chemical compositions of the alteration products in the porphyry/volcanics. Separation of the extrusive rocks into pyroclastic and non-pyroclastic varieties is much more difficult because of post eruptive alteration and devitrification, etc., but tentative classification of individual samples accompanies the descriptions in Appendix 1.

# CHAPTER 3
# GEOCHEMISTRY

Approximately fourty samples of clinopyroxene-fayalite granite (non-peralkaline), arfvedsonite-riebeckite granite (peralkaline) and Nuiklavick volcanics have been analyzed for major, minor and trace (including the rare earth) elements. Geochemical methods, results, and supplemental diagrams are located in Appendices B, C and D. This chapter will consist of a description of observed geochemical trends and a comparison of trends between the various rock types.

## CLINOPYROXENE-FAYALITE GRANITE

### Major Element Geochemistry

The clinopyroxene-fayalite granite is slightly alkaline with fayalite, iron-sodium clinopyroxene and amphibole a combination which reflects high concentrations of sodium, potassium, calcium and iron. Relative to an average granite composition, it is enriched in calcium, potassium, sodium, titanium, iron and manganese and slightly depleted in aluminum and magnesium (Fig. 5).

CIPW normative analyses (Appendix C) show a slightly alkaline but not peralkaline nature, i.e. they have no normative acmite or sodium metasilicate and have agpaitic indices significantly less than one (.68 - .84). On a Q-AB-Or normative diagram all except two samples fall between the liquidus minimum at $PH_2O$= 1000 $Kg/CM^3$ for the system $SiO_2$ $NaAlSi_3O_8$ - $KAlSi_3O_8$ and liquidus minima representing the addition of

Fig. 5 and 15 - Major and trace element enrichment factors for clinopyroxene-fayalite granite and arfvedsonite-riebeckite granite relative to an average granite composite. On this and all subsequent diagrams an average of 5 clinopyroxene-fayalite granite analyses and 14 arfvedsonite-riebeckite granite analyses were used. The average granite composition was taken from Roslor and Lange (1972) - major elements; and Krauskopf (1967) - trace elements.

Clinopyroxene-fayalite granite (- - -)
Arfvedsonite-riebeckite granite (——)

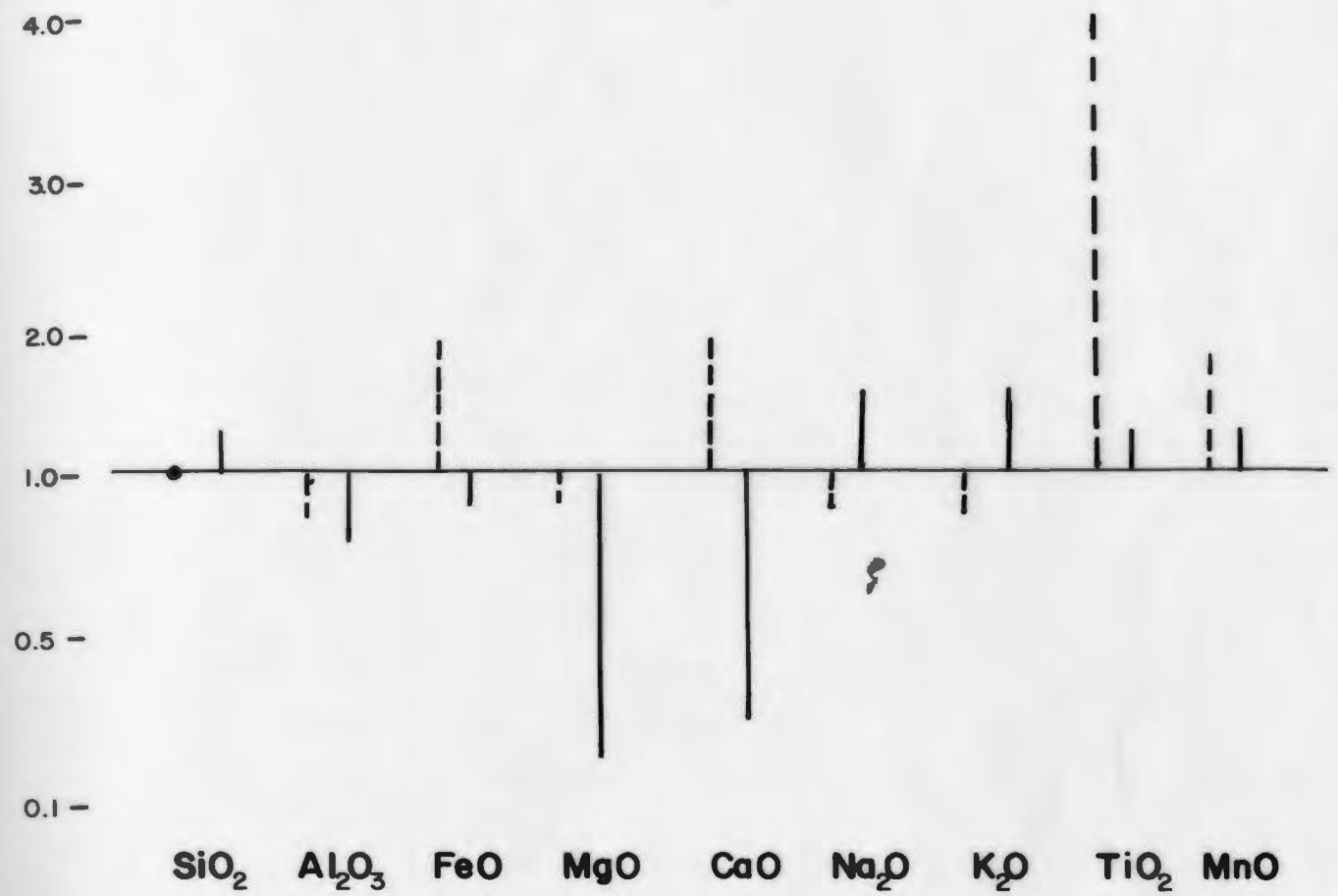
4.0
3.0
2.0
1.0
0.5
0.1
SiO2
Al2O3
FeO
MgO
CaO
Na2O
K2O
TiO2
MnO

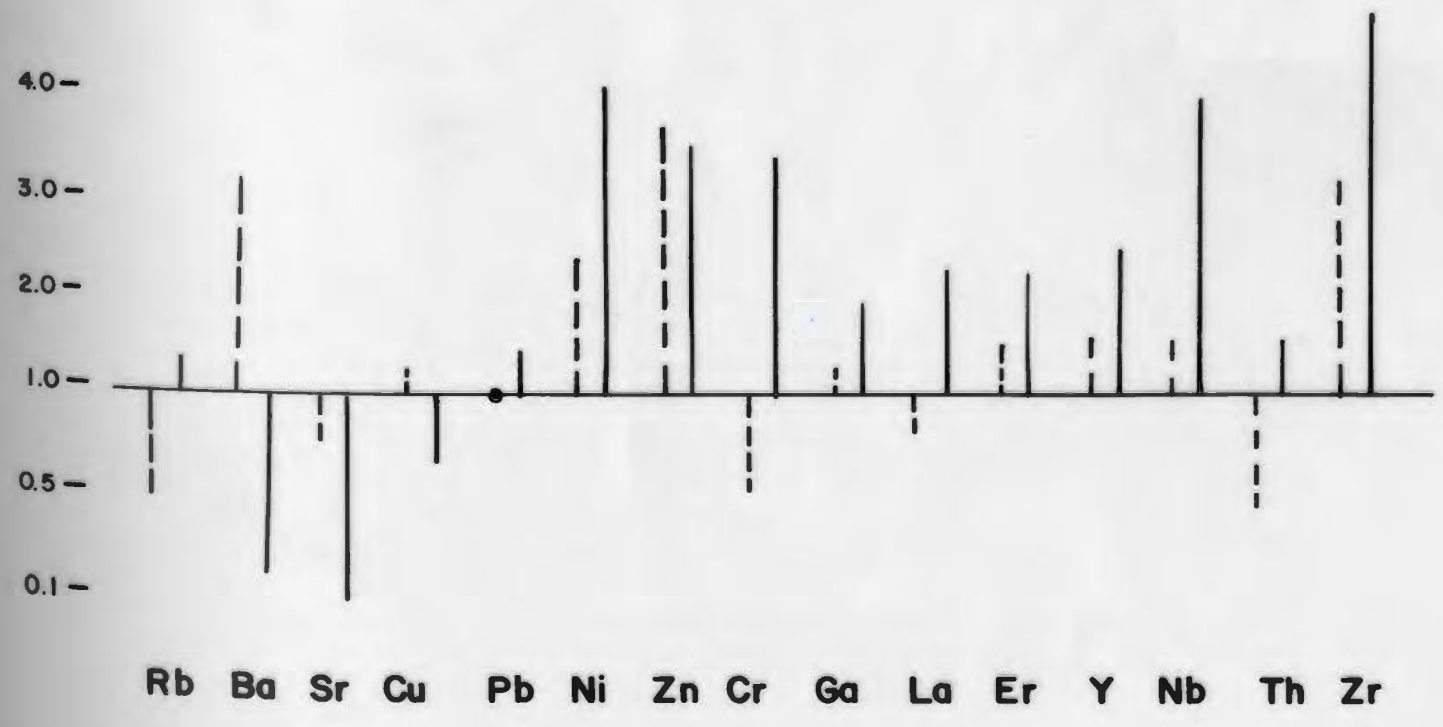
4.0
3.0
2.0
1.0
0.5
0.1
Rb
Ba
Sr
Cu
Pb
Ni
Zn
Cr
Ga
La
Er
Y
Nb
Th
Zr

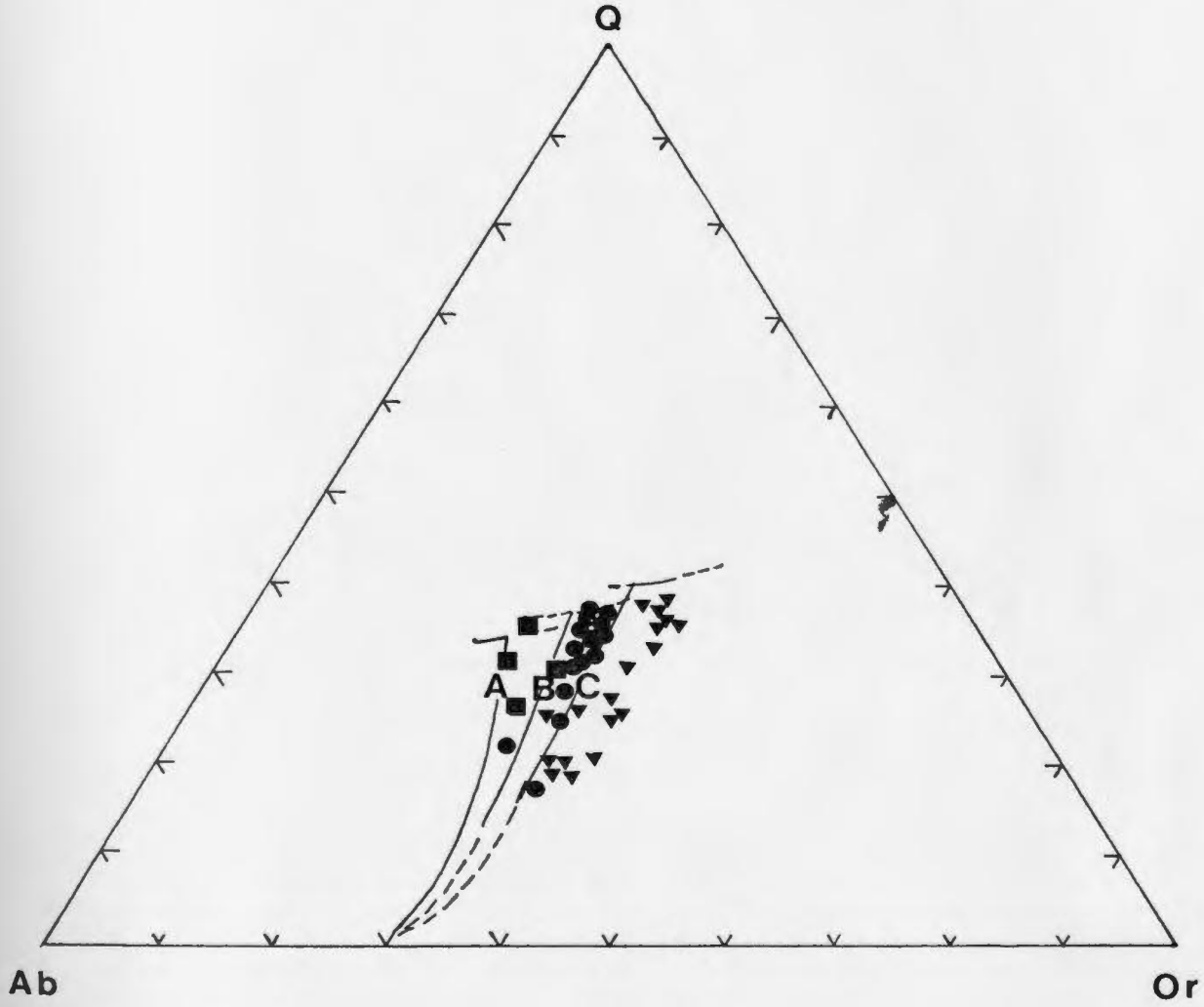


Fig. 6: **Q-Ab-Or Normative Diagram.** Composite diagram showing the isobaric projections of the thermal valleys, their intersections with the quartz-feldspar field boundaries, and the composition of the liquidus minimum for (A) the system $NaAlSi_3O_8$-$KAlSi_3O_8$-$SiO_2$-$H_2O$; (B) the 4.5% ac 4.5% ns plane; (C) the 8.3% ac 8.3% ns plane (Carmichaels and MacKenzie, 1963).

Symbols:
- ▼ 15 analyzed pantellerites from Pantellera (Carmichaels and MacKenzie, 1963)
- ■ clinopyroxene-fayalite granite
- ● arfvedsonite-riebeckite granite

Figs. 7-14. Harker diagrams for the arfvedsonite-riebeckite granite and the clinopyroxene-fayalite granite.

■ - Clinopyroxene-fayalite granite

● - Arfvedsonite-riebeckite granite

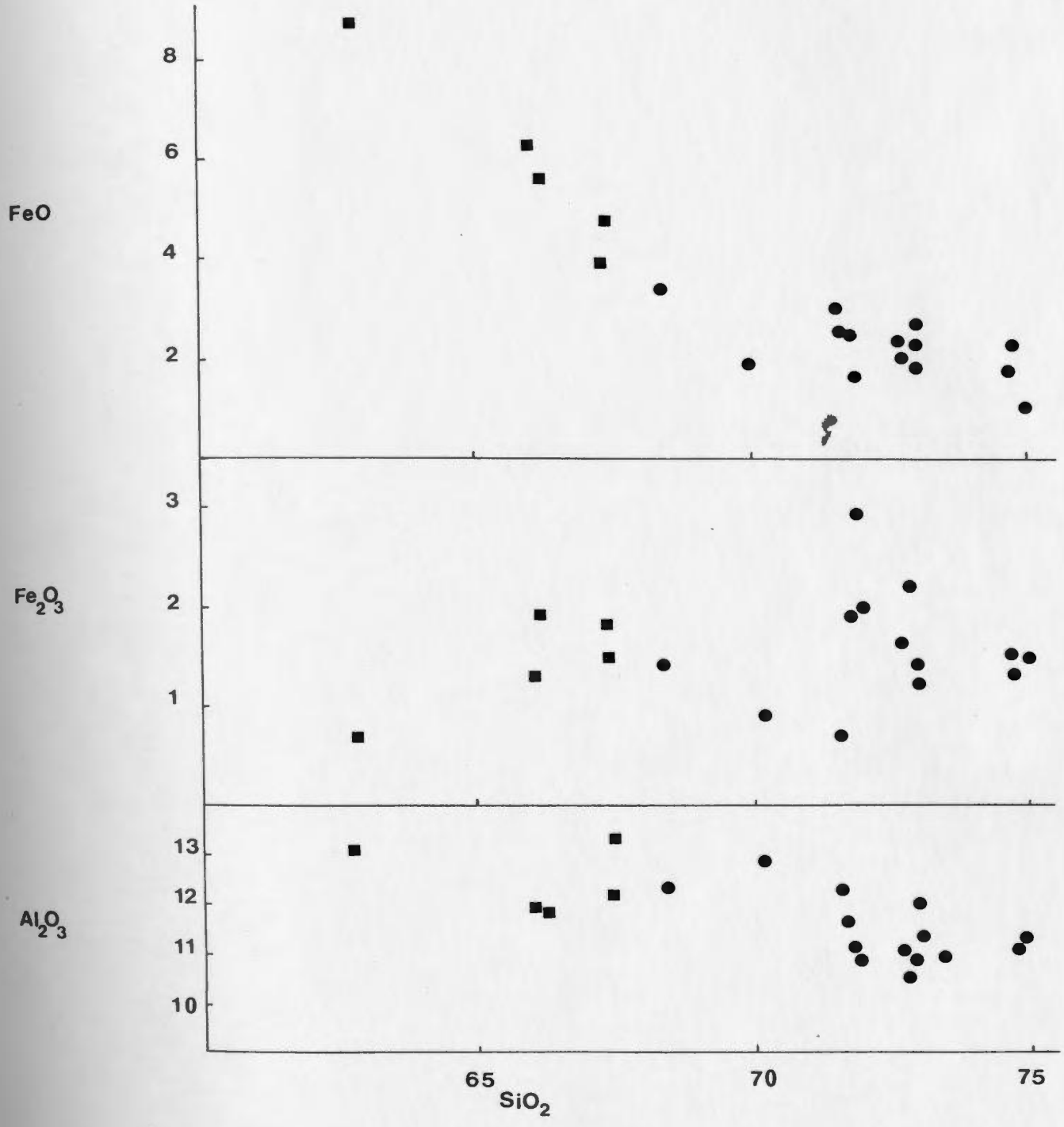


Figs.7-9: Harker diagrams for clinopyroxene-fayalite granite and arfvedsonite-riebeckite granite.

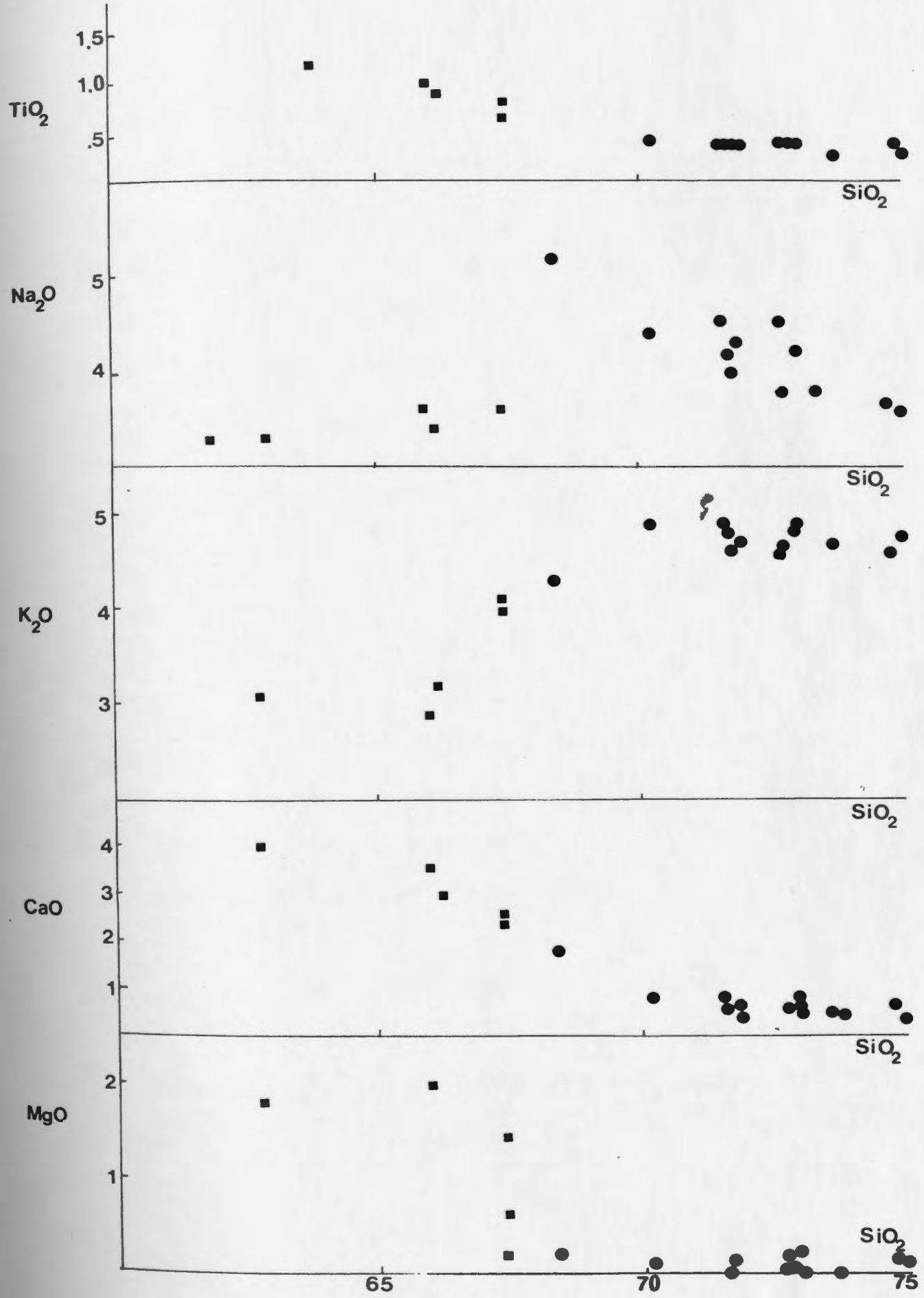
1.5
1.0
.5
TiO2
SiO2
5
4
Na2O
SiO2
5
4
3
K2O
SiO2
4
3
2
1
CaO
SiO2
2
1
MgO
SiO2
65
70
75

4.5% acmite and 4.5% sodium metasilicate (Charmichael and MacKenzie, 1963). Two samples 064b and 057 fall on the liquidus minimum for the system $SiO_2$ - $NaAlSi_3O_5$ - $KAlSi_3O_8$, 064b is very near the eutectic. Because only a small number of samples were collected, there are not sufficient data to display any well developed trends.

Harker diagrams (Fig. 7-14) are used to display trends of major/minor elements using silica as a differentiation index. The trends are quite normal and are unlike those of the peralkaline arfvedsonite-riebeckite granite.

Trace Element Geochemistry

Trace element trends for the clinopyroxene-fayalite granite are not well developed because of the small number of analyses but some observations can be made. The clinopyroxene-fayalite granite is enriched in Zr, Zn, Ni, Cr, Ba and depleted in Th and Rb (Sr, slightly depleted) relative to an average granite composition (Fig. 17). On Harker type correlation diagrams comparing those residual elements characteristic of peralkaline rocks, the clinopyroxene-fayalite granite defines its own field and trends unrelated to the arfvedsonite-riebeckite granite. The clinopyroxene-fayalite granite trends with Zr, Zn, Nb, Y, Th and Pb tend to have rather flat or negative slopes unlike the arfvedsonite-reibeckite granite which generally has positive, steep slopes (Figs. 15-18). K/Rb ratios for the clinopyroxene-fayalite granite are much higher than the peralkaline granite and fall near the normal field for granites (Shaw, 1968; Fig. 19).

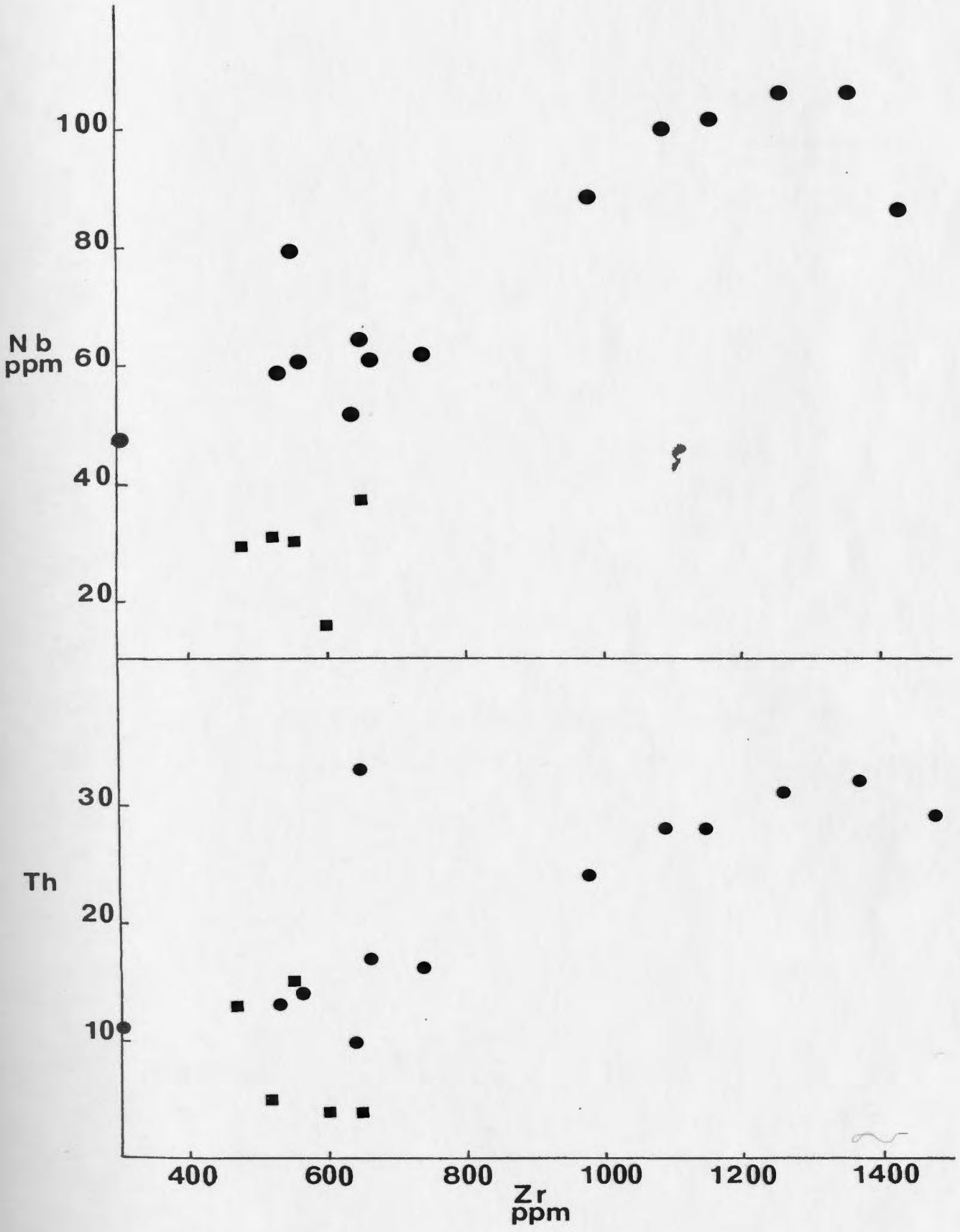


Fig. 16: Th vs. Zr and Nb vs. Zr for the clinopyroxene-fayalite granite and the arfvedsonite-riebeckite granite.

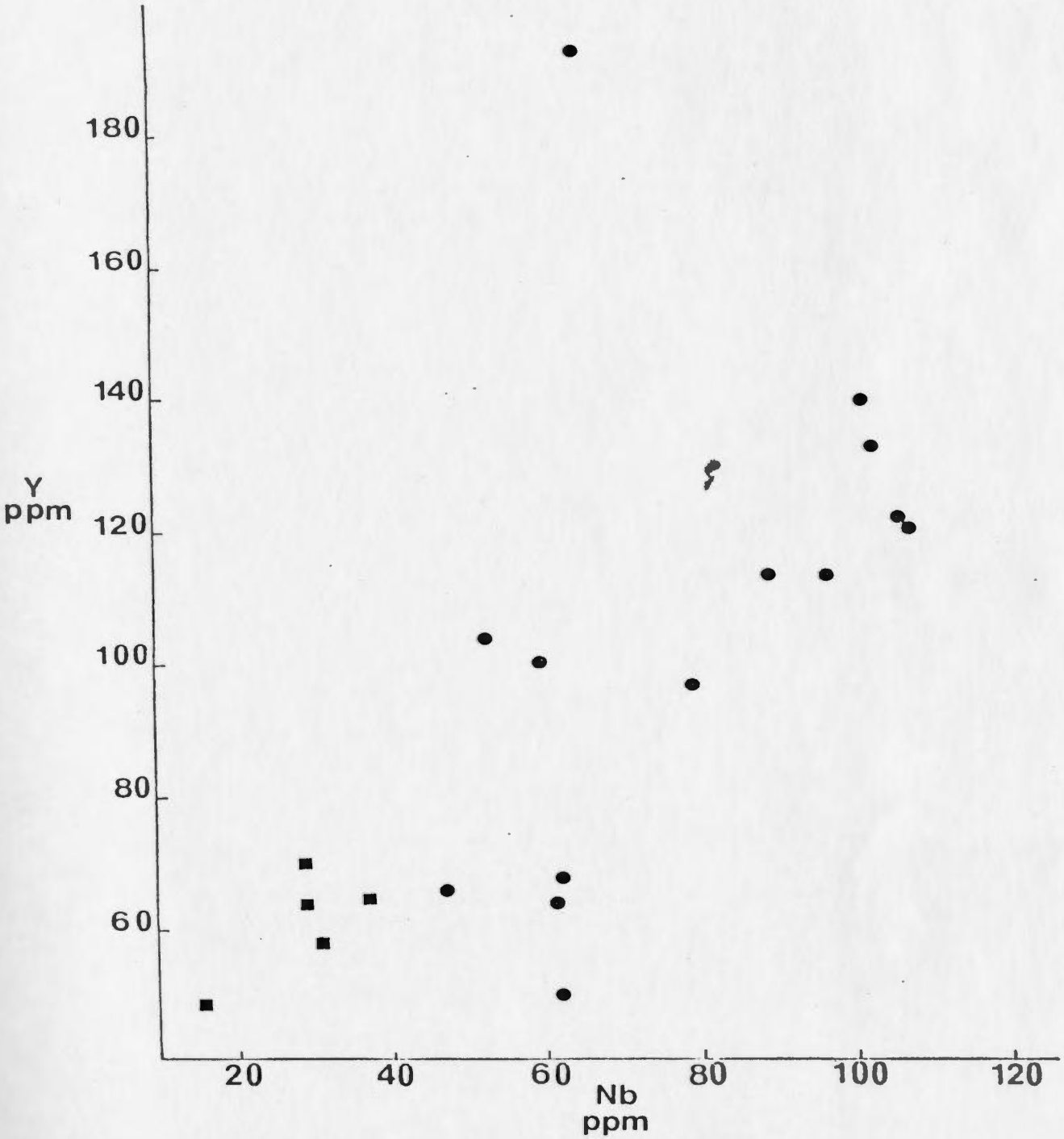


Fig. 17: Y vs. Nb for the clinopyroxene-fayalite granite and the arfvedsonite riebeckite granite.

Fig. 19. K/Rb vs Nb for the clinopyroxene-fayalite granite and the arfvedsonite-riebeckite granite

Fig. 18. Nb vs Zn for the clinopyroxene-fayalite granite and the arfvedsonite-riebeckite granite

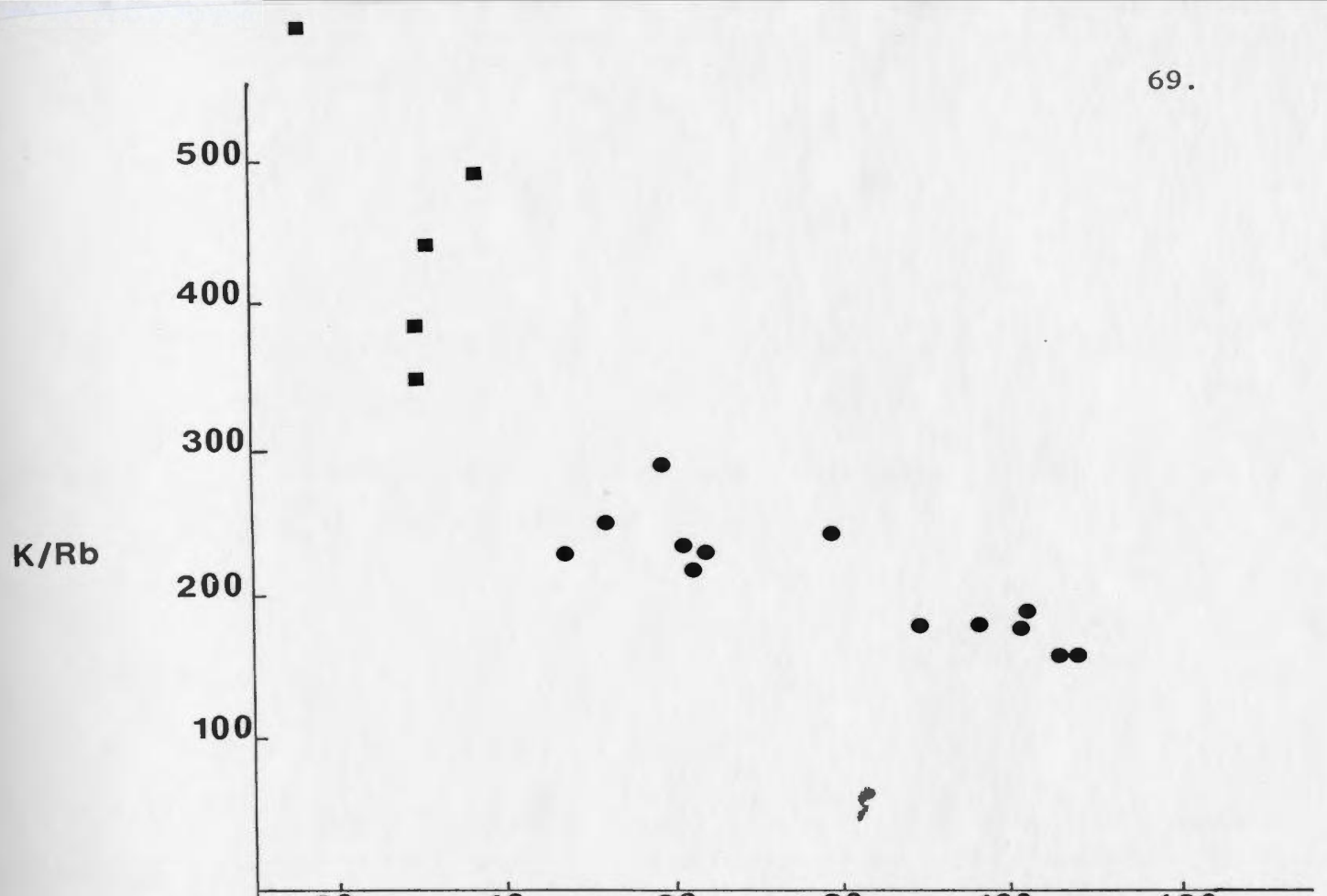
K/Rb
500
400
300
200
100
20
40
60
80
100
120
Nb
ppm

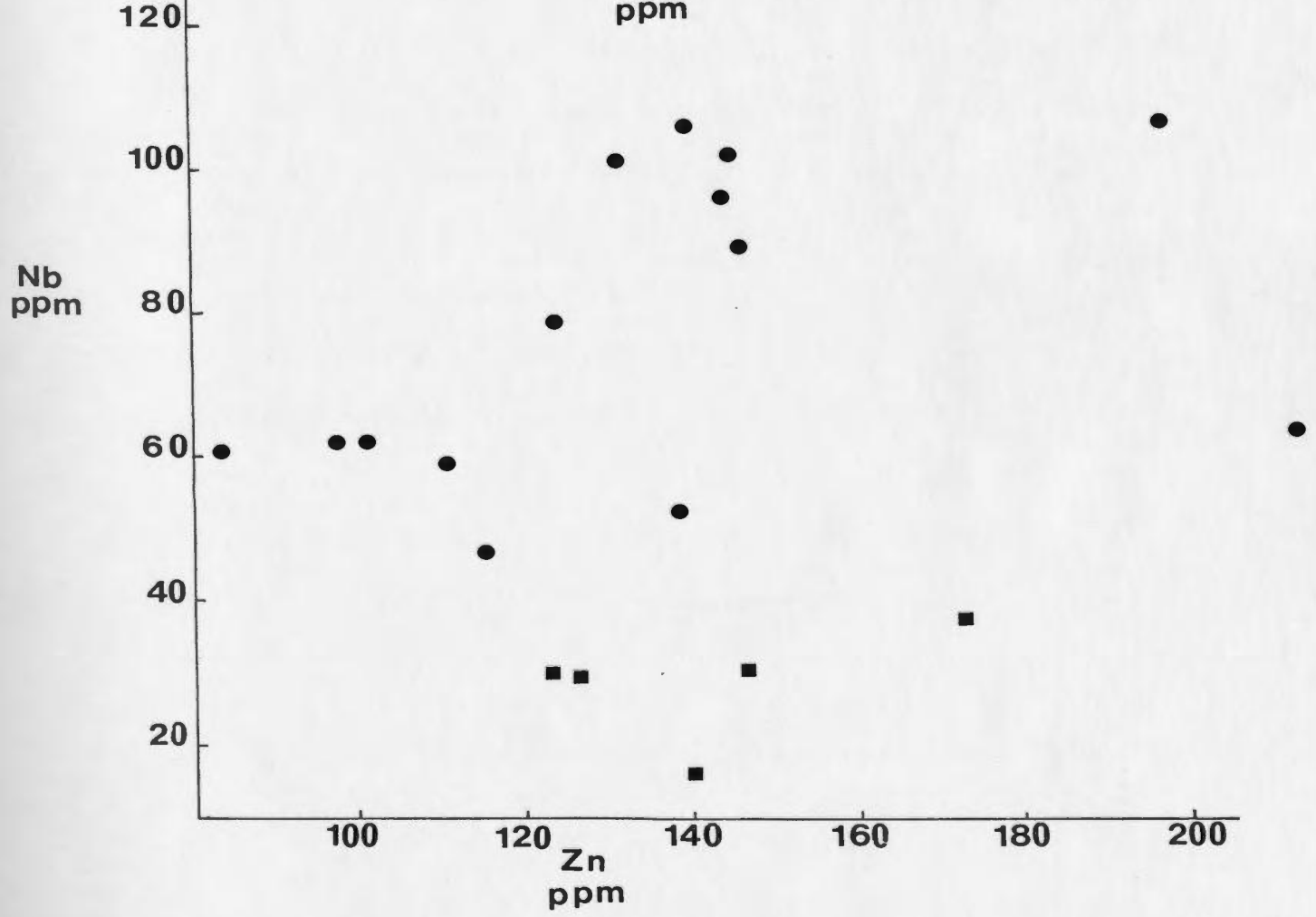
Nb
ppm
120
100
80
60
40
20
100
120
140
160
180
200
Zn
ppm

Rare Earth Element Geochemistry

Rare earth element concentrations for the clinopyroxene-fayalite granite are similar to those generally found in granitic rocks with total rare earth concentrations of 231-399 ppm (Fig. 20) (Haskin and Schmidt, 1967). The rare earth element pattern resembles that of a composite of average continental crust (Shaw et al., 1976; Fig. 21).

ARFVEDSONITE-RIEBECKITE GRANITE

Major Element Geochemistry

The peralkalinity of the arfvedsonite-riebeckite granite, documented on the basis of petrography, is substantiated by major, minor and trace (including REE) element geochemical evidence. The arfvedsonite-riebeckite granite is slightly enriched in silica, sodium, potassium and depleted in aluminum, magnesium, iron and calcium relative to an average granitic composition or the clinopyroxene-fayalite granite (Fig. 5 and 22).

CIPW normative analyses (Appendix C) establish the peralkaline affinity by the presence of normative acmite and in two samples sodium metasilicate. In addition all have agpaitic indices very near to or greater than one (.981-1.11). The three samples which do not contain normative acmite or sodium metasilicate have agpaitic indices of .98 (068, 071) and .999 (072).

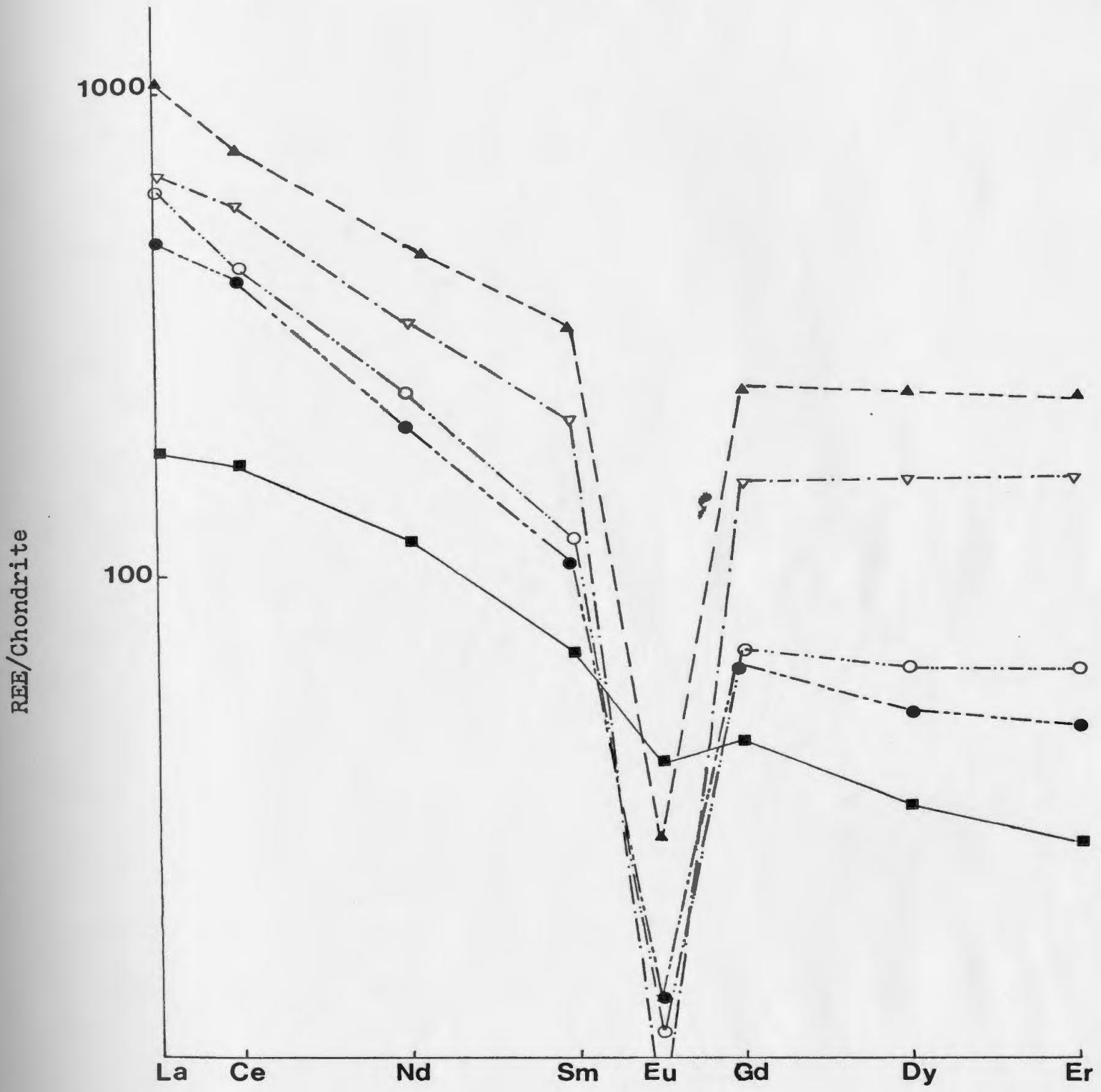


Fig. 20: Rare earth element patterns for the clinopyroxene fayalite granite, the arfvedsonite-riebeckite granite and the Nuiklavick Volcanics.

- ■ clinopyroxene-fayalite granite
- ● arfvedsonite-riebeckite granite
- ○ Nuiklavick Volcanics-group 1
- ▽ Nuiklavick Volcanics-group 2
- ▲ Nuiklavick volcanics-group 3

Fig. 21. REE patterns for an average crustal composition (Shaw et al., 1976), a peralkaline granite from New England (Buma et al., 1971), a comendite from the western U.S. (Noble et al., 1980), and a pantellerite from the western U.S. (Noble et al., 1980).

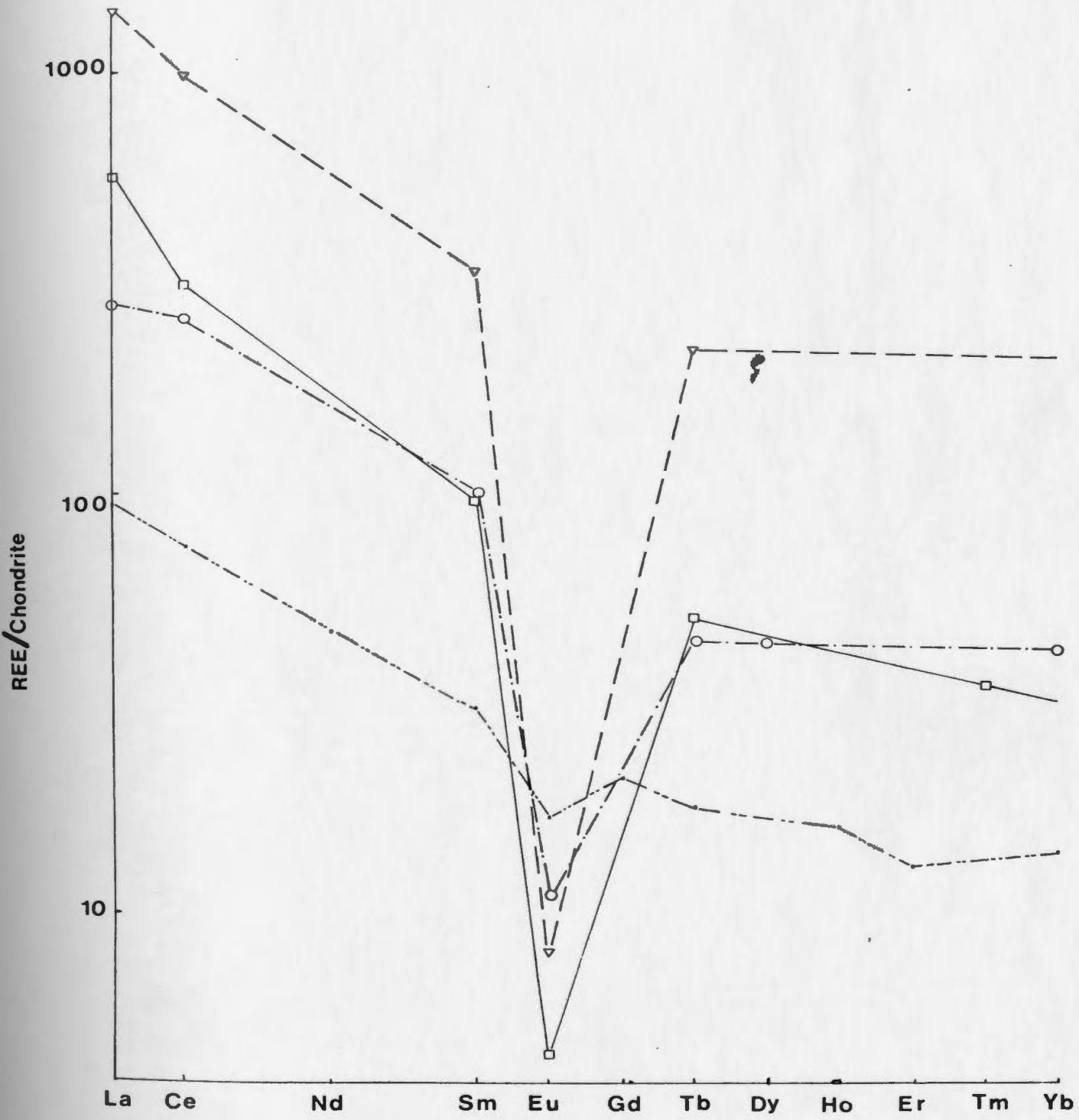
1000
100
10
REE/Chondrite
La
Ce
Nd
Sm
Eu
Gd
Tb
Dy
Ho
Er
Tm
Yb

Fig. 22. Major and trace element enrichment factors for the arfvedsonite-riebeckite granite relative to the clinopyroxene-fayalite granite.

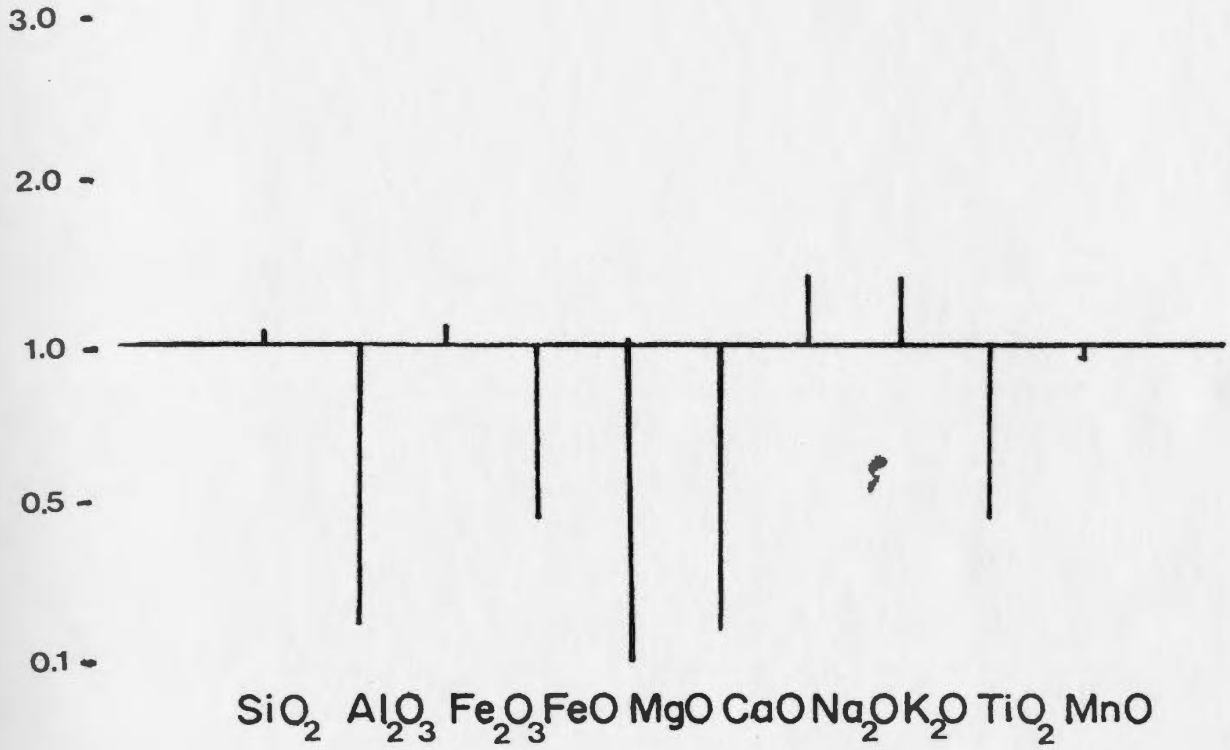
3.0
2.0
1.0
0.5
0.1
SiO2 Al2O3 Fe2O3 FeO MgO CaO Na2O K2O TiO2 MnO

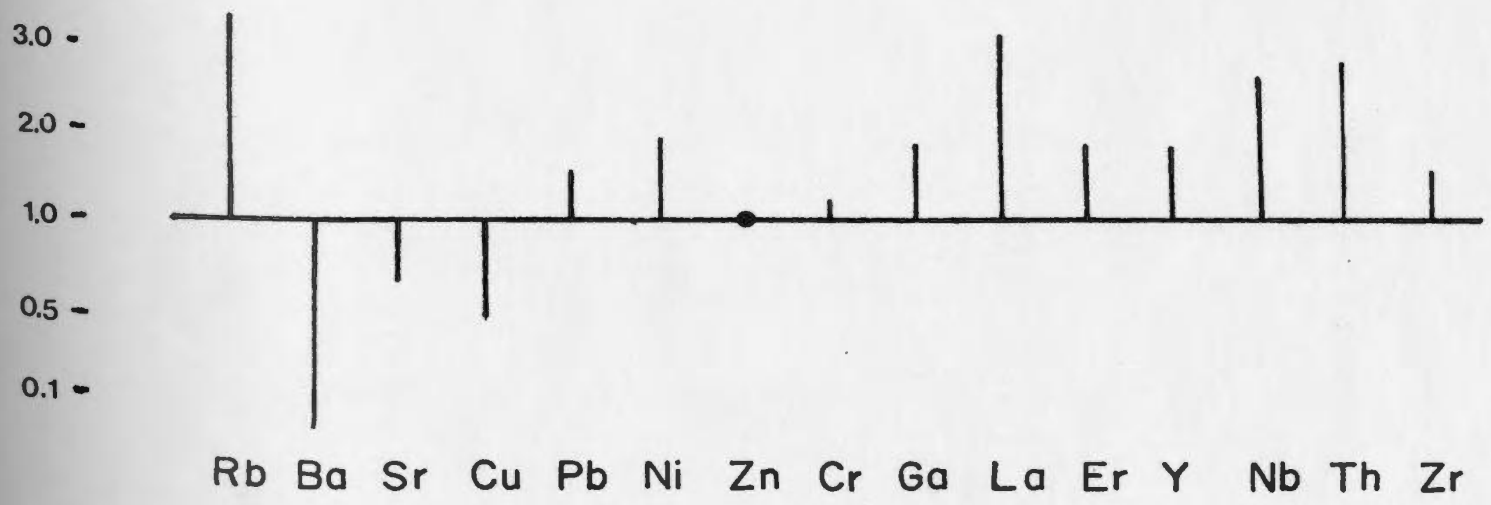
3.0
2.0
1.0
0.5
0.1
Rb Ba Sr Cu Pb Ni Zn Cr Ga La Er Y Nb Th Zr

Figs. 23-30. Harker diagrams for the arfvedsonite-riebeckite granite and the Nuiklavick Volcanics. On all diagrams the symbols are as follows:

- ● arfvedsonite-riebeckite granite
- ○ group 1 of Nuiklavick Volcanics
- △ group 2 of Nuiklavick Volcanics
- ▲ group 3 of Nuiklavick Volcanics

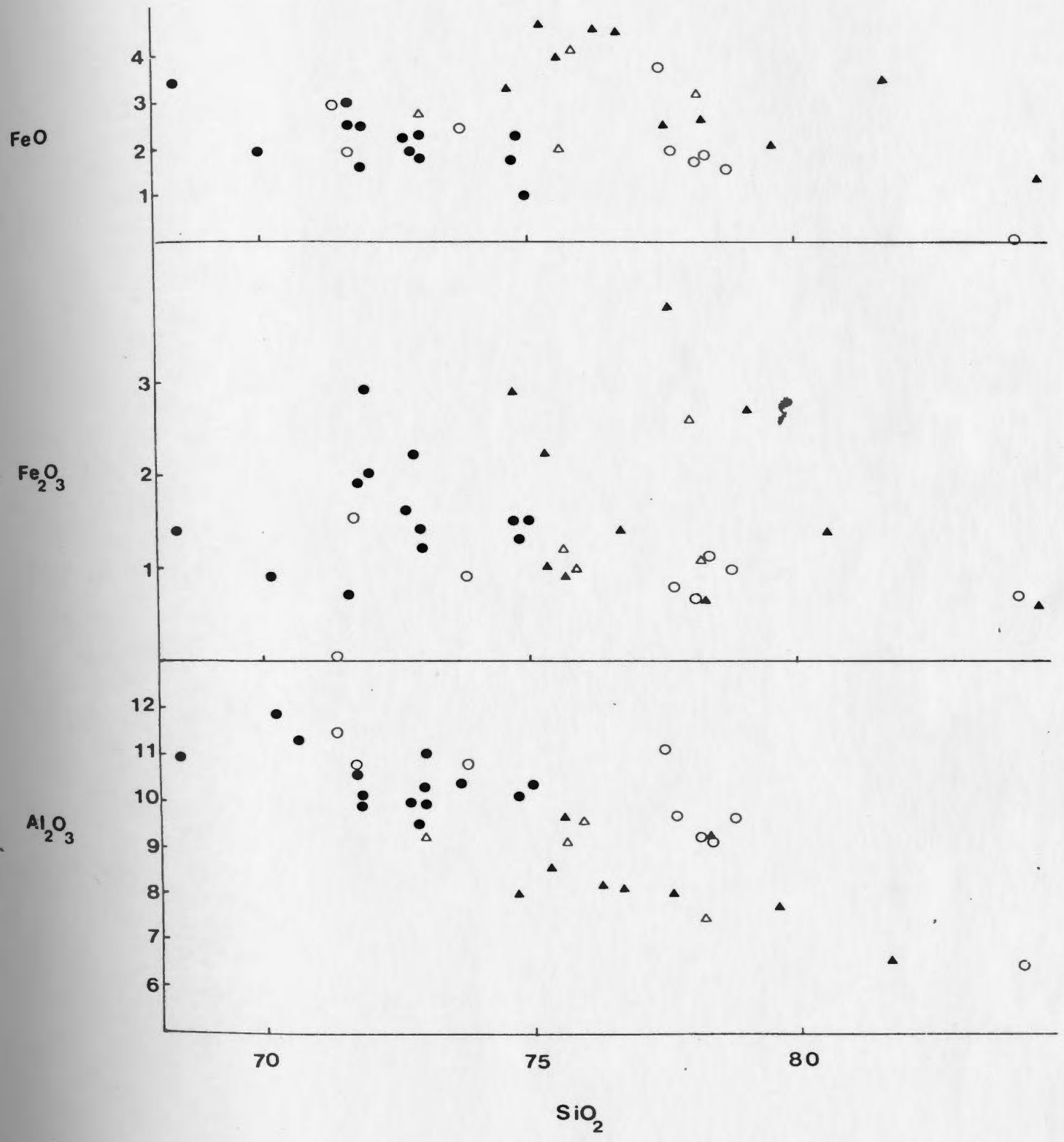
FeO
4
3
2
1
$Fe_2O_3$
3
2
1
$Al_2O_3$
12
11
10
9
8
7
6
70
75
80
$SiO_2$

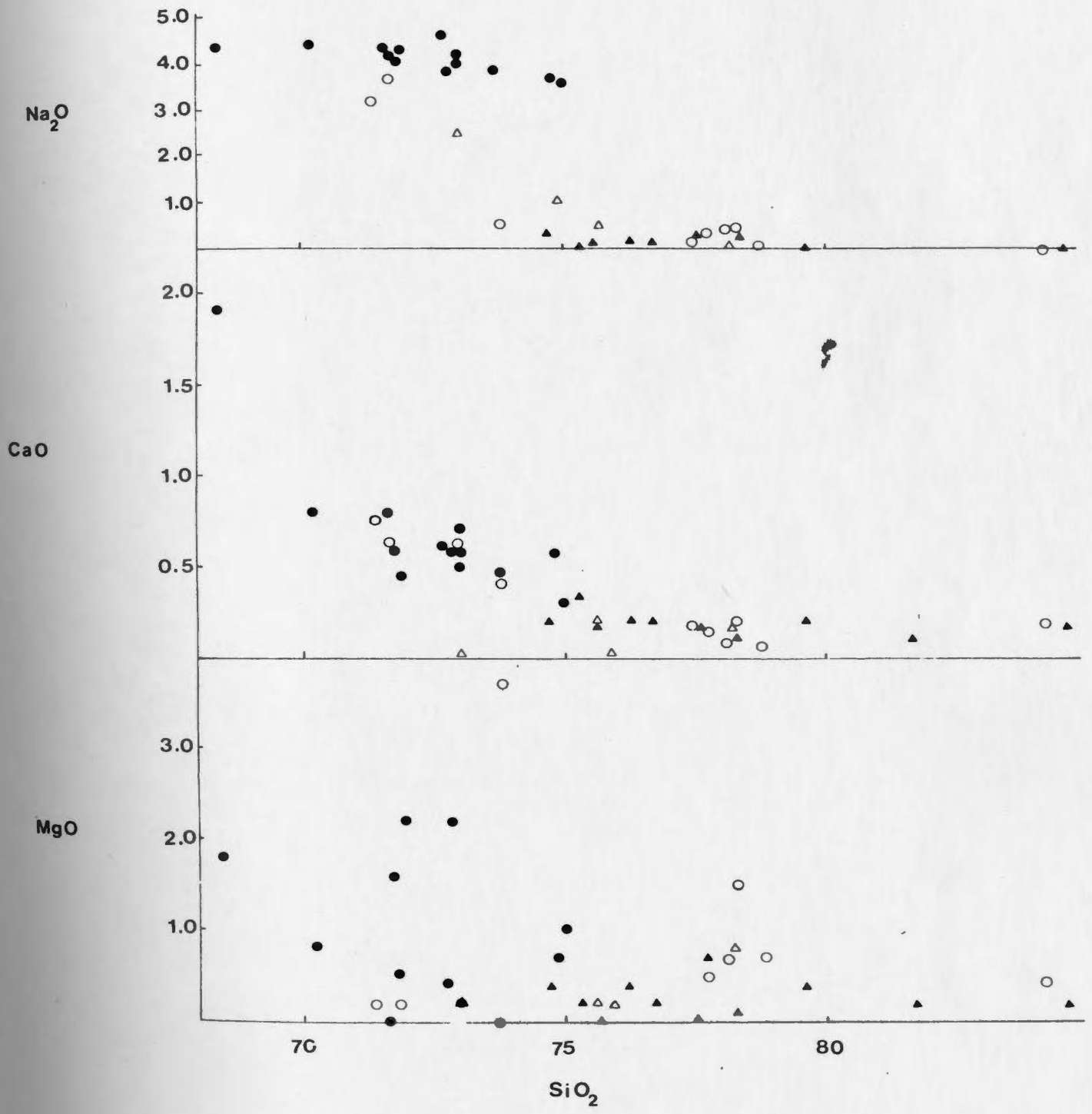
5.0
4.0
3.0
2.0
1.0
Na2O
2.0
1.5
1.0
0.5
CaO
3.0
2.0
1.0
MgO
70
75
80
SiO2

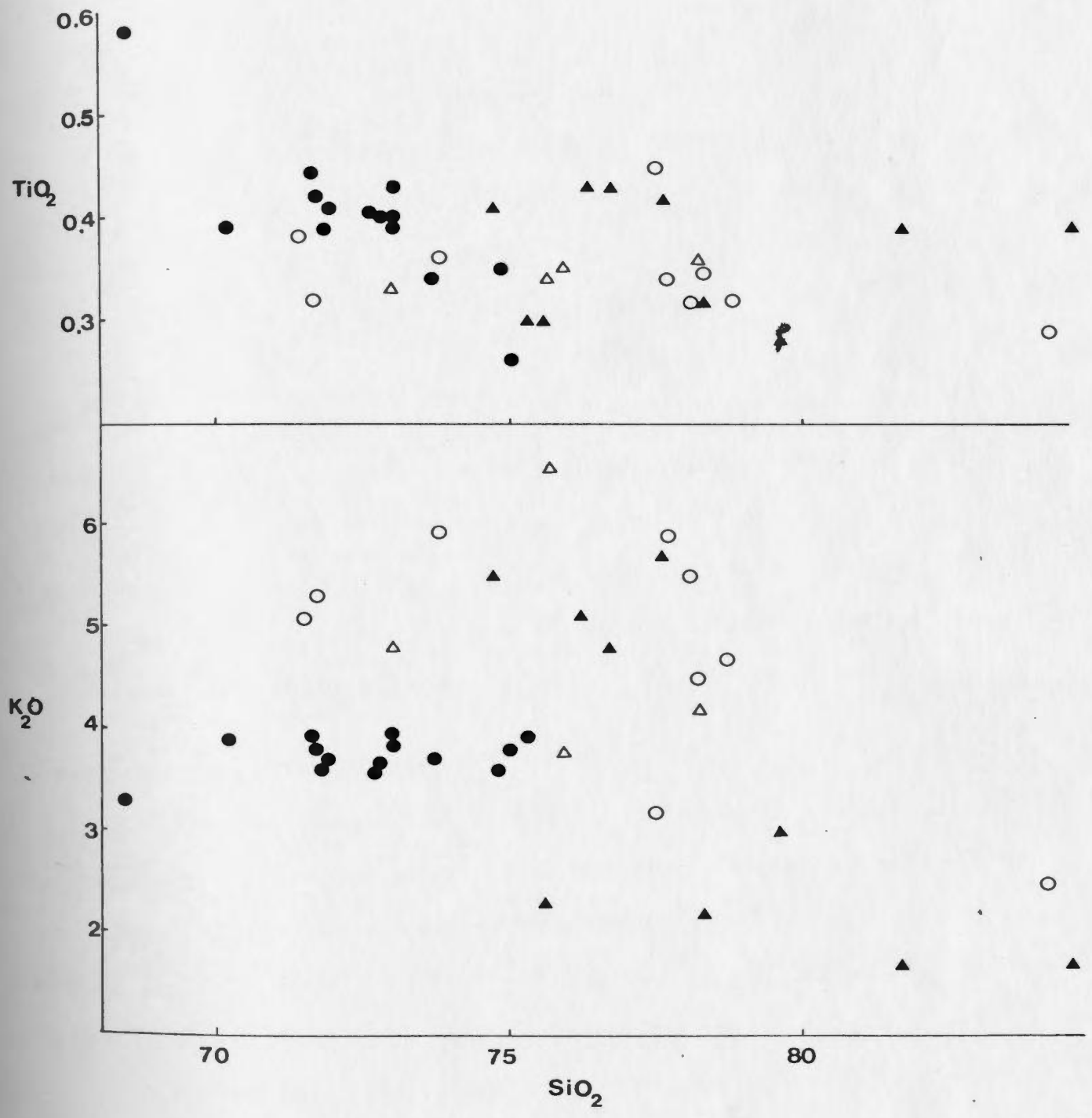
0.6
0.5
TiO2
0.4
0.3
6
5
K2O
4
3
2
70
75
80
SiO2

On a Q-Ab-Or normative diagram (Fig. 6) the arfvedsonite-riebeckite granite samples define a trend parallel to that of a suite of pantellerites from the island of Pantelleria (Carmichael and MacKenzie, 1969). The arfvedsonite-riebeckite granite trend falls between the experimentally determined liquidus surfaces for the planes containing 8.3 and 4.3% acmite plus sodium metasilicate (Carmichael and MacKenzie, 1963).

Again, Harker diagrams have been used to illustrate possible differentiation trends of major/minor elements relative to silica. The arfvedsonite-riebeckite granite has been plotted with the clinopyroxene-fayalite granite (Figs. 7-14) and with the Nuiklavick volcanics (Figs. 23-30) for ease of comparison. With the exceptions of sodium and potassium (Figs. 28 and 29), trends are generally similar to those normally found in over-saturated peralkaline rocks (Viliari, 1974; MacDonald, 1974), i.e. $Al_2O_3$, MgO, CaO, FeO decrease, $TiO_2$ is constant and $Fe_2O_3$ increases slightly with increasing $SiO_2$. Sodium and potassium generally increase with increasing silica for the granite samples.

Trace Element Geochemistry

With the exception of nickel and to some extent lead, trace element concentrations in the arfvedsonite-riebeckite granite are similar to those normally observed in over-saturated peralkaline rocks (e.g. Nicholls and Carmichael, 1969; Ferrara and Treuil, 1974). Relative to an average granitic composition and the clinopyroxene-fayalite granite, the arfvedsonite-riebeckite granite is enriched in Nb, Zr, Cr, Zn, Ni and REE, slightly enriched in Th, Rb, Ga and Pb and depleted in Sr, Cu and Ba (Fig. 22).

In most other studies of peralkaline rocks, nickel, lead and chromium are characteristically depleted (Ferrara and Treuil, 1974) but in this study chromium and lead are slightly enriched and nickel significantly so. At least two other cases of nickel enrichment in peralkaline rocks have been documented (Hussey, 1969; Taylor et al., 1980) but chromium and lead enrichments have not been previously noted.

The use of Harker-type correlation diagrams to show geochemical trends in an attempt to determine or characterize geochemical processes has gained widespread acceptance and favour. In this study, these diagrams are used extensively to show relationships between ratios or pairs of elements. On correlation diagrams of the residual elements characteristic of peralkalinity, the arfvedsonite-riebeckite granite samples separate into two distinct groups which together define generally linear trends with little scatter (Figs. 16-19, Appendix D). K/Rb ratios decrease with increasing concentrations of residual elements developing a negative trend when only the peralkaline granite is plotted and a curve when plotted with the clinopyroxene-fayalite granite (Fig. 19, Appendix D).

Diagrams of Zr vs the residual elements all have similar trends with the exceptions of Zn and Pb (Fig. 16, Appendix D). Zr plots are generally linear with a tendancy to level off at high concentrations. Plots with Y, Nb, Th vs the residual elements produce similar trends but do not usually level off at higher concentrations (Figs. 16 and 17,

Appendix D). Zn tends to produce a distinctly curved trend when plotted against the residual elements (Fig. 18, Appendix D). The similarities in the trends of various residual elements plotted against each other indicates positive correlations among those included in this group.

Lead and nickel are enriched in the peralkaline granite but no sulphides have been observed. Plots of lead and nickel vs the residual elements produce trends similar to those described above suggesting that these elements are positively correlated (Figs, 31, 32, 33, 34 and 35). Chromium is somewhat enriched but does not have a positive correlation and whereas the residual elements tend to become systematically enriched chromium becomes increasingly depleted (Appendix D).

Rare Earth Element Geochemistry

The arfvedsonite-riebeckite granite, like other peralkaline granites, is strongly enriched in rare earth elements (Figs. 20 and 21 and Buma et al., 1971). The light rare earths (La-Sm) are enriched relative to the heavy rare earths (Gd-Lu), however, the ratio $\Sigma$Ce: $\Sigma$Y is low compared to non-peralkaline granites (Baslashov, 1962; Buma et al., 1971). The rare earth element trend has a negative slope with a tendency to flatten or level off on the heavy rare earth end, Eu is strongly depleted (Fig. 20).

If the rare earth elements are plotted against a residual element such as Zr, there is a difference in the behaviour of a light rare earth element such as La or Ce and a heavy rare earth element such as Er

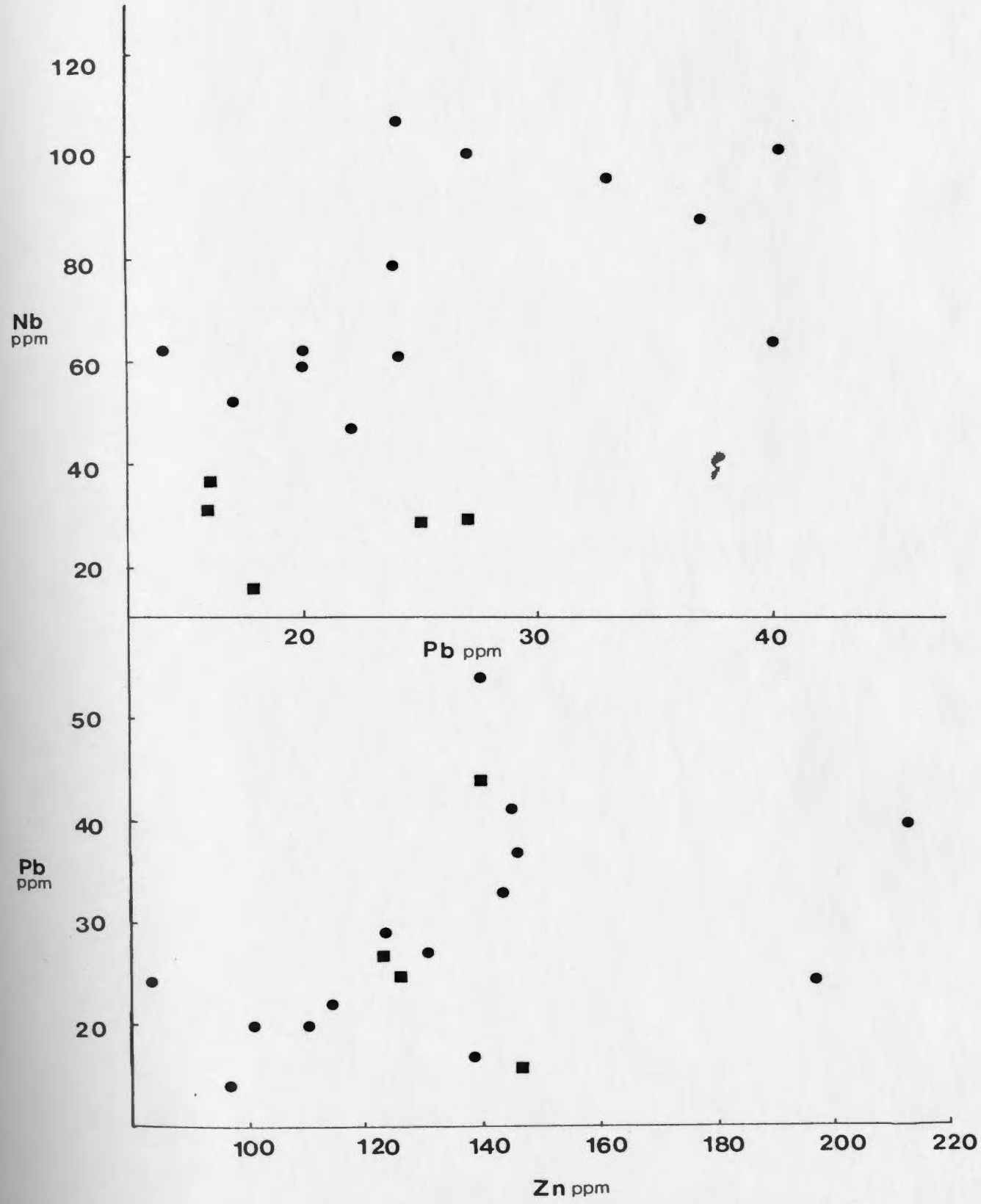


Figs. 31-32: Pb vs. Nb and Pb vs. Zn for the clinopyroxene-fayalite granite and the arfvedsonite-riebeckite granite

Fig. 34. Ni vs Zn for the clinopyroxene-fayalite granite and the arfvedsonite-riebeckite granite

Fig. 33. Ni vs Zr for the clinopyroxene-fayalite granite and the arfvedsonite-riebeckite granite

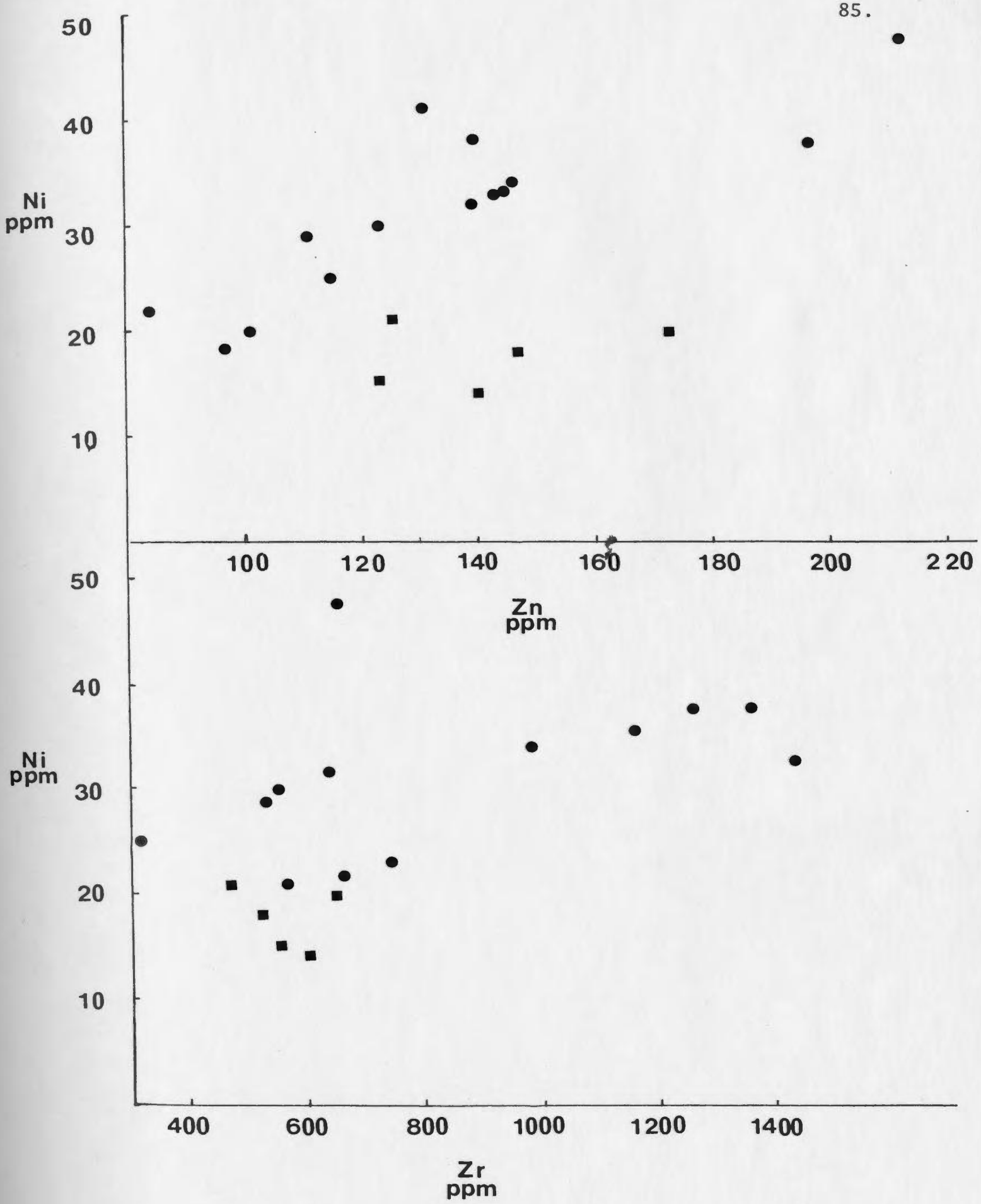
50
40
Ni
ppm
30
20
10
100
120
140
160
180
200
220
Zn
ppm
50
40
Ni
ppm
30
20
10
400
600
800
1000
1200
1400
Zr
ppm

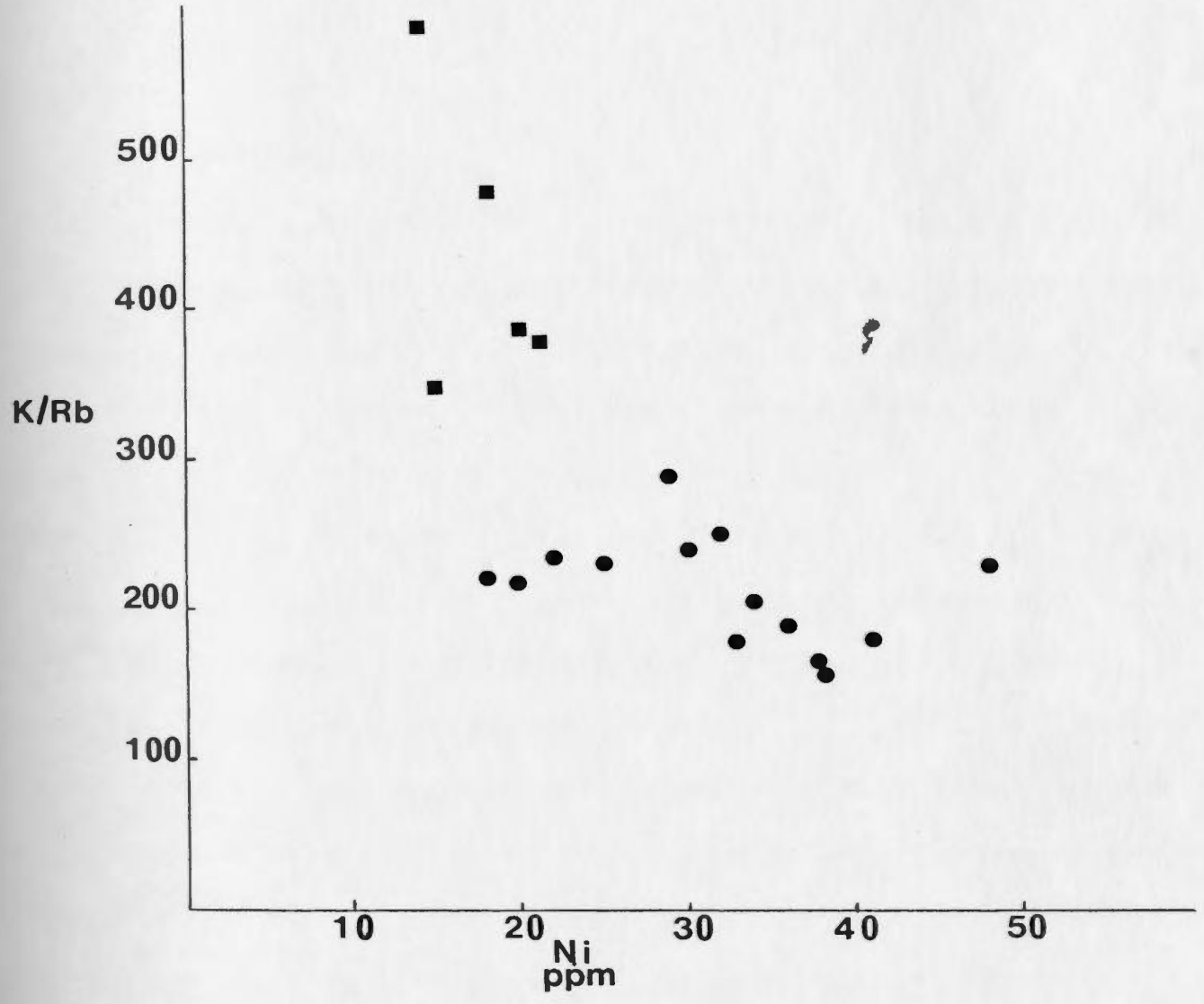


Fig. 35: K/Rb vs. Ni for the arfvedsonite-riebeckite granite and the Nuiklavick Volcanics.

(Figs. 54-55). The trends of Zr vs La or Ce have a considerable amount of scatter and are not well developed. The trend of Zr vs Er is similar to those described above for Zr vs other residual elements such as Nb or Th (Figs. 16 and 54).

## NUIKLAVIČK VOLCANICS

### Major Element Geochemistry

The Nuiklavick volcanics cannot be defined as peralkaline on the basis of petrography or major/minor element geochemistry. Their average is very slightly enriched in silica and potassium relative to an average granitic composition (Fig. 36). It should be noted, however, that although the average of the volcanics indicates potassium enrichment this reflects the high concentrations in the quartz-feldspar porphyry whereas the rhyolites/tuffs are somewhat depleted in potassium. In the average volcanic sample, sodium, magnesium, and calcium are strongly depleted, aluminum and titanium are less so.

CIPW normative analyses are meaningless because of sodium depletion. Element trends on Harker diagrams (Figs. 23-30), with the exceptions of sodium and potassium follow trends similar to those of the arfvedsonite-riebeckite granite. In general, $Al_2O_3$, MgO, CaO and FeO decrease with increasing $SiO_2$, $Fe_2O_3$ becomes slightly enriched and $TiO_2$ remains constant. In the granite $Na_2O$ and $K_2O$ increase with increasing $SiO_2$ but in the volcanics they tend to decrease in concentration.

Fig. 36. Major and trace element enrichment factors for groups 1 and 3 of the Nuiklavick Volcanics relative to an average granitic composition.

On all subsequent diagrams an average of 9 analysis was used for group 1 and an average of 10 analyses was for group 3.

Group 1 - quartz-feldspar porphyry plus 2 volcanic breccia samples (- - -)

Group 3 - rhyolite and tuff (——)

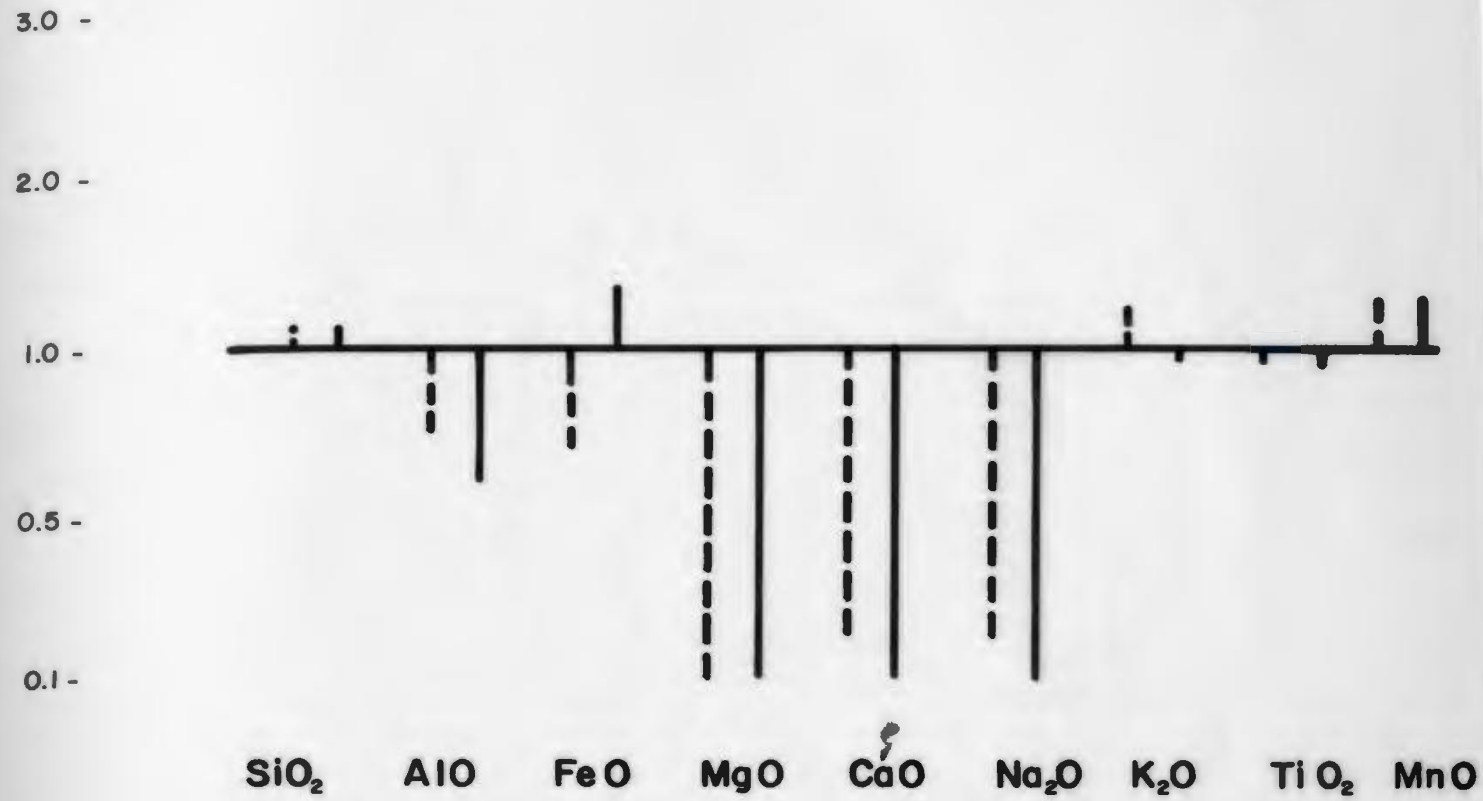
3.0 -
2.0 -
1.0 -
0.5 -
0.1 -
SiO2
AlO
FeO
MgO
CaO
Na2O
K2O
TiO2
MnO

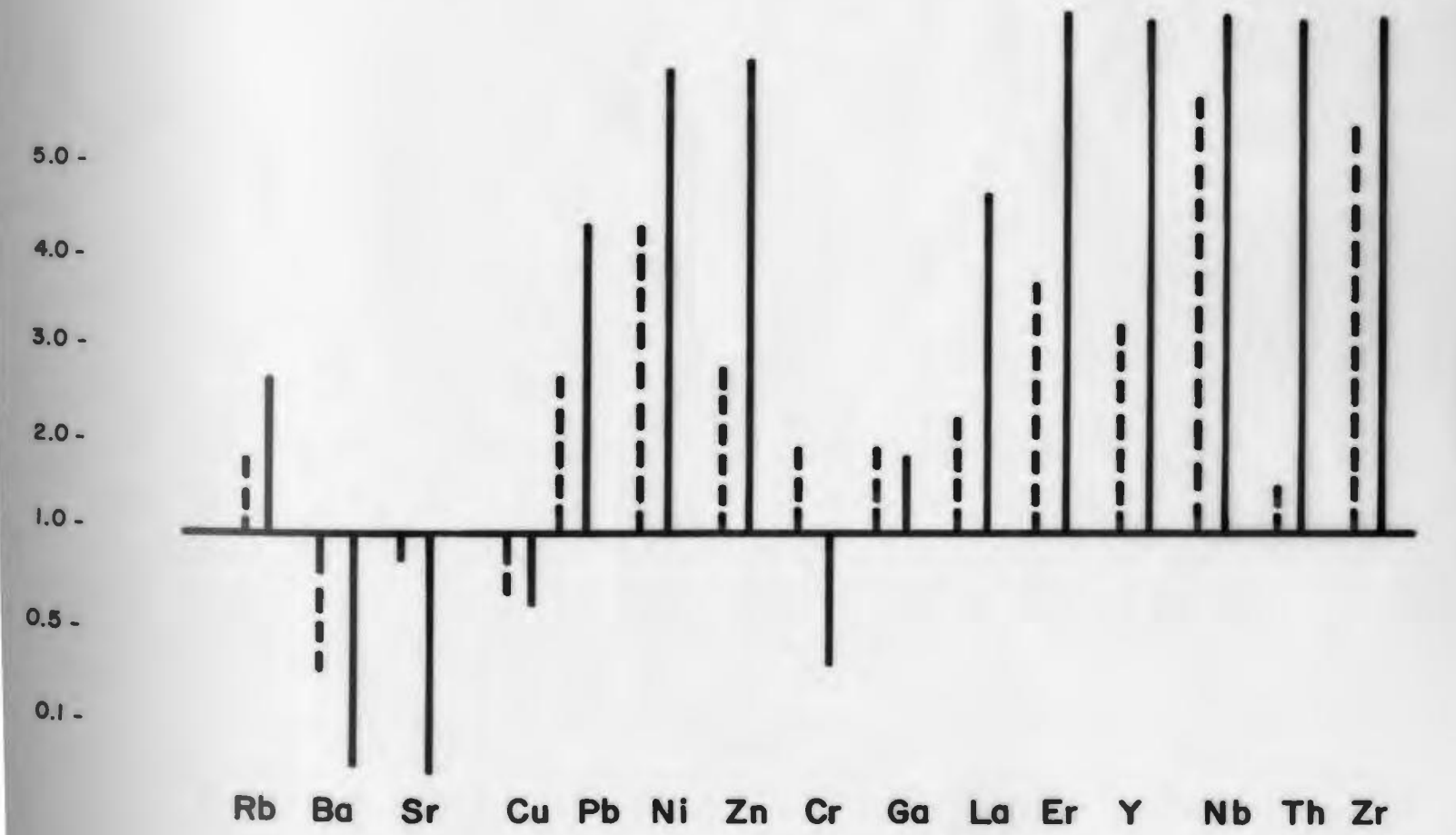
5.0 -
4.0 -
3.0 -
2.0 -
1.0 -
0.5 -
0.1 -
Rb
Ba
Sr
Cu
Pb
Ni
Zn
Cr
Ga
La
Er
Y
Nb
Th
Zr

Fig. 37. Major and trace element enrichment factors for the group 3 relative to group 1 of the Nuiklavick Volcanics.

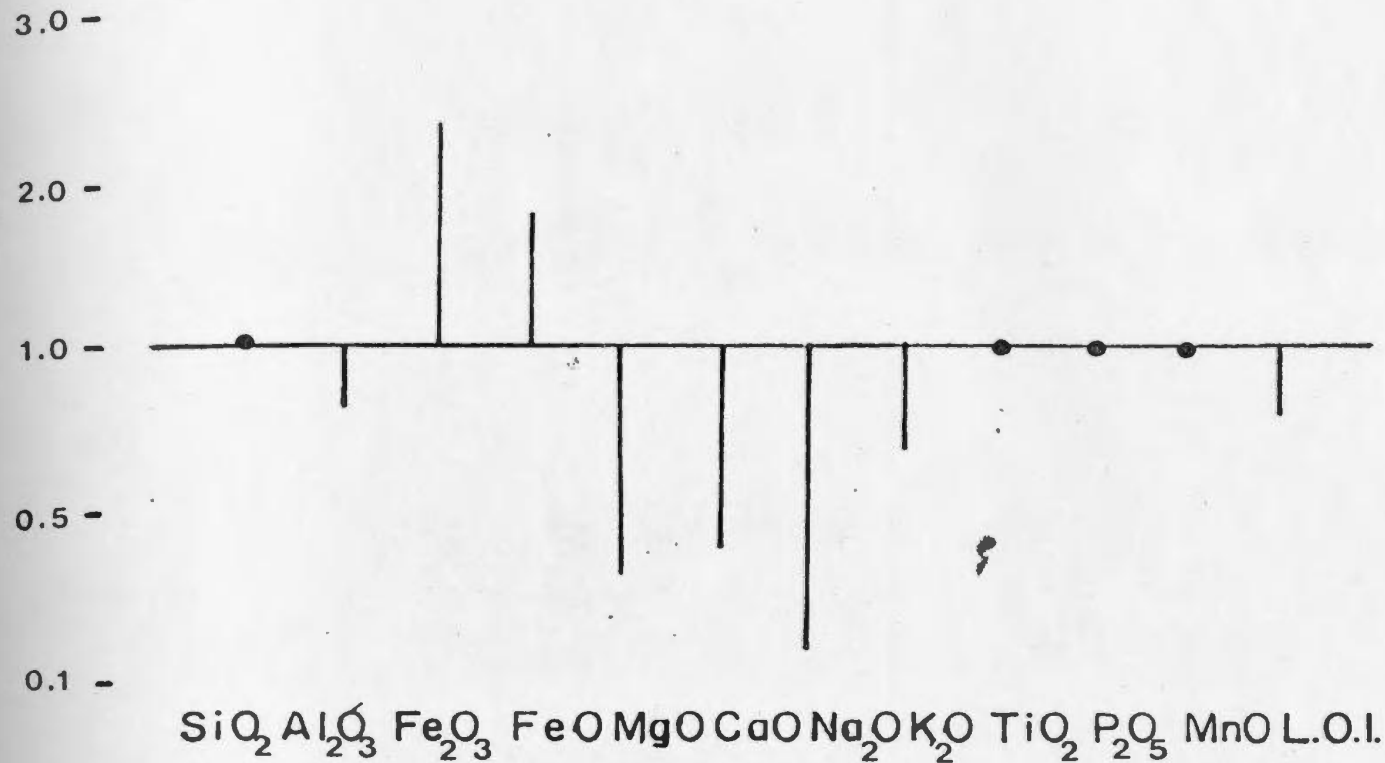
3.0
2.0
1.0
0.5
0.1
SiO2 Al2O3 Fe2O3 FeO MgO CaO Na2O K2O TiO2 P2O5 MnO L.O.I.

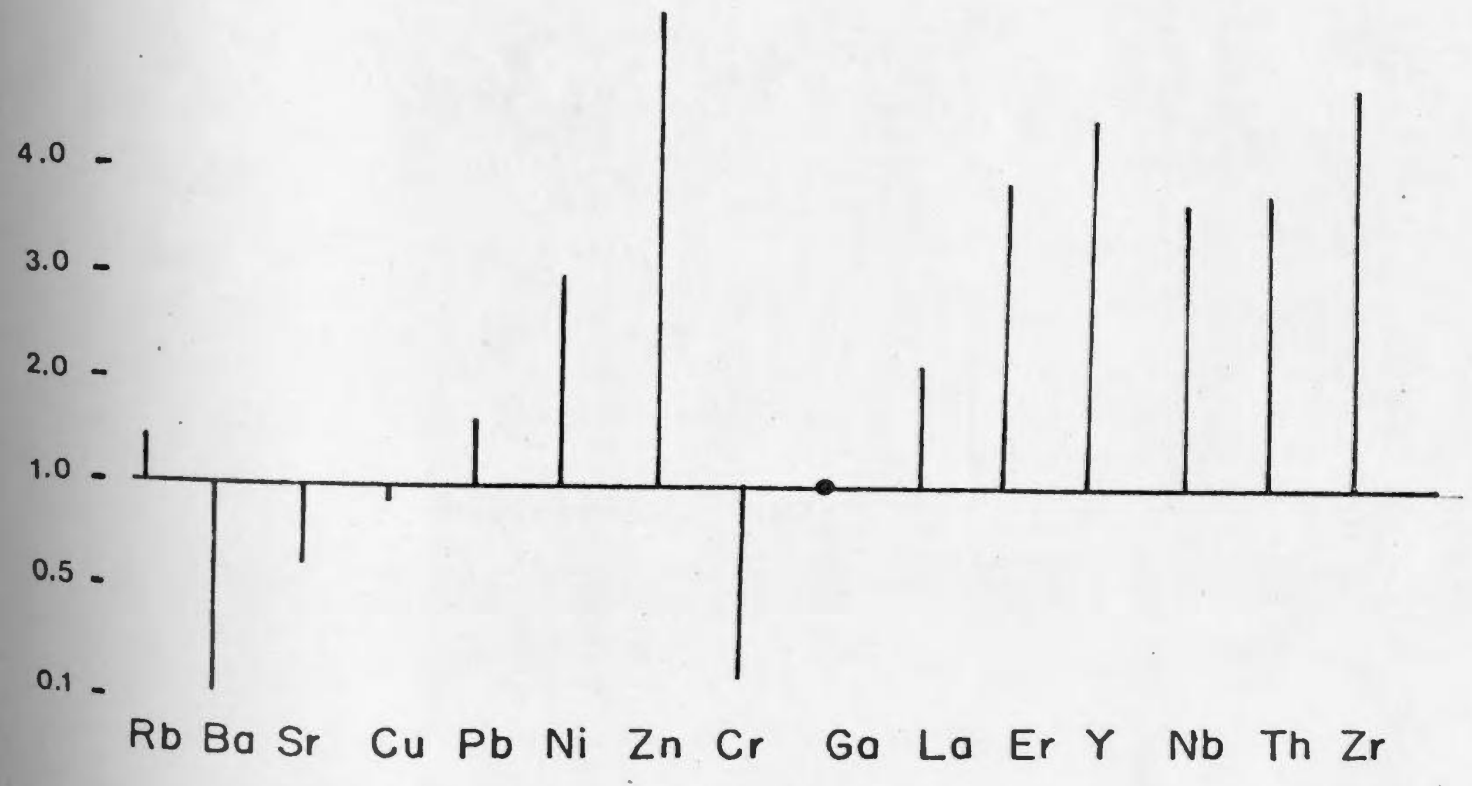
4.0
3.0
2.0
1.0
0.5
0.1
Rb Ba Sr Cu Pb Ni Zn Cr Ga La Er Y Nb Th Zr

On the basis of variations in chemistry, the Nuiklavick volcanics can be dividad into three geochemical groups:

Group 1: quartz-feldspar porphyry-subvolcanic plus 2 volcanic breccia samples

Group 2: 091A, 091B quartz-feldspar prophyry, 090 tuff-rhyolite, 100 volcanic breccia, all of which fall between Groups 1 and 3 and appear to be transitional between the extremes

Group 3: rhyolite and tuff-extrusive.

Group 3 is enriched in iron and depleted in aluminum, calcium magnesium, sodium and potassium relative to Group 1 (Fig. 37). The transitional group, Group 2, follows the same trends but has lower enrichment factors.

Trace Element Geochemistry

Although as noted previously, a peralkaline nature cannot be defined on the basis of petrography or major/minor element geochemistry, trace and rare earth element data provides enough evidence to show the peralkaline affinity of the volcanics and their relationship with the arfvedsonite-riebeckite granite. Trace element trends for the Nuiklavick volcanics are similar to those generally found in peralkaline volcanics with their extreme enrichment of the residual elements characteristic of peralkalinity and depletion of Ba and Sr (Nicholls and Carmichael, 1969; Ferrara and Treuil, 1974; Bailey and MacDonald, 1975). The Nuiklavick volcanics do not form a particularly coherent

group as there is a wide range of concentrations and most elements, especially Zr, have a tendency to separate them into the groups desribed above (Figs. 38 and 39, Appendix D).

Group 1, the quartz-feldspar porphyry has slightly higher concentrations of residual elements than the arfvedsonite-riebeckite granite but together the two plot as a coherent group on most diagrams (Figs. 38, 39, and 40, Appendix D). Groups 2 and 3 have significantly higher concentrations and are separated from Group 1 by a gap or discontinuity. On correlation diagrams, Group 2 tends to form a continuation of the trend begun by the arfvedsonite-riebeckite granite or cause an inflection centred on Group 2 (Figs. 39, 40 and 41, Appendix D). All of the residual elements - Zr, Nb, Y, Th - which are characteristic of peralkaline rocks have similar trends when plotted against each other (Figs. 40, 41, and 44). Trends of pairs of residual elements tend to be linear but regression lines do not pass through zero (Figs. 40 and 41). Plots with Zn have an inflection or curve centred on Group 2, the transitional group (Fig. 41, Appendix D); K/Rb ratios decrease with increasing concentrations of the residual elements (Fig. 44, Appendix D). Plots of lead and nickel vs the residual elements produce characteristic trends indicating a positive correlation and a seemingly residual nature (Figs. 41-43 and 45-47, Appendix D).

Gallium trends do not correspond with those of the residual elements. Trends for Ga vs Zr, Zn or K/Rb are not similar to those normally observed for the residual elements (Figs. 48-50, Appendix D). Gallium trends are similar to those produced by aluminum vs the residual elements reflecting the chemical coherence of these two elements (Figs. 48-51).

Fig. 38. Th vs Zr and Nb vs Zr for the arfvedsonite-riebeckite granite and the Nuiklavick volcanics.

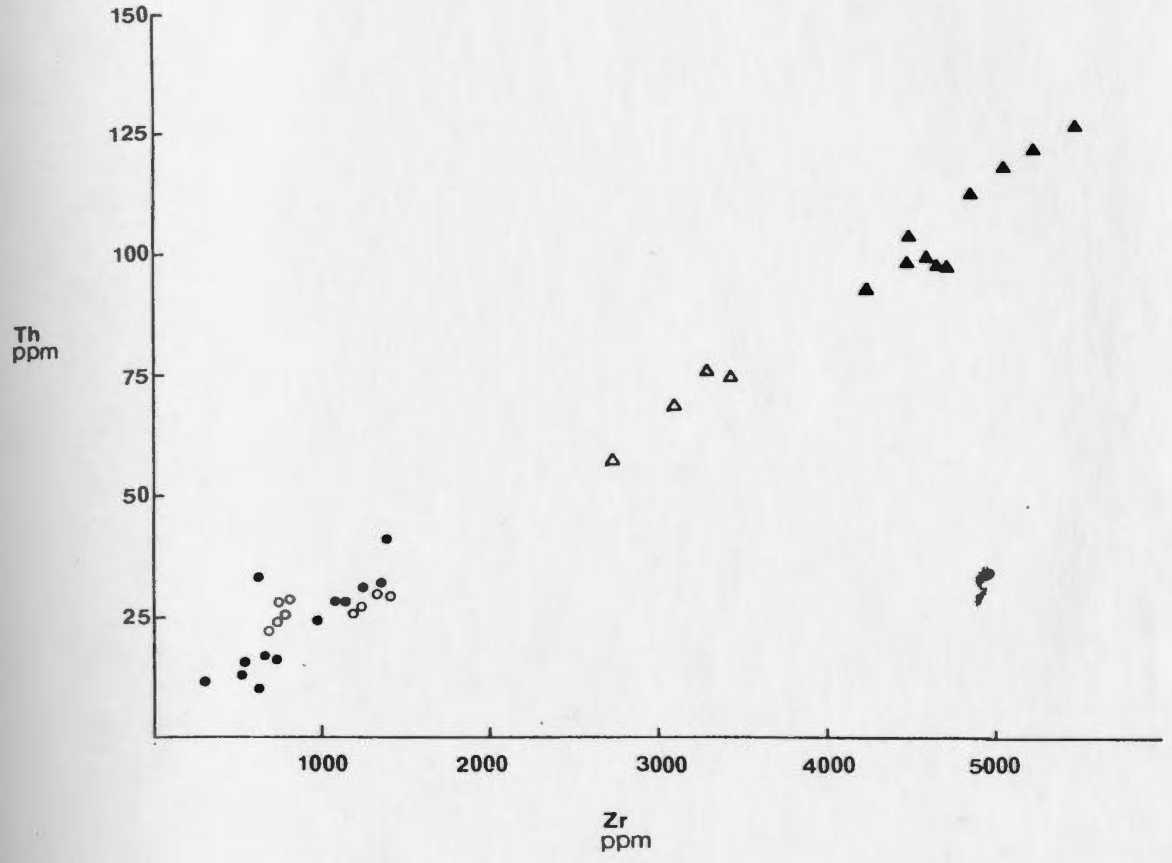
150
125
100
75
50
25
Th
ppm
1000
2000
3000
4000
5000
Zr
ppm

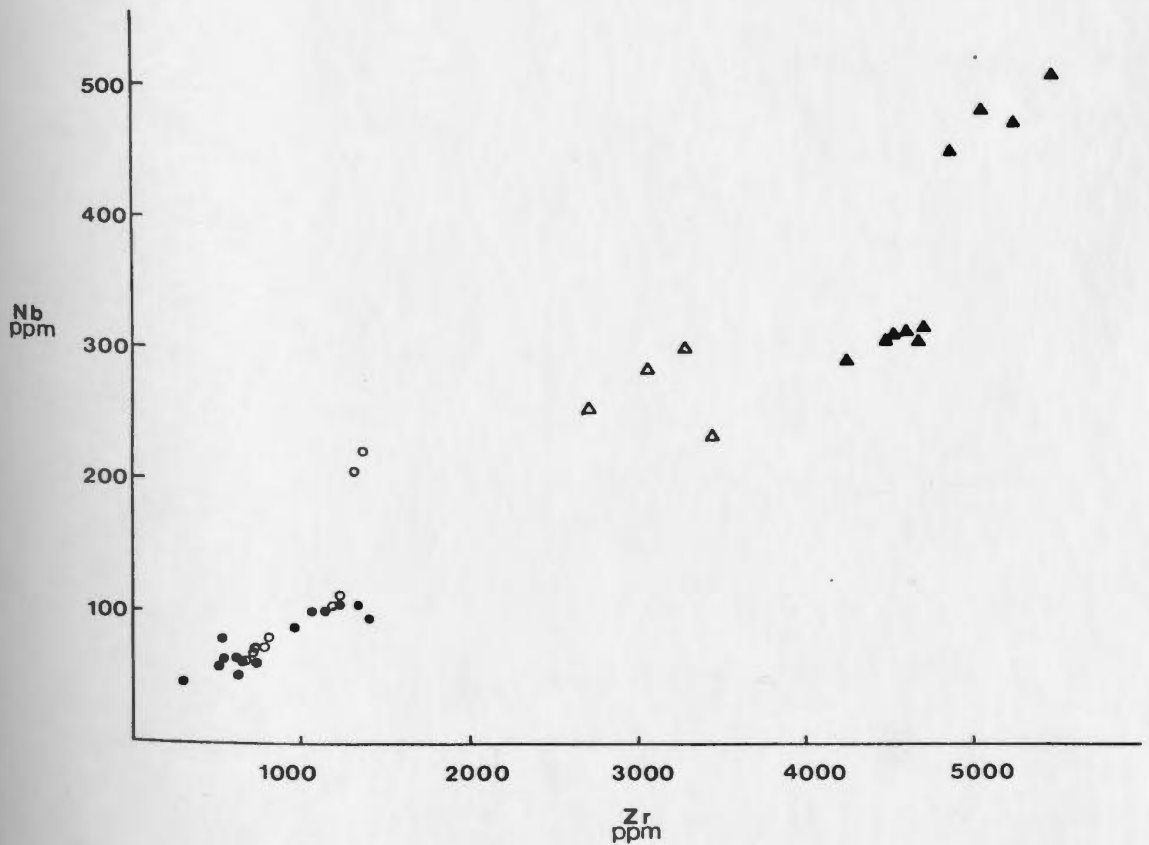
500
400
300
200
100
Nb
ppm
1000
2000
3000
4000
5000
Zr
ppm

Fig. 39. Major and trace element enrichment factors for the groups 1 and 3 of the Nuiklavick Volcanics relative to the arfvedsonite-riebeckite granite.

Group 1 (---

Group 2 (——

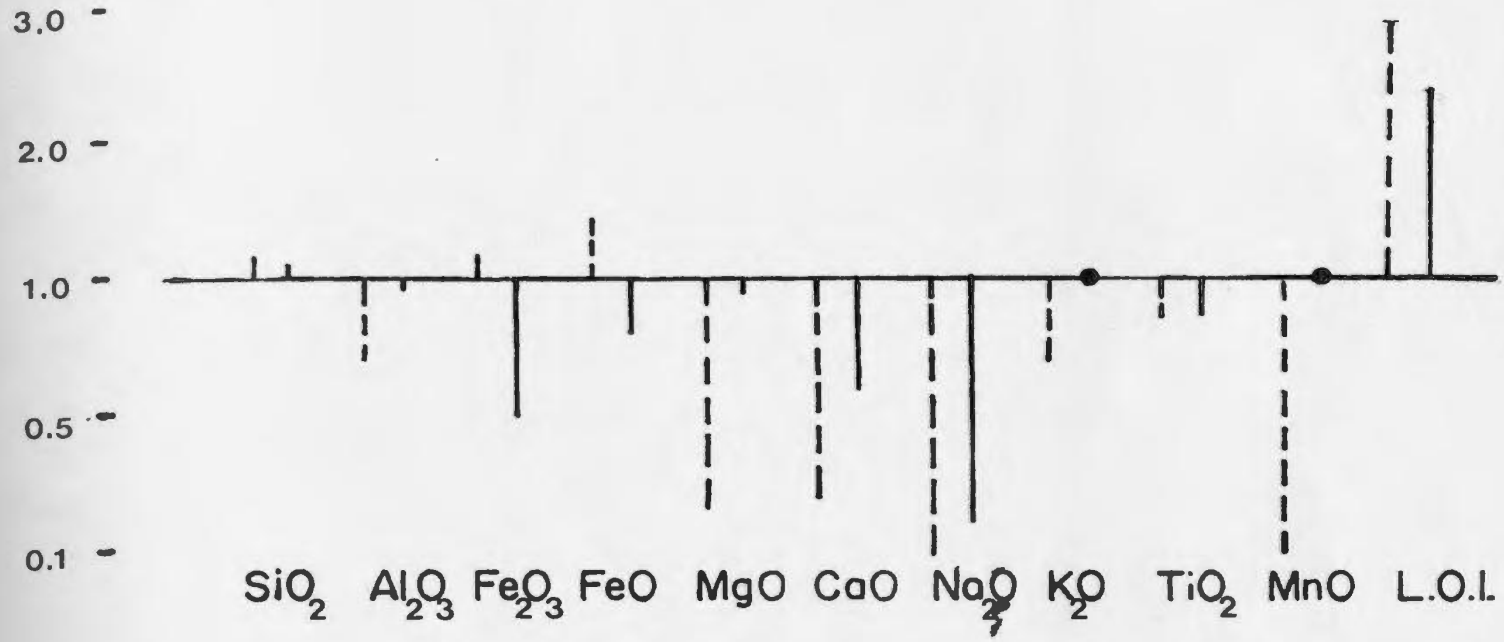
3.0
2.0
1.0
0.5
0.1
SiO2
Al2O3
Fe2O3
FeO
MgO
CaO
Na2O
K2O
TiO2
MnO
L.O.I.

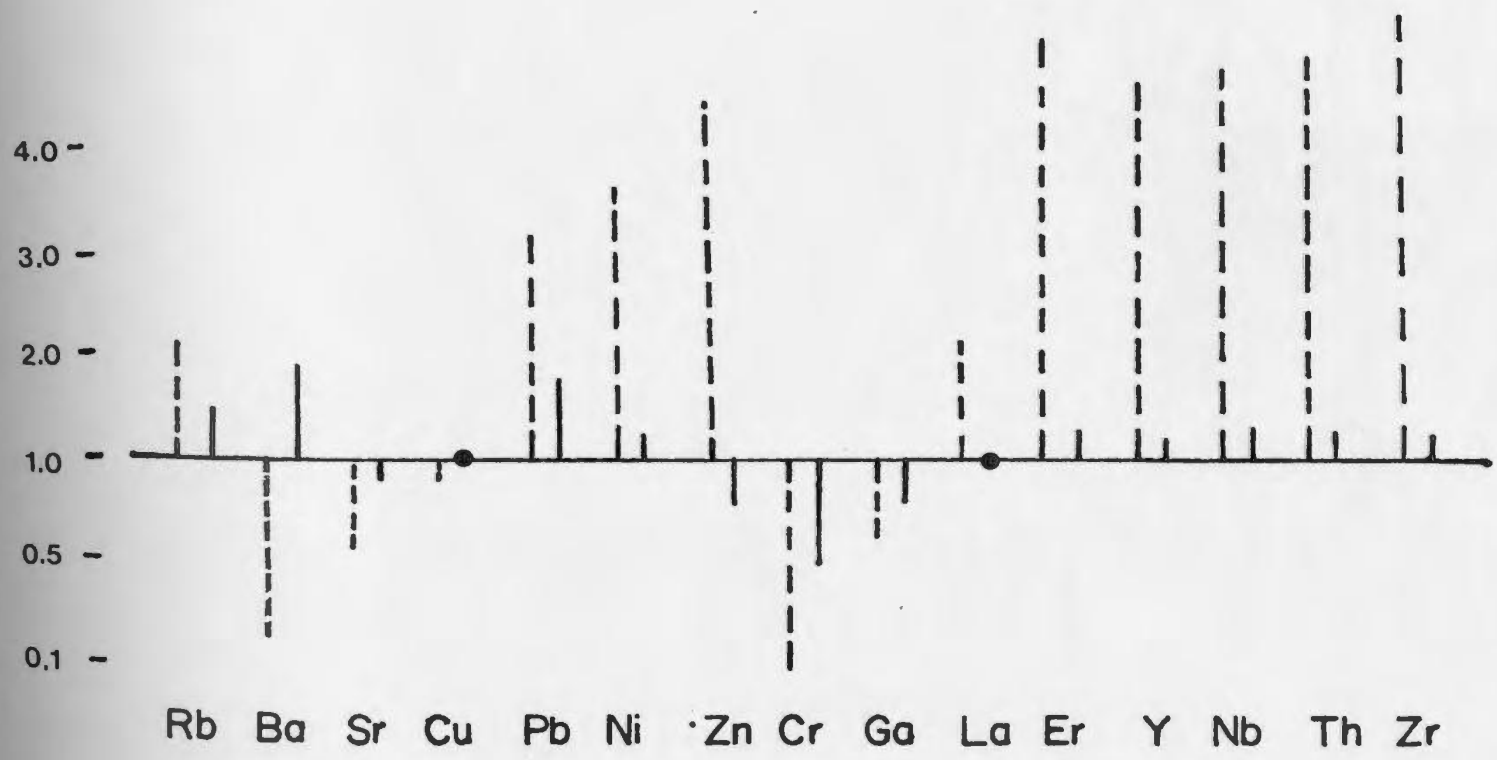
4.0
3.0
2.0
1.0
0.5
0.1
Rb
Ba
Sr
Cu
Pb
Ni
Zn
Cr
Ga
La
Er
Y
Nb
Th
Zr

Fig. 40. Y vs Nb for the arfvedsonite-riebeckite granite and the Nuiklavick volcanics



Fig. 41. Zn vs Zr for the arfvedsonite-riebeckite granite and the Nuiklavick volcanics

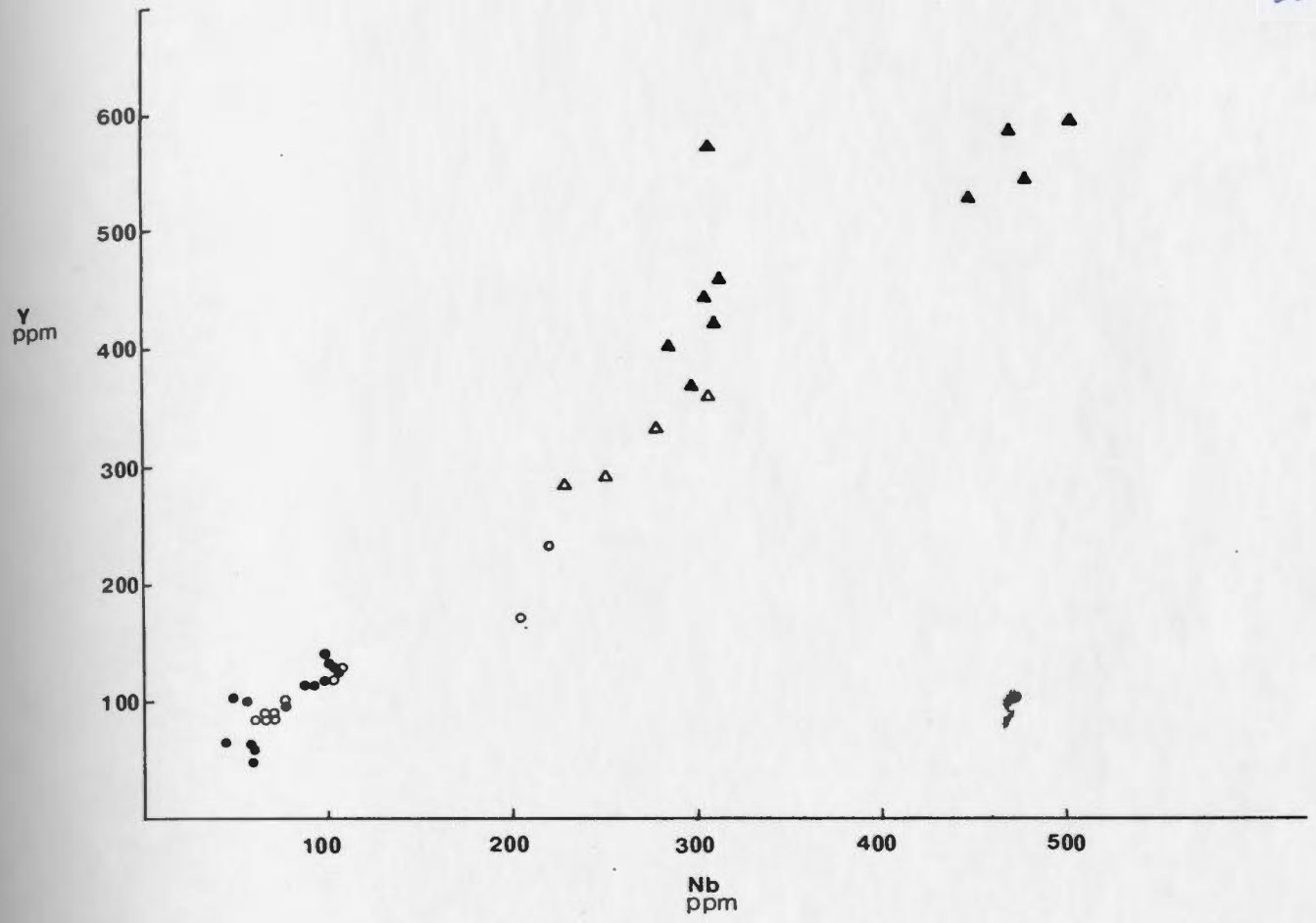
Y
ppm
600
500
400
300
200
100
100
200
300
400
500
Nb
ppm

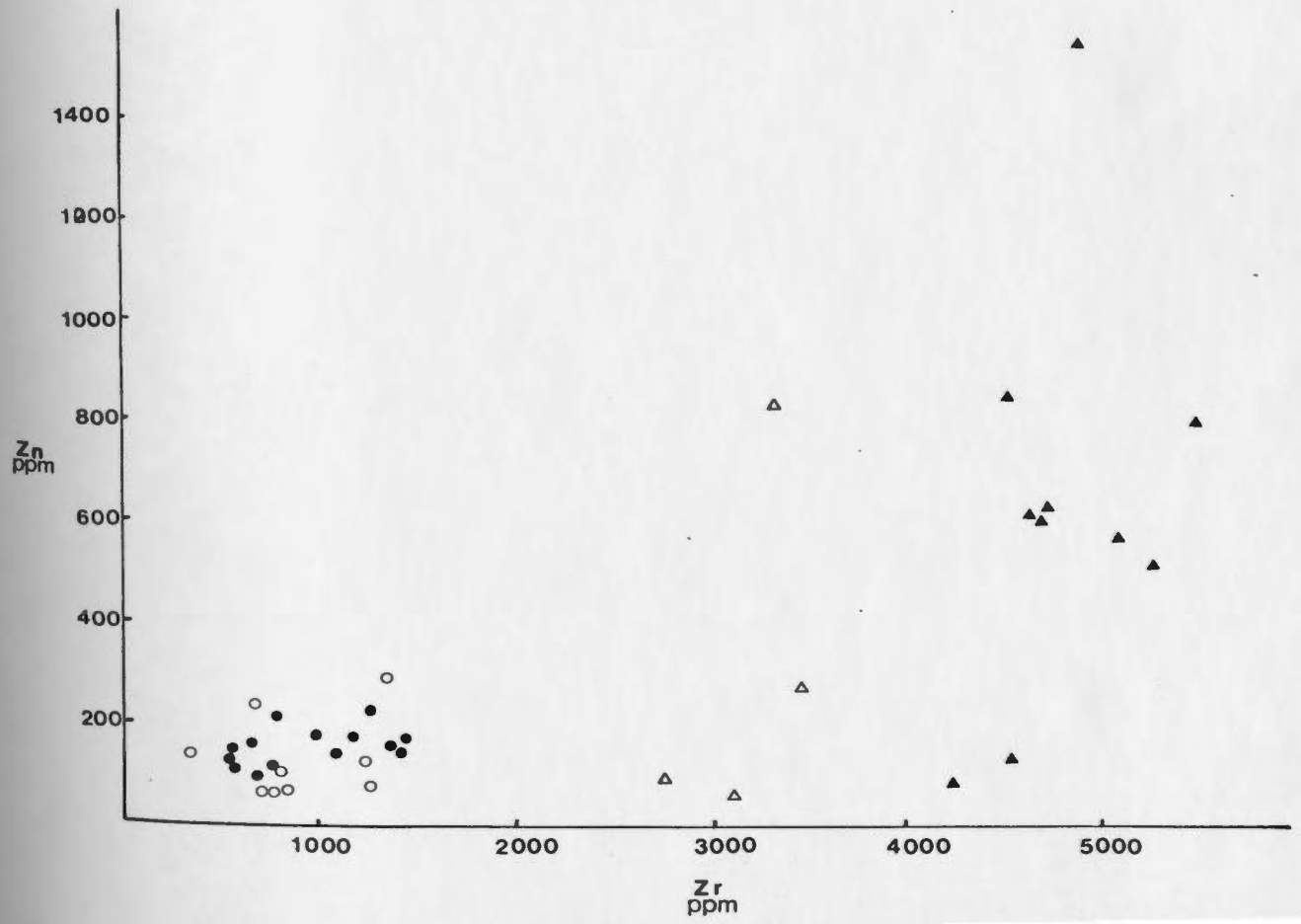
Zn
ppm
1400
1200
1000
800
600
400
200
1000
2000
3000
4000
5000
Zr
ppm

Fig. 42. Pb vs Zr for the arfvedsonite-riebeckite granite and the Nuiklavick volcanics

Fig. 43. Pb vs Zn for the arfvedsonite-riebeckite granite and the Nuiklavick volcanics

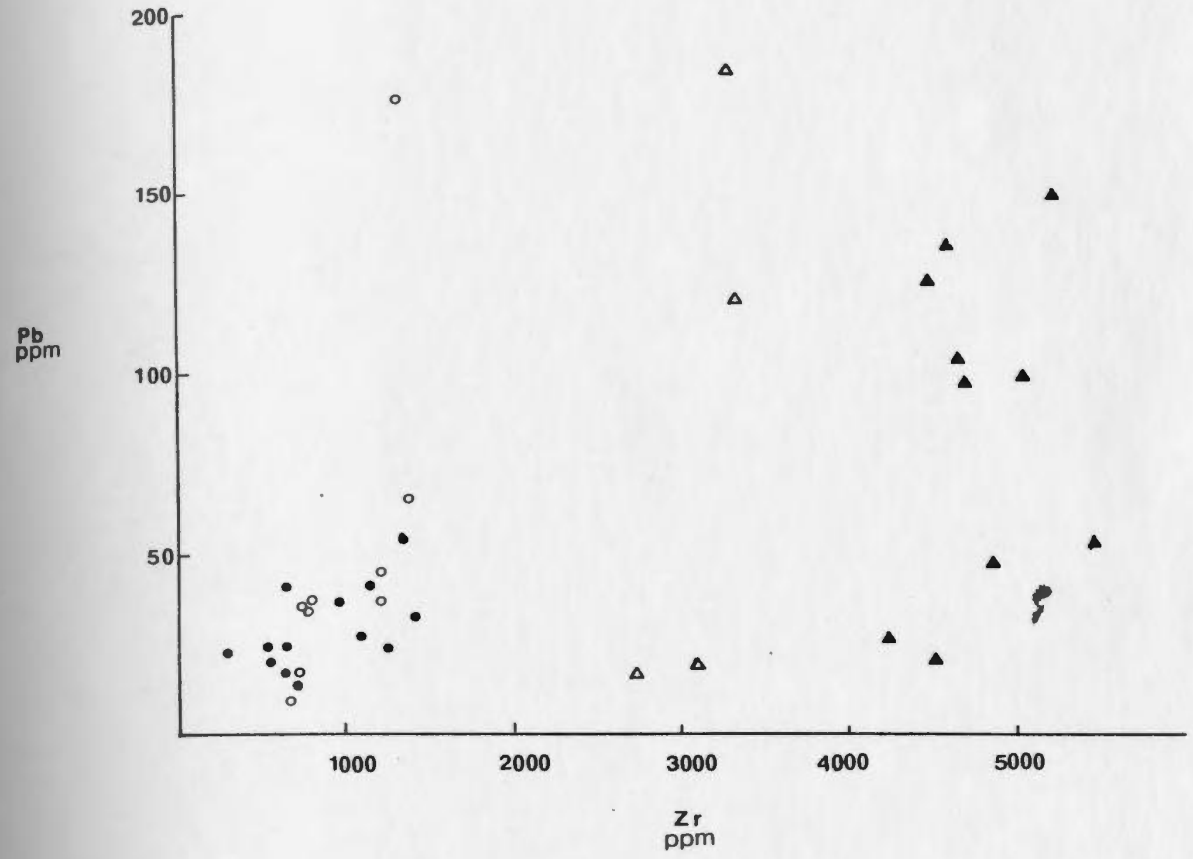
200
150
100
50
Pb
ppm
1000
2000
3000
4000
5000
Zr
ppm

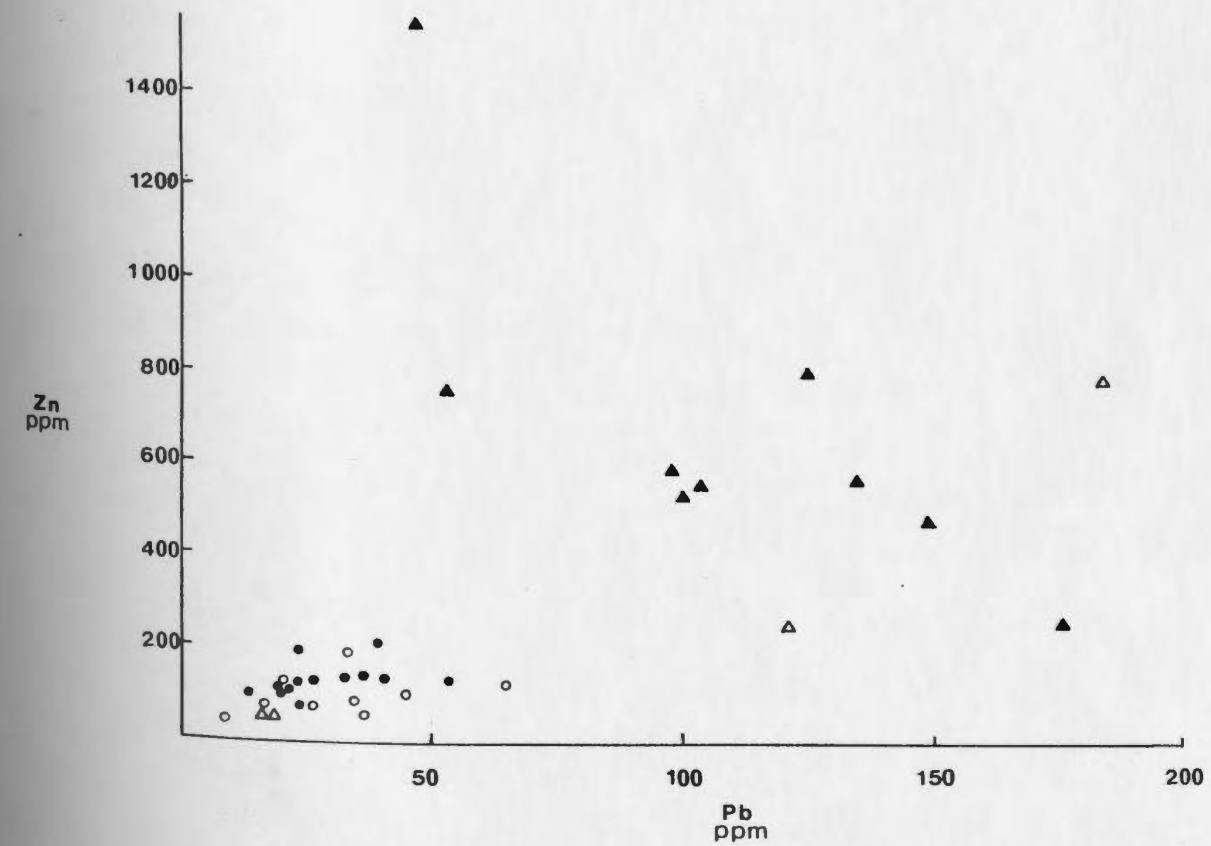
1400
1200
1000
800
600
400
200
Zn
ppm
50
100
150
200
Pb
ppm

Fig. 44. K/Rb vs Zr for the arfvedsonite-riebeckite granite and the Nuiklavick volcanics

Fig. 45. Ni vs Zr for the arfvedsonite-riebeckite granite and the Nuiklavick volcanics

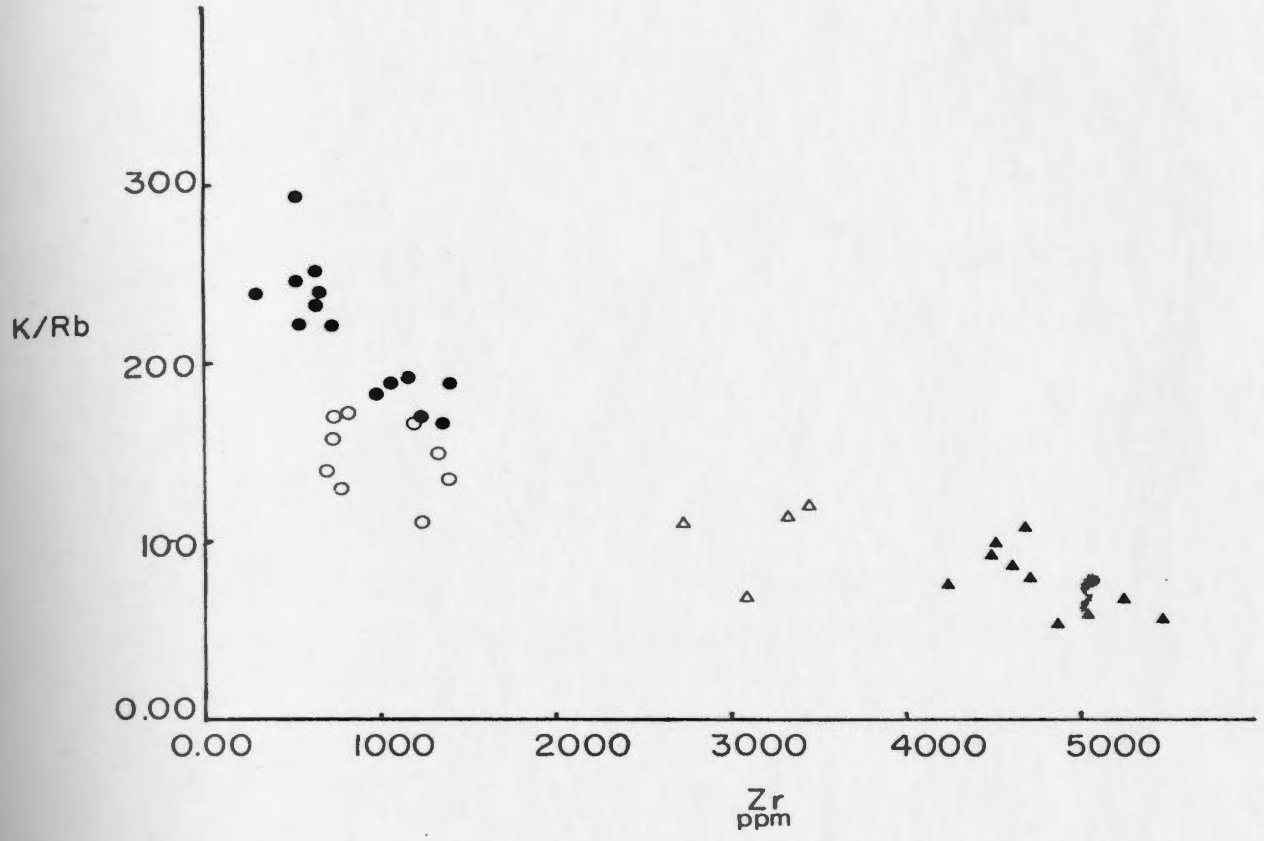
300
200
100
0.00
K/Rb
0.00
1000
2000
3000
4000
5000
Zr
ppm

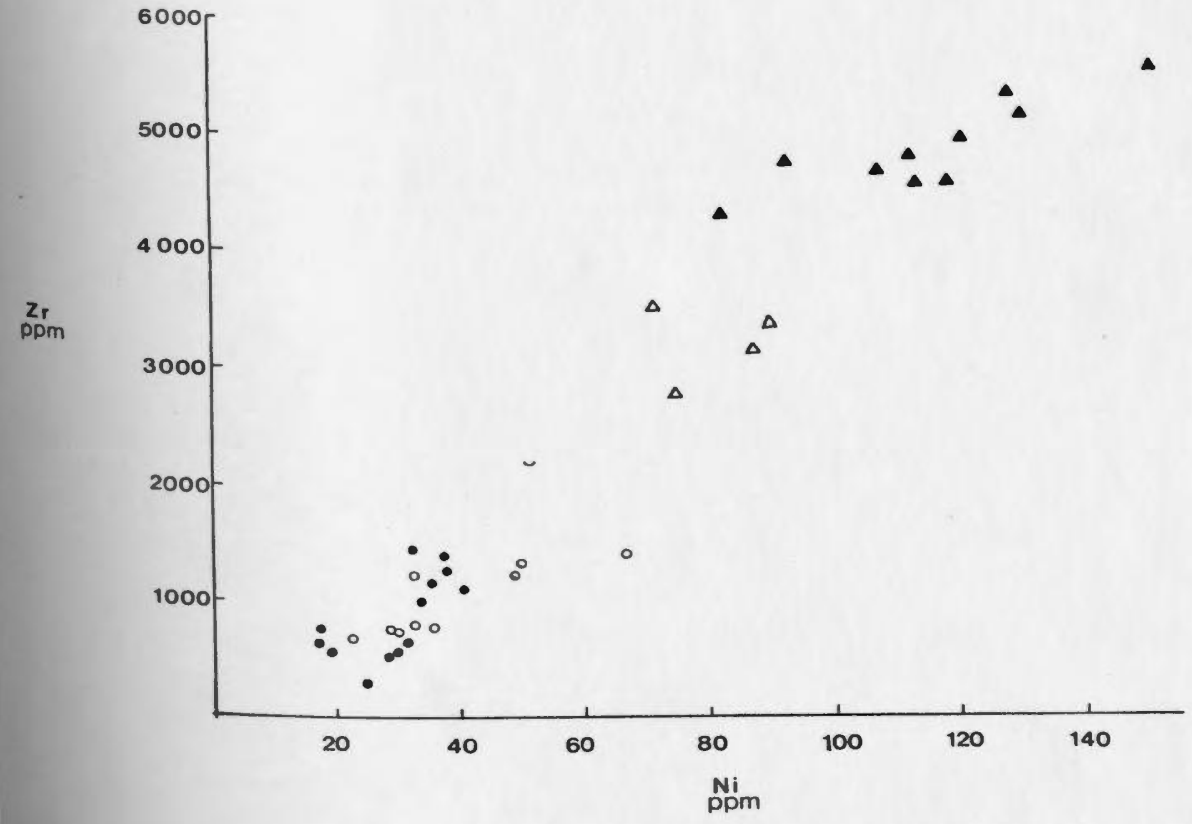
6000
5000
4 000
3000
2000
1000
Zr
ppm
20
40
60
80
100
120
140
Ni
ppm

Fig. 46. Ni vs Zn for the arfvedsonite-riebeckite granite and the Nuiklavick volcanics



Fig. 47. Ni vs K/Rb for the arfvedsonite-riebeckite granite and the Nuiklavick volcanics

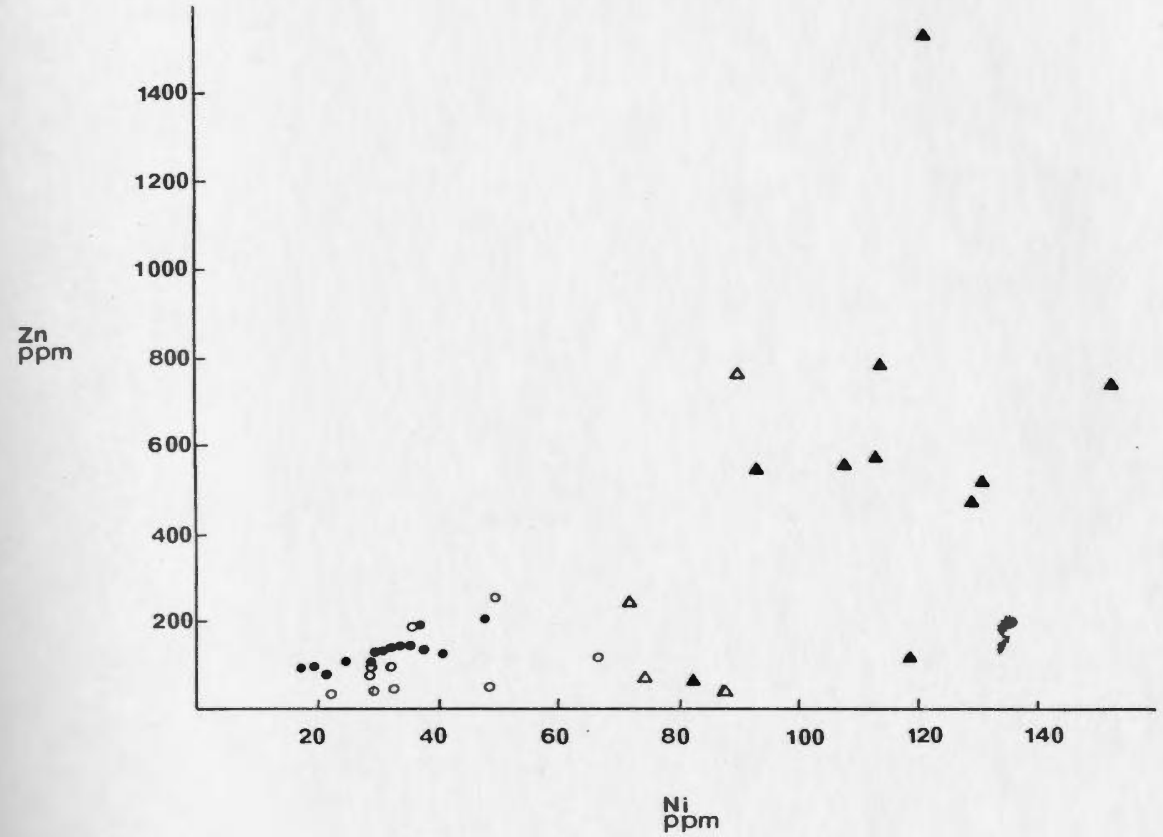
Zn
ppm
1400
1200
1000
800
600
400
200
20
40
60
80
100
120
140
Ni
ppm

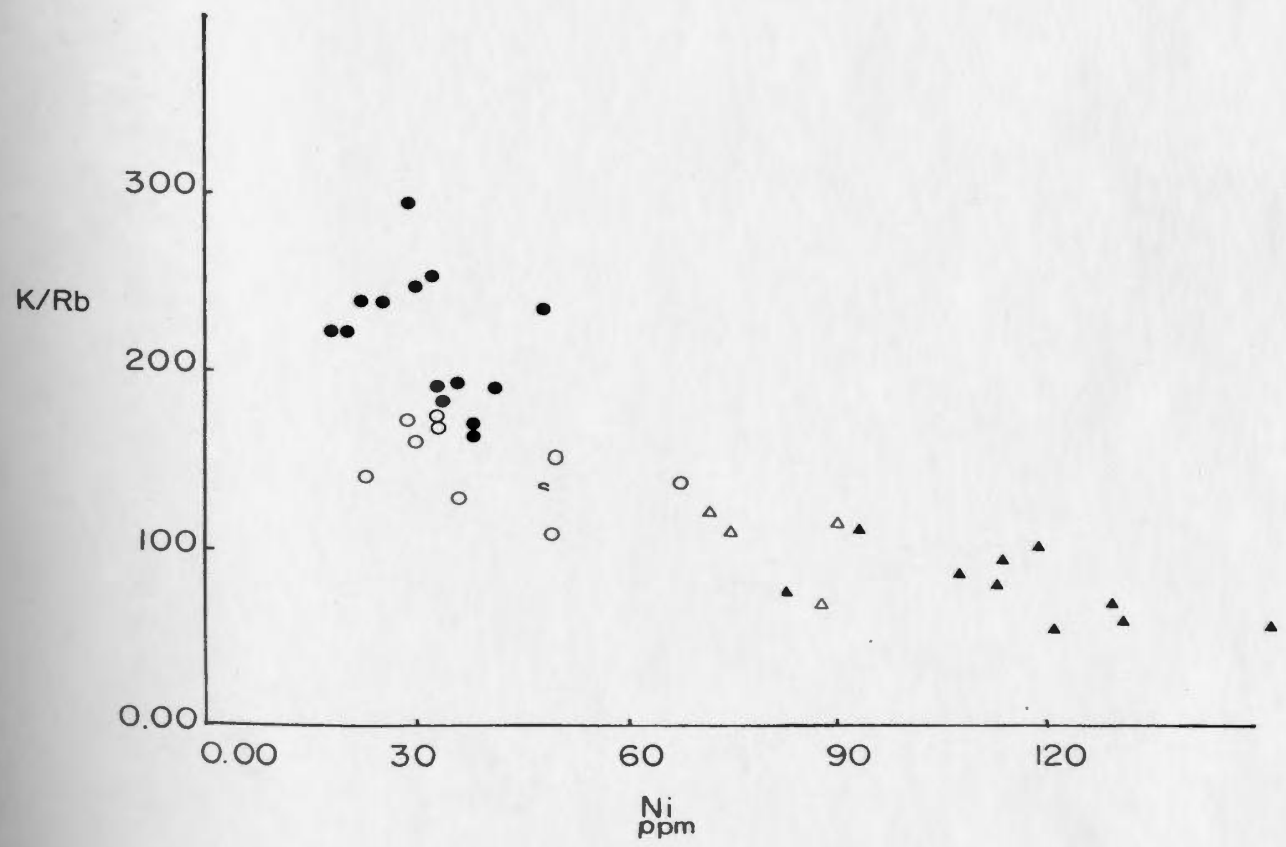
K/Rb
300
200
100
0.00
0.00
30
60
90
120
Ni
ppm

Fig. 48. Al vs Zr for the arfvedsonite-riebeckite granite and the Nuiklavick volcanics

Fig. 49. Ga vs Zr for the arfvedsonite-riebeckite granite and the Nuiklavick volcanics

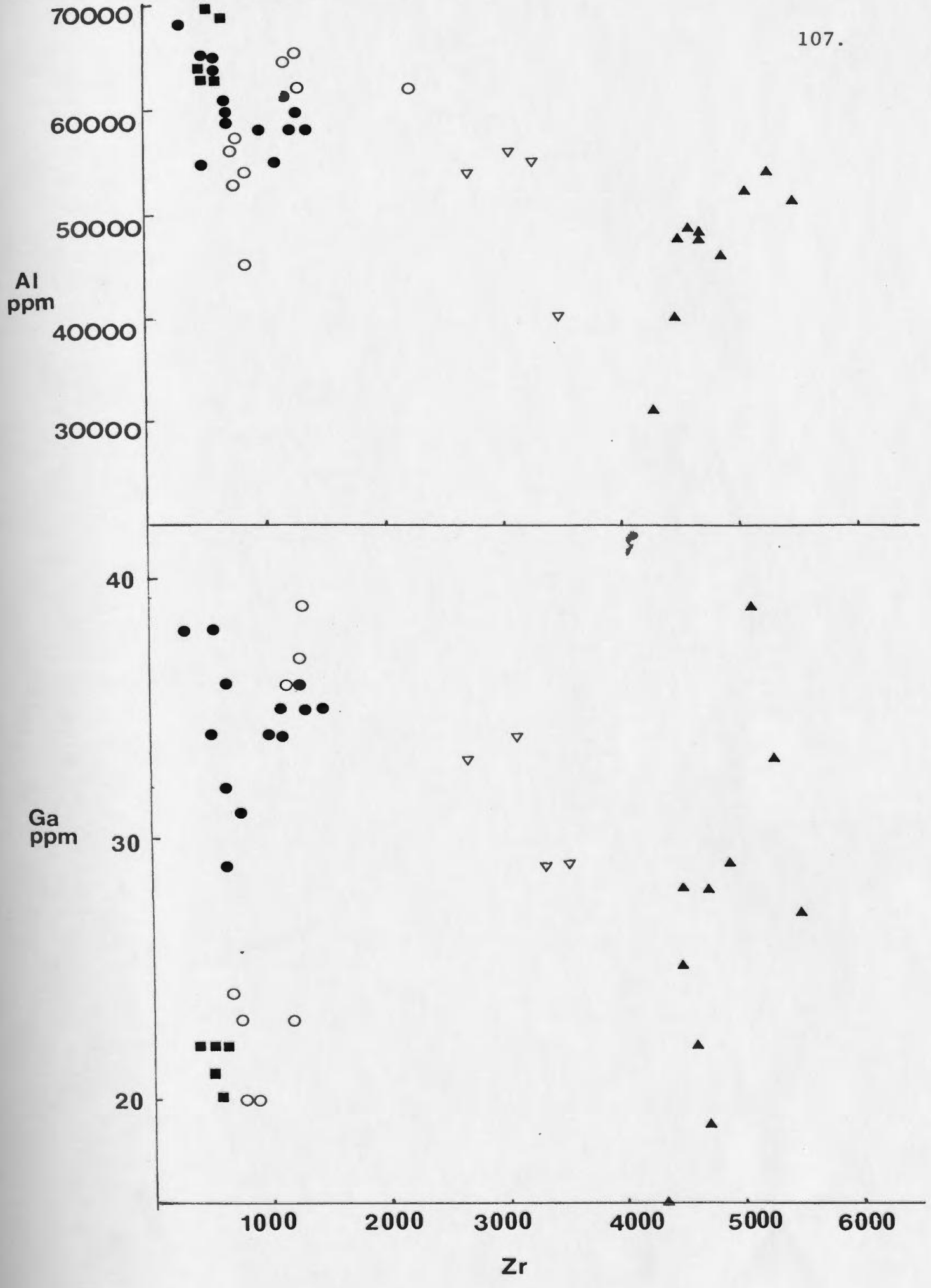
70000
60000
50000
Al
ppm
40000
30000
40
Ga
ppm
30
20
1000
2000
3000
4000
5000
6000
Zr

Fig. 50. Al vs Zn for the arfvedsonite-riebeckite granite and the Nuiklavick volcanics

Fig. 51. Ga vs Zn for the arfvedsonite-riebeckite granite and the Nuiklavick volcanics

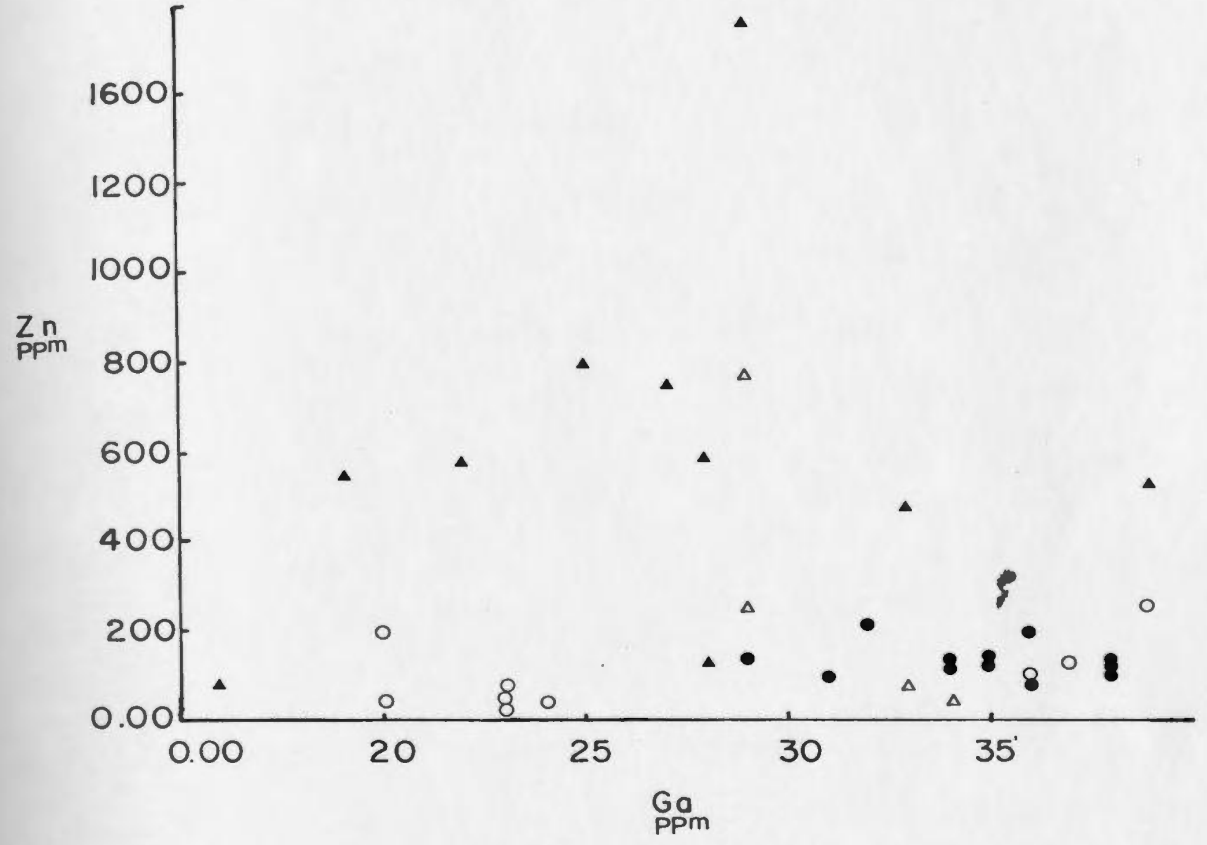
1600
1200
1000
Zn
PPm
800
600
400
200
0.00
0.00
20
25
30
35
Ga
PPm

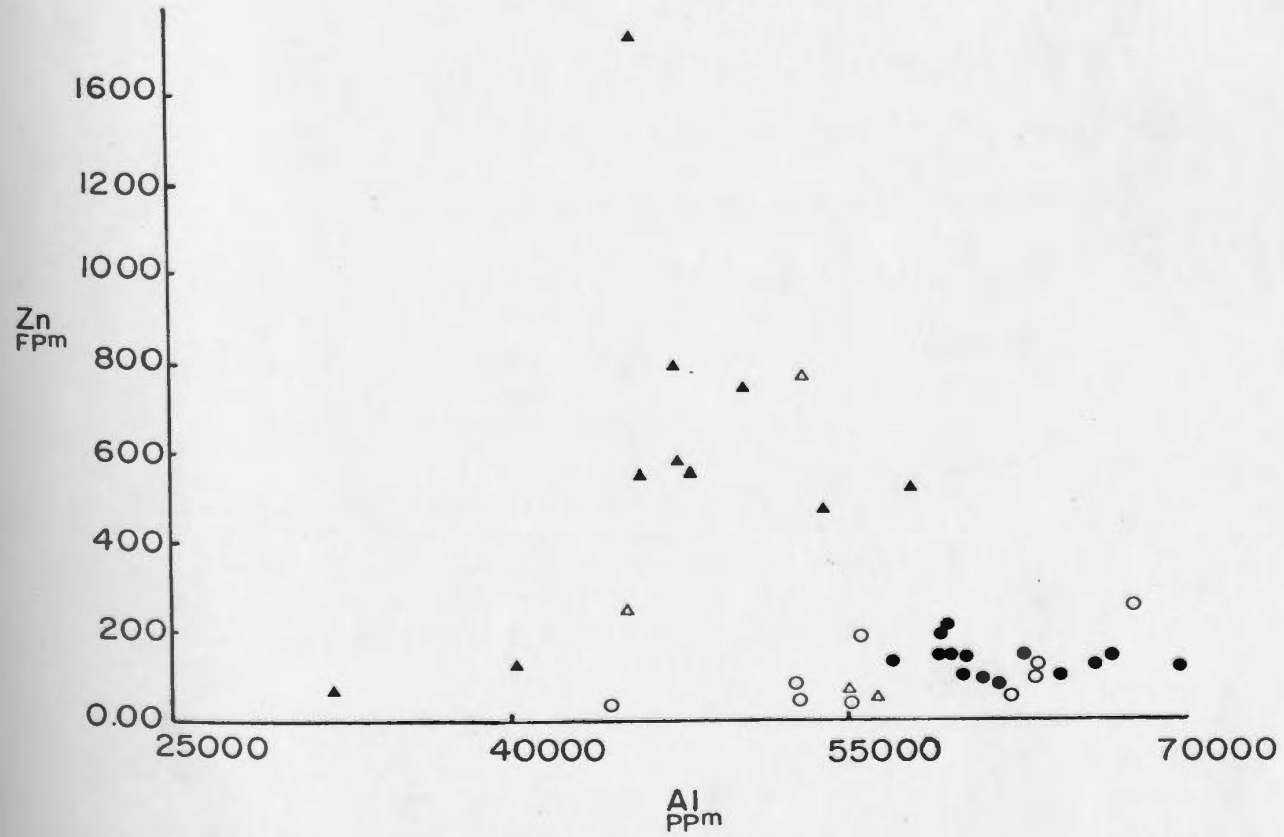
1600
1200
1000
Zn
FPm
800
600
400
200
0.00
25000
40000
55000
70000
Al
PPm

Rare Earth Element Geochemistry

The rare earth element patterns for geochemical Groups 1-3 are nearly identical but absolute abundances increase from Group 1 to Group 2 to Group 3 (Fig. 25). The light rare earths have a negative slope and are enriched relative to the heavy rare earths which have a tendency to flatten out. Eu is strongly depleted especially in Group 2. The total rare earth content of each group is greater than that of either the arfvedsonite-riebeckite granite or the clinopyroxene-fayalite granite.

Rare earth element trends of the Nuiklavick volcanics (especially Group 1) are similar to those of the arfvedsonite-riebeckite granite. Comparisons of the rare earth element patterns, ΣREE and the ratios ΣCe ΣY are particularly useful for demonstrating the similarity of the peralkaline granite and the volcanics (Fig. 20, Table 8).

Two samples of the peralkaline granite, 073 and 079, were selected for rare earth element analyses of their mafic and felsic fractions, and zircons in order to determine approximate partition coefficients. The felsic fraction consisted of quartz and feldspar, the mafic fraction contained all of the dark coloured, sodium-iron rich minerals. Analytical techniques and separation methods can be found in Appendix B.

True partition coefficients cannot be determined from granitic rocks but approximations can be derived from the ratio of concentrations in mineral separate to concentration in whole rock (Buma et al., 1971). Rare earth element patterns for approximate partition coefficients are

TABLE 8

AVEREGED ΣCe: ΣY RATIOS AND ΣREE FOR THE ARFVEDSONITE-RIEBECKITE GRANITE AND GROUPS 1-3 OF THE NUIKLAVICK VOLCANICS

| | ΣCe: ΣY | ΣREE* | |
|---|---|---|---|
| Arfvedsonite-riebeckeite granite | 13.9 | 668 | Ave. 13 |
| Group 1 | 13.5 | 781 | Ave. 9 |
| Group 2 | 4.2 | 1060 | Ave. 4 |
| Group 3 | 7.0 | 1578 | Ave. 10 |

*ΣREE = La + Ce + Nd + Sm + Gd + Dy + Er + Y

nearly identical for both the mafic and felsic fractions (Fig. 52). The only major difference between the two is in regards to concentration i.e. the mafic fraction is enriched ten times over the felsic fraction. The heavy rare earths are slightly enriched relative to the light rare earths with $\frac{Ce}{Y}$ less than one. Eu is depleted and both patterns have a minimum at Dy. Eu is somewhat dubious due to its very low levels and as a result it is difficult to know exactly what is happening.

Very little effort has been extended towards determination of partition coefficients in peralkaline rocks so it is difficult to make comparisons. Approximate partition coefficients have been determined for pyroxene, amphibole and feldspar for the Quincy granite in New England (Buma et al., 1971) but the resultant rare earth element patterns do not agree with those found in this study. Buma et al. (1977) did not find Eu depletion in the mafic minerals which had flat, negative slopes and the felsic fraction was enriched in Eu.

Examination of the zircon separate (Sample 73) indicated that both types described in Chapter 2 were present in the analyzed sample. Zircons contain very high concentrations of REE with the heavy rare earths enriched relative to the light rare earths but have no strong Eu anomaly (Fig. 53). Approximate partition coefficients have been determined and plotted. Zircons in a peralkaline environment produce a pattern similar to that of zircons from an alkaline environment (Buma et al., 1971, Fig. 53) but both are different from those found in non-alkaline environments (Nagasawa, 1970, Fig. 53). The heavy rare earth enrichment observed in

Fig. 52. REE for the mafic and felsic minual fractions each normalized to the whole rock.

●- mafic fraction/whole rock

◇- felsic fraction (x 10)/whole rock

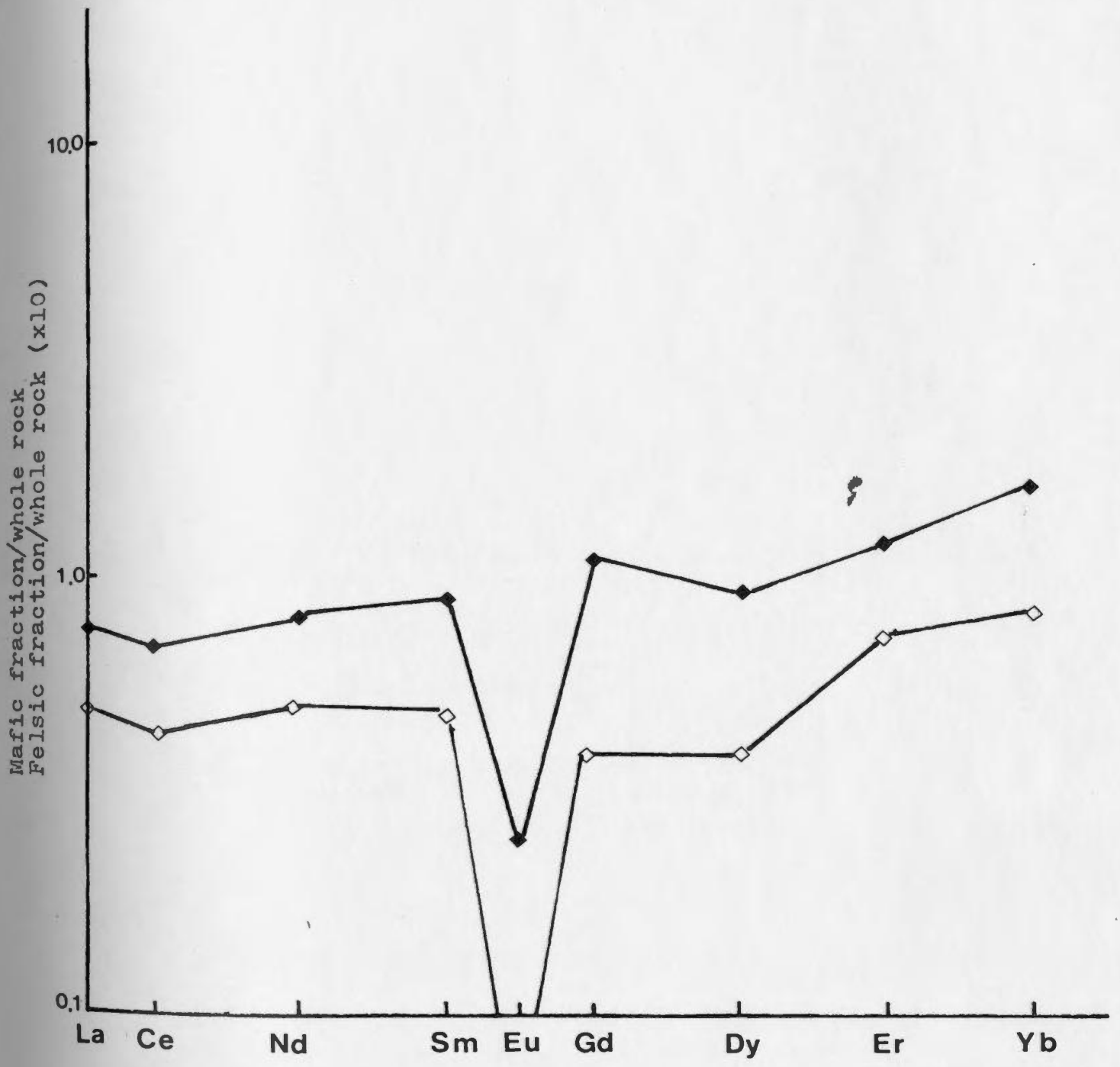
10,0
1,0
0,1
Mafic fraction/whole rock
Felsic fraction/whole rock (x10)
La
Ce
Nd
Sm
Eu
Gd
Dy
Er
Yb

Fig. 53. REE patterns for the zircon fraction normalized to the whole rock.

△ peralkaline granite - Davis Inlet

□ alkaline granite - New England (Buma et al., 1971)
(concentrations multiplied by 10)

○ calc-alkaline granite (Nagasawa, 1970)
(concentrations multiplied by 100)

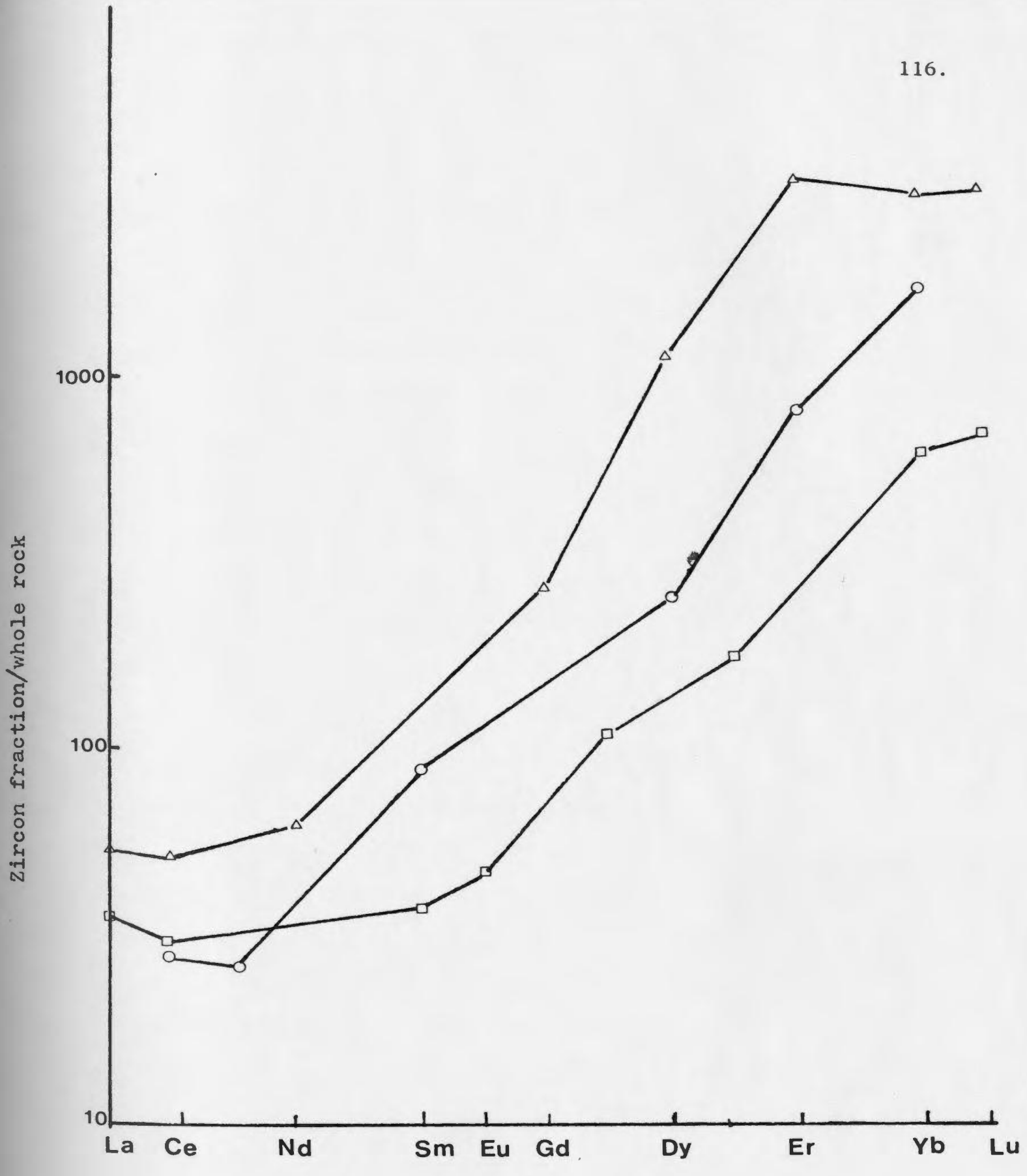
Zircon fraction/whole rock
1000
100
10
La
Ce
Nd
Sm
Eu
Gd
Dy
Er
Yb
Lu

zircons does not seem to be strongly affected by the alkalinity of the melt. The light rare earths, however, are affected by alkalinity, i.e. in non-alkaline granites there is a sharp upward trend from Ce to Sm but in an alkaline/peralkaline environment increasing concentrations between La and Sm are more gradual. In all three environments, Eu is strongly depleted in both the zircons and the host rock (Buma et al., 1971; Nagasawa, 1970).

Zircons become increasingly enriched in total REE with increasing alkalinity. REE concentrations are enriched as much as ten to one hundred times in alkaline and peralkaline environments (Fig. 53). Synthetic zircons that crystallized in a peralkaline environment produce a pattern similar to that of natural zircons but their concentrations are considerably higher (Watson, 1979, 1980).

REE patterns of both the granite and volcanics bear a strong resemblance to a peralkaline granite - Quincy granite in New England (Buma et al., 1971) and pantellerite and comendite from Nevada (Nobel et al., 1979) (Fig. 21). Group 3 of the Nuiklavick volcanics has concentrations very similar to those of the glassy pantellerite, the concentrations for all of the volcanics plus the arfvedsonite-riebeckite granite fall between those of the glassy comendite and pantellerite. In the Davis Inlet area, rare earth element enrichment corresponds to that of the residual elements. The two volcanic types used for comparison become increasingly enriched in rare earths in a manner which corresponds to increasing peralkalinity. In both cases, the volcanics are enriched relative to the intrusive phase(s), but it must be remembered that the granitic and volcanic samples used for comparison are not related.

Fig. 54. Er vs Zr for the arfvedsonite-riebeckite granite and the Nuiklavick volcanics

Fig. 55. La vs Zr for the arfvedsonite-riebeckite granite and the Nuiklavick volcanics

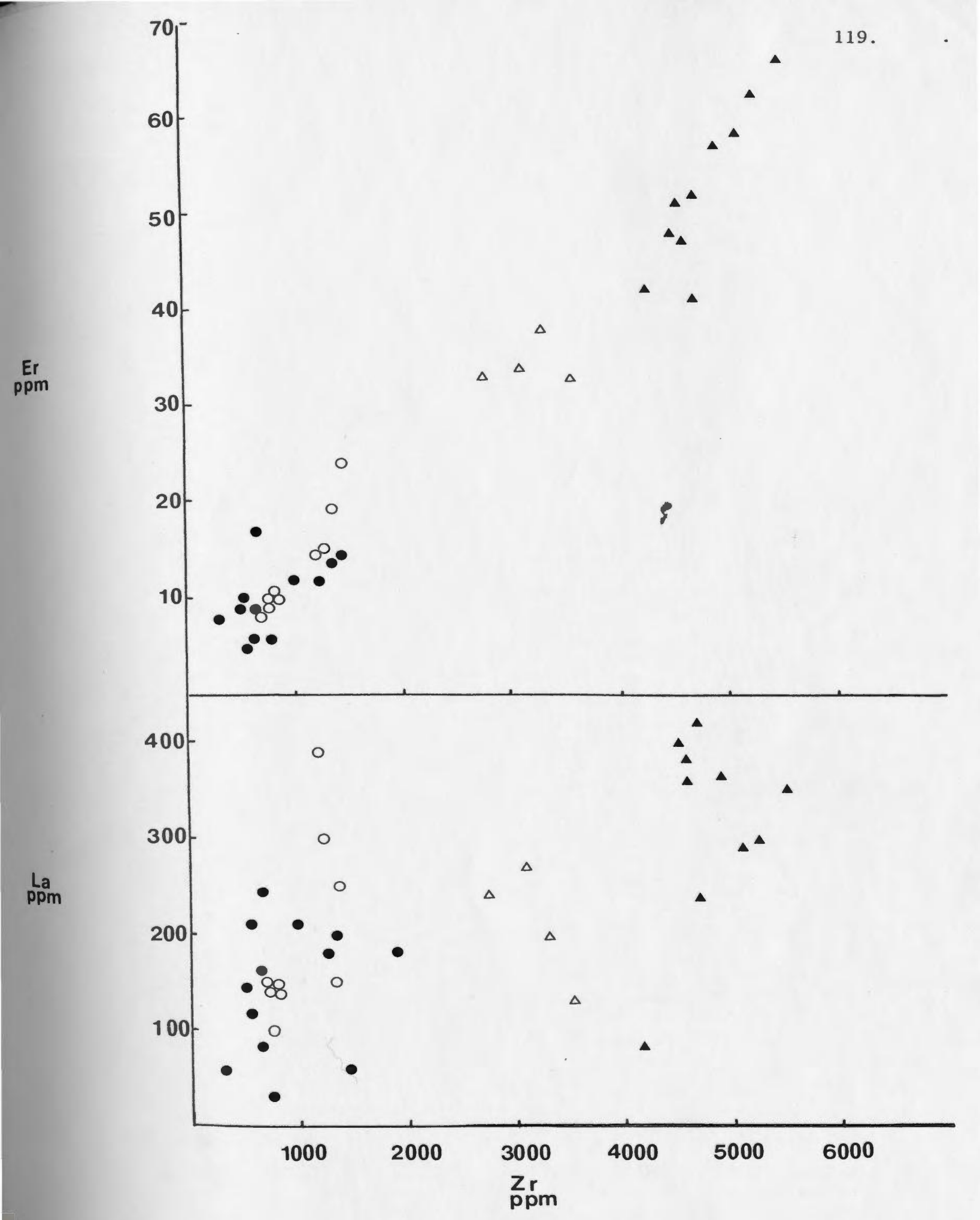
70
60
50
40
30
20
10
Er
ppm
400
300
200
100
La
ppm
1000
2000
3000
4000
5000
6000
Zr
ppm

Fig. 56. Ce vs Zr for the arfvedsonite-riebeckite granite and the Nuiklavick Volcanics

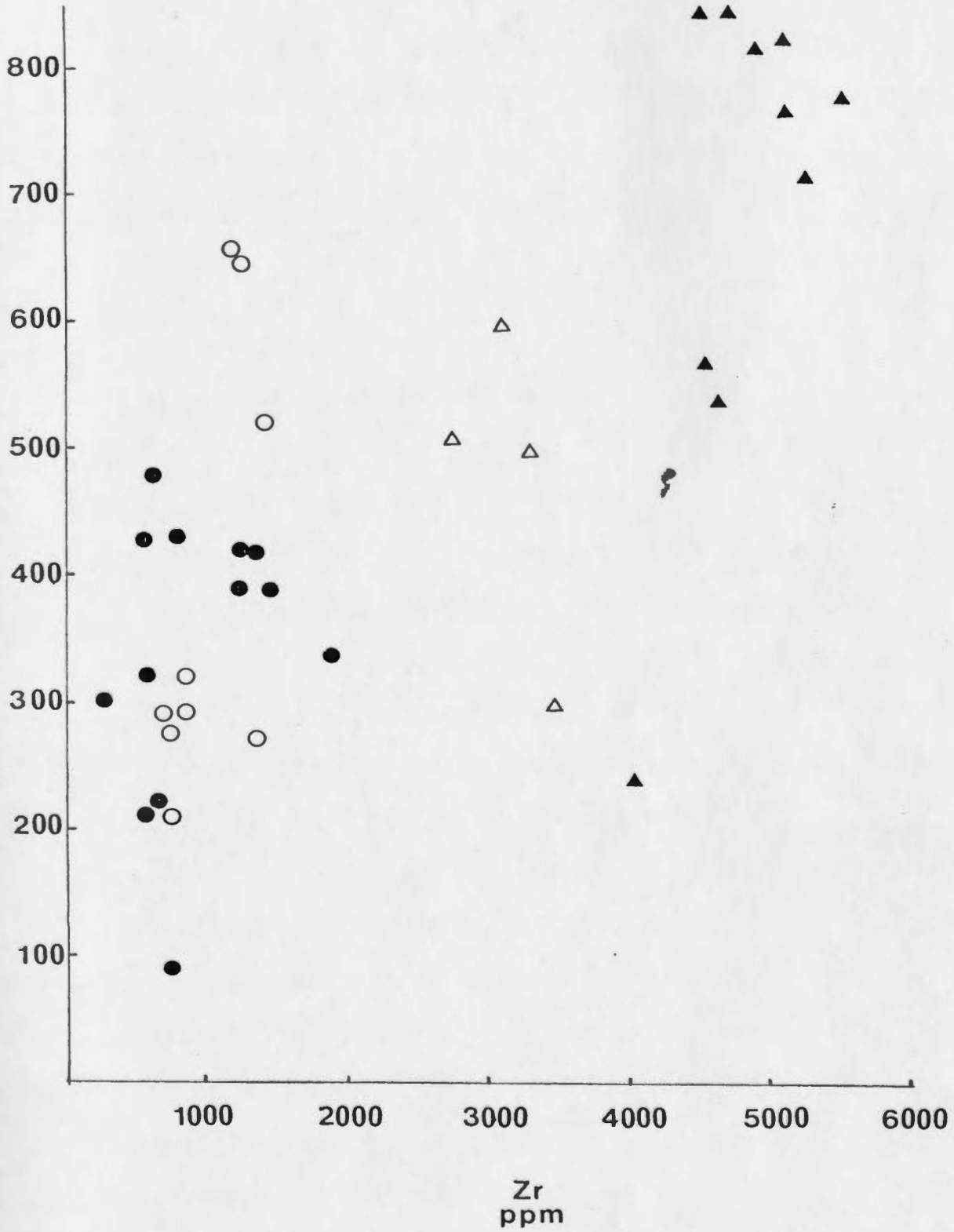
800
700
600
500
400
300
200
100
Ce
ppm
1000
2000
3000
4000
5000
6000
Zr
ppm

Like the arfvedsonite-riebeckite granite, there is a strong correlation between the heavy rare earths and residual elements such as Zr (Figs. 54-56). There is a strong similarity between the trends of Zr-Er and Zr-Th or Nb but not much resemblance for Zr-La or Ce.

SUMMARY

The geochemical characteristics of the clinopyroxene-fayalite granite are considerably different from those of the arfvedsonite-riebeckite granite or the Nuiklavick volcanics. Rare earth and other trace elements trends and in many cases concentrations are significantly different. Trends observed for the clinopyroxene-fayalite granite are often the complete opposite of those observed in arfvedsonite-riebeckite granite. A good example is the behaviour of Ba which is enriched in the clinopyroxene-fayalite granite but very depleted in the arfvedsonite-riebeckite granite. The REE patterns of these two granites are strikingly different, bearing almost no resemblance to each other.

The similarity of the arfvedsonite-riebeckite granite to the Nuiklavick volcanics has been documented on the basis of major, minor and trace (including the RE) elements. Group 1, the quartz-feldspar porphyry, is especially similar to the arfvedsonite-riebeckite granite indicating a direct petrogenetic relationship. Table 9 is a chart showing the similarities in behaviour of individual elements in the peralkaline suite. The most notable observations include the characteristic patterns produced by Zr, Zn and the ratio K/Rb. Table 9 and the figures in this chapter

TABLE 9

SUMMARY OF TRACE ELEMENT TRENDS ON CORRELATION DIAGRAMS

Plots of any combination of:

Zr, Y, Nb, Th, Ni

are essentially linear but may vary slightly for the highest values.

Plots of Zn or Pb vs

Zr, Y, Nb, Th, Ni

are curved with Zn and Pb increasing in concentration with increasing Zr, Y, Nb, Th, Ni.

Plots of K/Rb ratios vs

Zr, Y, Nb, Th, Ni, Zn, Pb

curves, K/Rb decreases with increasing concentrations of Zr, Y, Nb, Th, Ni, Zn, Pb.

Plots of Ga

are similar to plots with Al.

(and Appendix D) illustrate the consistency of the behaviour of the residual elements characteristic of peralkaline rocks. Ga, Ba, Sr, Cr, Cu cannot be included in this group but Ba and Sr do have a type of behaviour which is characteristic of peralkalinity, i.e. extreme depletion. The behaviour of Ga is quite compatible with that of Al. Cr is somewhat of an enigma because it is enriched relative to an average granite composition. The residual elements characteristic of peralkaline rocks increase with increasing peralkalinity (alkalinity) but Cr does not, it decreases in concentration as expected.

# CHAPTER 4

# DISCUSSION

The major components in felsic igneous rocks are silica, alumina and the alkalies. The alkalies are very susceptible to alteration which impedes the interpretation of major element chemistry. The granites at Davis Inlet can be classified on the basis of major elements as peralkaline (arfvedsonite-riebeckite granite) and non-peralkaline (clinopyroxene-fayalite granite). The Nuiklavick volcanics are severely depleted in sodium making interpretations based on major elements unrealistic. Therefore, loss of alkalies (predominantly sodium) from the Nuiklavick volcanics will be the only feature of major element chemistry to be discussed in detail.

## SODIUM DEPLETION

Sodium loss from peralkaline volcanics is not unusual nor unexpected. In the Nuiklavick volcanics sodium losses are as high as 100%, much greater than any reported in the recent literature (e.g. Baker and Henage, 1977). A small amount of potassium depletion accompanies sodium loss in the rhyolite and tuff but not in the quartz-feldspar porphyry. Sodium has been lost preferentially from the groundmass and altered feldspar phenocrysts. Unaltered feldspar phenocrysts have normal albitic lamellae.

Sodium depletion in peralkaline rocks has been attributed to groundwater rock interaction (Noble, 1967; Scott, 1971; Kochaar, 1977) and alkali ion exchange between the magma and an accompanying aqueous phase

and/or the expulsion of sodium rich vapours or fluids during the last stages of crystallization (Noble, 1970; Baker and Henage, 1977). Some evidence suggests that sodium loss may be proportional to the peralkalinity and the amount of normative sodium metasilicate (Noble, 1967; Kogarko, 1974; Baker and Henage, 1977).

Direct evidence of intense groundwater interaction and low temperature hydrothermal alteration is provided by devitrified glass and sericitized phenocrysts. These processes can also account for potassium depletion from the extrusive rocks. However, the extreme sodium losses encountered suggest that much of the sodium may have been lost through the expulsion of an alkali-rich volatile phase during the final stages of emplacement. The genetic relationship between the Nuiklavick volcanics and the peralkaline granite and the presence of a volatile phase (especially in the granite) has been documented in Chapters 2 and 3. Some workers have established that the amount of sodium lost may be determined by the degree of the peralkalinity of the original melt (Noble, 1970; Baker and Henage, 1977). Therefore, it is possible that the extreme sodium depletion of the Nuiklavick volcanics may reflect the extremely peralkaline nature of the original melt.

## TRACE ELEMENT RELATIONSHIPS

Trace elements have been used to describe the relationship of the two granites and the volcanics. The clinopyroxene-fayalite granite does not appear to be directly related to the peralkaline arfvedsonite-riebeckite granite. Geochemical trends on correlation diagrams (Figs.

16-19) give no indication of any genetic relationship between the two granites. Both the non-peralkaline and the peralkaline granites were compared with an average granite composition (Fig. 15). Enrichment trends of some elements such as Zn, Ni, Er, Y, Nb, and Zr are similar but the relative amounts differ (Fig. 22). Other elements, such as Rb, Ba, Cu, Pb, Cr, La and Th show divergent behaviour (Fig. 22).

The trace element characteristics of the arfvedsonite-riebeckite granite, like the Nuiklavick volcanics, are similar to those normally found in oversaturated peralkaline rocks and are summarized in Table 10. Both correlation and enrichment diagrams (Figs. 22, 38-51, Appendix D) demonstrate the similarity of trace element behaviour between the peralkaline granite and the Nuiklavick volcanics, especially the quartz-feldspar porphyry. Zinc is characteristically enriched in peralkaline rocks (Nicholls and Carmichael, 1969; Bowden and Kinnaird, 1978) and some cases of possible nickel enrichment have been reported (Hussey, 1979; Taylor et al., 1980). Occasionally lead is enriched in peralkaline rocks. In this case it seems to be associated with zinc. Plots of abundances of zinc or lead against Zr, Th, Y, Nb, Ni and K/Rb (Fig. 31 and Appendix D) are very similar. Zinc, zirconium and the K/Rb ratio exhibit especially distinctive behaviours, i.e. where these are plotted against the other trace elements characteristic patterns are produced. The correlation of Ni and Pb with the "residual elements" characteristic of peralkaline rocks suggests that they should be included in this group.

TABLE 10

SOME CHEMICAL CHARACTERISTICS OF PERALKALINE ROCKS

(Compiled from Nicholls and Carmichael, 1969)
and Ferrara and Treuil, 1974)

| | Enriched | | Depleted |
|---|---|---|---|
| a. | Alkalies, iron | a. | Alkaline earths especially Ba, Sr |
| b. | REE (except Eu) | b. | Majority of transition elements belonging to the 3rd series particularly S, U, Cr*, Co, Ni*, Ca |
| c. | Zn, Be | c. | Eu |
| d. | Halogens F, Cl | d. | Al, Mg, Ca |
| e. | Highly charged elements: Zr, Hf, Nb, Ta, Mo, W, U, Th | | |
| | low K/Rb, K/Cs, Zr/Hf | | |

* Cr and nickel are generally included in the list of depleted elements but several cases of enrichment have been reported (Hussey, 1979; Taylor et al., 1980).

Experimental studies of zirconium solubility show marked contrasts in peralkaline and non-peralkaline environments (Deitrich, 1968; Watson, 1979, 1980). In the $SiO_2$-$Al_2O_3$-$Na_2O$-$K_2O$ system, the saturation of Zr is governed by the agpaitic index of the melt but remains remarkably insensitive to temperature, silica concentration or the $Na_2O/K_2O$ ratio (Deitrich, 1968; Watson, 1979, 1980). In non-peralkaline melts, concentrations of zirconium as low as 100 ppm are sufficient for zircon crystallization but in a peralkaline melt, saturation levels are considerably higher (Watson, 1979). Zirconium in a peralkaline environment is retained in solution probably because it exists in the form of complexes with the alkalies which cause its increased solubility (Balashov, 1966; Watson, 1979). Because of the increased solubility of zirconium in peralkaline melts, zircons do not crystallize at an early stage as in other granitic melts. This explains how zirconium can be present in high concentrations ( 500 ppm) but with few if any zircons being present, as well as the different morphology of zircons in peralkaline granites (Watson, 1979; Pupin, 1980).

Like zirconium, zinc enrichment has come to be considered a characteristic of peralkaline rocks (Bowden and Kinnaird, 1978; Taylor et al., 1980). Under normal conditions zinc is chalcophile and thus concentrated in sulphides or more rarely in Fe-Mg silicates (Goldschmidt, 1954). In peralkaline rocks zinc is most commonly found replacing $Fe^{2+}$ in sodic pyroxene, sodic amphibole, aenigmatite and astrophyllite (MacDonald and Saunders, 1973; Bailey and MacDonald, 1975; Novak and Rankin, 1980).

During differentiation of a magma, the behaviour of zinc is generally governed by the basicity which is analogous to the concentration and behaviour of $Fe^{2+}$, Mg and Mn such that zinc may substitute for them in the common rock forming minerals during crystallization (Gaurilin and Pevtsova, 1975). However, in alkaline/peralkaline rocks, zinc behaves independently of the ferromagnesian elements (Zlobin and Gorshkova, 1961). This explains the presence of zinc in ferromagnesian minerals where $Fe^{2+}$:Zn ratios do not reflect any differentiation (Zlobin and Gorshkova, 1961).

The relationship between $Fe^{2+}$ and Zn reflects the increased solubility of zinc in peralkaline melts, hence its enrichment. Experimental studies have shown that zinc solubility in aqueous solutions with NaOH is directly related to Na concentration and temperature (Khodakovskiy and Yelkin, 1975). These studies suggest that zinc is present in the form of ionic complexes which results in its increased stability in aqueous solutions.

The behaviour of lead resembles zinc in alkaline melts and hydrothermal systems (Zlobin and Gorshkova, 1961; Gavrilin and Pevtsova, 1975). The behaviour of lead is generally governed by the alkalinity of the melt (primarily K) as it substitute for K in silicate minerals during crystallization (Zlobin and Gorshkova, 1961; Gavrilin and Pevtsova, 1975). However, K:Pb ratios in very sodic rocks do not significantly reflect any type of differentiation indicating that lead, like zinc, has been influenced by other processes during the evolution of peralkaline rocks.

Low K/Rb ratios are also characteristic of peralkaline rocks with ratios generally between 150-300 but some ratios, less than 100, have been reported (Shaw, 1968; Bowden and Turner, 1974; Taylor et al., 1980). Generally the K/Rb ratio is regarded as a sensitive measure of hydrothermal activity (Shaw, 1968). It has been shown that K/Rb ratios in pegmatites and metasomatized granitic rocks are considerably lower than those normally found in granites (Shaw, 1968). Low K/Rb ratios in oversaturated peralkaline rocks reflect an increase in Rb and not a decrease in K. The relationships of Rb to both major and trace elements cannot reflect a fractionation sequence and the system is open to Rb (Nicholls and Carmichael, 1969; Bailey and MacDonald, 1975; Taylor et al., 1980). The correlation between the behaviour of Rb and the other trace elements such as Zr, Nb, Th, Zn and others suggests that the system must be open to these other trace elements as well.

The peralkaline rocks at Davis Inlet exhibit strong enrichment of the highly charged cations (Nb, Th, Zr, Y) as well as Zn, Ni and Pb and extreme depletion of Ca, Mg, Ba and Sr with progressive enrichment of Rb. Enrichment depletion trends correlate systematically with: (1) increasing peralkalinity; (2) an increase in metasomatic alteration; and (3) increasingly higher levels, i.e. the extrusive rocks.

The observed trends and patterns of the Davis Inlet suite are similar to those of other peralkaline rocks from Nigeria (Bowden and Turner, 1974; Bowden and Kinnaird, 1978), the East African Rift zone (Ferrara and Treuil, 1974; Bailey and MacDonald, 1975), and the Topsails

Complex of central Newfoundland (Taylor et al., 1980). The Davis Inlet Suite is more highly evolved than other examples with greater abundances of elements such as Zr, Zn, Ni (Table 11). Study of the peralkaline rocks at Davis Inlet provides convincing evidence of a direct correlation between increasing nickel concentration and increasing peralkalinity which has been intimated by others (Hussey, 1979; Taylor et al., 1980). This behaviour is the converse of that expected for nickel, which suggests that in peralkaline environments nickel, like zinc and lead, is governed by processes other than normal crystal-silicate liquid differentiation.

Geochemical trends and enrichment patterns for the residual trace elements characteristic of peralkaline rocks (including Ni and Pb) suggests that common mechanisms are responsible for their concentration. Experimental and empirical evidence indicate that zirconium and zinc exist as complexes in peralkaline melts. The correlations between the behaviour of Zr, Zn and the other residual trace elements suggests that they too exist in the form of complexes. The highly charged cations form complexes more readily than zinc, nickel, lead and rubidium. As a result the latter are enriched to a lesser degree.

Rare earth element patterns of the rocks from Davis Inlet substantiate trace element evidence for: (1) the peralkaline nature of the Nuiklavick volcanics (Fig. 21, Table 8); (2) the absence of a direct genetic relationship between the peralkaline and non-peralkaline granites; and (3) the consanguinity of the peralkaline granite and the Nuiklavick volcanics.

Table 11

Comparison of average compositions for peralkaline granite, quartz, feldspar, porphyry and volcanics from the Davis Inlet area and from the Topsails Complex of Central Newfoundland (Taylor et al, 1980; Taylor pers. comm. 1980)

| | Davis Inlet | | | Topsails Complex | | |
|---|---|---|---|---|---|---|
| | Peralkaline Granite | Quartz-feldspar Porphyry | Rhyolite/ Tuff Group | Peralkaline Granite | Quartz-feldspar Porphyry | Volcanics |
| $SiO_2$ | 72.37 | 76.67 | 78.04 | 75.88 | 74.77 | 75.47 |
| $Al_2O_3$ | 11.51 | 10.92 | 8.46 | 12.16 | 11.93 | 10.60 |
| $Fe_2O_3$ | 1.58 | 0.77 | 1.80 | 1.10 | 2.01 | 2.32 |
| FeO | 2.47 | 2.07 | 3.47 | 1.08 | 1.9 | 1.02 |
| MgO | 0.095 | 0.09 | 0.03 | 0.08 | 0.18 | 0.09 |
| CaO | 0.68 | 0.42 | 0.18 | 0.25 | 0.34 | 0.14 |
| $Na_2O$ | 4.62 | 0.71 | 0.11 | 4.11 | 4.10 | 4.39 |
| $K_2O$ | 4.72 | 4.73 | 3.19 | 4.03 | 4.55 | 4.50 |
| $TiO_2$ | 0.40 | 0.35 | 0.36 | 0.23 | 0.18 | 0.20 |
| MnO | 0.09 | 0.10 | 0.10 | 0.06 | 0.06 | 0.05 |
| $P_2O_5$ | 0.02 | 0.006 | - | 0.01 | 0.10 | 0.003 |
| LOI | 0.76 | 1.79 | 1.40 | 0.38 | 0.77 | 0.63 |
| Nb | 78 | 112 | 375 | 25 | 43 | - |
| Th | 22 | 28 | 241 | - | 15 | 33 |
| Zr | 851 | 1000 | 4805 | 570 | 509 | 1466 |
| Y | 106 | 125 | 492 | 307 | 78 | 190 |
| Sr | 15 | 14 | 8 | 14 | 14 | 5 |
| Rb | 189 | 270 | 387 | 125 | 92 | 206 |
| Pb | 28 | 51 | 86 | 20 | 18 | 34 |
| Cr | 13 | 7 | 1 | 4 | 7 | 1 |
| Ga | 35 | 27 | 27 | 27 | 18 | 28 |
| Zn | 135 | 108 | 597 | 103 | 95 | 217 |
| Ca | 7 | 7 | 6 | 15 | 11 | 18 |
| Ni | 32 | 39 | 116 | 11 | 6 | 33 |
| Ba | 97 | 186 | 22 | 375 | 418 | 2 |

Systematic increases in REE and decreases in Ce: Y from the intrusive to extrusive rocks corresponds to trace element enrichment patterns. This suggests that there is a strong correlation between REE (especially HREE) and the residual elements characteristic of peralkaline rocks (Figs. 39, 54, and 55, Appendix D). Figure 56 shows trace and rare earth element distributions of the rhyolite-tuff group normalized to the peralkaline granite. This type of diagram effectively demonstrates the enrichment trends of the lanthanides and the residual elements characteristic of peralkaline rocks for the Davis Inlet suite.

Further evidence of a correlation between the HREE and the residual trace elements characteristic of peralkaline rocks is demonstrated by plotting the REE against Zr (Figs. 54 and 55). The correlation between Er and Zr is much stronger than that of La or Ce and Zr. The trend for Er vs Zr is very similar to those of Th, Nb or Ni vs Zr (Figs. 38, 40, 45, and 54, Appendix D), suggesting that both the HREE and the trace elements were affected by the same mechanisms.

## REE RELATIONSHIPS

Data on REE abundances and trends in peralkaline environments is limited but the available data indicates variations in their behaviour not only between peralkaline and non-peralkaline environments but between over-saturated and under-saturated melts. Some of these differences are vital to the interpretation of the rocks in this study. Thus, some of the properties and characteristics of REE in peralkaline environments will be discussed briefly.

The rare earth elements generally behave as a group but they exhibit two contrasting, variable properties: (1) ionic radius; and (2) degree of basicity, which gives rise to two schools of thought on their behaviour (Mineyev, 1963). One suggests that REE fractionation is explicable in terms of crystal chemistry alone, i.e. fractionation according to ionic radii (Mineyev, 1963). Others suggest that the REE are fractionated according to their degree of basicity, i.e. geochemical differences within the group account for differentiation trends (Mineyev, 1963). The latter, has become increasingly accepted especially for explaining such phenomena as REE complexing in alkaline/peralkaline melts. Various physicochemical parameters such as acidity and the ease with which elements form complexes play major roles in REE differentiation, migration and concentration in solution (Mineyev, 1963). These factors (and probably others) account for the characteristics of REE and their complexes which are summarized in Tables 12 and 13.

The complexes thought to be formed by trace and rare earth elements take various forms ranging from simple ones like $NaYF_4$ or $Na_5Ce_3F_{14}$ to much more complex ones (Balashov, 1963; Mineyev, 1963; Moeller, 1972). The characteristics of REE in Table 13 suggest that their concentration in peralkaline rocks is directly related to their greater ease of complex formation within highly sodic and/or hydrothermal systems. The ability of REE to form ionic complexes with volatiles results in increased stability and mobility which allows them to become concentrated by geochemical processes involving volatile activity such as in a discrete volatile phase or volatile migrations (Mineyev, 1963).

TABLE 12

A SUMMARY OF REE CHARACTERISTICS OF OVERSATURATED PERALKALINE ROCKS

(compiled from Balashov (1962, 1963, 1966), Mineyev (1963))

- REE concentrations are higher in oversaturated peralkaline rocks than in non-peralkaline or undersaturated peralkaline rocks

- $\Sigma Ce:\Sigma Y$ is lower in oversaturated peralkaline rocks than in non-peralkaline or undersaturated peralkaline rocks

- REE increase in a manner directly proportional to the agpaitic index or the degree of peralkalinity

- Increases in agpaitic index are accompanied by increased concentrations of the basic lanthanides (HREE)

- The rare earth elements tend to exist in the form of complexes in alkaline environments

TABLE 13

A SUMMARY OF THE CHARACTERISTICS OF REE COMPLEXES IN OVERSATURATED PERALKALINE ROCKS

1. The stability of complexes increases from La-Yb favouring longer retention of the basic HREE in the melt and a relative concentration of REE in the last stages of differentiation (Balshov, 1962)

2. Complexing is responsible for the high degrees of fractionation of REE in alkaline igneous intrusives

3. REE complexes are stable under hydrothermal and supercritical conditions

4. REE are often paragenetically associated with typical complex forming elements ($Al_3$, Be, Fe, Zr, Sn, etc.) and ligands ($F^-$, $Cl^-$, $CO_3^{2-}$, $PO_4^{3-}$, etc.)

5. High concentrations of HREE in agpaitic melts are due to their tendency to form complexes which increases their stability in agpaitic melts with high concentrations of alkalies and volatiles - relative stability of complexes is directly related to the acidity of the solutions

The most effective complexing agents are carbonates, fluorides, hydroxides and chlorides (in order of decreasing efficiency) and somewhat less commonly phosphates (Balashov and Krigman, 1975). The lower stability constants of chloride complexes makes them less efficient complexing agents than the others (Balashov and Krigman, 1975), but there is some evidence that they may be instrumental in the concentration of the light and intermediate REE in some cases (Flynn and Burnham, 1977; Taylor and Fryer, 1980). The HREE show a much stronger tendency to be transported and concentrated by carbonate and/or fluoride complexes (Kapustin, 1961; Balashov and Krigman, 1975; Wendlant and Harrison, 1979). Studies have shown that the REE are stable in the form of carbonate complexes in very alkaline and oxidizing conditions and under both high and low pressures (Wendlant and Harrison, 1979). Hence, REE carbonate complexes are stable in carbonate-rich fluids under both mantle and crustal conditions (Wendlant and Harrison, 1979).

In the Davis Inlet peralkaline suite, systematic variations in REE concentrations seem to be related to increasing peralkalinity, alteration and the intrusive to extrusive sequence which reflects an increase in volatile activity similar to those documented by Taylor et al. (1980) for the Topsails Complex.

These systematic increases cannot be explained by crystal fractionation. Using the approximate partition coefficients from Chapter 3, 70% of the felsic fraction and 10% of the mafic fraction were fractionated from the average composition of the arfvedsonite-riebéckite granite, in

an attempt to reproduce the REE pattern of the rhyolite-tuff group (Fig. 57). The resultant pattern does not resemble the observed rhyolite-tuff pattern. Similar attempts were made by Neumann et al. (1977) who tried to produce the REE of an ekerite (peralkaline granite) by fractionation from several possible parent materials. He found that this was impossible with the available data. Analyses of the Davis Inlet peralkaline suite provide a good example of REE differentiation that was governed by geochemical variations among the REE and not crystal chemistry or ionic radii alone (Mineyev, 1963). The lack of similarity between the patterns produced in the mafic and felsic fractions at Davis Inlet and those normally found for amphiboles/pyroxenes or feldspars probably reflects the strong tendancies of the REE to form complexes which gives them increased stability and mobility in peralkaline environments.

ZONED MAGMA CHAMBERS

Systematic variations in trace and rare earth elements have been documented for the peralkaline suite in the Davis Inlet area in Chapter 3. The enrichment/depletion patterns are similar to those described by Hildreth (1980) and Smith (1980) for zoned magma chambers related to ash-flow tuffs located in the western United States. The geochemical characteristics commonly found in zoned magma chambers such as the Bishop Tuff have been summarized and compared with the Davis Inlet suite in Table 14. The Davis Inlet peralkaline suite varies slightly from the Bishop Tuff in that:

Fig. 57. A comparison of REE patterns for:

(a) fractionation of 70% felsic phase and 10% mafic phase from the average arfvedsonite-riebeckite composition—■

(b) the observed pattern for the Nuiklavick Volcanics (group 3)—▲

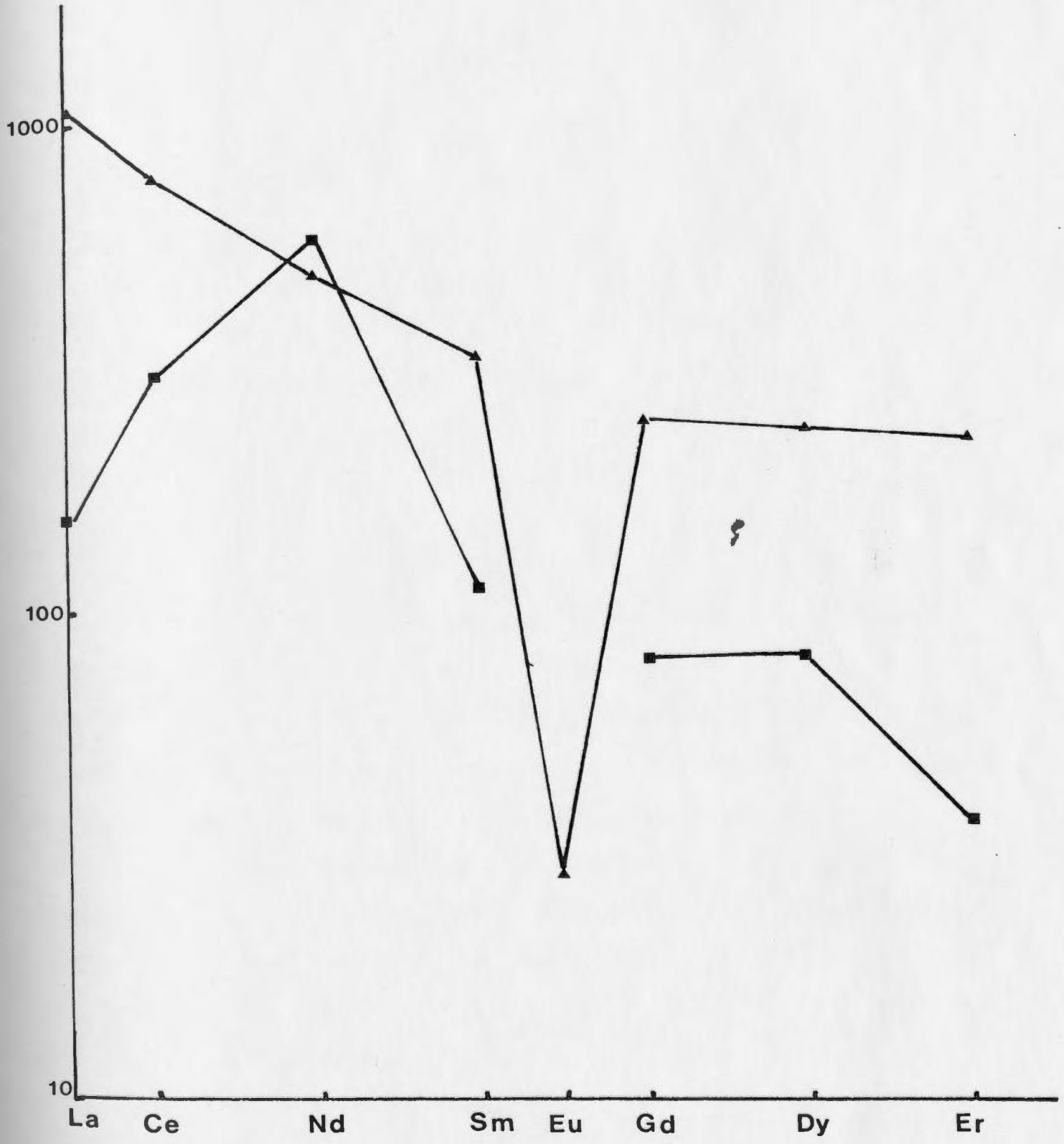
1000
100
10
La
Ce
Nd
Sm
Eu
Gd
Dy
Er

(1) directions of trends are reversed for Fe, Mn, Na, Ni, Zn, Cr, LREE and Zr (Fig. 58);

(2) enrichment factors are higher at Davis Inlet. These variations are due primarily to the peralkaline nature of the rocks of the Davis Inlet area. Hildreth (1980) noted that enrichment factors have a tendency to be higher in alkaline suites and that trend reversals may occur in peralkaline magmas.

Any differentiation model for the peralkaline suite at Davis Inlet must account for all of the geochemical trends summarized in Table 14. A brief discussion of why various differentiation models cannot produce the observed patterns in both the Bishop Tuff and the Davis Inlet area will be presented. For a more detailed discussion of this problem, especially in reference to the Bishop Tuff, see Hildreth (1980).

Petrogenetic models such as crystal fractionation, assimilation of country rock, basaltic underplating, liquid immiscibility, or progressive partial melting cannot satisfy all of the enrichment trends in a zoned magma chamber such as the Bishop Tuff (Hildreth, 1980). Because enrichment factors are even greater in the Davis Inlet rocks, it is even more difficult to ascribe one or more of these processes to their evolution. Some specific geochemical features that cannot be produced by these various models have been summarized from Hildreth (1980) in Table 15.

Hildreth (1980) suggests that the compositional zoning in the Bishop Tuff developed in an essentially liquid state by convection-driven chemical diffusion. Briefly, he says that in rhyolitic liquids, the

Fig. 58. A comparison of the trace (including the RE) elements for:

(a) the Nuiklavick volcanics normalized to the arfvedsonite-riebeckite granite. ▲

(b) the Bishop Tuff early phase normalized to the late phase (Hildreth, 1980) □

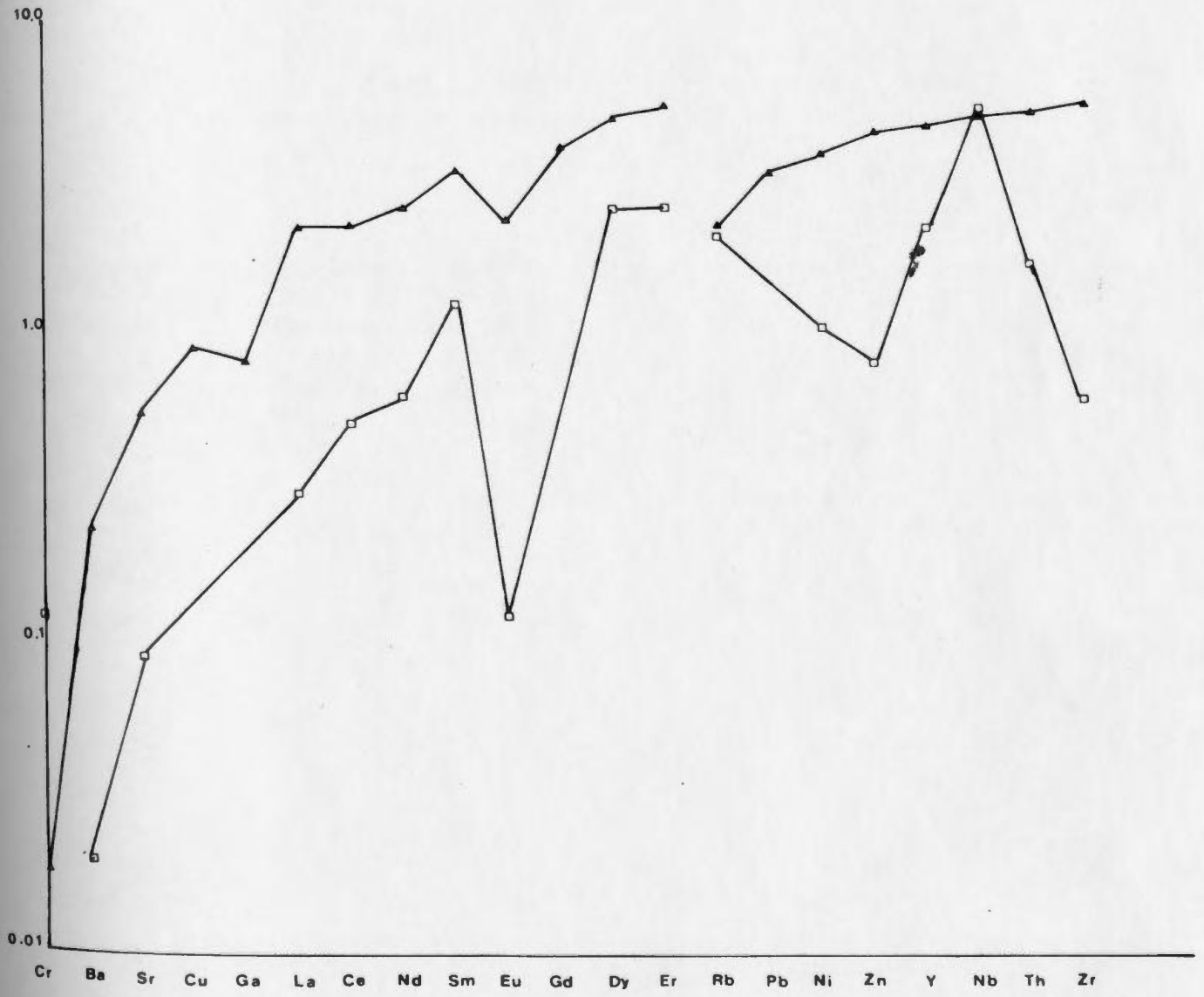
10.0
1.0
0.1
0.01
Cr
Ba
Sr
Cu
Ga
La
Ce
Nd
Sm
Eu
Gd
Dy
Er
Rb
Pb
Ni
Zn
Y
Nb
Th
Zr

TABLE 14

COMPARISON OF ENRICHMENT/DEPLETION TRENDS OBSERVED IN THE BISHOP TUFF (HILDRETH, 1980) AND THE DAVIS INLET PERALKALINE SUITE

| | BISHOP TUFF | DAVIS INLET |
|---|---|---|
| 1. | large roofward enrichments of small highly charged elements Nb, Sb, Ma, Ta, W, U, Th | large enrichments of small, highly charged cations Nb, Th, Zr (Sb, Mo, Ta, W, U, no analyses) in extrusive relative to intrusive rocks |
| 2. | sysmetatic enrichment pattern of the trivalent lanthanides in a roofward direction | systematic enrichment pattern of the trivalent lanthanides and Y in the extrusive rocks |
| 3. | extreme roofward depletion of Mg, Sr, Ba, Eu and Ca (lesser degree for Ca) | extreme depletion of Mg, Sr, Ba, Eu and Ca in the extrusive rocks |
| 4. | progressive enrichment of Rb, and Cs roofward and K downward | progressive enrichment of Rb in the extrusive rocks, some K depletion from groundwater interaction in extrusive rocks |

TABLE 15

VARIOUS POSSIBLE MODELS FOR GENERATION OF THE BISHOP TUFF ACCOMPANIED BY REASONS WHY THEY ARE UNFEASIBLE AS SUMMARIZED FROM HILDRETH (1980)

| | |
|---|---|
| Crystal settling, fractionation | - incompatible with phenocryst compositions and behaviour |
| | - Sr, Ba, Eu depletions in the roof zone require absurd amounts of crystal settling |
| | - separation of mafic phases or high density accessory minerals would cause HREE and small highly charged cation depletion not enrichment in the roof zone |
| | - ratios for Rb/Sr, Mg, Fe, Ba/K, K/Rb and Na/Ca cannot be accounted for by crystal fractionation |
| | - extreme trace element gradients are not compatable with modest major element gradients |
| Assimilation of country rock | - U, Th, Ta concentrations in volcanics relatively unaffected by granitic country rocks |
| | - REE patterns cannot be generated from associated granitic country rocks |
| Basaltic underplating | - enhanced Ba, LREE in lower magmatic levels |
| | - Sc and Mn should decrease in a roofward direction |
| | - V, Cr, Co, Ni and Cu should be present in higher concentrations in the deepest levels |
| Liquid immiscibility | - small degree of change among major elements and virtual continuity of all compositional parameters from base to roof of magmatic chamber |
| | - separation of a silicic melt from an underlying basaltic magma should cause basal enrichment of Ti, Mn, Au, REE, not Ba or Sr |

TABLE 15 (continued)

| | |
|---|---|
| Progressive partial melting | - thermal gradients and physical properties of the magma and its chamber would make convection and mixing a certainty |
| | - gradients such as Ba and Sr could not be reproduced by partial melting using various modeling schemes |

diffusion rates of $H_2O$, let alone most cations, is too slow to permit the observed chemical separations within a reasonable time framework in a static magma chamber. But, observed isotope and water concentration gradients attest to large scale mass transport while the magma was in a liquid state. He invokes a thermogravitational convection-driven model based on the little known Soret effect. Briefly, the Soret effect is active in a multi-component liquid and gas system which is characterized by a temperature gradient. In this system a temperature gradient is accompanied by a compositional gradient which builds up until a steady-state distribution is attained (Hildreth, 1980). Thereafter, throughout time, invarient compositional gradients will exist until the thermal gradient decays. Hildreth suggested that in essence element migration was related to the formation of cationic complexes involving volatiles but that a separate volatile phase did not necessarily exist. However, he acknowledges that associated pegmatites and metasomatism were the result of the exsolution of a separate vapour phase.

In the Davis Inlet area, a volatile/fluid phase did exist and it is suggested that the development of compositional zoning was the result of migration of fluids along a pressure gradient. Further, the compositional zoning reflects increasing peralkalinity towards the top of the magma chamber. As a result, it is evident that the fluids/volatiles also played a major role in the evolution of the peralkaline nature of the magma.

THE ROLE OF FLUIDS

In the Davis Inlet area there is both field and petrographic evidence of volatile activity. Field evidence includes the presence of pegmatites and veinlets which contain riebeckite, gas breccias and miarolitic cavities (Hill, 1978, 1979a,b, 1980). Extensive albitization, alteration of feldspar (and mafic) phenocrysts, corroded and altered zircons, devitrification and hydrothermally formed mafic minerals constitute petrographic evidence of volatile or fluid activity. Peralkaline granite and associated volcanics in the Topsails Complex are very similar both petrographically and chemically to the Davis Inlet suite except that the volcanics are more severely altered at Davis Inlet (Taylor et al., 1980; Taylor, pers. comm., 1979). The presence of a fluid phase is certain but its composition is almost impossible to discern. There is some evidence from microprobe studies to indicate that fluids associated with peralkaline melts are enriched in Fe, Na, Ti and Mn (e.g. Ferguson, 1978; Grapes et al., 1979; this work Chapter 2). High concentrations of Zr, Zn, REE and other trace elements have been reported in various late stage minerals of peralkaline rocks suggesting that these elements were concentrated in the residual fluids from which they subsequently crystallized (MacDonald and Saunders, 1973; Ferguson, 1978; Novak, 1980).

Some evidence from other peralkaline rock suites suggests that the fluids associated with their evolution may be mantle derived. Bailey (1964, 1972, 1978) and MacDonald (1974) have pointed out numerous times the association of peralkaline rocks with tensional zones, areas of

crustal upwarping or rifting. Rifting is accompanied by release of volatiles and as a result peralkaline rocks associated with tensional, or rift, zones are intimately associated with mantle derived volatiles such as $CO_2$, F and Cl (Bailey and MacDonald, 1975; Bailey, 1978, 1980).

Usually Sr initial ratios are high in peralkaline rocks but at least two cases Evisa, Corsica (Bonin et al., 1978) and the Topsails Complex (Taylor et al., 1980) have very low initial ratios. Both of these suites show good evidence that the peralkaline nature may have been strongly influenced by ($CO_2$ rich?) mantle derived fluids.

The major roles of a fluid phase associated with a peralkaline melt are to provide a medium for element transport and to supply complexing agents which hold certain cations in solution. Cations such as Na, Zr, Nb, Y, Zn, Ni Pb and HREE are maintained in solution in the form of ionic complexes because of their increased solubility resulting in increased concentrations which is essentially what makes the melt peralkaline. It has been shown that in highly alkaline melts, $CO_2$ is bound more stably in the liquid structure and has a higher activity than $H_2O$. Thus, $H_2O$ is relegated to a subordinate level during the evolution of alkaline magmas. Very preliminary studies of fluid inclusions indicate that there are two sets of inclusions in the peralkaline granite of the Davis Inlet area, one of which is $CO_2$ rich (Kay, pers. comm., 1980).

Hildreth (1980) suggests that the diffusion rate of $H_2O$ in rhyolitic melts is too slow to permit the observed chemical separations within a feasible time framework. However, volatiles such as F and $CO_2$ have

greater diffusion rates and therefore are more capable of being responsible for element distribution (Fyfe et al., 1979). Volatiles tend to move down a pressure gradient which, in a magma chamber, is toward the roof zone. The migrating volatiles will bring additional heat decreasing the melting range of the rocks (Bailey, 1970). Furthermore fluids can transport mobile elements, such as the alkalies and residual trace elements, which are characteristic of peralkaline rocks (Bailey, 1974a,b) resulting in the enormous concentrations of these elements in the volatile-charged extrusive rocks and in the autometasomatized intrusive rocks.

## SUMMARY

During the course of this work, it has been possible to demonstrate that the clinopyroxene-fayalite granite is not genetically related to the associated peralkaline rocks by any kind of differentiation scheme. The peralkaline rock suite consists of the arfvedsonite-riebeckite granite and the Nuiklavick volcanics. The peralkaline nature of the Nuiklavick volcanics was established primarily on the basis of trace (including RE) element data. The consanguinity of the peralkaline granite and volcanics is suggested by trace (including RE) element trends and the spatial relationship between the two rock units.

The peralkaline nature of the rocks near Davis Inlet reflects intense volatile activity which seems to have been most important in the development of the volcanic chemistry. The volatile phase was enriched in Na, Fe, Ti, Mn and trace (including the RE) elements. Expulsion of this phase during

volcanism was probably responsible for a large part of the loss of sodium experienced by the volcanics. Some sodium (and in the rhyolite/tuff, potassium) was lost by groundwater activity and low temperature hydrothermal/deuteric effects.

The volcanics are presumed to represent the upper levels of a magma chamber. The rhyolite/tuff represents the top of the magma chamber which was explosively erupted after the (volatile?) pressure reached its critical point. The quartz-feldspar porphyry represents a lower level which was not erupted and the granite represents the lowest levels which intruded its own volcanic pile during emplacement. Trace element patterns are similar to those of the Bishop Tuff and thus may be representative of a zoned magma chamber.

# CHAPTER 5

## CONCLUSIONS

The origin of peralkaline rocks has been enigmatic and a topic of dissention among igneous petrologists for sometime. The first and most traditional mechanism for generation of peralkaline magmas was extreme crystal fractionation and the "plagioclase effect" (Bowen, 1937, 1945) which was subsequently challenged by Bailey (1964; Bailey and Schairer, 1964, 1966) who advocated partial melting and the "orthoclase effect". Despite the growing mass of evidence against fractionation, there are still those who believe in it, often accompanied by various modifications, i.e. volatile phases, gaseous transfer, to explain the evolution of peralkaline suites (Ewart et al., 1968; Nicholls and Carmichael, 1969; Weaver et al.; 1972; Noble, 1968, 1970; Noble et al., 1969; Noble et al.; 1979).

For some time, Soviet geologists have placed a great deal of emphasis on the role of autometasomatic or hydrothermal fluids in the generation of alkaline, peralkaline magmas (e.g. Balashov, 1962, 1963, 1966; Mineyev, 1963; Balashov and Krigman, 1975; Wendlant and Harrison, 1979). Recently, the role of fluids and volatiles in the generation of peralkaline magmas has been recognized by other geologists such as Bailey (1970, 1974a, 1974b, 1978) who advocated deep crustal or mantle metasomatism associated with mantle degassing as a possible mechanism for generation of peralkaline magmas.

Petrogenetic models for any peralkaline rocks are at their very best, extremely speculative because: (1) the processes involved are complex and not well understood; and (2) relationships with possible parent materials are undecipherable. The peralkaline rocks at Davis Inlet present a good example of a highly evolved suite of peralkaline rocks without associated basic or intermediate rocks. Because of the highly evolved nature of this suite, it is impossible, with the data available, to speculate on possible parent materials. The major contribition of this work is to provide evidence that a fluid phase is instrumental in the evolution and composition of over-saturated peralkaline rocks.

## FURTHER WORK

The study of peralkaline rocks and their mode of origin have come a long way since Bowen (1937) first published his paper on Petrogeny's Residua System or the plagioclase effect. However, there is still a long way to go to obtain a more complete understanding of over-saturated peralkaline rocks. More effort needs to be expended towards documentation of fluid activity, its effects and composition. Partition coefficients for the sodic pyroxenes, amphiboles and other iron and sodium rich phases commonly found in peralkaline rocks should be determined. This information will provide a firmer foundation for testing differentiation and partial melting as modes of origin of peralkaline rocks. Both empirical and experimental studies should be directed towards investigation of the role of complexing during the evolution of peralka-

line rocks. As well trace element, especially the REE, behaviour in peralkaline environments should be documented more thoroughly. Studies of fluid inclusions both in peralkaline rocks and in associated pegmatites or veins will contribute largely to our knowledge of fluid composition and activity. Similarly study of oxygen and hydrogen isotopes will provide evidence to suggest a mantle or crustal source for the fluids which are present.

In summary, it is felt that extensive efforts should be expended predominantly in the area of documentation of trace (especially the RE) element behaviour, fluid inclusions and isotopes, in order to obtain a more comprehensive understanding of the origin of peralkaline rocks.

REFERENCES

Arth, J.G., 1976. Behaviour of trace elements during magmatic processes - a summary of theoretical models and their applications. J. Res., U.S. Geol. Soc., v. 4, pp. 41-47.

Bailey, D.K., 1964. Crustal warping - a possible tectonic control of alkaline magmation. J. Geophys. Res., v. 69, pp. 1103-1111.

Bailey, D.K., 1969. The stability of acmite in the presence of $H_2O$. Am. J. Sci., (Schairer Volume), pp. 1-16.

Bailey, D.K., 1970. Volatile flux, heat focusing and the generation of magma. Geol. J., Spec. Issue, No. 2, pp. 177-186.

Bailey, D.K., 1974a. Continental Rifting and Alkaline Magmation. In H. Sørenson (ed.), The Alkaline Rocks. J. Wiley and Sons, N.Y., pp. 148-159.

Bailey, D.K., 1974b. Melting in the Deep Crust. In H. Sørenson (ed.), The Akaline Rocks. J. Wiley and Sons, N.Y., pp. 436-442.

Bailey, D.K., 1978. Continental Rifting and Mantle Degassing. In E.R. Neumann and I.B. Ramberg (eds.), Petrology and Geochemistry of Continental Rifts. Dordrecht: D. Reidel, pp. 1-13.

Bailey, D.K., 1980. Volcanism, earth degassing and replenished lithosphere mantle. Phil. Trans. Roy. Soc. Lond. A, v. 297, pp. 309-322.

Bailey, D.K., and MacDonald, R., 1975. F and Cl in peralkaline liquids and the need for magma generation in an open system. Min. Mag., v. 40, pp. 405-414.

Bailey, D.K., and Schairer, J.F., 1964. Feldspar - liquid equilibria in peralkaline liquids - the orthoclase effect. Am. J. Sci., v. 262, pp. 1195-1206.

Bailey, D.K., and Schairer, J.F., 1966. The System $Na_2O$-$Al_2O_3$-$Fe_2O_3$-$SiO_2$ at 1 atm and the petrogenesis of alkaline rocks. J. Pet., v. 7, pp. 114-170.

Baker, B.H., and Henage, L.F., 1977. Compositional Changes during Crystallization of some Peralkaline Silicic Lavas of the Kenya Rift Valley. J. Volcanology and Geothermal Res., v. 2, pp. 17-28.

Balashov, Yu. A., 1962. Evolution of the rare earth composition and content in the intrusive phases of the Lovozero Alkalic Massif (Kola Peninsula). Geochemistry, pp. 233-247.

Balashov, Yu. A., 1963. Regularities in the distribution of the rare earth elements in the Earth's crust. Geochemistry, v. 3, pp. 97-124.

Balashov, Yu. A., 1966. Differentiation of rare earth elements during magmatic processes. In Vinogradov (ed.), Geochemistry of the Earth's Crust, pp. 372-387.

Balashov, Yu. A., and Krigman, L.D., 1975. The effects of alkalinity and volatiles on rare earth separation in magmatic systems. Geochem. Int., v. 12, pp. 165-170.

Bandurkin, G.A., 1961. Behaviour of the rare earth elements in fluorine-bearing media. Geochemistry, pp. 159-167.

Bevan, A.P., 1954. Report on Exploration in Labrador and Newfoundland. Unpub. Rept. of British Nfld. Corp. Ltd., Tor.

Bonin, B., Orsini, C.G., and Vialette, Y., 1978. Age, origin and evolution of anorogenic complex of Evisa (Corsica): A K-Li-Rb-Sr study. Contr. Min. Pet., v. 65, pp. 425-432.

Bowden, P. and Turner, D.C., 1974. Peralkaline and Associated Ring Complexes in the Nigeria-Niger Province, West Africa. In H. Sørenson (ed.), The Alkaline Rocks. John Wiley and Sons, N.Y., p. 330-351.

Bowden, P. and Kinnaird, J.A., 1978. Younger Granites of Nigeria - a zinc-rich tin province. Trans. Inst. Min. Metall., v. 87, pp. B66-B69.

Bowen, N.L., 1937. Recent high temperature research on silicates and its significance in igneous geology. Am. J. of Sci., v. 33, pp. 1-21.

Bowen, N.L., 1945. Phase-equilibria bearing on the origin and differentiation of alkaline rocks. Am. J. Sci., v. 243A (Daley v.), pp. 75-89.

Brooks, C., 1980. Geochronology report - Newfoundland and Labrador. In C.F. O'Driscoll and R.V. Gibbons (eds.), Current Research, Min. Dev. Div., Nfld. Dept. Mines and Energy, Rept. 80-1, pp. 143-146.

Buma, G., Frey, F.A., and Wones, D.R., 1971. New England granites: trace element evidence regarding their origin and differentiation. Contr. Min. Pet., v. 31, pp. 300-320.

Carmichael, J.J., Turner, F.J., and Verhoogen, J., 1974. Igneous Petrology: International Series in the Earth and Planetary Sciences. McGraw-Hill, Montreal, 739 p.

Carmichael, I.S.E., and MacKenzie, W.S., 1963. Feldspar-liquid Equilibria in Pantellerites: An Experimental Study. Am. J. Sci., v. 261, pp. 382-396.

Collerson, K.D., Jesseau, C.W., Ryan, A.B., and Hawkins, D.W., 1974. Mineral Potential evaluation in the Makkovick and Hopedale areas, Labrador. In R. Smyth (ed.), Report of Activities for 1973, Min. Dev. Div., Nfld. Dept. Mines and Energy, Rept. 74-1.

Dur, W.A., Howie, R.A., and Zussman, R., 1963. An Introduction to the Rock-Forming Minerals, Vol. II. The Chain Silicates, Longman Group Ltd., London, 379 p.

Dietrich, R.V., 1968. Behaviour of Zr in certain artificial magmas under diverse P-T conditions. Lithos, v. 1, pp. 20-29.

Ernst, W.G., 1962. Synthesis, stability relations, and occurrence of riebeckite and riebeckite-arfvedsonite solid solutions. J. Geol., v. 70, pp. 689-736.

Ewart, A., Taylor, S.R., and Capp, A.C., 1968. Geochemistry of the pantellerites of Mayor Island, New Zealand. Contr. Min. Pet., v. 17, pp. 116-140.

Ferguson, A.F., 1978. The Crystallization of Pyroxenes and Amphiboles in some Alkaline Rocks and the Presence of a Pyroxene Compositional Gap. Contr. Min. Pet., v. 67, pp. 11-15.

Ferrara, C., and Treuil, M., 1974. Petrological Implications of Trace Element and Sr Isotope Distributions in Basalt.- Pantellerite Series. Bull. Volc., v. 38, pp. 548-574.

Fisher, R.V., 1960. Proposed classification of volcaniclastic rocks. B.G.S.A., v. 71, pp. 1864-1865 (abst.).

Flynn, R.T., and Burnham, C.W., 1978. An experimental determination of rare-earth partition coefficients between a chloride-containing vapour phase and a silicate melt. Geochem. Cosmochem. Acta, v. 42, pp. 685-702.

Frohberg, M.H., 1939. Occurrence of riebeckite in the Michipicoten district, Ontario. Am. Min., v. 24, p..382.

Fryer, B.J., 1977. Rare earth evidence in iron formations for changing Precambrian oxidation states. Geochim. Cosmochem. Acta, v..41, pp. 361-367.

Fyfe, W.S., Price, N.J., and Thompson, A.B., 1978. Fluids in the Earth's Crust. Elsevier Scientific Publishing Company, N.Y., pp. 47-53.

Gavrilin, R.D., and Peutsova, L.A., 1970. Behaviour of lead and zinc in rocks of a single intrusive phase (in syenite intrusions of northern Tien Shan). In N.I. Khetarov (ed.), Problems in Geochemistry. Keter Press, Jerusalem, pp. 406-414.

Goldschmidt, W.M., 1954. Geochemistry. Clarendon Press, Oxford, 730 p.

Grapes, R., Yagi, K., and Okunura, K., 1979. Aenigmatite, sodic pyroxene, arfvedsonite and associated minerals in syenites from Morotu, Sakhalin. Con. Min. Pet., v. 69, pp. 97-103.

Haskin, L.A., and Schmidt, R.A., 1967. Rare earth distributions. In P.H. Abelson (ed.), Researches in Geochemistry, v. 2. J. Wiley and Sons Inc., N.Y.

Hatch, F.H., Wells, A.K., and Wells, M.K., 1972. Petrology of the Igneous Rocks. Thomas Murby and Co., London, 551 p.

Hawley, J.E., 1937. Riebeckite in quartz veins from the Michipicoten district, Ontario. Am. Min., v. 22, p. 1099.

Hildreth, W., 1980. The Bishop Tuff: evidence for the origin of compositional zonation in silicic magma chambers. In C.E. Chapin and W.E. Elston (eds.), Ash-flow Tuffs. G.S.A. Spec. Paper 180, pp. 43-76.

Hill, J., 1978a. Preliminary investigation of the anorthosite-adamellite igneous suite in the Davis Inlet area, Labrador. In R.V. Gibbons (ed.), Report of Activities for 1977, Min. Dev. Div., Nfld. Dept. Mines and Energy, Rept. 78-1, pp. 22-26.

Hill, J.D., 1978b. The Geology of the Helikian igneous rocks suite, Davis Inlet area, Labrador. Min. Dev. Div., Nfld. Dept. Mines and Energy, Rept. 78-7 (open file).

Hill, J.D., 1979. Geological Mapping in the Davis Inlet-Mistastin Lake Corridor, Labrador. In R.V. Gibbons (ed.), Report of Activities for 1978, Min. Dev. Div., Nfld. Dept. Mines and Energy, Rept. 79-1, pp. 148-153.

Hill, J.D., 1980. Continued geological mapping in the Davis Inlet-Mistastin Lake Corridor, Labrador. In C.F. O'Driscoll and R.V. Gibbons (eds.), Current Research, Min. Dev. Div., Nfld. Dept. Mines and Energy, pp. 222-229.

Hussey, E.M., 1979. The Stratigraphy, Structure and Petrochemistry of the Clode Sound Map Area, Northwestern Avalon Zone, Newfoundland. Unpub. M.Sc. Thesis, M.U.N., St. John's, Nfld.

Kapustin, Yu. L., 1966. Geochemistry of rare earth elements in carbonatites. Geochem. Int., v. 3, pp. 1054-1064.

Khodakovskiy, I.L., and Yelkin, A. Ye., 1975. Measurement of the solubility of zincite in aqueous NaOH at 100, 150, 200°C. Geochem. Int., v. 12, pp. 127-133.

Kochhar, N., 1977. Post-emplacement alkali modifications in rapidly cooled volcanic rocks. Am. Min., v. 62, pp. 333-335.

Kogarko, L.N., 1974. Role of volatiles. In H. Sørenson (ed.), The Alkaline Rocks. John Wiley and Sons, N.Y., pp. 474-487.

Krauskopf, K.B., 1967. Introduction to Geochemistry. McGraw-Hill, 720 p.

Larsen, L.M., 1977. Aenigmatites from the Ilimaussaq intrusion, south Greenland: Chemistry and Petrological Implications. Lithos, v. 10, pp. 257-270.

Lilljequist, R., and Svenson, S.A., 1974. Exceptionally well preserved Precambrian ignimbrites and basic lavas in North Sweden. Geologiska Foreningens i Stockholm Förhandlingar, v. 96, pp. 221-229.

MacDonald, R., 1974. Nomenclature and petrochemistry of the peralkaline oversaturated extrusive rocks. Bull. Volc., v. 38, pp. 498-517.

MacDonald, R., and Saunders, M.J., 1973. Chemical variation in minerals of the astrophyllite group. Min. Mag., v. 39, pp. 97-111.

Martin, R.C., 1959. Some field and petrographic features of New Zealand and American ignimbrites. New Zealand J. Geol. Geophys, v. 2, pp. 394-411.

Mineyev, D.A., 1963. Geochemical differentiation of the rare earth elements. Geochemistry, pp. 1129-1148.

Moeller, T., 1972. Complexes of the lanthanides. In MTP International Review of Science Lantharides and Actinides. Inorganic Series 1, v. 7, pp. 275-298.

Moorehouse, W.W., 1959. The Study of Rocks. In Thin Section. Harper and Row Pub., N.Y., 514 p.

Neuman, E.R., 1976. Compositional relations among pyroxenes, amphiboles and other mafic phases in the Oslo Region plutonic rocks. Lithos, v. 9, pp. 85-109.

Neuman, E.R., Brunfelt, A., Ofinstad, K.C., 1977. Rare earth elements in some igneous rocks in the Oslo rift, Norway. Lithos, v. 10, pp. 311-319.

Nicholls, J., and Carmichael, J.S.E., 1969. Peralkaline acid liquids: a petrological study. Contr. Min. Pet., v. 20, pp. 268-294.

Noble, D.C., 1967. Sodium, Potassium and Ferrous Iron Contents of some Secondarily Hydrated Natural Silicic Glasses. Am. Min., v. 52, pp. 280-286.

Noble, D.C., 1970. Loss of Sodium from Crystallized Comendite Welded Tuffs of the Miocene Grouse Canyon Member of the Belted Range Tuff, Nevada. Geol. Soc. Am. Bull., v. 81, pp. 2677-2688.

Noble, D.C., Rigot, W.C., and Bowman, H.R., 1979. Rare earth element content of some highly differentiated ash-flow tuffs and lavas. In C.E. Chapin and W.E. Elston (eds.), Ash-Flow Tuffs. G.S.A. Spec. Paper 180, pp. 77-85.

Novak, S.W., and Rankin, D.W., 1980. Mineralogy and geochemistry of an ash-flow tuff of peralkaline affinity from the Mt. Rogers Formation. Geol. Soc. Am. Bull., Abst. with Prog., SE section.

Pupin, J.P., 1980. Zircon and Granite Petrology. Contr. Min. Pet., v. 73, pp. 207-220.

Rosler, H.J., and Lange, H., 1972. Geochemical Tables. Elsevier Pub. Co., N.Y., pp. 252-253.

Ross, C.S., and Smith, R.L., 1961. Ash-flow tuffs: their origin, geologic relations and identification. U.S. Geol. Soc. Prof. Paper 366.

Ryan, A.B., 1974. Metamorphic and structural investigation of the Hopedale gneiss, Flowers Bay, Labrador. B.Sc. thesis, M.U.N., St. John's.

Scott, R., 1966. Origin of Chemical Variations within Ignimbrite Cooling Units. Am. J. Sci., v. 264, pp. 273-288.

Shaw, D.M., 1968. A review of K-Rb fractionation analysis. Geochem. Cosmochim. Acta, v. 32, pp. 573-601.

Shaw, D.M., Dostal, J., and Keays, R.R., 1976. Additional estimates of continental surface Precambrian shield composition in Canada. Geochem. Cosmochim. Acta, v. 40, pp. 73-83.

Smith, J.V., 1974. Feldspar - Vol. 2 - Chemical and Textural Properties. Springer-Verlag, N.Y., 690 p.

Smith, R.L., 1980. Ash-flow magmatism. Geol. Soc. Am. Spec. Paper 180, pp. 5-27.

Tauson, L.V., 1967. Geochemical behaviour of rare elements during crystallization and differentiation of granitic magma. Geochem. Int.; v. 4, pp. 1067-1075.

Taylor, F.C., 1971. A revision of PG structural provinces in north-eastern Quebec and northern Labrador. Can. J. Earth Sci., v. 8, pp. 579-584.

Taylor, F.C., 1972. Reconnaissance geology of a part of the Precambrian Shield, northeastern Quebec and northern Labrador; Part III. Geol. Soc. Canada Paper 71-48.

Taylor, R.P., and Fryer, B.J., 1980. Multiple-stage hydrothermal alteration in porphyry systems in northern Turkey: the temporal interplay of potassic, propylitic, and phyllic fluids. Can. J. Earth Sci., v. 17, pp. 901-926.

Taylor, R.P., Strong, D.F., and Kean, B.F., 1980. The Topsails Igneous Complex: Silurian-Devonian Peralkaline Magmatism. Can. J. Earth Sci., v. 17, pp. 425-439.

Villari, L., 1974. The Island of Pantelleria. Bull. Volc., v. 38, pp. 680-724.

Watson, E.B., 1979. Zircon saturation in felsic liquids: experimental results and applications to trace element geochemistry. Contr. Min. Pet., v. 70, pp. 407-419.

Watson, E.B., 1980. Some experimentally determined zircon/liquid partition coefficients for the rare earth elements. Geochem. Cosmochim. Acta, v. 44, pp. 895-897.

Wendlandt, R.F., and Harrison, W.J., 1979. Rare earth partitioning between immiscible carbonate and silicate liquids and $CO_2$ vapour: Results and implications for the formation of light rare earth-enriched rocks. Contr. Min. Pet., v. 69, pp. 409-419.

Wentworth, C.F., and Williams, H., 1932. The classification and terminology of the pyroclastic rocks. U.S. Nat. Res. Coun. Bull. 89, pp. 19-53.

Wheeler, E.P., 1942. Anorthosite and associated rocks about Nain, Labrador. J. Geology, v. 50, pp. 611-642.

Wheeler, E.P., 1955. Adamellite intrusive north of Dauco Inlet, Labrador. Geol. Soc. Am. Bull., v. 66, pp. 1031-1060.

Wheeler, E.P., 1960. Anorthosite-adamellite complex of Nain, Labrador. Geol. Soc. Am. Bull., v. 71, pp. 1775-1762.

Zlobin, B.I., and Gorshkova, M.S., 1961. Pb+Zn in alkalic rocks and their bearing on some petrological problems. Geochemistry, v. 1, pp. 317-328.

# APPENDIX A

## PETROGRAPHIC DESCRIPTIONS

## CLINOPYROXENE FAYALITE GRANITE

| Samp. | q | p | o | alb | fa | has | hed | Z | fl | ap | sp | opq | R |
|---|---|---|---|---|---|---|---|---|---|---|---|---|---|
| 057 | 22% | 65% | 5% | 5% | 1% | 2% | 19% | x | x | x | x | x | x |
| 060 | 30% | 60% | 5% | 2% | 1% | 5% | 10% | x | x | x | | x | |
| 061 | 30% | 60% | 5% | 2% | 1% | 5% | 2% | x | x | x | | x | x |
| 062a | 25% | 50% | 10% | 10% | | 5% | | x | | x | | x | |
| 062b | 15% | 50% | 15% | 15% | 2% | 1% | 4% | x | x | x | | x | |
| 062c | 15% | 45% | 15% | 20% | 3% | 1% | 4% | x | | x | | x | x |
| 064a | 25% | 30% | 30% | 20% | 1% | 1% | 3% | x | x | x | | x | x |
| 064b | 30% | 40% | 15% | 10% | 2% | 1% | 3% | x | x | x | | x | |

Explanation of symbols:

q - quartz
p - perthite
o - orthoclase
alb - ablite/albitization
fa - fayalite
has - hastingsite
hed - hedenbergite
Z - zircon
fl - flourite
ap - apatite
sp - sphene
opq - opaques
R - rutile

x - present but less than 1%

Additional notes:

057 - coarse grained equigranular

060 - coarse grained, oikocrystic mafics, equigranular
very small amounts of arfvedsonite on rims of hastingsite

061 - coarse grained, equigranular, some oikocrysts of hastingsite, some altering to biotite

062a - coarse grained, equigranular, some feldspar is phenocrystic, more altered than most

062b - medium grained, equigranular, hastingsite altering to biotite, arfvedsonite on rims of some crystals

062c - vermicular quartz, some arfvedsonite rimming hastingsite

064a - some arfvedsonite rimming hastingsite

064b - some arfvedsonite rimming hastingsite

## Arfvedsonite-riebeckite Granite

| Sample | q | p | a-r | aeg | alb | aen | aln | ast | fl | ap | z | opq | eq | gs | oik | grph |
|---|---|---|---|---|---|---|---|---|---|---|---|---|---|---|---|---|
| 066C | 25% | 70% | 1% | 4% | x | x | x | | | | x | | x | c | x | x |
| 067 | 25% | 70% | 2% | 2% | x | x | | x | x | x | | x | x | c | x | |
| 068 | 25% | 70% | 2% | 1% | x | x | x | | x | | x | x | x | c | x | |
| 069A | 25% | 70% | 3% | 1% | x | x | | x | x | x | x | x | x | c | x | |
| 069 | 25% | 60% | 5% | 2% | x | 1% | x | x | x | x | x | x | x | m | x | |
| 071 | 25% | 70% | 2% | | x | x | x | x | | x | x | | x | c | x | |
| 072 | 25% | 70% | 3% | x | x | | | x | x | | x | | x | m | x | x |
| 073 | 25% | 70% | 1% | 2% | x | 1% | x | x | x | | | | x | c | x | x |
| 074 | 25% | 70% | 3% | 1% | x | x | x | x | | | x | | x | m | x | x |
| 075 | 25% | 70% | 1% | x | x | 1% | x | x | | | x | | x | m-c | x | |
| 078 | 25% | 70% | 3% | x | | x | x | x | x | | x | x | x | m-c | x | |
| 079 | 25% | 70% | 2% | x | | x | | x | x | | x | x | x | m-c | | |
| 080 | 30% | 65% | 2% | 1% | x | 1% | | x | x | x | x | | x | c | x | x |
| 081 | 25% | 70% | 2% | x | x | 1% | | x | | | x | | x | c | x | |
| 082 | 25% | 70% | 3% | 1% | | 1% | | x | x | | x | | x | c | x | |
| 083 | 25% | 70% | 2% | 1% | x | 1% | x | x | x | | x | | x | c | x | |

Explanation of symbols:

q--quartz p--perthite a-r--arfvedsonite-riebeckite aeg--aegirien-augite
alb--albite aen--aenigmatite aln--allanite ast--astrophyllite fl--fluorite
ap--apatite z-zircon opq--opaques eq--equigranular gs--grain size
oik--oikocrysts grph--graphic intergrowths of quartz and feldspar

x--present but less than 1%

Additional notes:

066c - graphic granite

070a - fine grained, poikolitic, sample taken near contact with gneiss

079 - sample taken .4 m east of contact with monzonite

Explanation of symbols used in petrographic description of Nuiklavick Volcanics:

%p - % phenocrysts

q - quartz phenocrysts

fs - feldspar phenocrysts

q fs - % quartz phenocrysts % feldspar phenocrysts

af - altered feldspar (pseudoperthite) phenocrysts

ms - matrix size (mm units)

Z - zircon

fr - fragments

fb - flow banding

s - sulphides (pyrite)

sp - spherulites

fe - felsitic texture

e - eutaxitic

og - lacy overgrowths on quartz phenocrysts

l - lenticular structures, possible pumice fragments, lithophysae

opq - opaques

ps - phenocryst size (mm units)

## Nuiklavick Volcanics

| Sample | | %p | q | fs | q>f | af | ms | z | fr | fb | s | sp | e | fe | og | l | opq | ps |
|---|---|---|---|---|---|---|---|---|---|---|---|---|---|---|---|---|---|---|
| 084 | p | 50 | x | x | | | .25 | | | | | | | x | x | | | .5-3 |
| 085 | p | 50 | x | x | | | .1 | x | | | | | | x | x | | | .5-4.5 |
| 086A | p | 50 | x | x | | x | .1/.2 | x | | | | | | x | x | | | .5-3.5 |
| 086B | p | 50 | x | x | | | .1/.2 | x | | | | | | x | x | | | .5-3.5 |
| 087 | t | 1 | x | x | | x | .05 | | | | | | | | x | | | .5-1.75 |
| 088 | t | 5 | x | x | | x | .05 | | x | x | | | x | | x | x | | .25-2 |
| 089 | p | 70 | x | x | | x | .1 | | x | x | | x | x | x | | | | .2-4 |
| 090 | t | 1 | x | | | | .05 | | | x | | x | | | | | | .25-1 |
| 091A | p | | x | x | | | .1 | | | | | | | | | | | .5-1.5 |
| 091B | t | 5 | x | x | | | .1 | | x | | x | | | | | | | .5-1.5 |
| 092 | p | 50 | x | x | | x | .1/.25 | | | | x | | | x | x | | | .1-4.75 |
| 93A | t | 5 | x | | | | .05 | x | x | | x | x | | | | x | | .1-1 |
| 093B | t | 1 | x | | | | .05 | x | | x | x | x | x | | | x | | .2-2 |
| 094 | t | | | | | | .05 | | x | x | x | x | x | | | x | | |
| 095 | t | | | | | | .05 | | x | x | x | x | x | | | x | | |
| 097A | t | 3 | x | x | | | .05 | | x | x | | | | | | | | .5 |
| 097B | r | 5 | x | x | | | .05 | | | x | x | | | | | | x | .5-1 |
| 097C | r | 5 | x | x | | | .05 | | | x | x | | | | | | | .25-1.5 |
| 098 | r | 5 | x | x | | | .05 | | | x | x | | | | | x | | .25-1.25 |
| 099 | p | 30 | x | x | | | .1 | | | | | | | x | x | | | .5-2.75 |
| 100 | b | 40 | x | x | | | .1 | | x | x | | x | x | | | | | |
| 101 | b | 3 | x | x | | | .05/.2 | | x | | | | | | | | | .4-1.5 |
| 102 | b | 75 | x | x | | | .05 | | x | | | | | | | | | .25-2.5 |

Additional Notes:

084 - pink, aphanitic, xenolith of black, aphanitic material, appears to be ash, secondary quartz veins

086b - accessory fluorite

087 - dark red to black aphanitic with quartz and feldspar phenocrysts, fragments look stretched as by flowage, stringers of black alteration material in thin section dark laminations representative of flowage, fragments are porphyritic rhyolite or rhyolite porphyry

088 - red aphanitic groundmass with yellow patches stringers of black alteration materials; thin section shows flow banding, possible devitrified pumice fragment

090 - flowbanded, possible perlitic fractures in thin section, autobrecciated

092 - in thin section, patches or layers of fine and coarser grained quartz-feldspar mosaics

093a - grey-green aphanitic fragments of porphyry, stringers of black alteration material; in thin section, fragment of devitrified material possibly pumice

093b - possible pumice fragment (devitrified) in thin section

094 - quartz veinlets, autobrecciated

095 - autobrecciated, possible perlitic fractures, relic pumice fragments - lunate, cuspate in form, slightly folded, brown rims

097c - relict mafic phenocrysts in thin section; faint flowbanding similar to 97b, 97a

098 - relict mafic phenocrysts, possible lithophysae

099 - black, aphanitic with phenocrysts of quartz and feldspar, colour leached around phenocrysts, some feldspar phenocrysts stained yellowish green

100 - fragments 1mm-10cm

101 - pink, brecciated (autobrecciated), fragments of aphyric and porphyritic rhyolite, largest fragments 3.5 cm, stringers or veinlets of black alteration material; in thin section, some relict mafic material, alteration product unidentifiable

# APPENDIX B

## ANALYTICAL TECHNIQUES

SAMPLE PREPARATION

Surface weathering was sawn off and samples were scrubbed and washed before crushing. Samples were crushed to 1-2 cm chips using an eight pound sledge hammer and steel plate and in a Brawn steel jaw crusher. A representative sample of chips was powdered in a tungsten carbide, pulverizer for 2 minutes producing a rock powder of -200 mesh.

ANALYTICAL PROCEDURES

Major Elements

Analysis of the major and minor elements $SiO_2$, $Al_2O_3$, $Fe_2O_3$ (total), CaO, $K_2O$, MnO and $P_2O_5$ were done using a Phillips 1450 automatic X-ray fluorescence spectrometer with an Ag tube. $Na_2O$, MgO were done by atomic absorption on a Perkin-Elmer 303 Atomic Absorption Spectrometer.

Fused pellets were made by the following method:

(1) 4 $\pm$ .2 g of lithium tetraborate was weighted into a previously dried and weighed platinum crucible which was then heated on a Claisse Fluxer until melted. The melt was poured into a platinum mold until cooled then returned to the crucible and reweighed.

(2) 4 $\pm$ .2 g of lithium tetraborate, .5 $\pm$ .019 g rock powder and .5 $\pm$ .019 g of $La_2O_3$ were weighed into a previously dried and weighed platinum crucible

(3) the crucible was heated on a Calisse Fluxer until the mixture was completely melted

(4) the melt was poured into platinum molds and cooled then returned to the crucible and reweighed. The weights of the fused pellets for the sample and the tetraborate were used to determine a dilution factor which was used to calculate the percent of oxides in each sample. The dilution factor was calculated by the following equation:

(wt. of fused pellet - wt. of crucible)/(wt. of sample - wt. of tetraborate) x 10).

The difference between the weight of the fused pellet of the rock sample and the fused pellet of tetraborate can be used to determine the Loss on Ignition of the sample.

The fused pellets were then analyzed by X-ray fluorescence on a Phillips 1450 automatic XRF using a silver tube.

Samples were prepared for sodium analyses by the following procedure:

(1) .2 g of rock powder was weighed into a polyethylene digestion bottle

(2) 5 ml of concentrated HF was added using an automatic pipette then the bottle was placed on a steam bath for 30 min.

(3) the sample was cooled and 50 ml of saturated boric acid was added

(4) after cooling the solution was made up to a 200 ml volume by addition of distilled water

Analyses for MgO were carried out using the same solution to which 10 ml of $La_2O_3$ were added followed by further dilution with distilled water.

Ferrous Iron Analysis

Ferrous iron/FeO was determined by potentiometric titration, following hot acid decomposition of the sample by the modified Pratt method. $Fe_2O_3$ was recalculated by the following equation:

$$Fe_2O_3 = Fe_2O_3 \text{ (Total)} - 1.11 \times FeO.$$

Loss on Ignition

Loss on ignition analyses were conducted by observing the weight loss after heating a sample for two hours at 1050°C.

Trace Element Analyses

A total of 13 non-lanthanide trace element abundances were obtained for each sample. Pressed pellets that were used for analyses were made by the following method:

(1) 10 ± .1 g of rock powder was weighed into a clean bottle

(2) 1.4-1.5 g of phenyl formaldehyde binder (a heat setting plastic) was added to each bottle which was then shaken in a Spex-Mill shaker to completely homogenize the powder

(3) the powder was then placed in a Herzog hydraulic pellet press for 1 min.

(4) the pellets were removed from the press and placed in an oven for 10 min. at 200°C.

The pellets were analyzed by X-ray flourescence on a Phillips 1450 XRF using a Rh tube.

Rare Earth Element Analyses

Rare earth element abundances were determined by the thin film x-ray fluorescence method of Fryer (1977). Sample weights varied accoring to rock type as follows: .7 g clinopyroxene-fayalite granite, .5 g arfvedsonite-riebeckite granite and group 1 of the Nuiklavick volcanics, and .2 g of groups 2 and 3 of the Nuiklavick volcanics. A generalized method is given below:

(1) samples were weighed into a 100 ml teflon beaker, wetted with demineralized water and treated with a drop of 2 N HCl to dissolve any carbonate.

(2) 5 ml of a Tm Spike was added with 2 ml of $HCLO_4$ and then the sample was treated with 15 ml of HF and heated until dry

(3) 10 ml of HF was added and heated again until dry at which time 10 ml of 2 N HCl and 2 ml of $HCLO_4$ were added and again heated until dry

(4) 10 ml of 2 N HCl and 1-2 ml $H_2O$ were added to redissolve the solid

(5) the solutions were then transferred to previously cleaned and pH balanced on exchange columns filled with 100-200 mesh Amberlite resin CG-120 Na Type 1

(6) the columns were eluted with 85 ml of 2 N HCl which removed all the elements except the REE, Ba, Hf, Zr, Y and Sc

(7) the REE, Y, Sc and Ba were collected in teflon beakers by eluting the columns with 100 ml of 6 N HCl. This solution was heated to dryness and subsequently dissolved in 25 ml of $H_2O$.

(8) 2 drops of $H_2SO_4$ were added to precipitate out the Ba as $BaSO_4$ which was filtered off. Then the sample was again heated until dry.

(9) 5 ml of 6 NHCl was added to dissolve the sample which was again heated until dry then redissolved, with 5 ml of demineralized $H_2O$

(10) SA-2 ion exchange resin loaded papers, previously cut to fit the sample holders were added to the solution which was allowed to equilibrate for 24 hours

(11) the ion-exchange papers were gradually dried under an infra-red heat lamp

(12) both sides of the ion-exchange papers were then run on the XRF using a Rh tube

MINERAL SEPARATION METHOD

Each sample was ground and seived to -320 mesh. The -230 mesh fraction was then separated into two fractions by a heavy liquid separation. Using a separatory funnel and bromoform, a clean felsic fraction was obtained. The heavy fraction was again separated by heavy liquid using methyl iodide. This resulted in a zircon fraction and a heavy mineral fraction which was predominantly a mafic fraction. The mafic fraction was then pulverized in an agate mortar and pestal. This was subjected to numerous runs through a Franz magnetic separator to obtain a clean mafic fraction. Each fraction, mafic, felsic and zircon was examined optically to determine the amount of contamination.

The mafic and felsic fractions were prepared for REE analyses by the same method as the whole rock samples. The zircon fraction was dissolved and run through the ion exchange columns using the technique described under the REE Analyses Section. The zircons were dissolved by:

(1) weighing .002 g of sample which was placed in a Parr Teflon Lined Digestion Bomb with 2.5 ml of mixed hydrofluoric and nitric acid

(2) the bombs were placed in an oven and heated for 36 hours at which time they were removed and the sample put on the ion-exchange columns.

# Appendix C

## Geochemical Tables

On the following tables, all silicate analyses are in oxide percent, trace and rare earth element concentrations are in ppm., and n.d. represents none detected.

## Clinopyroxene-fayalite Granite

| Sample Number | 054 | 060 | 061 | 062c | 064b |
|---|---|---|---|---|---|
| $SiO_2$ | 66.02 | 67.36 | 67.39 | 62.83 | 66.15 |
| $Al_2O_3$ | 11.97 | 12.09 | 13.31 | 13.09 | 11.94 |
| $Fe_2O_3$ | 1.27 | 1.45 | 1.84 | 0.71 | 1.88 |
| FeO | 6.30 | 4.81 | 3.92 | 8.71 | 5.61 |
| MgO | 1.51 | 0.37 | 0.22 | 1.81 | 0.33 |
| CaO | 3.59 | 2.62 | 2.37 | 4.04 | 2.99 |
| $K_2O$ | 2.90 | 3.97 | 4.09 | 3.12 | 3.15 |
| $Na_2O$ | 3.58 | 3.56 | 3.18 | 3.32 | 3.43 |
| $TiO_2$ | 1.03 | 0.75 | 0.69 | 1.17 | 0.86 |
| MnO | 0.11 | 0.11 | 0.09 | 0.10 | 0.10 |
| $P_2O_5$ | 0.24 | 0.14 | 0.12 | 0.28 | 0.18 |
| LOI | 1.53 | 1.38 | 1.50 | 0.94 | 1.34 |
| Total | 100.05 | 98.61 | 98.72 | 98.64 | 97.99 |
| | | | | | |
| Nb | 31 | 29 | 30 | 37 | 16 |
| Th | 5 | 13 | 15 | 4 | 4 |
| Zr | 522 | 468 | 553 | 648 | 597 |
| Y | 59 | 70 | 64 | 65 | 49 |
| Sr | 307 | 170 | 173 | 253 | 204 |
| Rb | 55 | 87 | 98 | 53 | 44 |
| Pb | 16 | 25 | 27 | 16 | 18 |
| Cr | 11 | 10 | 10 | 11 | 12 |
| Ga | 21 | 22 | 22 | 22 | 20 |
| Zn | 147 | 126 | 123 | 173 | 140 |
| Cu | 13 | 10 | 4 | 19 | 14 |
| Ni | 18 | 21 | 15 | 20 | 14 |
| Ba | 1604 | 1787 | 1656 | 2229 | 1984 |

| Sample Number | 068 | 069A | 069 | 071 | 072 | 073 | 074 | 075 | 078 | 079 | 080 | 081 | 082 | 083 |
|---|---|---|---|---|---|---|---|---|---|---|---|---|---|---|
| $SiO_2$ | 70.24 | 71.64 | 68.43 | 74.96 | 74.79 | 73.74 | 72.80 | 72.71 | 71.71 | 73.02 | 73.04 | 71.87 | 71.82 | 72.95 |
| $Al_2O_3$ | 12.86 | 12.25 | 12.36 | 11.31 | 11.12 | 11.42 | 10.45 | 11.03 | 11.61 | 11.99 | 11.25 | 10.87 | 11.06 | 10.94 |
| $Fe_2O_3$ | 0.90 | 0.70 | 1.42 | 1.52 | 1.31 | 1.47 | 2.15 | 1.56 | 1.68 | 1.35 | 1.97 | 2.68 | 1.87 | 1.15 |
| FeO | 2.92 | 3.04 | 3.42 | 1.04 | 2.29 | 1.81 | 1.95 | 2.28 | 2.51 | 1.84 | 2.28 | 1.61 | 2.53 | 2.67 |
| MgO | 0.08 | n.d. | 0.18 | 0.10 | 0.07 | n.d. | 0.22 | 0.04 | 0.16 | 0.02 | 0.02 | 0.22 | 0.05 | 0.02 |
| CaO | 0.78 | 0.78 | 1.81 | 0.31 | 0.64 | 0.47 | 0.57 | 0.61 | 0.57 | 0.52 | 0.69 | 0.43 | 0.59 | 0.62 |
| $K_2O$ | 4.92 | 4.88 | 4.28 | 4.79 | 4.63 | 4.72 | 4.65 | 4.58 | 4.77 | 4.92 | 4.88 | 4.69 | 4.64 | 4.62 |
| $Na_2O$ | 4.44 | 4.30 | 5.18 | 3.60 | 3.71 | 3.84 | 3.82 | 4.74 | 4.23 | 4.21 | 4.20 | 4.26 | 3.99 | 4.14 |
| $TiO_2$ | 0.39 | 0.44 | 0.58 | 0.26 | 0.35 | 0.34 | 0.40 | 0.40 | 0.42 | 0.39 | 0.43 | 0.41 | 0.39 | 0.40 |
| MnO | 0.10 | 0.08 | 0.11 | 0.08 | 0.11 | 0.08 | 0.09 | 0.09 | 0.09 | 0.10 | 0.08 | 0.11 | 0.09 | 0.09 |
| $P_2O_5$ | 0.03 | 0.01 | 0.12 | n.d. | n.d. | 0.02 | n.d. | n.d. | n.d. | 0.01 | 0.02 | n.d. | n.d. | n.d. |
| LOI | 0.50 | 0.44 | 0.61 | 0.50 | 0.64 | 0.61 | 0.79 | 0.19 | 0.96 | 0.65 | 0.53 | 2.94 | 0.67 | 0.61 |
| Total | 95.26 | 98.56 | 98.50 | 98.47 | 99.66 | 98.52 | 98.29 | 98.23 | 98.71 | 99.02 | 99.09 | 100.09 | 95.80 | 98.21 |
| Nb | 47 | 79 | 52 | 62 | 64 | 61 | 101 | 89 | 102 | 62 | 59 | 107 | 106 | 96 |
| Th | 11 | 15 | 10 | 16 | 33 | 17 | 28 | 24 | 28 | 14 | 13 | 31 | 32 | 29 |
| Zr | 306 | 552 | 643 | 738 | 649 | 660 | 1090 | 983 | 1156 | 561 | 527 | 1256 | 1363 | 1431 |
| Y | 67 | 97 | 104 | 50 | 193 | 64 | 140 | 114 | 133 | 58 | 100 | 121 | 122 | 114 |
| Sr | 8 | 10 | 66 | 7 | 15 | 10 | 10 | 13 | 16 | 10 | 10 | 10 | 11 | 12 |
| Rb | 175 | 168 | 144 | 183 | 165 | 167 | 211 | 210 | 212 | 187 | 140 | 236 | 239 | 208 |
| Pb | 22 | 24 | 17 | 14 | 40 | 24 | 27 | 37 | 41 | 20 | 20 | 24 | 54 | 33 |
| Cr | 24 | 9 | 11 | 14 | 24 | 10 | 5 | 36 | 8 | 8 | 5 | 5 | 14 | 10 |
| Ga | 38 | 38 | 29 | 31 | 32 | 36 | 35 | 34 | 34 | 38 | 34 | 36 | 35 | 35 |
| Zn | 115 | 124 | 139 | 97 | 213 | 84 | 131 | 146 | 145 | 101 | 111 | 197 | 140 | 144 |
| Cu | 6 | 9 | 4 | 7 | 4 | 6 | 8 | 9 | 7 | 7 | 7 | 6 | 8 | 8 |
| Ni | 25 | 30 | 32 | 18 | 48 | 22 | 41 | 34 | 36 | 20 | 29 | 38 | 38 | 33 |
| Ba | 81 | 70 | 416 | 57 | 89 | 42 | 43 | 92 | 96 | 64 | 57 | 61 | 83 | 104 |

Nuiklavick Volcanics - Group 1

| Sample Number | 084 | 085 | 086A | 086B | 089 | 092 | 099 | 101 | 102 |
|---|---|---|---|---|---|---|---|---|---|
| $SiO_2$ | 78.33 | 78.11 | 78.76 | 84.22 | 73.82 | 77.46 | 77.74 | 71.38 | 71.71 |
| $Al_2O_5$ | 10.06 | 10.21 | 10.56 | 8.48 | 11.84 | 12.12 | 10.71 | 12.45 | 11.75 |
| $Fe_2O_3$ | 1.11 | 0.65 | 1.02 | 0.68 | 0.90 | n.d. | 0.78 | 0.05 | 1.55 |
| FeO | 1.78 | 1.79 | 1.61 | 0.55 | 2.38 | 3.83 | 1.96 | 2.88 | 1.85 |
| MgO | 0.15 | 0.07 | 0.07 | 0.04 | 0.37 | n.d. | 0.05 | 0.02 | 0.02 |
| CaO | 0.20 | 1.07 | 0.15 | 0.16 | 0.41 | 0.17 | 0.16 | 0.75 | 0.62 |
| $K_2O$ | 4.53 | 5.47 | 4.71 | 2.50 | 5.86 | 3.21 | 5.91 | 5.05 | 5.32 |
| $Na_2O$ | 0.43 | 0.41 | 0.05 | n.d. | 0.50 | 0.04 | 0.27 | 3.22 | 3.73 |
| $TiO_2$ | 0.35 | 0.32 | 0.32 | 0.29 | 0.36 | 0.11 | 0.34 | 0.38 | 0.32 |
| MnO | 0.08 | 0.08 | 0.08 | 0.08 | 0.08 | 0.08 | 0.09 | 0.10 | 0.09 |
| $P_2O_5$ | n.d. | 0.02 | n.d. | n.d. | n.d. | n.d. | 0.01 | n.d. | n.d. |
| LOI | 1.57 | 1.42 | 1.88 | 1.47 | 1.92 | 2.59 | 2.31 | 1.60 | 1.35 |
| Total | 98.59 | 98.72 | 99.08 | 98.47 | 98.44 | 99.97 | 100.33 | 97.81 | 98.31 |
| Nb | 73 | 79 | 70 | 63 | 109 | 107 | 75 | 207 | 222 |
| Th | 28 | 29 | 24 | 22 | 27 | 26 | 25 | 30 | 41 |
| Zr | 761 | 819 | 742 | 690 | 1236 | 1221 | 792 | 1339 | 1399 |
| Y | 92 | 103 | 90 | 86 | 129 | 121 | 86 | 172 | 233 |
| Sr | 18 | 21 | 13 | 5 | 19 | 6 | 15 | 16 | 14 |
| Rb | 216 | 255 | 242 | 145 | 435 | 156 | 368 | 286 | 330 |
| Pb | 35 | 37 | 17 | 9 | 37 | 45 | 34 | 176 | 65 |
| Cr | 7 | 7 | 6 | 9 | 7 | n.d. | 8 | 7 | 8 |
| Ga | 23 | 20 | 23 | 24 | 23 | 36 | 20 | 39 | 37 |
| Zr | 87 | 55 | 47 | 43 | 56 | 104 | 190 | 260 | 128 |
| Ca | 7 | 3 | 8 | 10 | 12 | 7 | 5 | 7 | 4 |
| Ni | 29 | 33 | 30 | 23 | 49 | 33 | 36 | 50 | 67 |
| Ba | 192 | 223 | 218 | 99 | 188 | 63 | 224 | 314 | 149 |

Nuiklavick Volcanics - Group 2

| Sample Number | 090 | 091A | 091B | 100 |
|---|---|---|---|---|
| $SiO_2$ | 75.57 | 72.99 | 75.90 | 78.16 |
| $Al_2O_3$ | 10.10 | 10.23 | 10.60 | 8.53 |
| $Fe_2O_3$ | 1.24 | 2.64 | 0.97 | 1.05 |
| FeO | 2.02 | 2.73 | 4.06 | 3.22 |
| MgO | 0.02 | 0.02 | 0.02 | 0.08 |
| CaO | 0.19 | 0.02 | 0.02 | 0.17 |
| $K_2O$ | 6.31 | 4.78 | 3.82 | 4.15 |
| $Na_2O$ | 0.47 | 2.49 | 1.00 | 0.05 |
| $TiO_2$ | 0.34 | 0.33 | 0.35 | 0.36 |
| MnO | 10.09 | 0.09 | 0.08 | 0.09 |
| $P_2O_5$ | n.d. | n.d. | n.d. | n.d. |
| LOI | 1.36 | 1.34 | 1.11 | 1.80 |
| Total | 97.71 | 98.17 | 98.35 | 97.66 |
| | | | | |
| Nb | 299 | 252 | 280 | 231 |
| Th | 76 | 58 | 69 | 75 |
| Zr | 3317 | 2742 | 3108 | 3465 |
| Y | 366 | 291 | 335 | 286 |
| Sr | 9 | 6 | 7 | 12 |
| Rb | 460 | 367 | 464 | 286 |
| Pb | 184 | 17 | 19 | 121 |
| Cr | 2 | 1 | 5 | 7 |
| Ga | 29 | 33 | 34 | 29 |
| Zn | 772 | 76 | 46 | 248 |
| Cu | n.d. | n.d. | n.d. | 7 |
| Ni | 90 | 75 | 88 | 72 |
| Ba | 10 | 20 | 9 | 34 |

## Nuiklavick Volcanics - Group 3

| Sample Number | 087 | 088 | 093A | 093B | 094 | 095 | 097a | 097b | 097c | 098 |
|---|---|---|---|---|---|---|---|---|---|---|
| $SiO_2$ | 81.68 | 84.63 | 78.33 | 75.58 | 75.31 | 79.63 | 76.65 | 77.58 | 74.73 | 76.27 |
| $Al_2O_3$ | 7.61 | 6.04 | 10.19 | 10.74 | 9.61 | 8.70 | 9.11 | 8.98 | 8.96 | 9.18 |
| $Fe_2O_3$ | 1.40 | 1.08 | 0.65 | 0.78 | 2.24 | 2.74 | 1.37 | 3.80 | 2.89 | 1.04 |
| FeO | 3.49 | 1.93 | 3.63 | 3.99 | 4.68 | 2.11 | 4.54 | 2.45 | 3.31 | 4.59 |
| MgO | 0.02 | 0.02 | 0.01 | n.d. | 0.02 | 0.04 | 0.02 | 0.07 | 0.04 | 0.04 |
| CaO | 0.10 | 0.16 | 0.11 | 0.17 | 0.34 | 0.18 | 0.18 | 0.17 | 0.18 | 0.19 |
| $K_2O$ | 1.73 | 1.69 | 2.19 | 2.32 | 3.91 | 3.00 | 4.82 | 5.71 | 5.51 | 5.05 |
| $Na_2O$ | n.d. | n.d. | 0.15 | 0.13 | n.d. | n.d. | 0.10 | 0.32 | 0.27 | 0.13 |
| $TiO_2$ | 0.39 | 0.39 | 0.32 | 0.30 | 0.35 | 0.28 | 0.43 | 0.42 | 0.41 | 0.43 |
| MnO | 0.11 | 0.08 | 0.10 | 0.09 | 0.10 | 0.10 | 0.09 | 0.09 | 0.10 | 0.11 |
| $P_2O_5$ | n.d. | n.d. | n.d. | n.d. | n.d. | n.d. | n.d. | n.d. | n.d. | n.d. |
| LOI | 2.10 | 1.73 | 1.54 | 3.40 | 2.34 | 2.34 | 1.59 | 1.33 | 1.62 | 1.33 |
| Total | 98.63 | 97.75 | 97.22 | 97.50 | 98.90 | 99.12 | 99.01 | 100.92 | 98.02 | 98.36 |
| | | | | | | | | | | |
| Nb | 309 | 288 | 472 | 481 | 507 | 450 | 315 | 309 | 306 | 312 |
| Th | 104 | 93 | 122 | 118 | 127 | 113 | 98 | 98 | 99 | 100 |
| Zr | 4530 | 4257 | 5255 | 5075 | 5495 | 4885 | 4727 | 4692 | 4510 | 4625 |
| Y | 574 | 401 | 588 | 545 | 597 | 529 | 461 | 361 | 442 | 424 |
| Sr | 4 | 4 | 6 | 7 | 9 | 6 | 9 | 11 | 10 | 10 |
| Rb | 145 | 185 | 271 | 335 | 583 | 463 | 502 | 419 | 487 | 482 |
| Pb | 21 | 27 | 149 | 100 | 53 | 47 | 98 | 104 | 125 | 135 |
| Cr | 3 | 9 | n.d. | n.d. | n.d. | n.d. | n.d. | 1 | n.d. | n.d. |
| Ga | 28 | 16 | 33 | 39 | 27 | 29 | 28 | 19 | 25 | 22 |
| Zn | 125 | 17 | 475 | 525 | 749 | 1538 | 579 | 552 | 790 | 562 |
| Cu | n.d. | n.d. | n.d. | 2 | n.d. | 57 | n.d. | n.d. | 9 | n.d. |
| Ni | 119 | 83 | 29 | 131 | 152 | 57 | 113 | 93 | 114 | 108 |
| Ba | 35 | 20 | 23 | 13 | 17 | 121 | 17 | 28 | 25 | 31 |

CIPW Normative Analyses (In Mole %)

Clinopyroxene-fayalite granite

| Sample Number | 057 | 060 | 061 | 062c | 064b |
|---|---|---|---|---|---|
| Q | 55.66 | 58.83 | 61.78 | 45.32 | 60.78 |
| Or | 9.19 | 12.38 | 12.32 | 11.21 | 9.59 |
| Ab | 17.25 | 16.88 | 14.56 | 18.12 | 15.87 |
| An | 4.31 | 2.79 | 5.08 | 7.05 | 4.06 |
| Di | 4.64 | 3.81 | 0.70 | 4.35 | 3.22 |
| Hy | 5.58 | 2.44 | 2.56 | 10.38 | 3.06 |
| Mt | 1.19 | 1.33 | 1.63 | 0.75 | 1.69 |
| Il | 1.92 | 1.38 | 1.23 | 2.48 | 1.54 |
| Ap | 0.25 | 0.14 | 0.12 | 0.33 | 0.18 |
| Agpaitic Index | .754 | .840 | .726 | .675 | .758 |

## Arfvedsonite-riebeckite granite

| Sample Number | 068 | 069A | 069 | 071 | 072 | 073 | 074 | 075 | 078 | 079 | 080 | 081 | 082 | 083 |
|---|---|---|---|---|---|---|---|---|---|---|---|---|---|---|
| Q | 57.11 | 60.34 | 50.04 | 70.94 | 69.20 | 68.28 | 67.97 | 63.92 | 62.61 | 64.20 | 64.33 | 64.89 | 65.44 | 65.75 |
| Or | 15.82 | 14.90 | 14.89 | 12.43 | 12.19 | 12.80 | 12.67 | 13.07 | 14.07 | 14.14 | 13.86 | 13.38 | 13.21 | 13.00 |
| Ab | 21.70 | 19.66 | 24.83 | 14.20 | 14.85 | 15.81 | 13.64 | 16.01 | 17.57 | 17.69 | 15.66 | 15.28 | 15.88 | 15.44 |
| An | 0.34 | 0.00 | 0.00 | 0.24 | 0.01 | 0.00 | 0.00 | 0.00 | 0.00 | 0.00 | 0.00 | 0.00 | 0.00 | 0.00 |
| Ns | | | | | | | | 0.96 | 0.00 | 0.00 | 0.00 | 0.00 | 0.00 | 0.18 |
| Di | 1.63 | 1.88 | 4.86 | 0.52 | 1.26 | 0.95 | 1.19 | 1.37 | 1.31 | 1.11 | 1.44 | 0.89 | 1.27 | 1.33 |
| Hy | 1.72 | 1.54 | 1.28 | 0.06 | 0.58 | 0.35 | 0.46 | 1.26 | 1.40 | 0.57 | 0.94 | 0.86 | 1.12 | 1.58 |
| Ac | 0.00 | 0.30 | 2.55 | 0.00 | 0.00 | 0.01 | 2.18 | 2.63 | 1.44 | 0.69 | 2.47 | 3.20 | 1.38 | 1.91 |
| Mt | 0.85 | 0.48 | 0.18 | 1.16 | 1.02 | 1.17 | 0.64 | 0.00 | 0.74 | 0.80 | 0.42 | 0.66 | 0.88 | 0.00 |
| Il | 0.74 | 0.79 | 1.19 | 0.00 | 0.54 | 0.54 | 0.64 | 0.67 | 0.73 | 0.86 | 0.72 | 0.69 | 0.65 | 0.66 |
| Ap | 0.03 | 0.01 | 0.14 | 0.00 | 0.00 | 0.02 | 0.00 | 0.00 | 0.00 | 0.01 | 0.02 | 0.00 | 0.00 | 0.00 |
| Agpaitic Index | .982 | 1.008 | 1.064 | .982 | .999 | 1.000 | 1.083 | 1.156 | 1.045 | 1.022 | 1.083 | 1.112 | 1.047 | 1.079 |

## REE Analyses

### Clinopyroxene-fayalite Granite

| Sample | 057 | 060 | 061 | 062C | 064B |
|---|---|---|---|---|---|
| La | 60 | 70 | 64 | 51 | 34 |
| Ce | 144 | 167 | 148 | 128 | 89 |
| Pr | 17 | 19 | 18 | 16 | 12 |
| Nd | 76 | 82 | 71 | 71 | 53 |
| Sm | 14 | 15 | 14 | 13 | 11 |
| Eu | 3 | 3 | 3 | 3 | 3 |
| Gd | 12 | 14 | 12 | 13 | 10 |
| Du | 11 | 12 | 11 | 12 | 10 |
| Er | 6 | 7 | 6 | 7 | 4 |

### Arfvedsonite-riebeckite Granite

| Sample | 068 | 069A | 069 | 071 | 072 | 073 | 074 | 075 | 079 | 080 | 081 | 082 | 083 |
|---|---|---|---|---|---|---|---|---|---|---|---|---|---|
| La | 59 | 214 | 85 | 36 | 244 | 160 | 180 | 211 | 120 | 145 | 180 | 207 | 189 |
| Ce | 126 | 428 | 224 | 93 | 533 | 321 | 340 | 433 | 208 | 303 | 390 | 421 | 392 |
| Pr | 18 | 42 | 27 | 9 | 56 | 32 | 42 | 45 | 25 | 36 | 35 | 44 | 42 |
| Nd | 60 | 153 | 100 | 28 | 206 | 109 | 135 | 157 | 89 | 124 | 121 | 148 | 144 |
| Sm | 10 | 24 | 19 | 4 | 36 | 16 | 23 | 26 | 14 | 20 | 20 | 25 | 24 |
| Eu | n.d. | 2 | 1 | n.d. | 2 | 1 | 0.1 | 1 | 1 | 1 | 1 | 1 | 1 |
| Gd | 10 | 18 | 18 | 5 | 31 | 13 | 23 | 22 | 10 | 18 | 16 | 20 | 21 |
| Du | 11 | 19 | 16 | 6 | 31 | 11 | 21 | 20 | 10 | 21 | 19 | 22 | 18 |
| Er | 8 | 10 | 9 | 6 | 17 | 5 | 15 | 15 | 12 | 5 | 9 | 12 | 13 |

## REE Analyses

### Nuiklavick Volcanics - Group 1

| Sample Number | 084 | 085 | 086A | 086B | 089 | 092 | 099 | 101 | 102 |
|---|---|---|---|---|---|---|---|---|---|
| La | 98 | 140 | 139 | 147 | 307 | 395 | 148 | 152 | 246 |
| Ce | 210 | 294 | 277 | 288 | 649 | 660 | 318 | 267 | 525 |
| Pr | 21 | 33 | 32 | 28 | 66 | 88 | 28 | 32 | 57 |
| Nd | 80 | 106 | 106 | 102 | 220 | 256 | 102 | 116 | 190 |
| Sm | 13 | 19 | 18 | 17 | 34 | 34 | 16 | 26 | 35 |
| Eu | n.d. | 0.3 | 0.4 | 1 | 2 | n.d. | 2 | 1 | 1 |
| Gd | 14 | 17 | 14 | 15 | 27 | 25 | 13 | 25 | 34 |
| Du | 14 | 17 | 16 | 15 | 23 | 21 | 14 | 30 | 39 |
| Er | 9 | 11 | 10 | 9 | 15 | 15 | 10 | 19 | 24 |

### Nuiklavick Volcanics - Group 2

| Sample Number | 090 | 091A | 091B | 100 |
|---|---|---|---|---|
| La | 219 | 238 | 271 | 129 |
| Ce | 499 | 523 | 596 | 303 |
| Pr | 61 | 56 | 63 | 34 |
| Nd | 212 | 202 | 225 | 145 |
| Sm | 47 | 40 | 46 | 28 |
| Eu | n.d. | n.d. | 1 | n.d. |
| Gd | 48 | 43 | 45 | 32 |
| Du | 58 | 48 | 53 | 49 |
| Er | 38 | 33 | 34 | 33 |

REE Analyses

Nuiklavick Volcanics - Group 3

| Sample Number | 087 | 088 | 093A | 093B | 094 | 095 | 097A | 097B | 097C | 098 |
|---|---|---|---|---|---|---|---|---|---|---|
| La | 381 | 86 | 319 | 342 | 347 | 365 | 424 | 238 | 403 | 360 |
| Ce | 569 | 240 | 721 | 769 | 777 | 815 | 853 | 544 | 849 | 784 |
| Pr | 87 | 24 | 79 | 86 | 90 | 89 | 93 | 61 | 96 | 88 |
| Nd | 339 | 110 | 283 | 304 | 315 | 323 | 346 | 235 | 355 | 317 |
| Sm | 73 | 41 | 64 | 68 | 69 | 68 | 67 | 54 | 69 | 62 |
| Eu | 2 | 1 | n.d. | 2 | 1 | 3 | 6 | 1 | 4 | 1 |
| Gd | 71 | 48 | 67 | 68 | 75 | 72 | 68 | 55 | 67 | 60 |
| Du | 82 | 66 | 86 | 88 | 93 | 82 | 76 | 63 | 77 | 74 |
| Er | 51 | 42 | 62 | 59 | 67 | 57 | 52 | 41 | 48 | 48 |

| Sample Number | 073 Felsic Fraction | 079 Mafic fraction | 073 Zircons |
|---|---|---|---|
| La | 97 | 910 | 8249 |
| Ce | 141 | 1827 | 1647 |
| Pr | 12 | 199 | 1893 |
| Nd | 54 | 706 | 6829 |
| Sm | 8 | 124 | 1434 |
| Eu | n.d. | 2 | n.d. |
| Gd | 5 | 104 | 3512 |
| Py | 4 | 89 | 12310 |
| Er | 4 | 59 | 19064 |

# APPENDIX D

This Appendix consists of supplementary Harker type correlation diagrams on all diagrams, concentrations are in ppm and symbols represent:

- □ arfvedsonite-riebeckite granite
- Δ Nuiklavick volcanics - group 1
- \+ Nuiklavick volcanics - group 2
- ● Nuiklavick volcanics - group 3

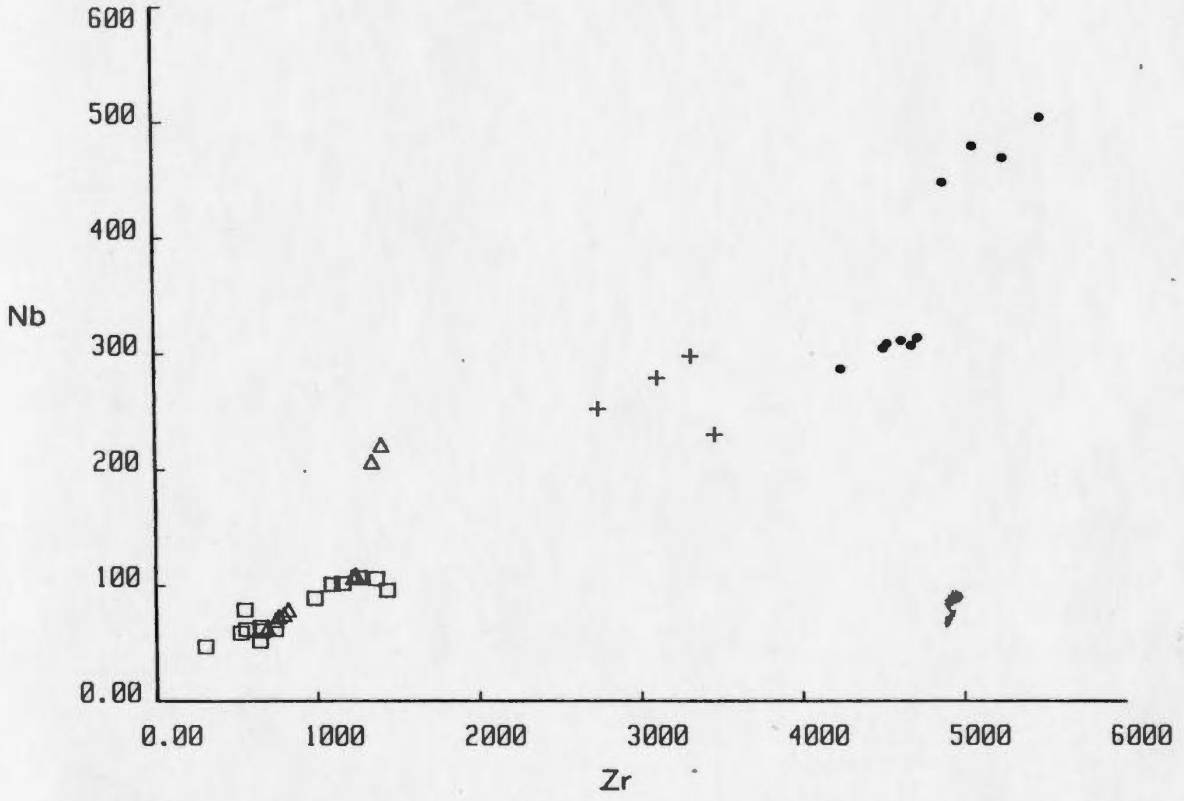
600
500
400
Nb
300
200
100
0.00
0.00
1000
2000
3000
4000
5000
6000
Zr

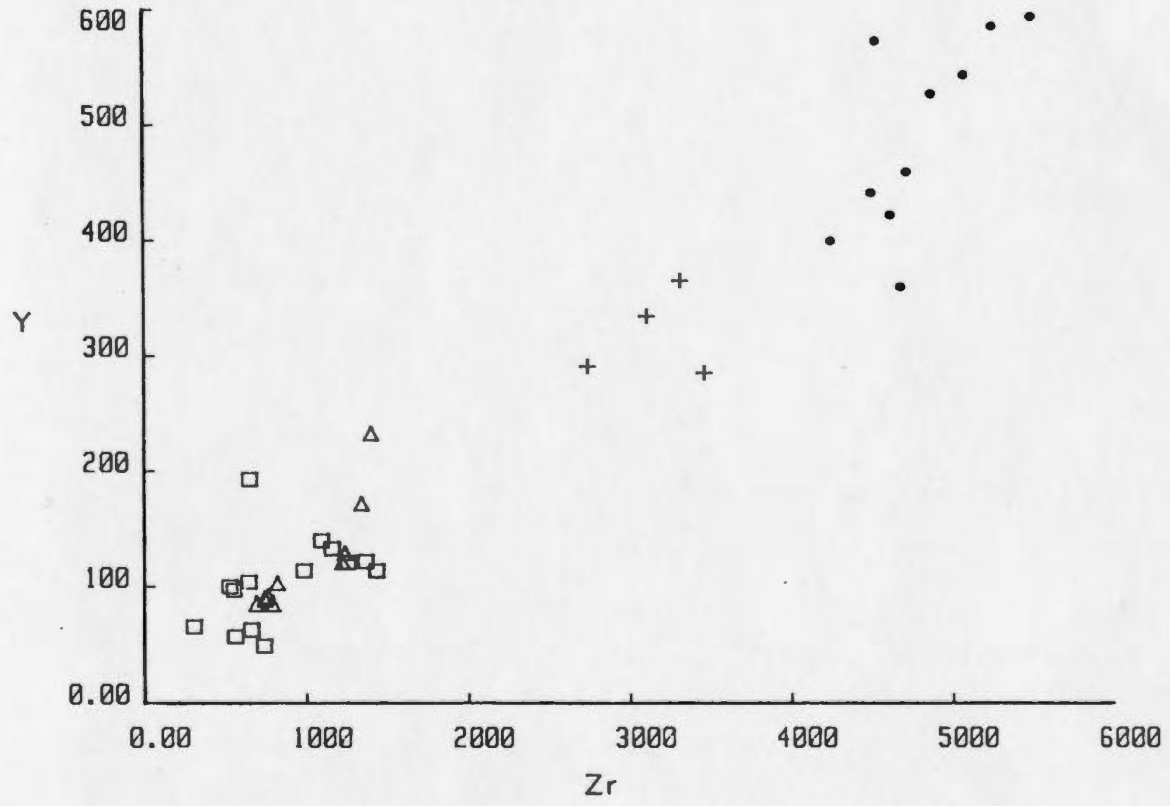
600
500
400
Y
300
200
100
0.00
0.00
1000
2000
3000
4000
5000
6000
Zr

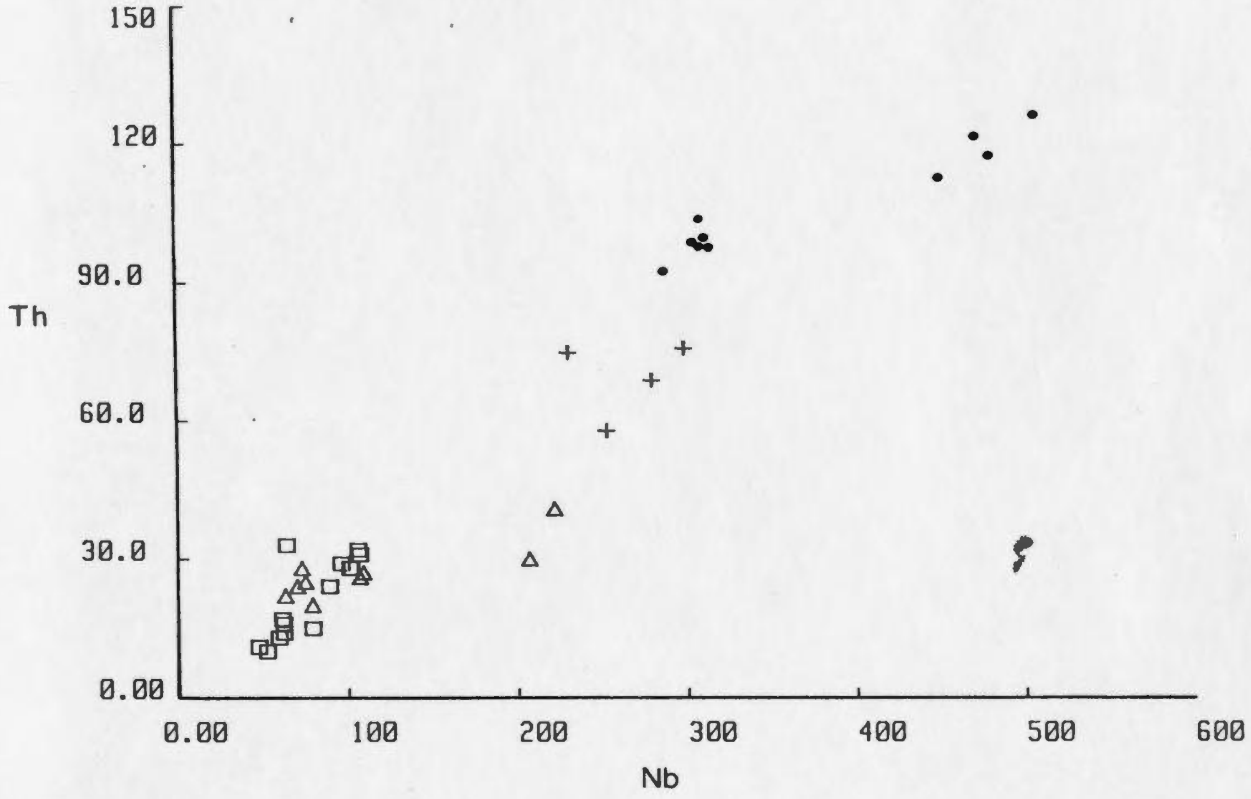
150
120
90.0
60.0
30.0
0.00
Th
0.00
100
200
300
400
500
600
Nb

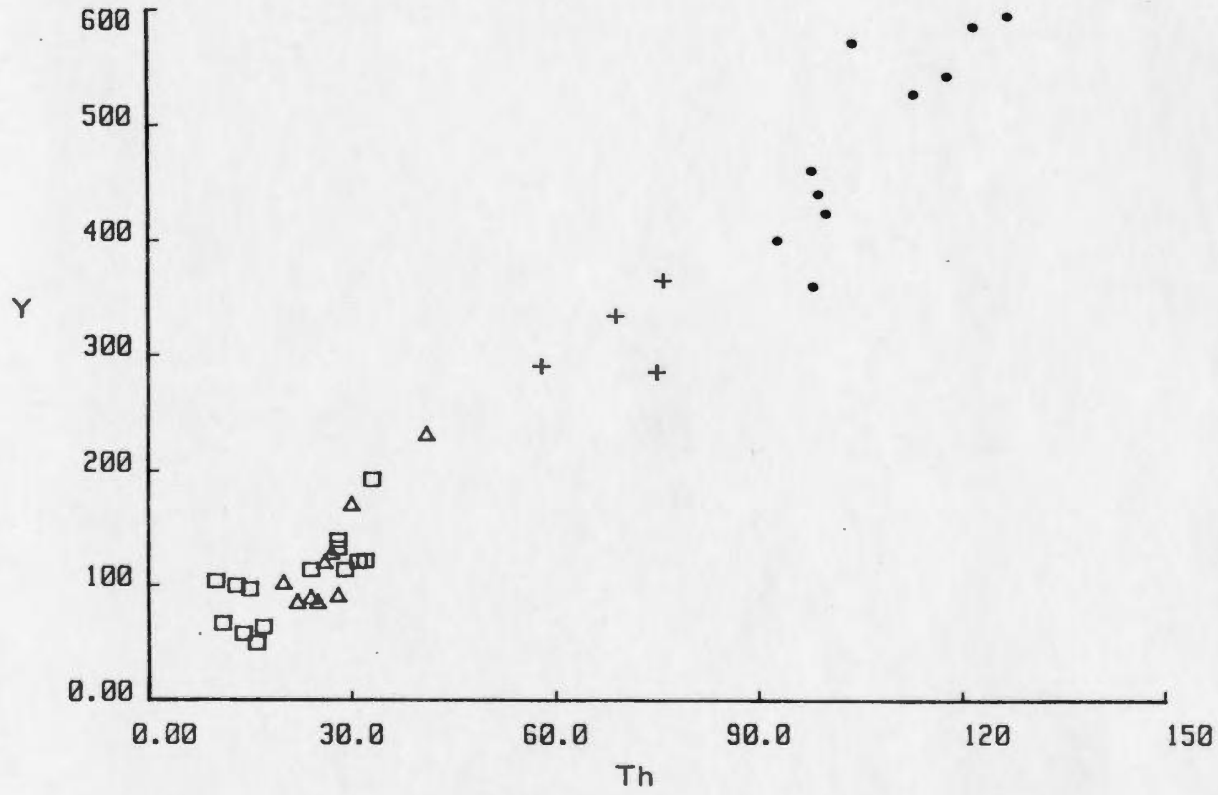
600
500
400
300
200
100
0.00
Y
0.00
30.0
60.0
90.0
120
150
Th

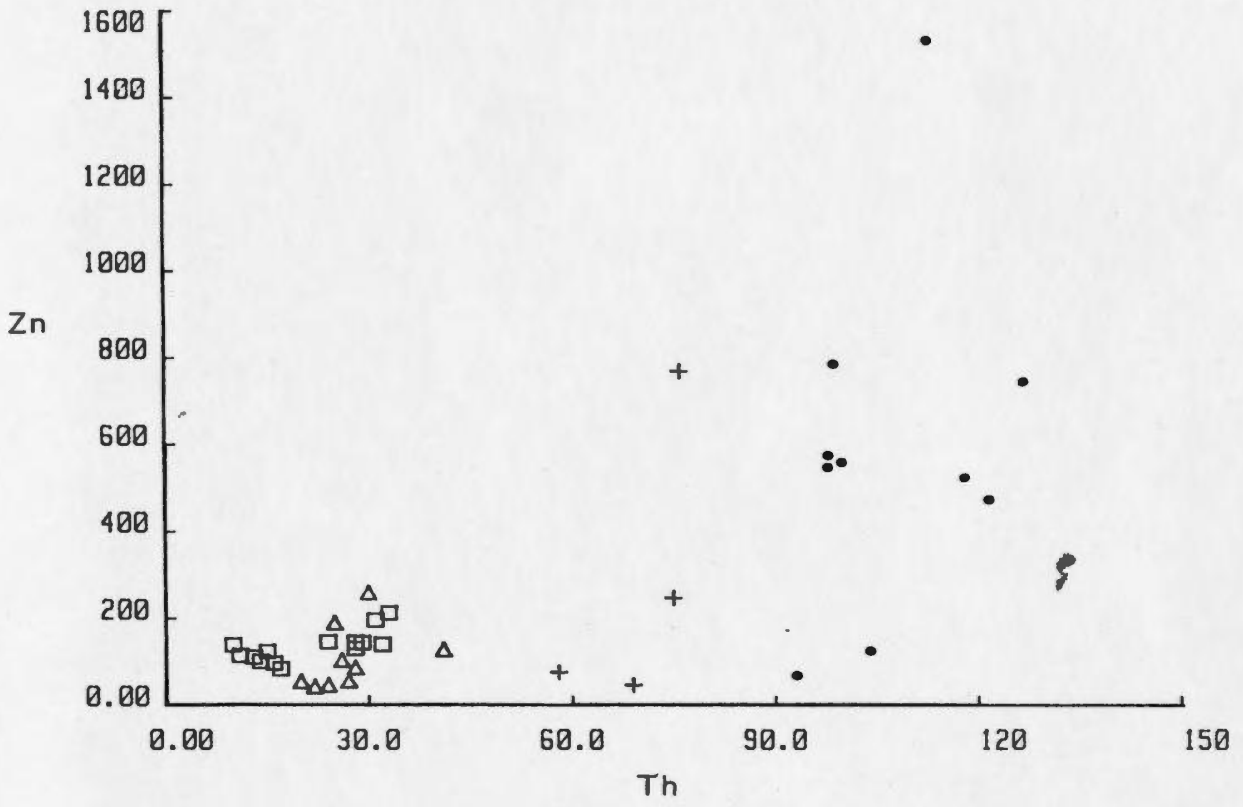
1600
1400
1200
1000
Zn
800
600
400
200
0.00
0.00
30.0
60.0
90.0
120
150
Th

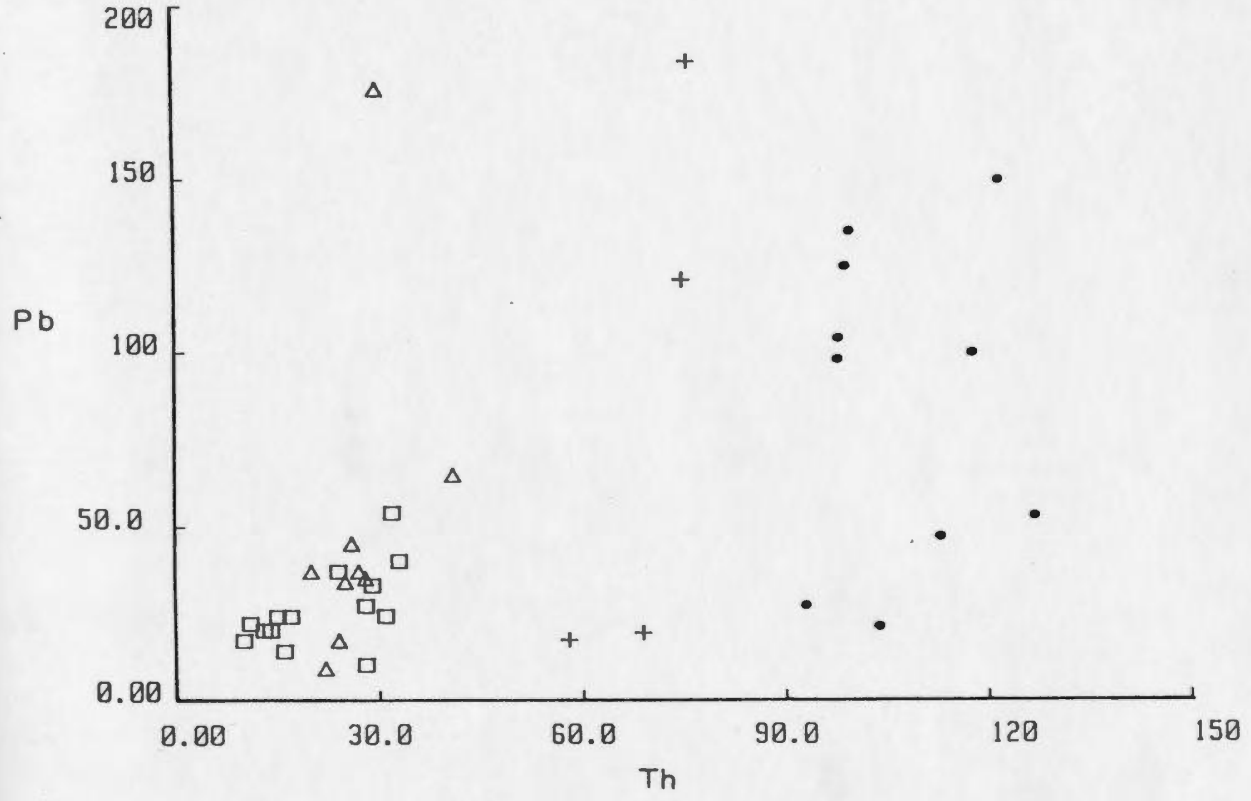
200
150
Pb
100
50.0
0.00
0.00
30.0
60.0
90.0
120
150
Th

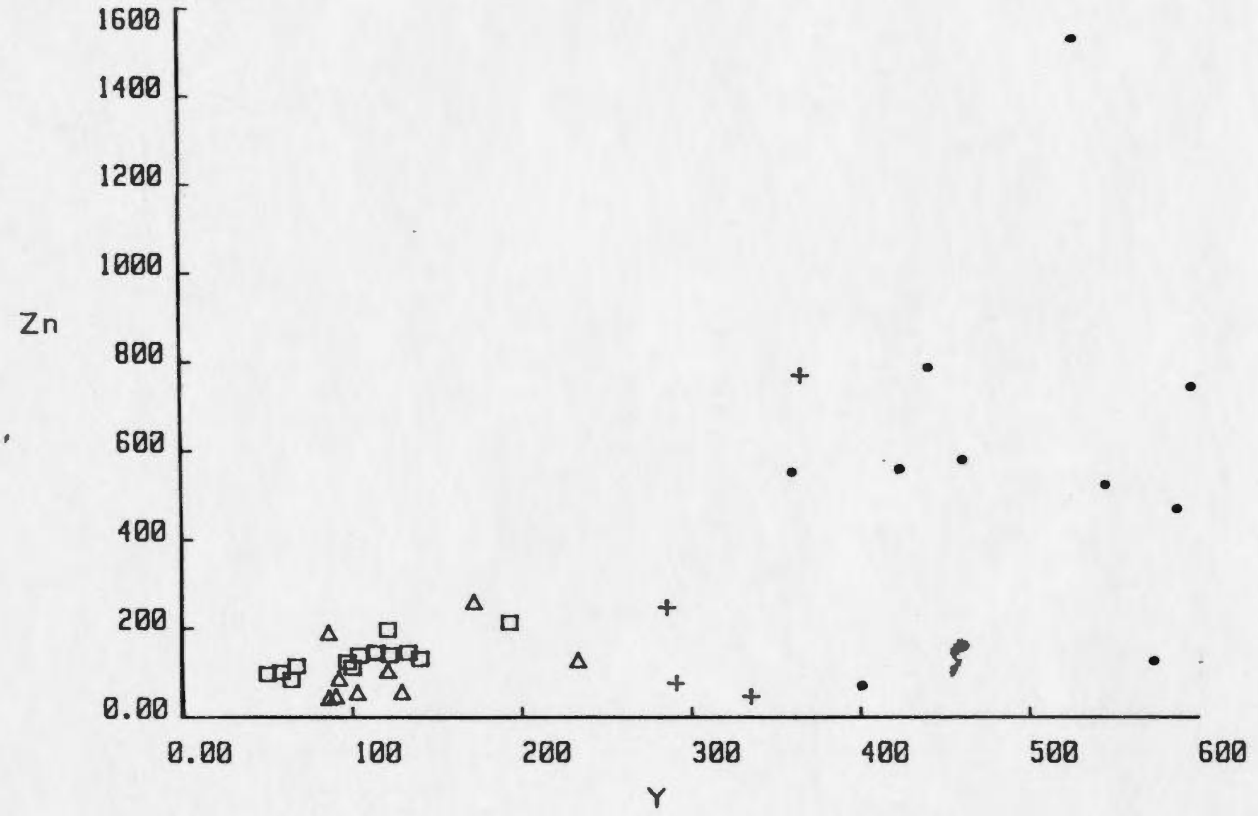
1600
1400
1200
1000
Zn
800
600
400
200
0.00
0.00
100
200
300
400
500
600
Y

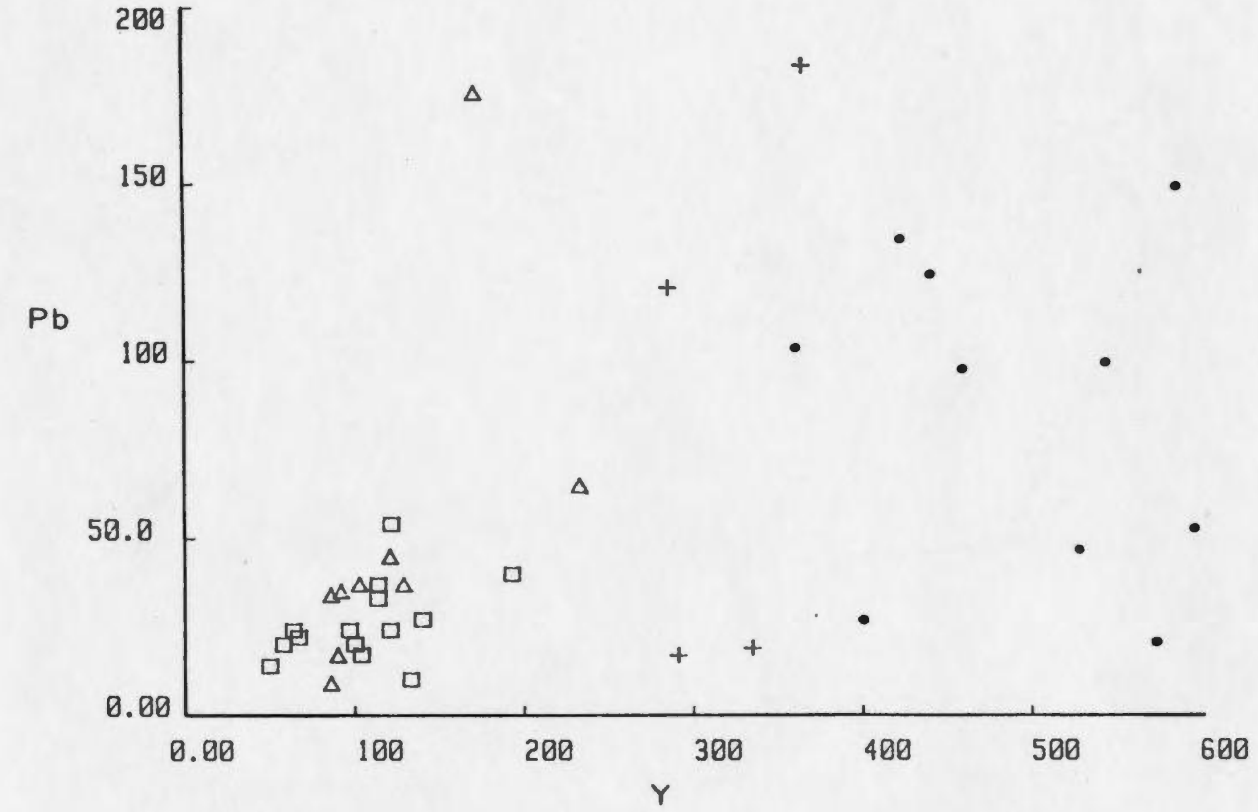
200
150
Pb
100
50.0
0.00
0.00
100
200
300
400
500
600
Y

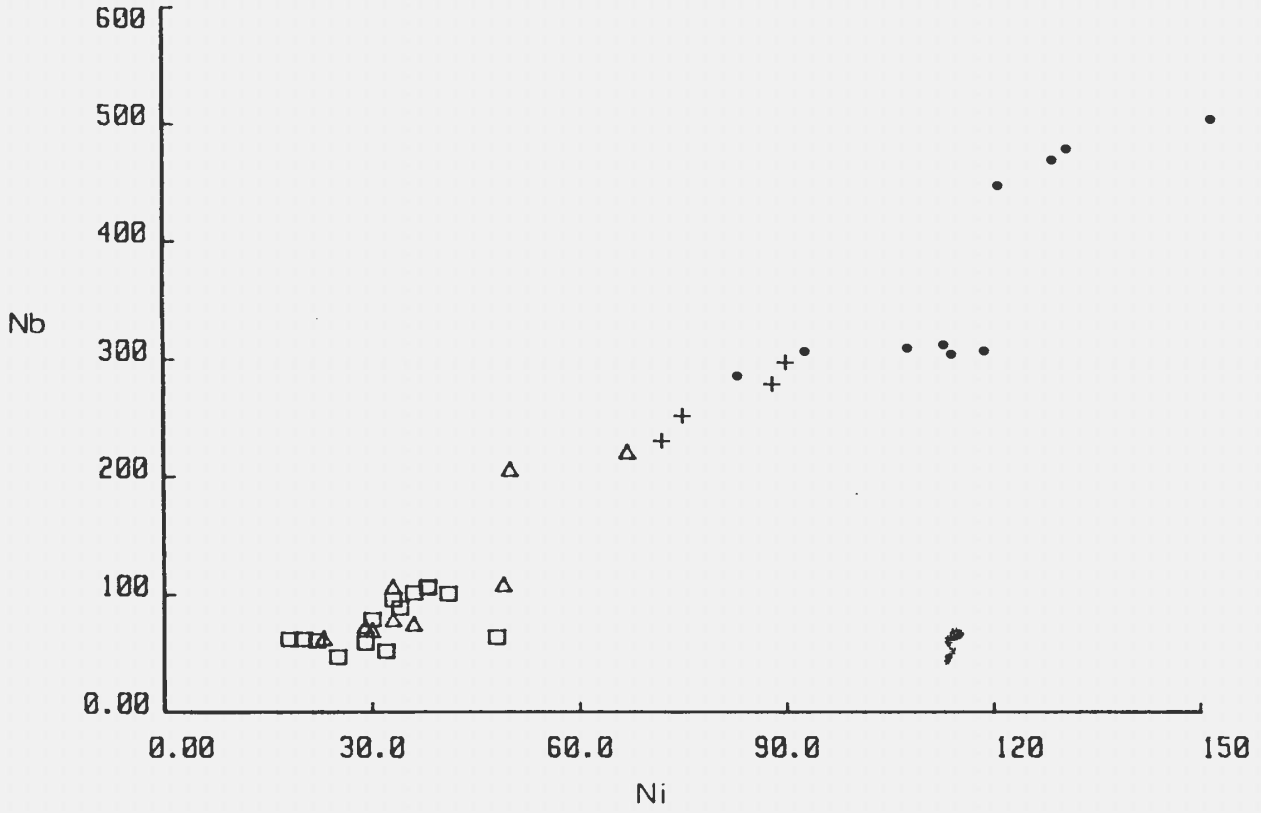
600
500
400
Nb
300
200
100
0.00
0.00
30.0
60.0
90.0
120
150
Ni

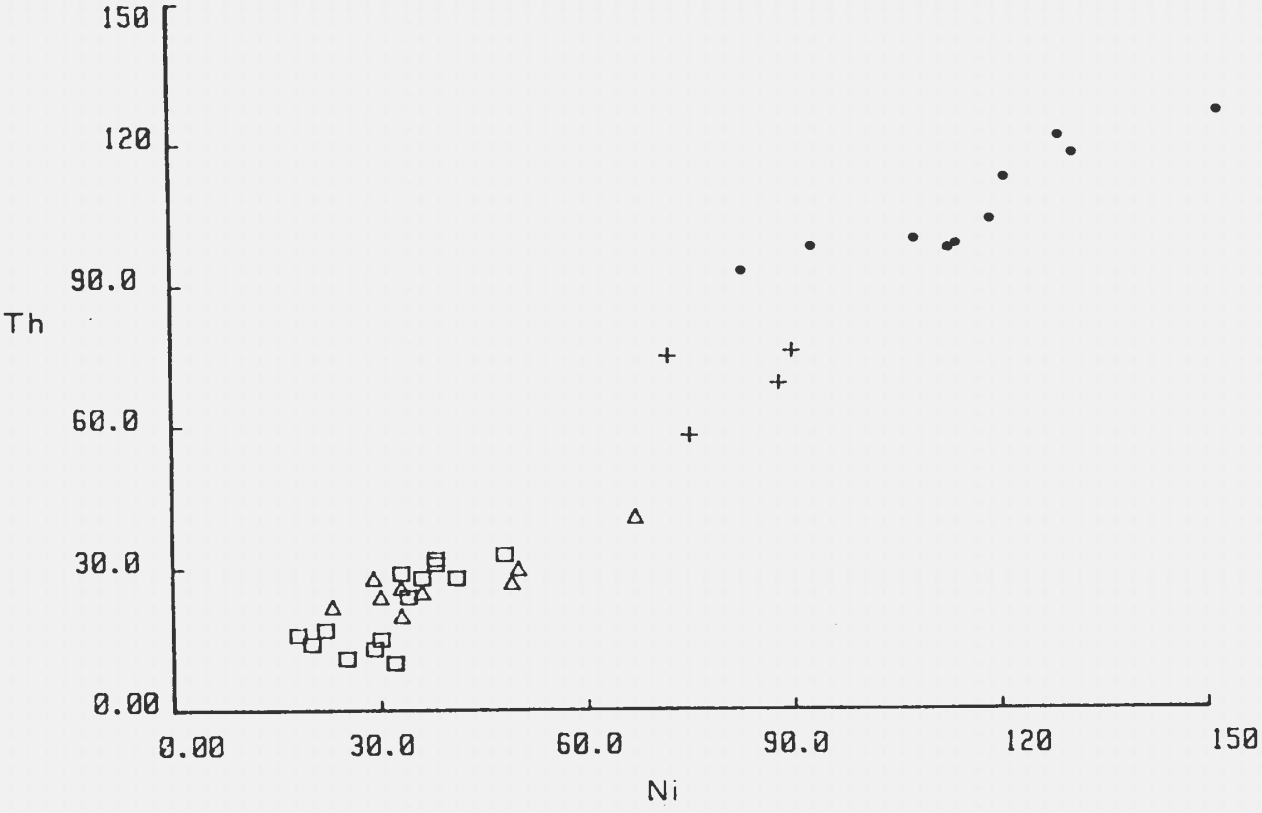
150
120
90.0
Th
60.0
30.0
0.00
0.00
30.0
60.0
90.0
120
150
Ni

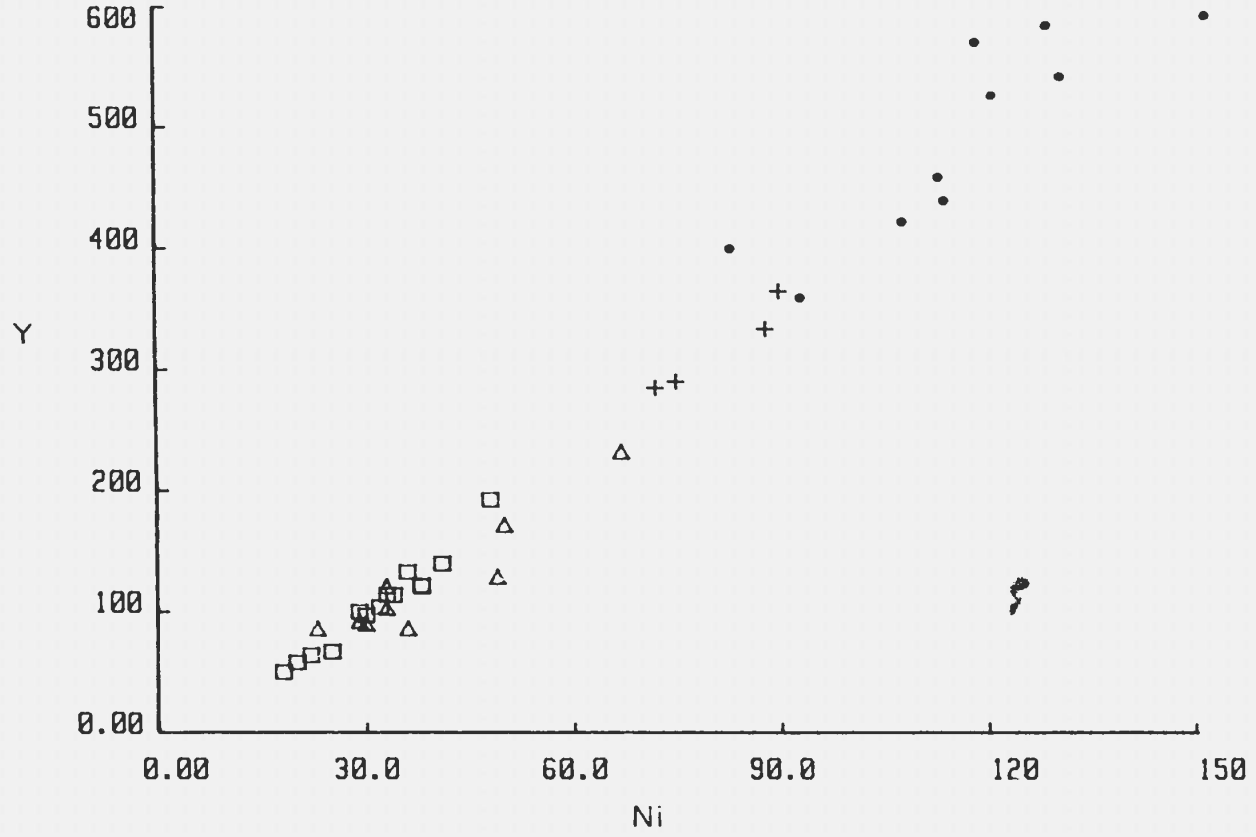
600
500
400
300
200
100
0.00
Y
0.00
30.0
60.0
90.0
120
150
Ni

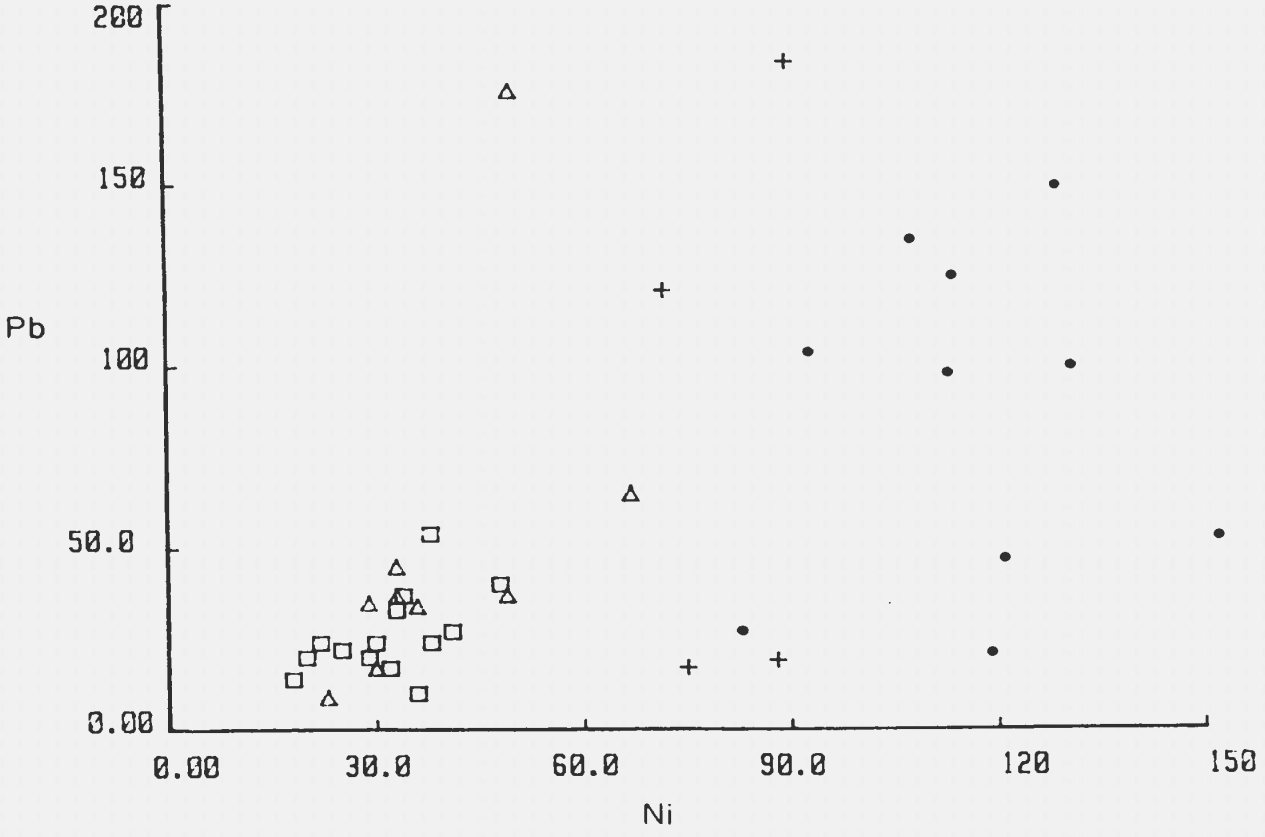
200
150
100
50.0
0.00
Pb
0.00
30.0
60.0
90.0
120
150
Ni

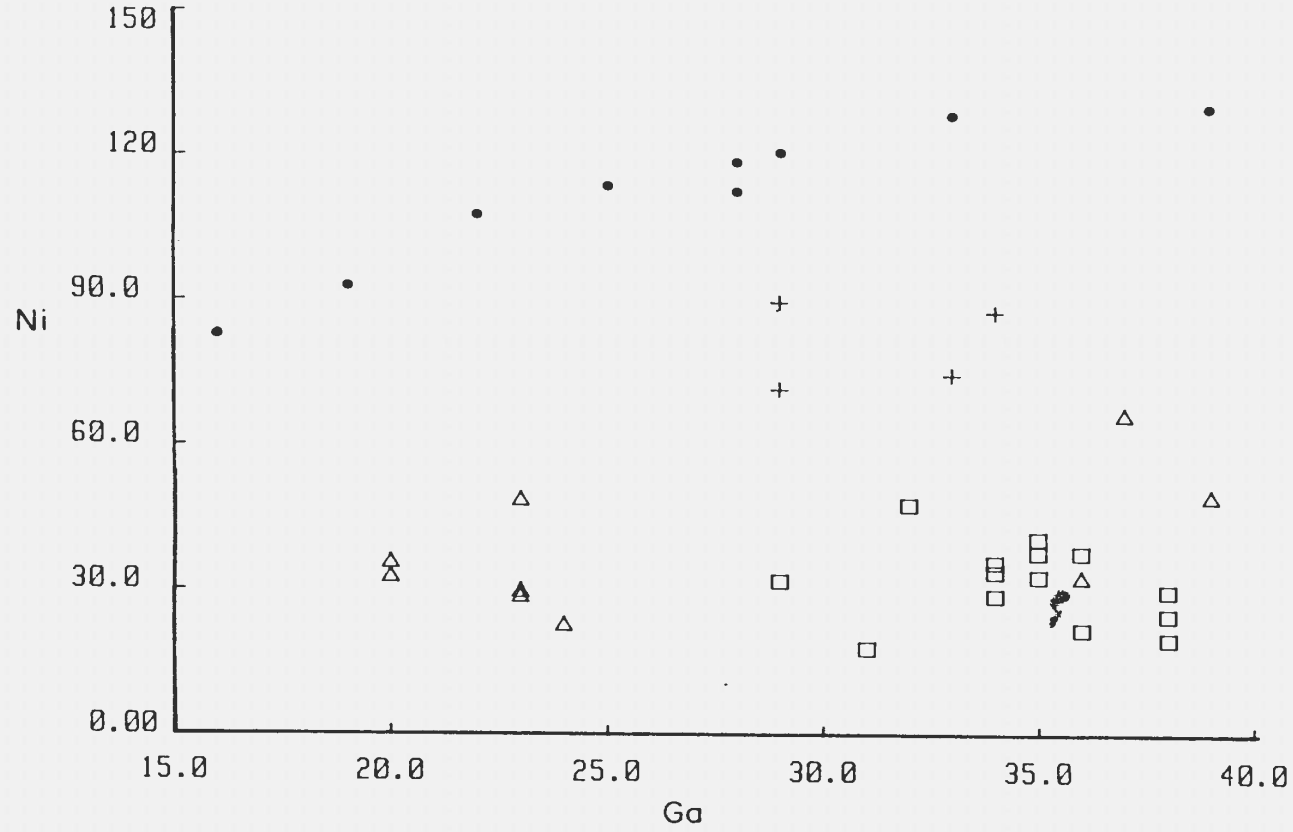
150
120
90.0
60.0
30.0
0.00
Ni
15.0
20.0
25.0
30.0
35.0
40.0
Ga

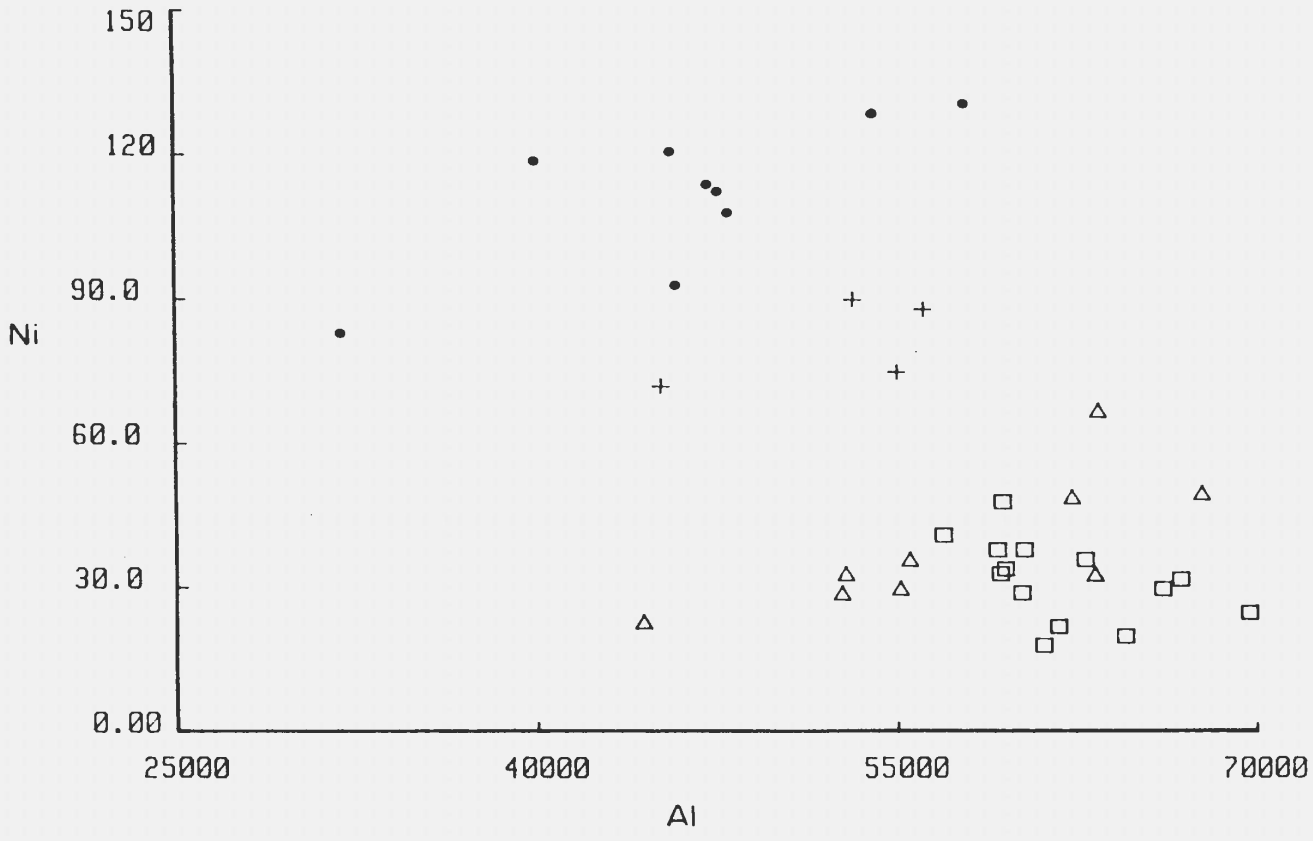
150
120
90.0
60.0
30.0
0.00
Ni
25000
40000
55000
70000
Al

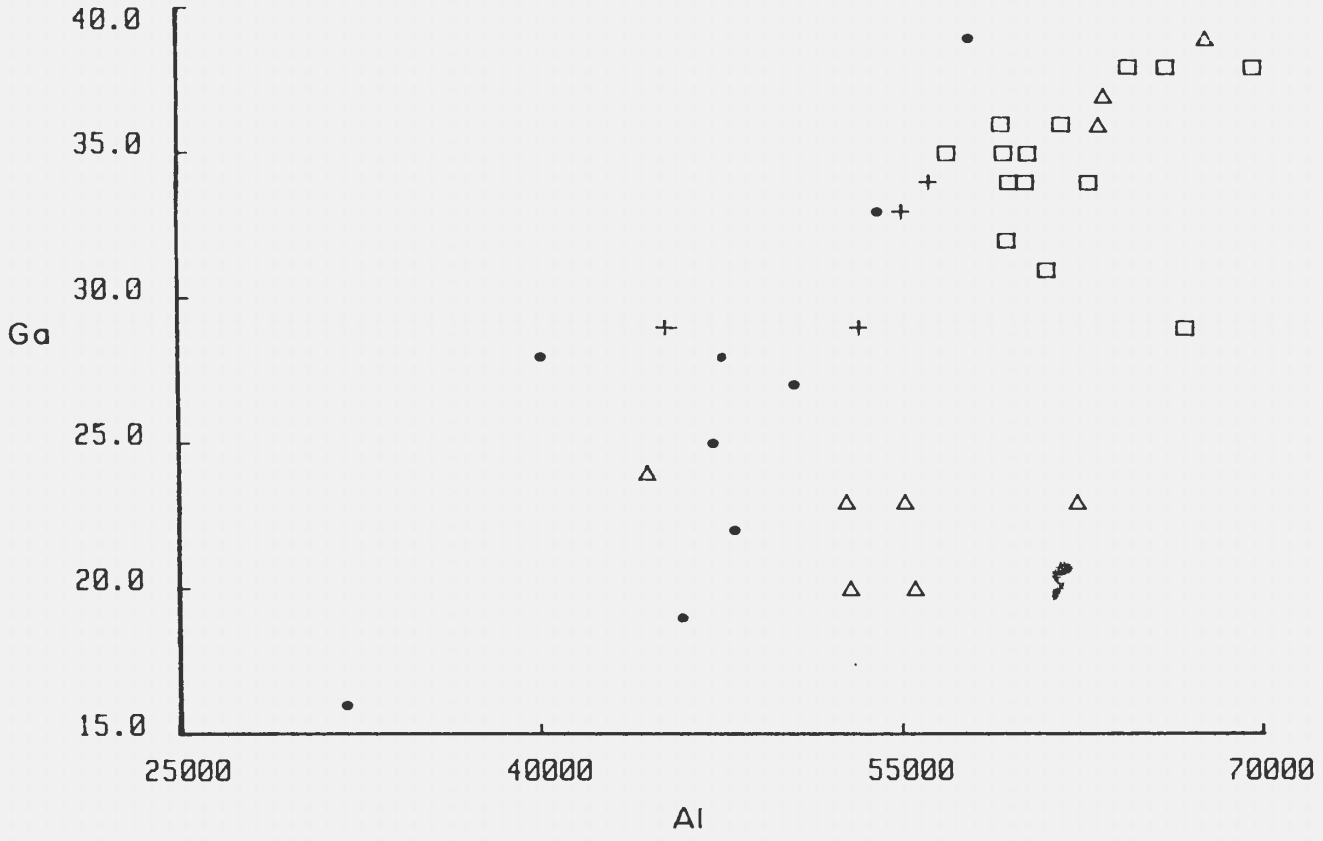
40.0
35.0
30.0
25.0
20.0
15.0
Ga
25000
40000
55000
70000
Al

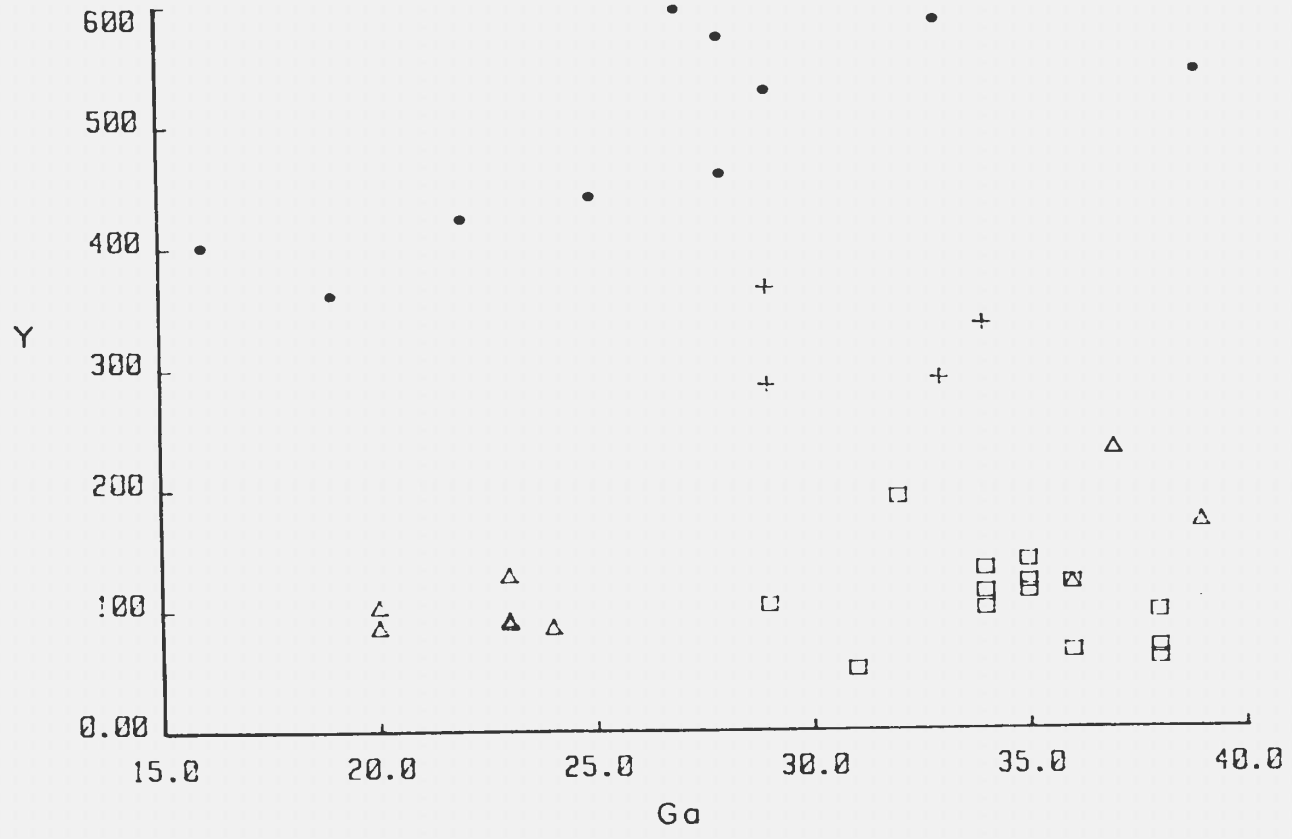
600
500
400
300
200
100
0.00
Y
15.0
20.0
25.0
30.0
35.0
40.0
Ga

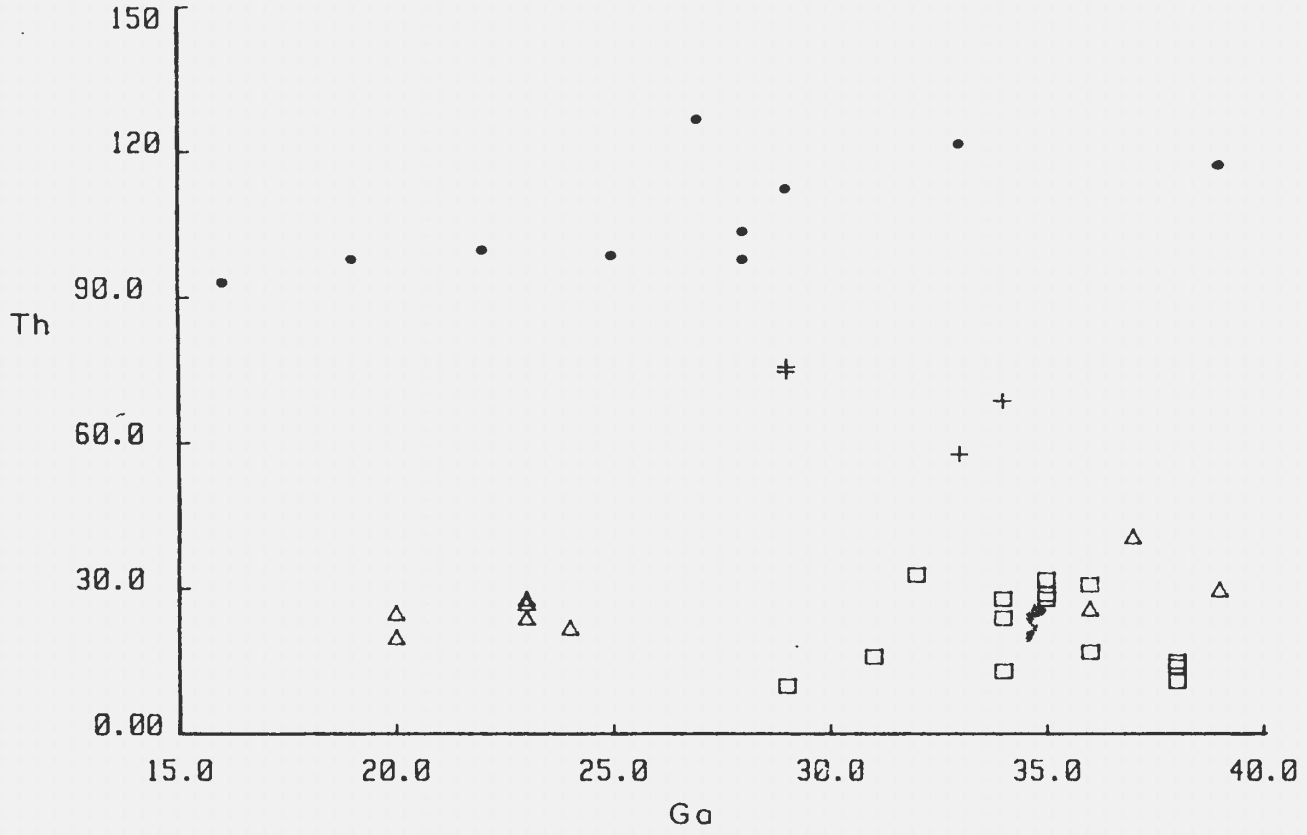
150
120
90.0
60.0
30.0
0.00
Th
15.0
20.0
25.0
30.0
35.0
40.0
Ga

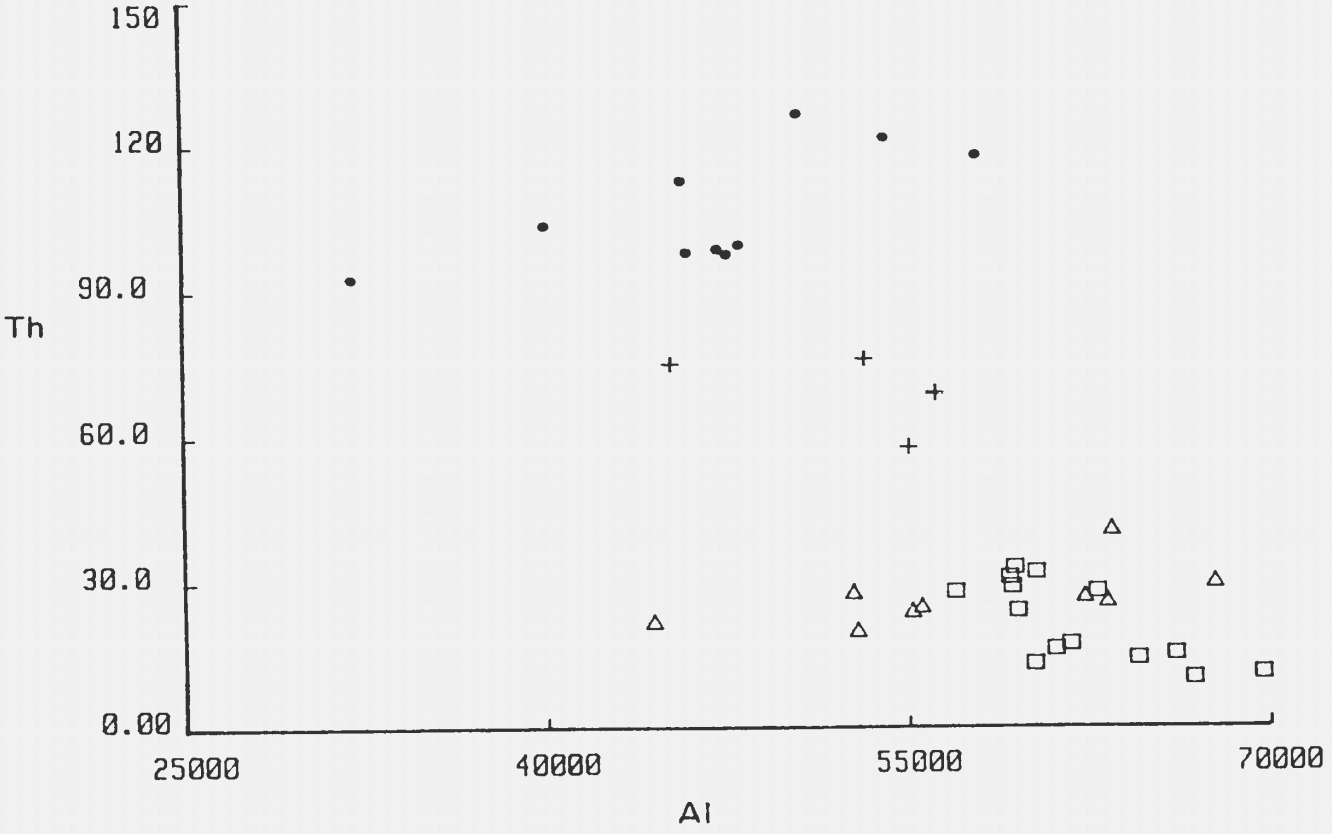
150
120
90.0
60.0
30.0
0.00
Th
25000
40000
55000
70000
Al

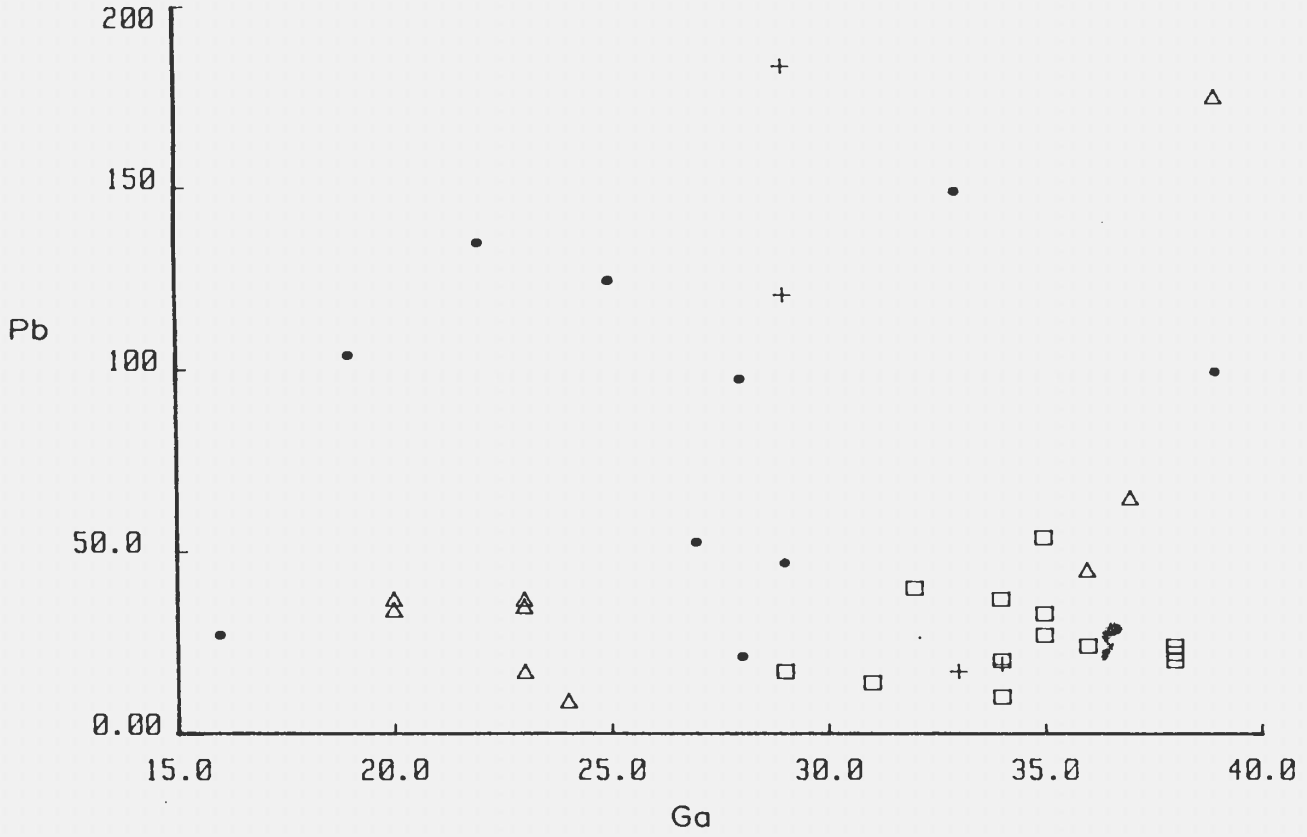
200
150
100
50.0
0.00
Pb
15.0
20.0
25.0
30.0
35.0
40.0
Ga

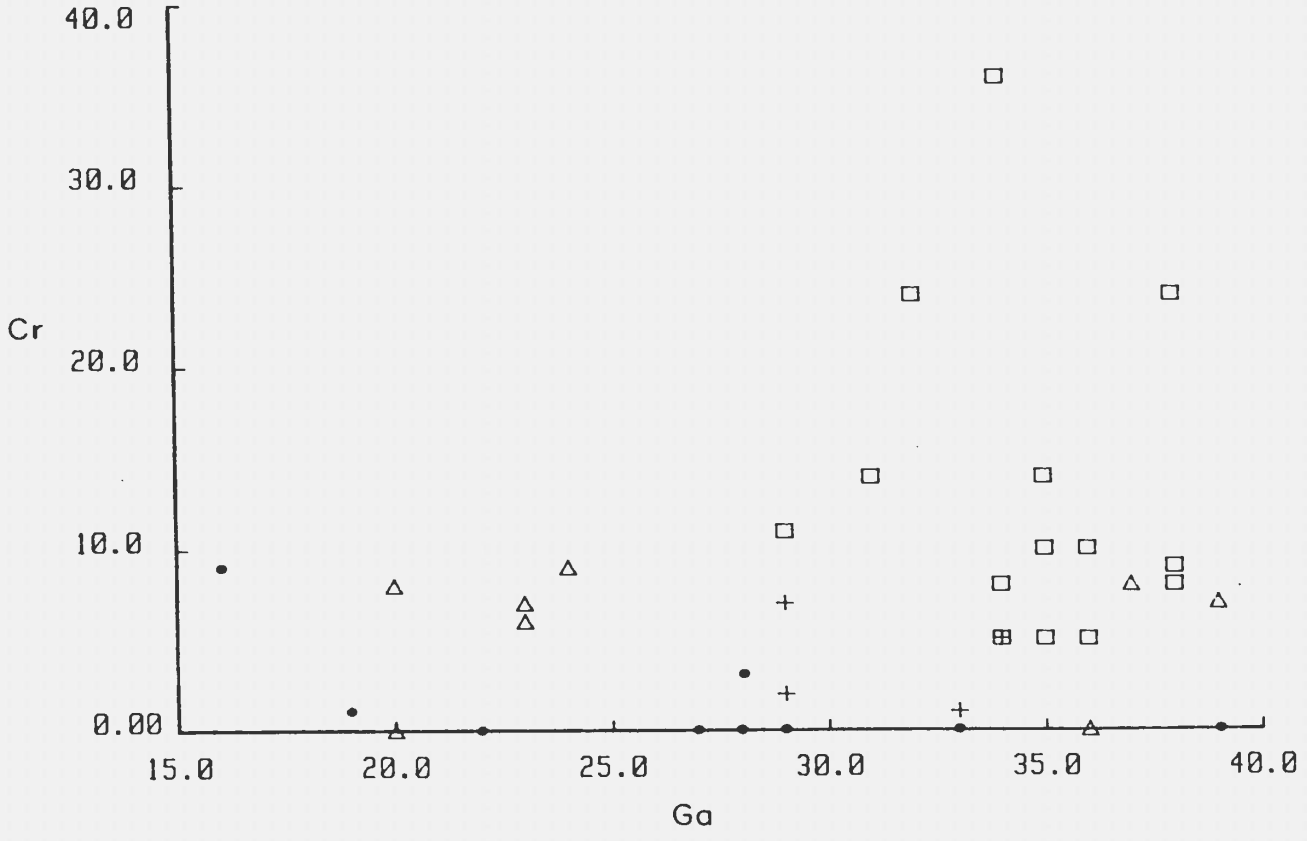
40.0
30.0
20.0
10.0
0.00
Cr
15.0
20.0
25.0
30.0
35.0
40.0
Ga

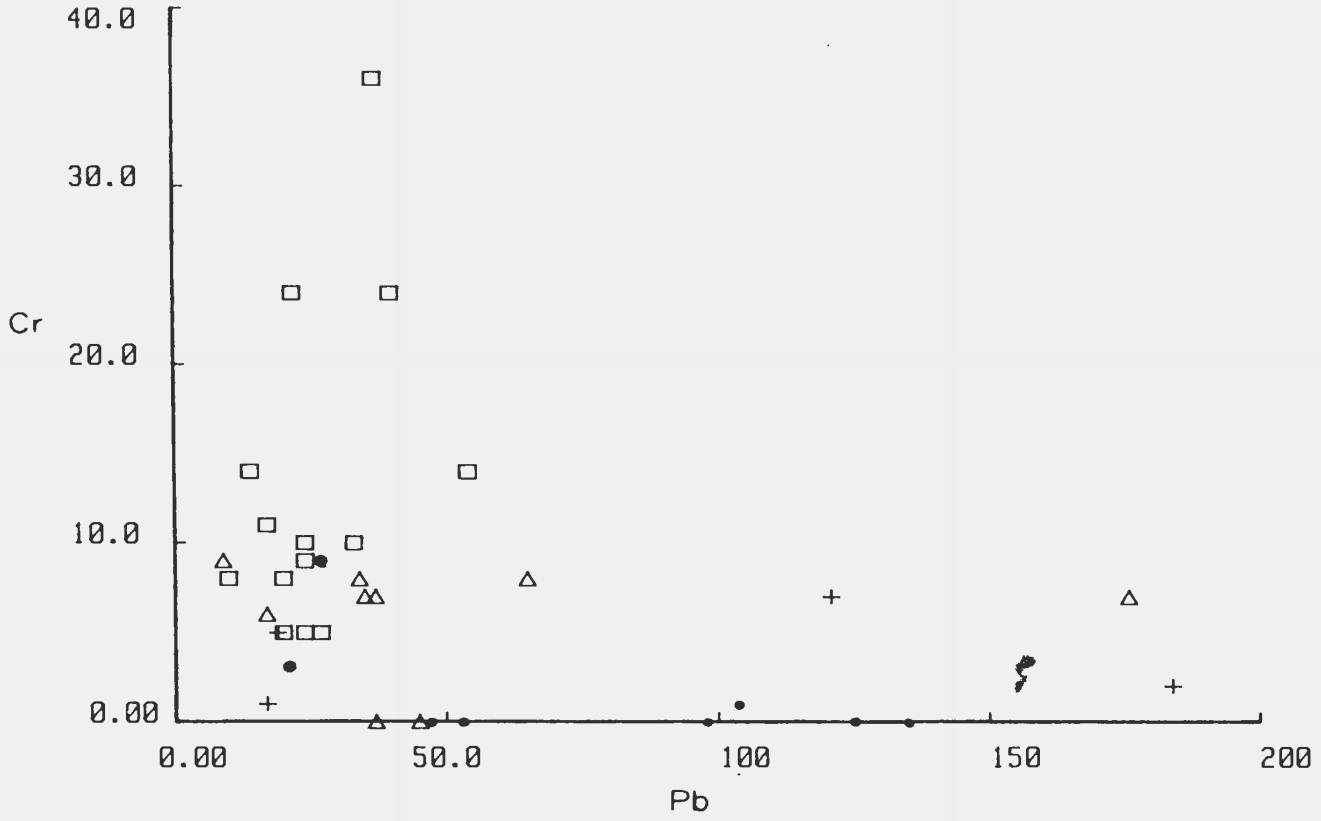
40.0
30.0
20.0
10.0
0.00
Cr
0.00
50.0
100
150
200
Pb

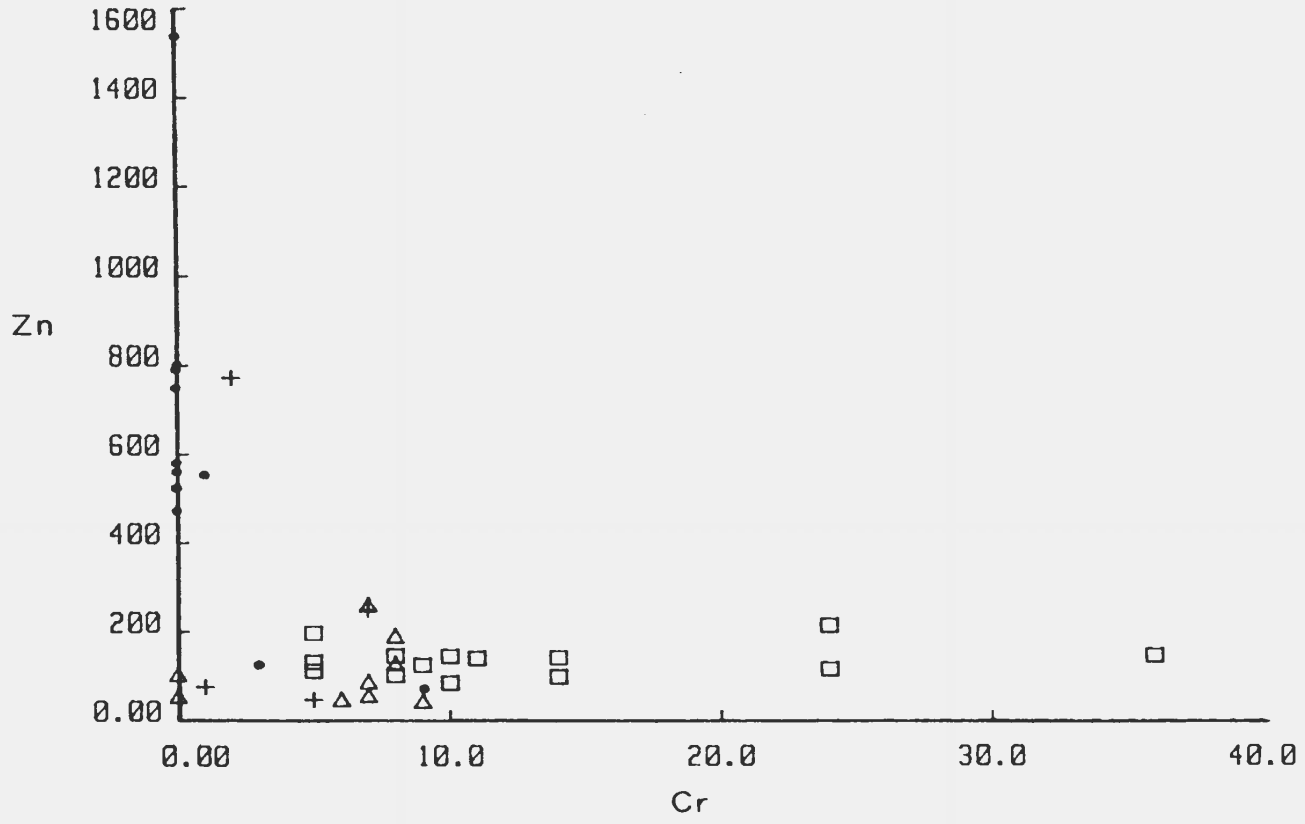
1600
1400
1200
1000
800
600
400
200
0.00
Zn
0.00
10.0
20.0
30.0
40.0
Cr

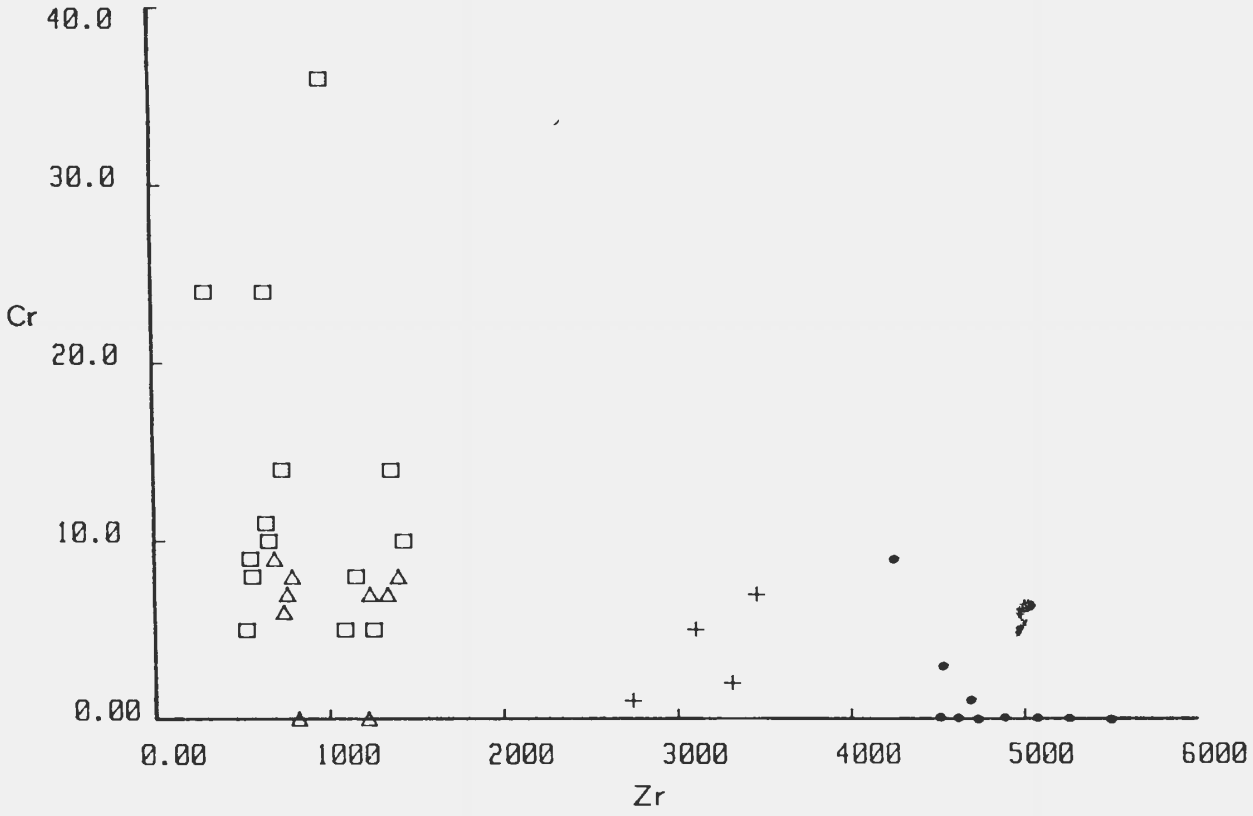
40.0
30.0
Cr
20.0
10.0
0.00
0.00
1000
2000
3000
4000
5000
6000
Zr

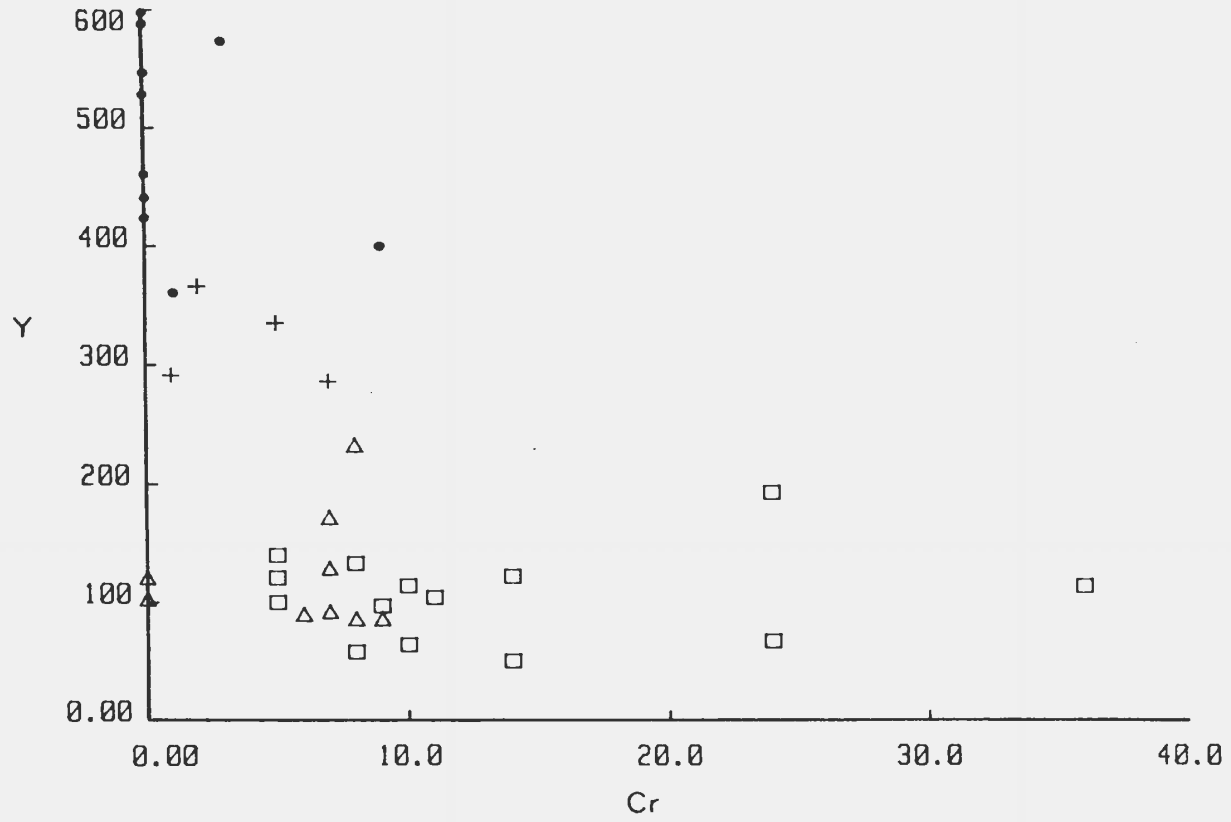
600
500
400
Y
300
200
100
0.00
0.00
10.0
20.0
30.0
40.0
Cr

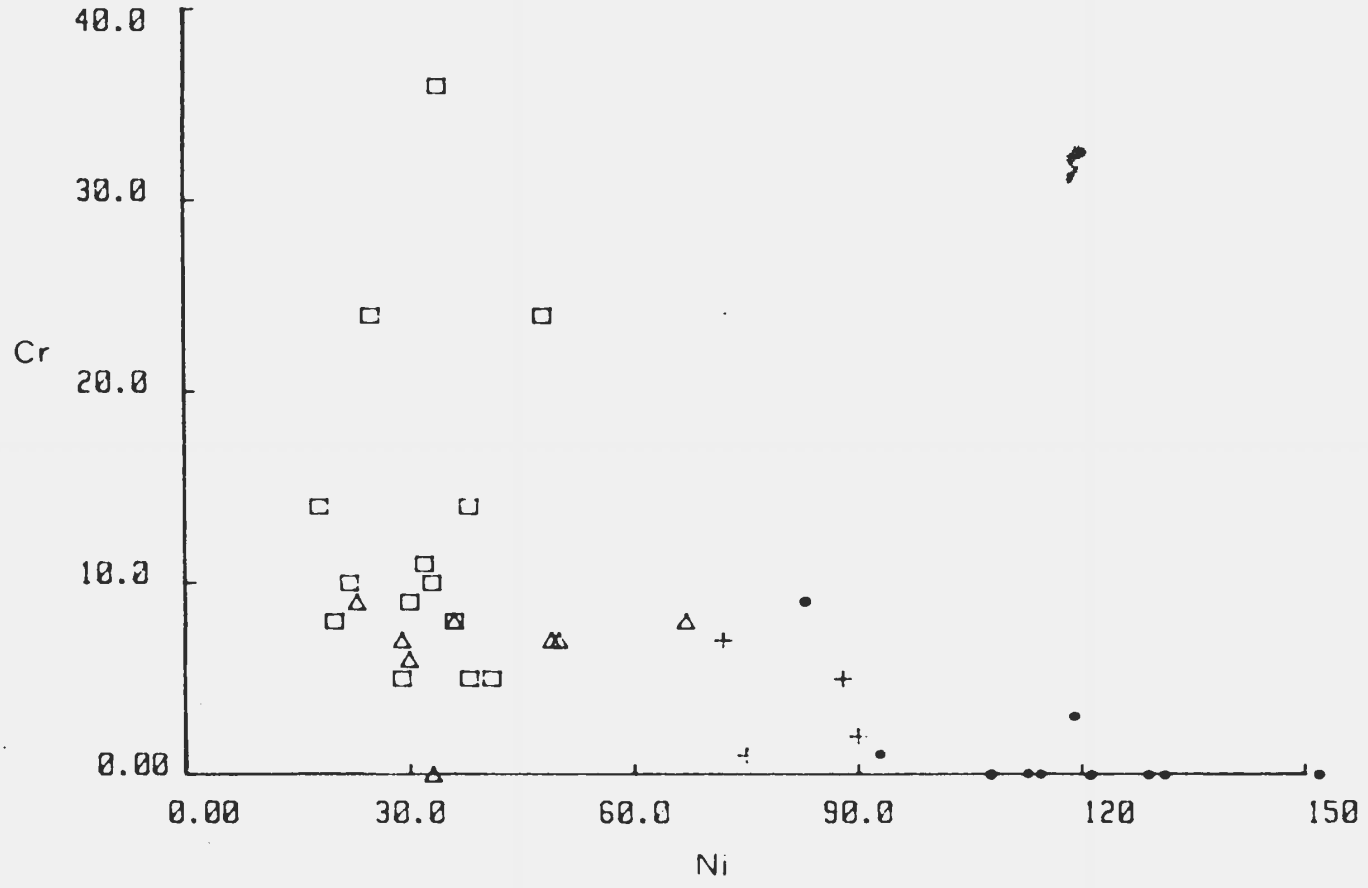
40.0
30.0
20.0
10.0
0.00
Cr
0.00
30.0
60.0
90.0
120
150
Ni

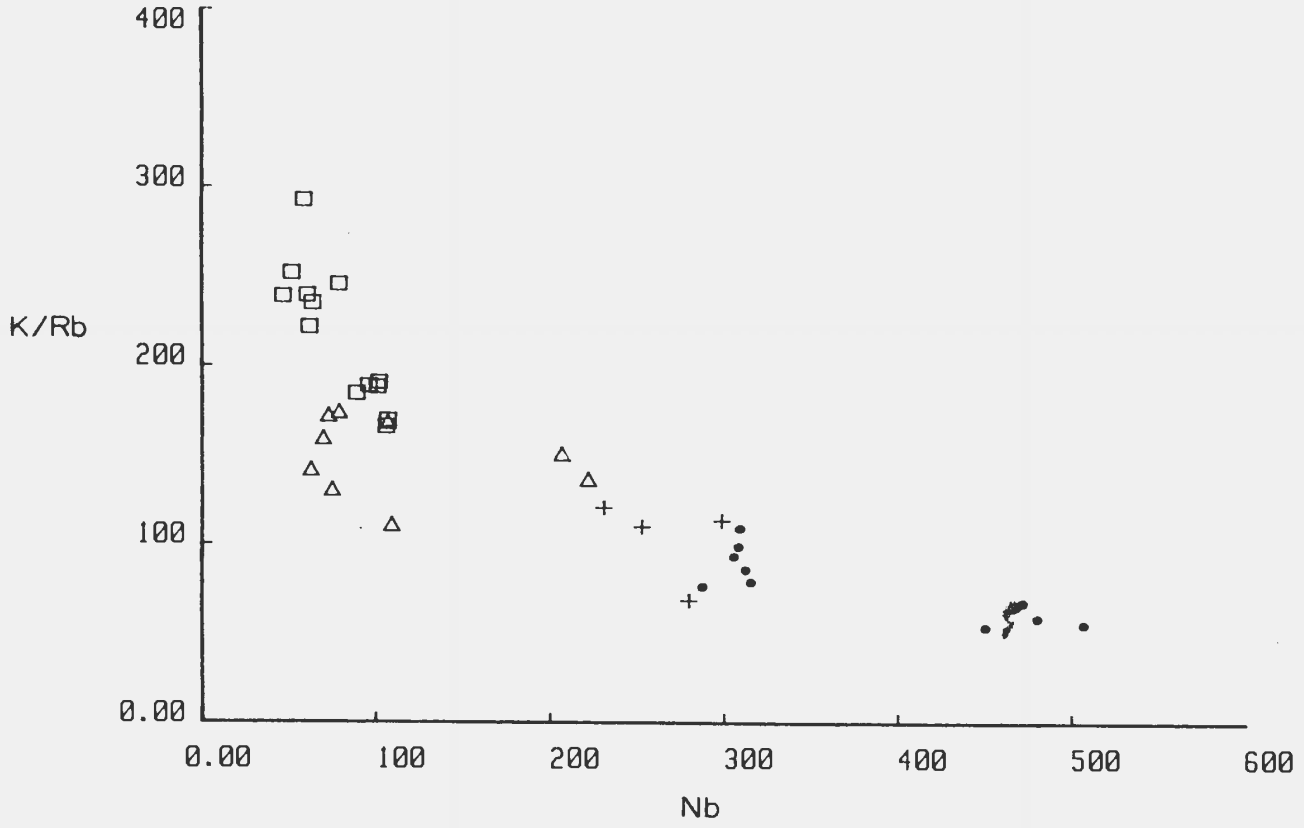
400
300
200
100
0.00
K/Rb
0.00
100
200
300
400
500
600
Nb

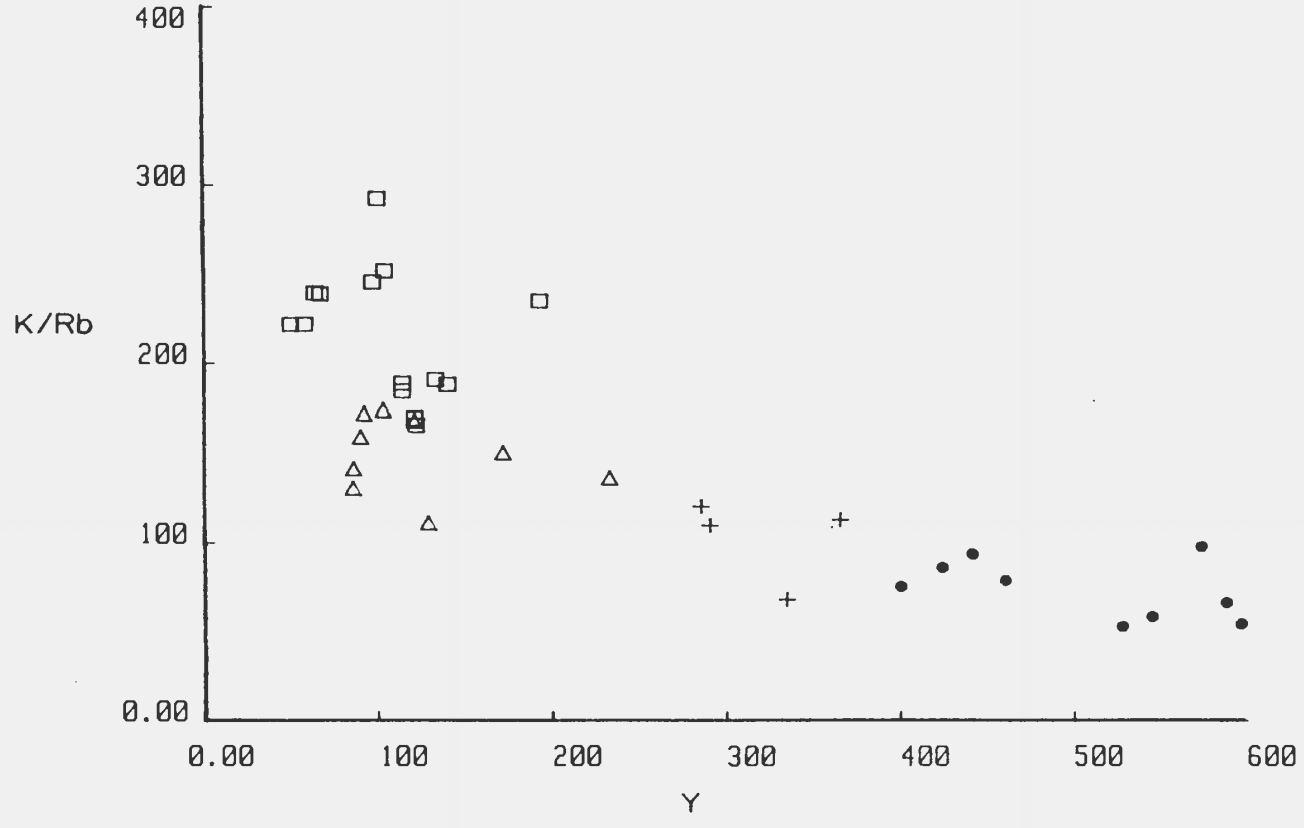
400
300
200
100
0.00
K/Rb
0.00
100
200
300
400
500
600
Y

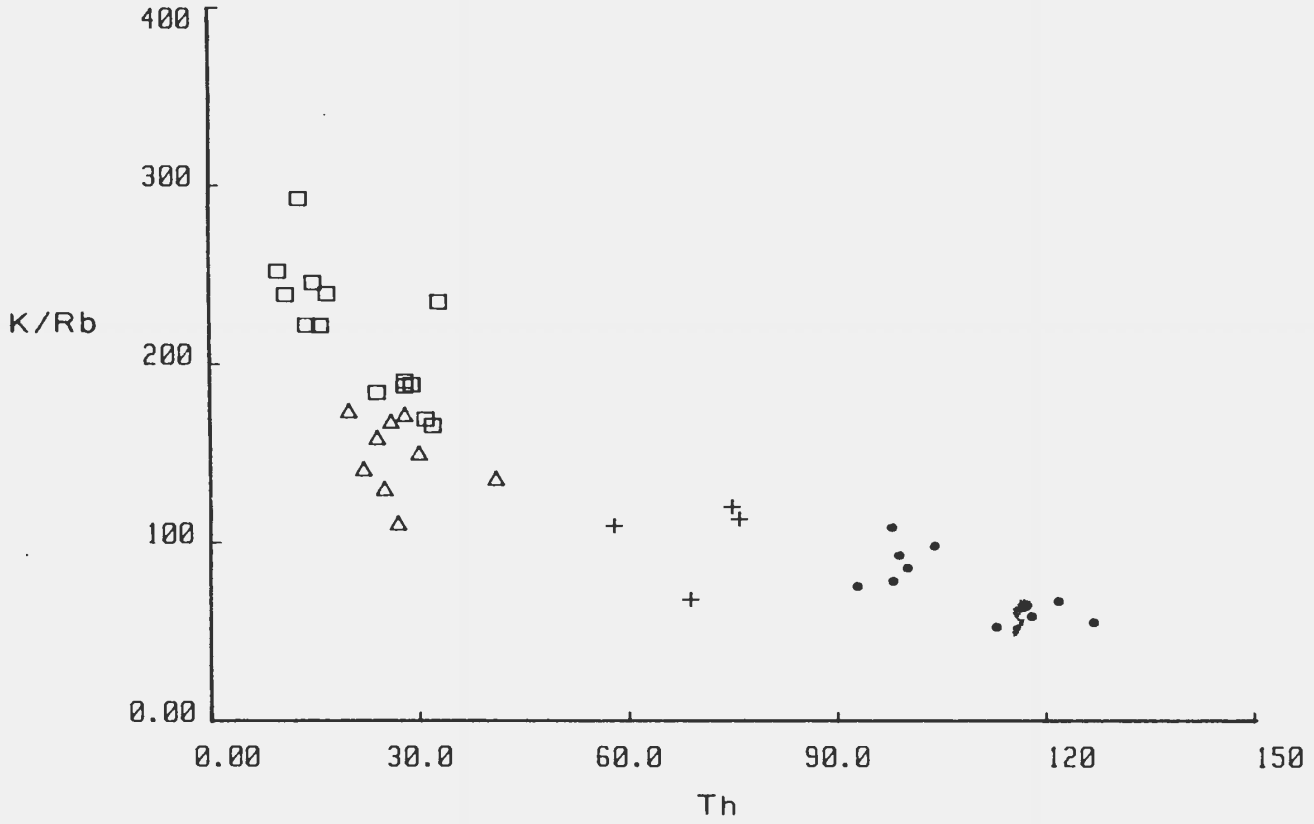
400
300
200
100
0.00
K/Rb
0.00
30.0
60.0
90.0
120
150
Th

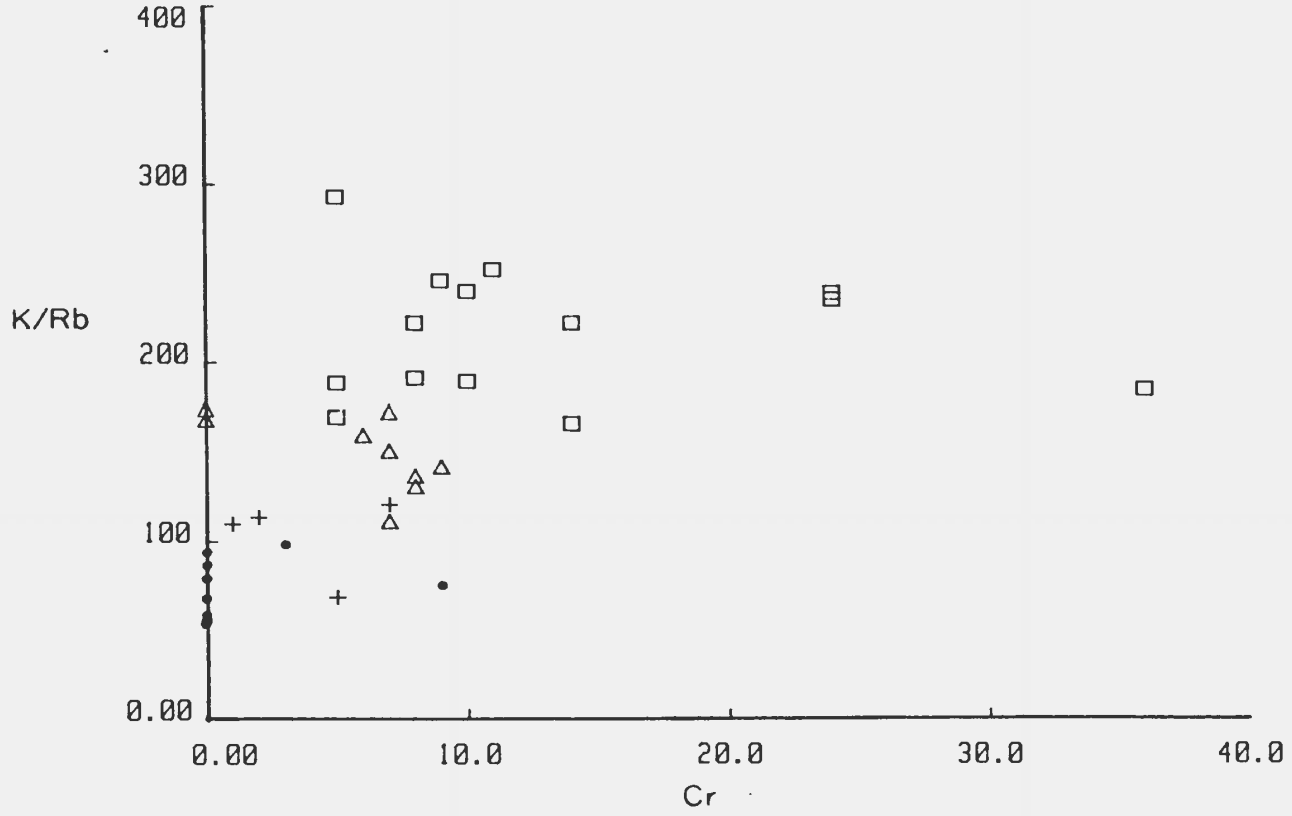
400
300
200
100
0.00
K/Rb
0.00
10.0
20.0
30.0
40.0
Cr

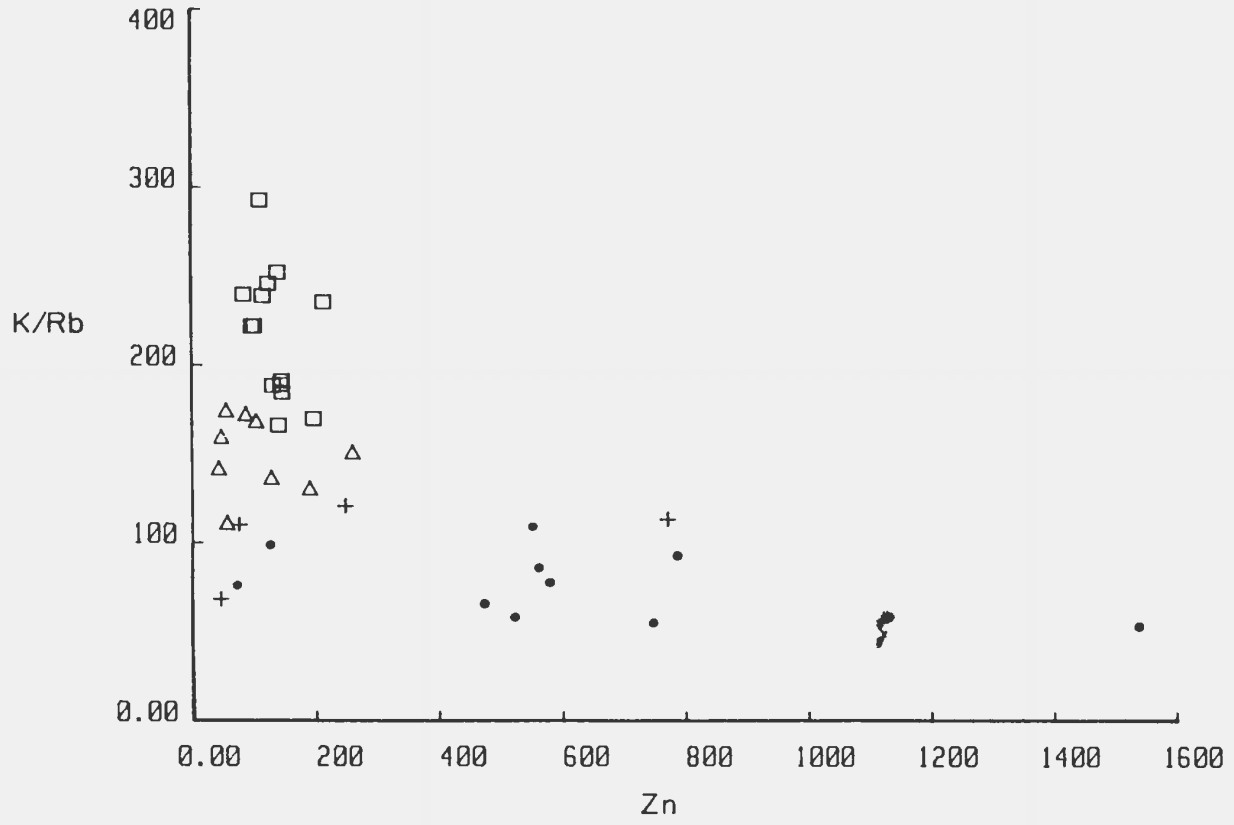
400
300
200
100
0.00
K/Rb
0.00
200
400
600
800
1000
1200
1400
1600
Zn

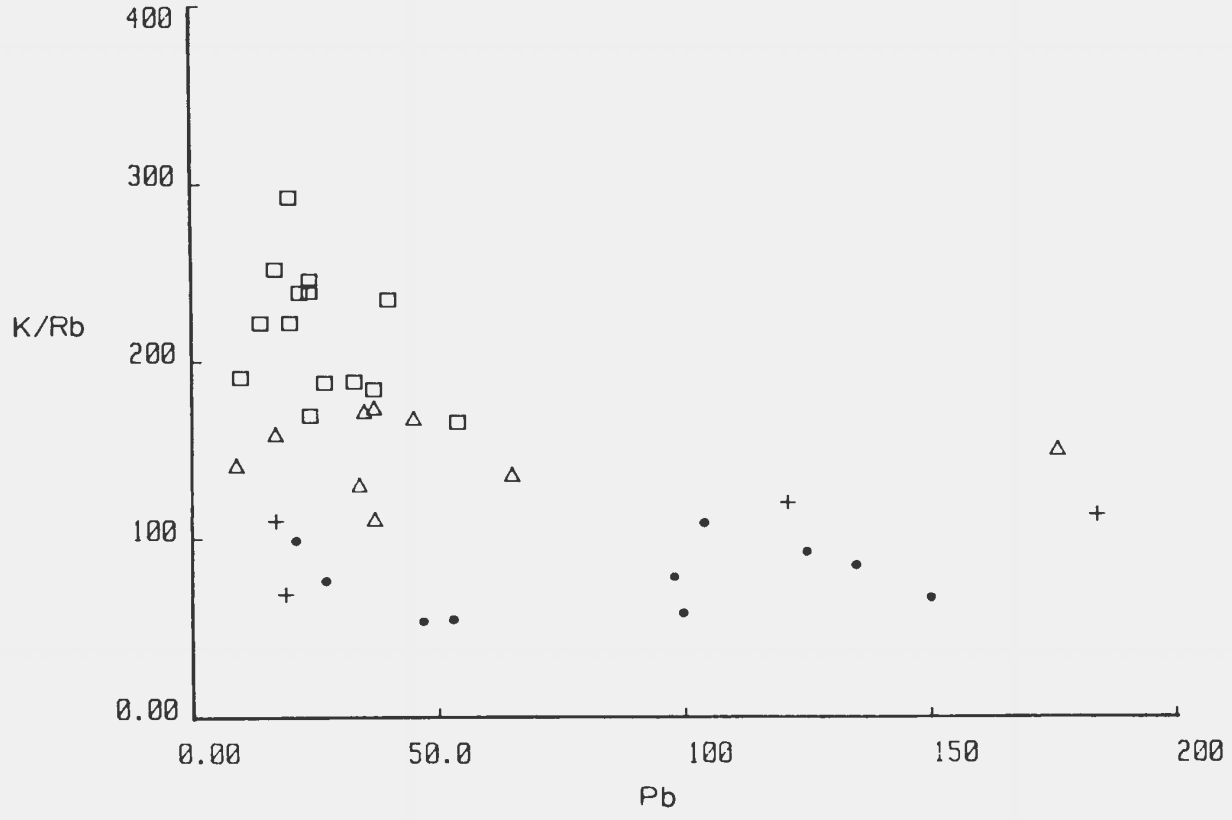
400
300
200
100
0.00
K/Rb
0.00
50.0
100
150
200
Pb

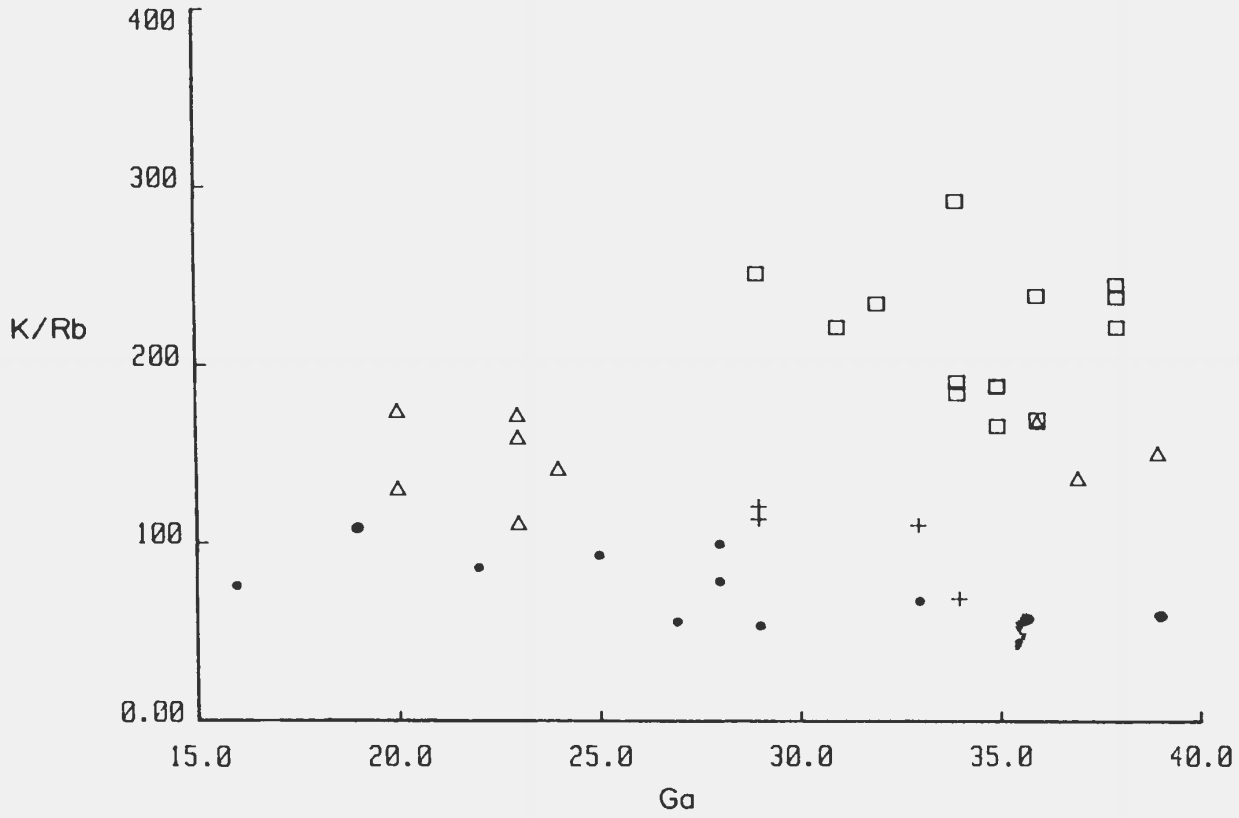
400
300
200
100
0.00
K/Rb
15.0
20.0
25.0
30.0
35.0
40.0
Ga

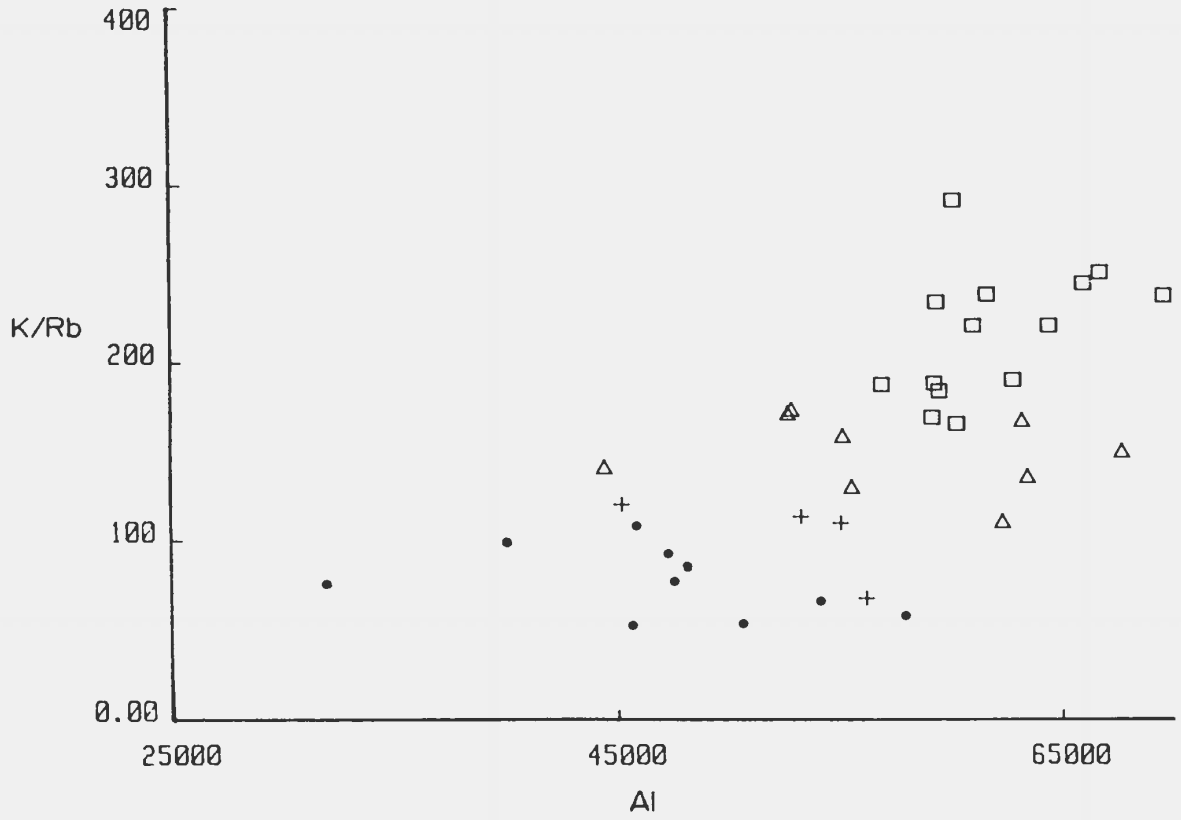
400
300
200
100
0.00
K/Rb
25000
45000
65000
Al


CENTRE FOR NFLD. STUDIES
MAR 23 198
MEMORIAL UNIVERSITY
OF NEWFOUNDLAND